IMPACT OF CASCADING FAILURES ON PERFORMANCE ASSESSMENT OF CIVIL INFRASTRUCTURE SYSTEMS

A Dissertation
Presented to
The Academic Faculty

By

Takao Adachi

In Partial Fulfillment
Of the Requirements for the Degree
Doctor of Philosophy in the
School of Civil and Environmental Engineering

Georgia Institute of Technology

May 2007

IMPACT OF CASCADING FAILURES ON PERFORMANCE ASSESSMENT OF CIVIL INFRASTRUCTURE SYSTEMS

Dr. Bruce R. Ellingwood, Advisor
School of Civil and Environmental Engineering
Georgia Institute of Technology

Dr. Reginald DesRoches
School of Civil and Environmental Engineering
Georgia Institute of Technology

Dr. James I. Craig
School of Aerospace Engineering
Georgia Institute of Technology

Dr. Kenneth M. Will
School of Civil and Environmental Engineering
Georgia Institute of Technology

Dr. Abdul-Hamid Zureick
School of Civil and Environmental Engineering
Georgia Institute of Technology

Date Approved: February 20, 2007

I dedicate this dissertation to my wife Mihoko.

I'd like to express my enduring gratitude to her for being an emotional support to me.

ACKNOWLEDGMENTS

This dissertation might not have been written without the advice and support of Dr. Bruce R. Ellingwood, who encouraged me during my entire doctoral program. I would like to thank him and my other doctoral committee members - Dr. Abdul-Hamid Zureick, Dr. Kenneth M. Will, Dr. Reginald DesRoches and Dr. James I. Craig - for their patient guidance. I also am grateful to the other faculty and my fellow students at the Georgia Institute of Technology for their advice and friendship during my time on campus.

I have found my coursework throughout the curriculum to be stimulating and thoughtful, providing me with the necessary tools with which to understand past and present ideas and to explore future engineering issues and challenges.

TABLE OF CONTENTS

LIST OF TABLES

LIST OF FIGURES

SUMMARY

Water distribution systems, electrical power transmission systems, and other civil infrastructure systems are essential to the smooth and stable operation of regional economies. Since the functions of such infrastructure systems often are inter-dependent, the systems sometimes suffer unforeseen functional disruptions. For example, the widespread power outage due to the malfunction of an electric power substation, which occurred in the northeastern United States and parts of Canada in August 2003, interrupted the supply of water to several communities, leading to inconvenience and economic losses. The sequence of such failures leading to widespread outages is referred to as a cascading failure. Assessing the vulnerability of communities to natural and man-made hazards should take the possibility of such failures into account.

In seismic risk assessment, the risk to a facility or a building is generally specified by one of two basic approaches: through a probabilistic seismic hazard analysis (PSHA) and a stipulated scenario earthquake (SE). A PSHA has been widely accepted as a basis for design and evaluation of individual buildings, bridges and other facilities. However, the vulnerability assessment of distributed infrastructure facilities requires a model of spatial intensity of earthquake ground motion. Since the ground motions from a PSHA represent an aggregation of earthquakes, they cannot model the spatial variation in intensity. On the other hand, when a SE-based analysis is used, the spatial correlation of seismic intensities must be properly evaluated.

This study presents a new methodology for evaluating the functionality of an infrastructure system situated in a region of moderate seismicity considering functional interactions among the systems in the network, cascading failure, and spatial correlation

of ground motion. The functional interactions among facilities in the systems are modeled by fault trees, and the impact of cascading failures on serviceability of a networked system is computed by a procedure from the field of operations research known as a shortest path algorithm. The upper and lower bound solutions to spatial correlation of seismic intensities over a region are obtained.

CHAPTER 1

INTRODUCTION

Commerce and public health and safety depend strongly on the proper functioning of civil infrastructure systems, including electrical power transmission, water and gas distribution, and public transportation systems. The serviceability of such systems can be measured as the ratio of customers in an area that can be served to customers requiring service within that area. If the serviceability of these infrastructure systems is impaired or destroyed as a consequence of extreme natural events such as hurricanes or earthquakes, accidents, or deliberate man-made incidents, business and industrial activities in the community serviced are interrupted, productivity is diminished or lost and social welfare is impaired. The recovery period is longer when the systems are severely damaged, and the losses increase exponentially as the period required to fully recover infrastructure serviceability lengthens (Tierney, 2000). Furthermore, the demands placed on an infrastructure system, as well as the capacity of components and systems to withstand those demands, are highly uncertain. Accordingly, a probability-based vulnerability assessment of infrastructure systems is necessary to forecast the likely impact of a disaster on their operating requirements, the degree of damage or diminished functionality in key system components, and the social impact of the disaster on the community served. This vulnerability assessment is one basis for estimating probable losses and the impact of diminished functionality on the affected community.

Civil infrastructure systems that may be impacted by a natural or man-made disaster consist of many interconnected components and delivery systems. These

components may be widely distributed over an urban area and may sustain different levels of damage when subjected to an extreme event. For example, a municipal water system includes water storage tanks, pumping stations and pipelines. Electrical power systems in an urban area may have one or more generation plants, numerous substations, and extensive transmission and distribution lines. Furthermore, civil infrastructure systems often are functionally interdependent, in the sense that the proper functioning of one system requires service from other systems. One familiar example of the impact of functional dependence between infrastructure systems on their operating characteristics is furnished by the widespread power outage in the northeastern United States and parts of Canada in August, 2003. During that power outage, water systems in Cleveland, OH (and other municipalities) failed to operate because the pumping stations required electrical power, even though the water system itself did not sustain any physical damage (Cascos et al., 2004). More recently, as a result of a power outage in Tokyo, Japan on August 14, 2006 caused by an industrial accident, urban road traffic networks were affected due to traffic light failures at more than 260 places, passenger travel on the subway system was impaired, and the Tokyo Stock Exchange was forced to cease its foreign exchange operations (CNN.COM, 2006). Earthquakes are likely to be a source of such failures. In the Mid Niigata Prefecture, Japan earthquakes of 2004 (four earthquakes of Japanese magnitudes 5.8, 5.9, 6.4 and 6.5 occurred in 40 minuets), about 260 houses in Yamakoshi village lost electrical power; power transmission could not be restored for an extended period because transportation networks were severely damaged by the earthquakes. In this village, the supply of potable water was also damaged; the repair of the damaged potable water supply system was delayed for four months because

the other infrastructure systems on which it depended were severely damaged. Many similar situations were reported after this earthquake (Niigata Prefecture, 2004).

In many parts of the world, earthquakes pose a major threat to the operation of civil infrastructure systems. Seismic fragility and vulnerability assessment are key ingredients of decision-making for mitigating earthquake risks to civil infrastructure in an urban area. In recent years, such assessments have been performed for networked civil infrastructure systems that provide essential services - natural gas, water, electric power, telecommunications and transportation - to urban communities. When the fragility or functionality of a component or facility in a networked infrastructure system or the vulnerability of the system as a whole are considered, the performance of a facility in that networked system may be affected by the functionality of other facilities and connecting elements in interfacing systems. For example, during the electrical power blackout of August, 2003 noted above, some undamaged electrical power substations were unable to deliver power to a service area because other substations in the electrical grid on which they depended lost functionality (US-Canada Power System Outage Task Force, 2004). Such failures are referred to as cascading failures (Rinaldi et al., 2001; Rinaldi, 2004).

Earthquake hazards used in vulnerability assessment of civil infrastructure systems generally are specified using two basic approaches: through a probabilistic seismic hazard analysis (PSHA) (McGuire, 1995) or scenario earthquake (SE) based seismic analysis. In a PSHA, the seismic hazard is described by a complimentary cumulative distribution function defining the probability of exceeding specific earthquake intensities. This probabilistically stated seismic hazard reflects the aggregated effect of possible earthquakes in proximity to a site, weighted by the probability of occurrence of

each earthquake (McGuire, 1995 and 2004). Probabilistic seismic hazard maps that display contours of seismic intensities corresponding to peak ground acceleration or velocity (PGA, PGV) or spectral parameters at specific return periods are published by the United States Geological Survey (U.S. Geological Survey, 2002b). The intensities from these uniform hazard maps are used in building design (Federal Emergency Management Agency, 2004; American Society of Civil Engineers, 2005). A PSHA is particularly suited for designing individual facilities because the aggregated effects of all seismic events affecting the facility can be represented at a probabilistically stipulated level of the seismic hazard in the governing codes and regulatory documents (e.g., 2% probability of exceedance in 50 years). On the other hand, no single earthquake can generate the spatial distribution of seismic intensity that is reflected in the probabilistic seismic hazard map, as the mapped contours represent the aggregated effects of numerous earthquakes. This fact does not pose a problem when only one facility is analyzed or designed, since a risk assessment of that one facility does not require information on the spatial distribution of seismic intensities. However, when the damage or risk to a spatially distributed networked infrastructure system must be assessed, information regarding the spatial distribution of seismic intensities is also important (Eguchi, 1991b; Chang et al., 2000). This impact is difficult to assess on the basis of a PSHA because information on the spatial distribution of ground motion intensity due to one (severe) earthquake is lost in the process of aggregation on which the uniform hazard contours are based.

In contrast to a PSHA, a SE-based seismic hazard analysis is aimed at investigating the impact of a specific earthquake (usually stipulated in terms of

magnitude and epicenter) on a facility or group of facilities. Such a specification of seismic hazard also is useful in communicating the hazard or risk, especially in explaining seismic risk to civil infrastructure systems to public decision-makers who seldom are familiar with the mathematical concepts that underlie a PSHA but understand the concept of an earthquake magnitude from exposure in the popular media.

Assessments of civil infrastructure network performance during and after an earthquake often are based on a postulated scenario earthquake (SE). A scenario-based seismic risk analysis, despite its conditional nature, avoids some of the conceptual and practical difficulties in applying a probabilistic seismic hazard analysis (PSHA) (Tierney, 2000) to evaluate network serviceability (Shinozuka et al., 1992; Hwang et al, 1998; Cascos et al., 2004). Among the particular challenges in scenario-based risk analysis are modeling the effect of spatial correlation in ground motion intensity in the absence of information on seismic wave propagation and local site conditions, and evaluating the impact of this spatial correlation on response of distribution elements that are found in distributed civil infrastructures systems. Furthermore, the effect of infrastructure interdependency must be properly modeled and evaluated when the serviceability of infrastructure systems are assessed.

1.1 Research Objectives

Experience during and following past earthquakes has clearly shown that the residual serviceability of a civil infrastructure system is strongly dependent on the residual serviceability of other infrastructure systems that interface with it. More specifically, once infrastructure systems have become damaged or their function has been impaired, other interfacing infrastructure systems can lose their serviceability though they

are not physically damaged. Furthermore, stochastically dependent seismic intensities lead to stochastically dependent damage in infrastructure systems, and facilities and distribution elements, yielding damage situation nor forseen from ordinary seismic assessments which have not considered stochastic dependence. For example, if a seismic intensity at one site is much higher than estimated by its epicentral distance and local soil condition, seismic intensities around the site might be higher than estimated, and this yields more severe damage situation than would otherwise be expected.

The proposed research introduces a new methodology for assessing serviceability of infrastructure systems exposed to earthquake hazard. The distinctive features of this methodology are its consideration of interactions between infrastructure systems at risk, its inclusion of cascading failures from components within the infrastructure system, and its accounting for spatially correlated seismic intensities in the affected region. The applicability of probabilistic seismic hazard analysis to a spatially distributed infrastructure system and limitations in comparison to a scenario analysis are assessed. To illustrate the methodology, a vulnerability assessment is conducted of the municipal water system in an urban area of the Central United States exposed to moderate seismic risk.

This new serviceability assessment methodology leads to improvements in the residual serviceability estimation that can be utilized in decision making regarding design and retrofit plan of infrastructure systems.

1.2 Organization of Dissertation

This dissertation is divided into seven chapters. Chapter 1 introduces the subject and identifies the major research issues, and presents the research objectives. Chapter 2

reviews existing research methods in the field of operations research and system reliability that might be used for serviceability assessment of infrastructure systems and for evaluating interdependency effects among infrastructure systems. Chapter 3 presents the approaches for modeling infrastructure interdependencies, illustrating the theories and algorithms that are used in the following chapters with simple examples. Chapter 4 illustrates alternatives for characterizing the seismic demands on infrastructure systems. Probabilistic seismic hazard analysis and the scenario based seismic hazard analysis are introduced, in the context of describing the earthquake threat on a distributed system. Attenuation equations for the peak ground acceleration and the peak ground velocity, the local soil amplification factors and the spatial correlation of seismic intensities are introduced. Chapter 5 considers the applicability of the probabilistic seismic hazard analysis approach to a spatially distributed infrastructure system. The simple network models are used to identify situations in which probabilistic seismic hazard analysis can reasonably be applied and to explain its limitations through quantitative examples. Chapter 6 illustrates the new serviceability assessment methodology of interdependent infrastructure systems subjected to spatially correlated seismic demands, through a case study involving the water distribution system and the electrical power transmission system in Shelby County, TN. Easily computed upper and lower bounds on serviceability ratio under the spatially correlated seismic intensities are developed. Chapter 7 illustrates the serviceability assessment of infrastructure systems under uniform seismic intensities. By applying the probabilistic seismic hazard analysis to the real network system, the deficiencies in use of probabilistic seismic hazard analysis for this purpose are illustrated. Using a deaggregation of the probabilistic seismic hazard, the

serviceability of infrastructure systems is evaluated at several return periods. Chapter 8 illustrates the impact of epistemic uncertainty on the serviceability assessment are illustrated. Using event tree models, the effect of epistemic uncertainty due to the choice of modeling parameters are evaluated. Furthermore, the sensitivities of water distribution and electrical power transmission systems to the modeling parameters are evaluated. Chapter 9 summarizes the major research findings and suggests future avenues for research in this area.

CHAPTER 2

SERVICEABILITY ASSESSMENT OF INFRASTRUCTURE SYSTEMS

Methodologies to analyze the serviceability of an infrastructure system following an extreme natural event, such as an earthquake, have been improved in recent years and have become more efficient and sophisticated as a number-crunching power of personal computers has improved. In addition, some research recognizes the important effects of infrastructure interdependency when serviceability of an infrastructure system is analyzed. However, most of the research does not consider the functional interaction among infrastructure systems. Rather, it considers financial interaction among the monetary losses due to the lost performance of infrastructure systems and underestimates the total monetary loss since the monetary loss due to a single infrastructure system must be affected by the functional interaction among infrastructure systems.

In this section, previous research applicable to civil infrastructure network analysis is reviewed, with the goal of identifying the current state-of-the-art and research issues and challenges that must be addressed. This review lays the groundwork for, and clarifies the objectives of, the proposed research.

2.1 Review of Previous Work

Many assessment methodologies applicable to the serviceability of infrastructure systems have been proposed. These methodologies are classified as follows:

- To model an infrastructure system,

- To assess the serviceability of an infrastructure system, and
- To evaluate effects of infrastructure interdependency.

During these steps, uncertainties of parameters such as seismic intensities or failure events of components in an infrastructure system should be integrated properly. In this section, prior research achievements are reviewed, and issues which have not been dealt with previously and are to be addressed in this study are presented.

(1) Modeling an infrastructure system

An infrastructure system is a collection of many components such as facilities and distribution elements. Each facility or distribution element has its own structural characteristics and its own independent role to maintain a function of the infrastructure system. While an office building or a bridge is also a collection of components, the major characteristic of an infrastructure system not shared by an office building or bridge is that its components are spatially distributed over a large region, and key components may located at some distance from one another. For example, a hydro-power generation station is located close to a water dam in a valley; electrical power is transmitted through transmission lines and substations to urban areas located some distance from the hydro-power generation plant. Thus, the modeling approach must take these distinct features into account.

To address this modeling problem, Satyanarayana and Wood (1985), Wagner et al. (1988a and 1988b) and Quimpo et al. (1997) used graph theory to model an infrastructure system. In these studies, an infrastructure system was modeled using edges and vertices. The edge represents components of an infrastructure system such as a

facility or a distribution element, and the vertex represents a connecting point which has perfect reliability. When two components such as a water pumping station and a water pipe are physically connected, the two edges, which represent the water pumping station and the water pipe, are connected at a vertex. Conversely, when two components (e.g., an electrical power substation and a water dam) are not physically connected, the two edges representing the two components do not share a vertex. Later, Yang and Shaoping (2003) also used a graph to model an infrastructure system although the methodology was not clearly mentioned.

Recently, Dueñas-Osario (2005), Dueñas-Osario et al. (2006a and 2006b) also modeled an infrastructure system using graph theory. In contrast with the earlier studies mentioned above, a vertex represented a facility such as an electrical power substation, water pumping station or a water storage tank, and an edge represented a distribution element such as a water pipe or an electrical power transmission line. When a distribution element and a facility are physically connected, the vertex and one end of the edge are connected. Compared with the modeling approach proposed by Satyanarayana and Wood (1985), Wagner et al. (1988a and 1988b) and Quimpo et al. (1997), the modeling approach proposed by Dueñas-Osario (2005), Dueñas-Osario et al. (2006a and 2006b) is more realistic since an infrastructure system in the real world is composed of vertices (facilities) and edges (distribution elements) in broad perspective.

(2) Assessing the serviceability of an infrastructure system

Seismic damage to a single building can be estimated from a fragility curve of the building and knowledge of the seismic intensity at the site of the building. Similarly, the

seismic damage to each facility comprising an infrastructure system, such as a water storage tank, an electrical power generating plant or an electrical power substation, can be assessed by an appropriate fragility curve and the seismic intensity at the site of the component. For a distribution element such as a water pipe, the pipe break density, which is defined as the number of pipe break per unit pipe length (e.g. 1,000 feet), is dependent on seismic intensity distributed over the length of the distribution element. Thus, the seismic damage level of components of an infrastructure system can be computed individually. However, the seismic damage level (or residual serviceability after an earthquake) of an entire infrastructure system cannot be computed simply from the fragility curves and seismic intensities which are used to evaluate the seismic damage to each component. For example, though a water pumping station may not be damaged after an earthquake, it may lose its function if water cannot be provided because water storage tanks and/or water pipes that supply the pump are damaged and lose their functions. Evaluating this type of failure (cascading failure) has been one of the main thrusts of the present study.

Many methodologies for the serviceability assessment of an infrastructure system have been proposed. Satyanarayana and Wood (1985), Wagner et al. (1988a and 1988b) and Quimpo et al. (1997) used the techniques of series reduction, parallel reduction and polygon-chain reduction. By applying these techniques, a subsystem, which is a portion of an entire model of an infrastructure system can be replaced a single component whose failure probability is same as the failure probability of the original subsystem. When a subsystem is modeled as a polygon, this also can be replaced by a pure series system or a single component, which is called the polygon-chain reduction (Satyanarayana and

Wood, 1985). By continuing the replacements, the entire model of an infrastructure system becomes a pure parallel system, a pure series system, or a single component which have the same reliability as that of an entire infrastructure system. Though this approach leads the correct serviceability of an infrastructure system, finding a polygon which can be replaced by a chain is very difficult and only one component can be analyzed at one time. Thus, the computation of the serviceability of an entire infrastructure system containing many components can be time-consuming and inefficient.

Pires et al. (1996) and Ang et al. (1996) assessed the serviceability of an infrastructure system using a matrix formulation of component connectivity. In this method, a coefficient $a_{i,j}$ of matrix A represents the connection between two components i and j. When two components i and j are physically and directly connected, $a_{i,j} = 1$; otherwise $a_{i,j} = 0$. An element $a^k_{i,j}$ of the matrix A^k, which is the matrix of A to the k^{th} power, represents that component i is connected with component j though the k-1 components that may exist between two components i and j. Thus, the connectivity matrix for the system, C, which is the sum of matrices A, A^2, … , A^n, where n is the number of components, represents whether an arbitrary pair of two components within the system is connected ($c_{i,j} \neq 0$) or disconnected ($c_{i,j} = 0$). In contrast to the polygon-chain reduction technique, this approach can analyze the serviceability of an entire infrastructure system at once, once the coefficients of matrix A are determined. However, the process must be applied many times to evaluate a reliable estimate of serviceability.

Kuwata and Takada (2003) evaluated the water availability at a hospital using a probabilistic approach. The probability of connectivity between the water reservoir and the hospital was determined as the product of failure probabilities of the water reservoir, water pipes connecting the reservoir and the hospital, and internal building utility systems, under the assumption that the three failure events are statistically independent. This approach can be useful if the connections among facilities and distribution elements are purely in series. Other cases were not discussed in their study.

In the graph theory approach of Dueñas-Osario et al (2005, 2006a and 2006b), when a component loses its functionality, the vertex or the edge is removed from the original graph which represents a non-damaged infrastructure system. The probability that a node is removed is computed using the fragility curve of a component, while the probability that an edge is removed is equal to the probability that a distribution element has at least one leakage or break. The serviceability ratio of the infrastructure system is defined as the connectivity loss, which is computed as the ratio of the number of paths between supply facilities and demand facilities within a damaged infrastructure system to the number of the paths within the same infrastructure system prior to damage. Following this approach, the infrastructure system can be modeled as a graph by simply replacing facilities and distribution elements by edges and nodes, respectively, of a graph. The shape of this graph directly reflects the shape of the infrastructure system. However, since the graph theory approach has not been commonly used in civil engineering, its results are difficult to integrate with the results of previous research.

Many studies which use computer applications have been proposed. However, the methodologies to analyze the connectivity were not described in detail (e.g., Chang et al., 1996; Shinozuka et al., 1998; Jin et al., 2002; Dong and Shinozuka, 2003).

(3) Evaluating effects of infrastructure interdependency

In addition to the fact that functions of components within an infrastructure system are dependent on each other, the functions of infrastructure systems are also interdependent. For example, electrical power is needed to operate a water distribution system properly, and water is needed to operate an electrical power generating plant to generate electrical power by watery vapor. To ignore such infrastructure interdependencies results in a non-conservative estimation of the serviceability of an infrastructure system.

Rinaldi et al. (2001), Peerenboom et al. (2002), Gillette et al. (2002), NERC (2004) and Fedora (2004) noted the importance of infrastructure interdependencies on economic, industrial and social activities. Rinaldi et al. (2001) and Peerenboom et al. (2002) classified infrastructure interdependencies based on relationships among infrastructure systems (the details will be discussed in Chapter 3). Chang et al. (1996) also noted the potential importance of infrastructure interdependency among the water distribution, the gas distribution and the electrical power transmission systems in Shelby County, TN, but did not determine the quantitative effects of infrastructure interdependency on serviceability. The research focusing on the quantitative effects of infrastructure interdependency on infrastructure system serviceability is limited.

The study by Robert (2004) is one of the first that attempted to assess network serviceability considering system interdependency effects directly. Interdependency among systems was modeled by direct links and indirect links. A direct link represents physical attachment of two facilities. Examples of direct links are water pipes and electrical power transmission lines. An indirect link represents a functional connection which "is not specifically planned or constructed but emerges from the dispersion of a substances coming from a lifeline network. This dispersion triggers a modification of the area in which other networks function, therefore creating a new link" (Robert, 2004). An example of an indirect link is the loss of function of a water pumping station due to electrical power unavailability. Though Robert's study recognizes the existence of infrastructure interaction effects and their importance when serviceability of a lifeline network is analyzed, it is applied to a hydroelectric power network, which is composed of a hydroelectric power generating station, a spillway, a dam, a storage basin and a river, and a power distribution network, which is composed of electrical power substations and transmission lines. The details of the methodology used to analyze the effect of infrastructure interdependencies were not reported.

In the graph theory approach of Dueñas-Osario et al. (2005, 2006a and 2006b), the probability that a node or an edge is removed is determined by not only the component fragility or the leakage or break ratio of a distribution element but also the probability that a facility did not receive commodities which are needed to maintain the function of the nodes or the edges. For example, the edge representing a water pumping station was removed when the electrical power was lost.

Many studies (e.g., Chang and Seligson et al., 1996; FEMA, 1997 and 2003; Rose, et al., 1997; Shinozuka, et al., 1997 and 1998) have considered financial losses incurred due to loss of serviceability arising from system interdependency effects using Input-Output (I-O) analysis (Leontief, 1951 and 1986; Haimes and Jiang, 2001; Haimes et al, 2005a and 2005b). This approach is necessary to compute the total monetary losses to industries damaged by an earthquake. However, none of the studies to date using I-O analysis have considered the additional serviceability loss due to infrastructure interdependency. Accordingly, such studies may underestimate the total monetary loss.

(4) Analysis of Uncertainty

The process of serviceability assessment of an infrastructure system involves numerous uncertainties. Earthquakes of sufficient magnitude to severely damage infrastructure systems are relatively infrequent. Data on performance of engineered systems are limited, mathematical regression models are used in lieu of physical models, and expert opinions substitute for data when empirical data are unavailable. For example, attenuation relationships that describe seismic intensities at a site in terms of magnitude and epicentral distance from the seismic source are computed from regression analysis of historical ground motion records, in which the mathematical form of the attenuation relationship is based on expert opinion (e.g., Boore, 1987 and 2003). The local soil amplification factors, the fragility curves of facilities and the leakage/break ratio of distribution elements are also evaluated by similar approaches. Thus, such mathematical relationships lead to estimates of mean or median values and uncertainties which reflect the deviation of real value from the estimates. Most studies presented

above did not consider or discuss such uncertainties. In addition, no study exists which considers the impact of spatial correlation of seismic intensities over a large area on the functioning of distributed networks within that area. The importance of spatially correlated seismic intensities and uncertainty modeling for network serviceability assessment is examined at length in Chapters 4, 6 and 7 of this dissertation.

2.2 Critical Appraisal of Existing Studies

The review of previous research studies of direct and indirect losses resulting from earthquake damage to civil infrastructure systems has identified the following research issues:

- Serviceability of infrastructure systems currently is measured without considering infrastructure interdependency effects in the most of existing studies. As a result, the estimate of the serviceability of an infrastructure system after an earthquake may be on the non-conservative side, predicting a shorter recovery time of damaged infrastructure and a lower monetary losses than would actually be the case.
- The uncertainty of seismic intensities is not considered in most existing research. Seismic intensities can deviate significantly from its mean or median value due to its natural uncertainty (aleatory uncertainty). Thus, neglecting the uncertainty in the seismic intensities fails to provide a proper context for decision making regarding infrastructure systems.
- Though the seismic intensities have been modeled as random variables in some existing research, the spatial correlation of seismic intensities over an urban area has not been considered. This disregard of the spatial correlation of seismic

intensities fails to model the stochastic field describing the seismic intensity properly, and may not capture the regional variation on infrastructure damage properly. This yields unexpected errors in the estimated residual serviceability of the networked system.

- The serviceability assessment of infrastructure systems has been addressed by a single seismic intensity attenuation equation, a single formula of local soil amplification factors and a single fragility curve of facilities comprising an infrastructure system. By neglecting the epistemic uncertainties due to selecting specific formulas or factors from many choices, the evaluated serviceability may not provide enough information for decision making.
- Most existing studies have been applied with a specific (scenario) earthquake which has low (but unknown) frequency. Thus, the serviceability of a damaged infrastructure system assessed on the basis of this scenario earthquake may not reflect the expected seismic hazard to the system. Such assessments may lead to costly design or retrofit strategies that provide excessive resistance or redundancy when they are not required.

In addition to these substantive concerns, some of the previous network analysis methodologies reviewed, e.g., serviceability assessment using matrix operations to identify cascading failures within a network, may be difficult to implement for practical systems. While such approaches, may determine the cascading failures correctly, the total computing time and cost might be a problem if a large and complicated infrastructure system were to be assessed. Computational efficiency is essential for practical infrastructure system network evaluation.

These research issues are addressed by the serviceability assessment methods introduced in the following chapters.

CHAPTER 3

MODELS OF INFRASTRUCTURE INTERDEPENDENCY

Civil infrastructure systems are highly inter-connected and each system requires support from other infrastructure systems to maintain its function. Recognizing such types of infrastructure interdependencies and types of failures is necessary to model infrastructure systems and to analyze effects of infrastructure interdependency on the reliability and serviceability of a networked system. In this chapter, the fundamental nature of the interrelationships between infrastructure systems is introduced, along with conceptual approaches to their analysis.

3.1 Mechanism of Infrastructure Interaction

Infrastructure systems are interdependent in various aspects. Rinaldi et al. (2001) classified the interdependency into four categories: physical, geographical, informational and logical.

The physical interdependency is defined as the situation where one infrastructure system needs commodities or outputs from other systems to maintain its function. For example, a pumping station may lose its function when an electrical power substation which supplies electrical power to the pumping station since electrical power is required to maintain the function of a pumping station.

The geographical interdependency among infrastructure systems is evident. For example, the function of a water pumping station in Shelby County, TN may be strongly

impacted by the failure of an electrical power substation in the same county, but little affected by the failure of an electrical power substation in California.

According to Rinaldi et al. (2001), the informational interdependency among infrastructure systems is defined where "the state of an infrastructure system depends on information transmitted through the information infrastructure." For example, systems that manage electrical power flow operate through internet systems, telecommunication networks or other cyber network systems. Logical interdependency is defined where "the state of one infrastructure system depends on the state of the other via a mechanism that is not a physical, cyber, or geographic connection." For example, increasing oil prices decrease purchasing power since people spend more for fuel. In this case, the petroleum and the financial infrastructures are logically connected. These latter two types of infrastructure interdependency are not considered in this study since the effects of the physical and geographical interdependency include the effects of the informational interdependency when seismic hazard is considered. Since serviceability of an infrastructure system after a seismic event is considered in this study, the logical interdependency is not of interest.

In order to better understand the vulnerability of interdependent networked systems, the nature of failures within these systems are classified into three categories: cascading failure, escalating failure and common cause failure (Rinaldi et al., 2001).

A cascading failure occurs when the failure or the malfunction of one facility in an infrastructure system causes the failure or the malfunction of another facility in the infrastructure system although the latter facility is not physically damaged. For example, an electrical power substation cannot perform its function when generating plants cannot

supply electrical power to the substation. This type of failure can be analyzed by checking the availability of commodities from supply facilities.

An escalating failure arises when the malfunction or the failure of a facility diminishes the function on another facility. For example, disconnection of telecommunication networks or internet systems increases the time required to eliminate traffic congestion due to a car accident since the arrival of police officers and rescue crews at the site of the accident may be delayed due to lack of information. This type of component failure may be included in the cascading failure when a seismic demand is considered.

A common cause failure occurs when two or more components fail at the same time due to an event that impacts both components. For example, since facilities which are located close each other both may be exposed to similar seismic intensities, such facilities may be damaged at the same time if their seismic resistances are similar. Analyzing this type of failure requires that spatial correlation of seismic intensities be modeled accurately.

3.2 System Reliability Theory

Civil infrastructure systems are modeled as consisting of facilities and distributing elements. A water distribution system consists of dams, storage tanks and pumping stations as facilities and pipes as distributing element. An electrical power transmission system involves generating plants, substations and transmission towers as facilities and transmission lines as distributing elements. The performance of such systems can be assessed using methods of system reliability analysis.

System reliability theory is used in a variety of engineering fields and has a central role in risk analysis, quality management, maintenance and operation optimization and engineering design. As a tool for evaluating infrastructure systems, system reliability theory can be used to assess potential risks of natural hazards for infrastructure systems, to improve redundancy of infrastructure systems efficiently, to create maintenance plans at lower cost and higher efficiency, and to design the layout of facilities and distributing elements of infrastructure systems.

There are several approaches to quantifying the failure modes of an infrastructure system. These include fault tree models, reliability block diagrams and event tree analysis.

A fault tree model is a logic diagram that displays the interrelationships between a potential critical event (accident) in a system and the causes for this event (Rausand and Hoyland, 2004). The fault tree model can deal with both qualitative and quantitative analysis. The primary (or top) failure event of interest is situated at the top of the fault tree; below the top event are located, in turn, the immediate causal failure events. The primary failure event and the immediate causal failure events are connected through logic gates (AND or OR gates). The process is continued until the top event is expressed as a combination of basic events which are located at the bottom of the fault tree, so the structure of the fault tree is deductive in nature. In a fault tree model, all failure events from primary to basic failure events are binary in nature: occurs or does not occur, fails or does not fail, etc. Events with intermediate states cannot be analyzed (U.S. Nuclear Regulatory Commission, 1981; Ang and Tang, 1984; Rausand and Hoyland, 2004).

Figure 3-3 illustrate three simple fault tree models. In Figure 3-1, the top event is the result of three basic events 1-3, linked through an OR-gate. Thus, the top event occurs if any of the basic events occur. In Figure 3-2, the top event is the result of three basic events 1-3, linked through an AND-gate. Here, the top event occurs only if all three basic events occur at the same time. In Figure 3-3, the top event is the result of basic event 1 or a sub-event, while the sub-event requires the occurrence of both events 2 and 3.

Quantitative analysis of a fault tree model requires the identification of minimal cut-sets or minimal path-sets after the fault tree is constructed. A minimal cut-set is defined as an essential set of basic events whose occurrence must result in occurrence of the top event. A minimal path-set is defined as an essential set of basic events whose non-occurrence results in the non-occurrence of the top event (Rausand and Hoyland, 2004). Table 3-1 describes the minimal path-sets and the minimal cut-sets of three events shown in Figures 3.1 - 3.3. In Table 3-1, $\{\bullet\}$ represents a set of basic events. For example, the occurrence of any of the basic events 1, 2 or 3 results in the occurrence of top event A, thus, each basic event 1, 2 or 3 is a minimal cut-set of event A. On the other hand, top event A does not occur when basic events 1, 2 or 3 does not occur at the same time, which is a minimal path-set of event A.

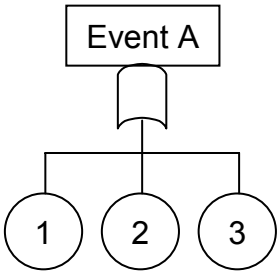

Figure 3-1 Fault tree model using OR gate

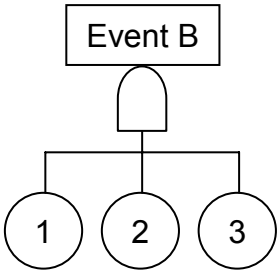

Figure 3-2 Fault tree model using AND gate

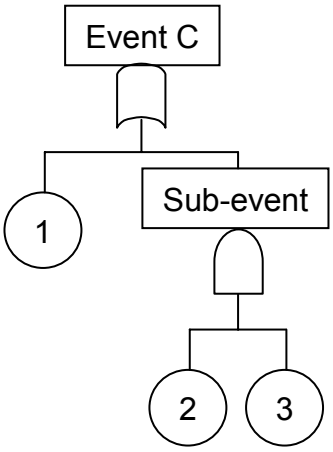

Figure 3-3 Fault tree model using OR and AND gates

Table 3-1 Minimal cut-sets and minimal path-sets of three events A, B and C

	Event A	Event B	Event C
Minimal cut-set	{1} {2} {3}	{1,2,3}	{1} {2,3}
Minimal path-set	$\{\overline{1},\overline{2},\overline{3}\}$	$\{\overline{1}\}\{\overline{2}\}\{\overline{3}\}$	$\{\overline{1},\overline{2}\}\{\overline{1},\overline{3}\}$

In a reliability block diagram, the function of a system is illustrated as a logical combination of functioning components which are not repairable. Thus, a reliability block diagram is the graphical representation of how components are connected in such a way as to comprise a system. The combinations of functioning components in a reliability block diagram are classified into series and parallel structures. A series system is defined as a system whose components are linked in a single row. Thus, a series system maintains its function only when all components maintain their function. A parallel system is defined as a system whose components cannot be linked together in a row. Thus, a parallel system maintains its function as long as at least one component maintains its function (Rausand and Hoyland, 2004).

For quantitative analysis of a system described by a reliability block diagram, a structure function must be constructed. A structure function $\phi(x)$ is a binary function assumed to take on values 1 if the system is functioning and 0 if the system is in a failed state. The structure function is a function of a state vector (x), whose coefficients (x_i) are binary variables representing the two states of the components that comprise the system; 1 if component *i* is functioning, 0 if component *i* is in a failed state. The structure function of a series system is expressed as a product of all coefficients in a state vector (Eq.3-1). The structure function of a parallel system is expressed as the maximum of the coefficients of the state vector (Eq.3-2) (Ross, 2003; Rausand and Hoyland, 2004).

$$\phi(x) = \prod_{i=1}^{n} x_i \tag{3-1}$$

$$\phi(x) = \max_{i=1}^{n}(x_i) \tag{3-2}$$

The failure probability of a system can be calculated (at least conceptually) when failure probabilities of the components of the system can be determined. When failure events of components are statistically independent, the failure probability of a series system is computed as Equation 3-3 and the failure probability of a parallel system is computed as Equation 3-4.

$$P_f = 1 - \prod_{i=1}^{n} \left[1 - P_{f_i}\right] \tag{3-3}$$

$$P_f = \prod_{i=1}^{n} P_{f_i} \tag{3-4}$$

If the component failures are not statistically independent, the failure probability of a system can be computed from an integral of the joint probability density function describing the random variables over the domain defined by the limit state function of a system failure (Thoft-Christensen and Baker, 1982; Ang and Tang, 1984; Thoft-Christensen and Muratsu, 1986; Melchers, 1999). Monte Carlo simulation may be used to perform this integral when the system behavior or limit state are complex or the component failure events are not statistically independent (Ang and Tang, 1984; Melchers, 1999).

Figures 3.4 - 3.6 illustrate three simple and typical reliability block diagrams. These diagrams represent the same events illustrated by the fault tree models in Figures 3.1 - 3.3. By determining that there is at least one connection between the two ends, the system is identified as being functioning. For example, when any one of the three components shown in Figure 3-4 fails, there is no connection between the ends, and the system fails. In Figure 3-5, the system loses its function only when all three components fail. In Figure 3-6, there is no connection between two ends when either component 1

fails or components 2 and 3 fail. The structure functions of these three systems are given by Eqs.3-5 to 3-7, respectively.

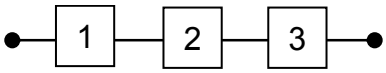

Figure 3-4 Reliability block diagram of a series system

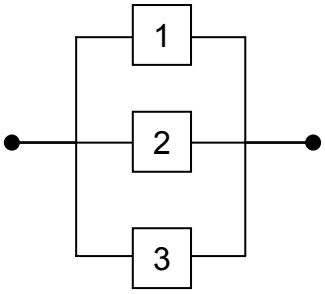

Figure 3-5 Reliability block diagram of a parallel system

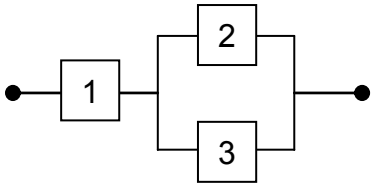

Figure 3-6 Reliability block diagram of a system with series and parallel structures

$$\phi(x) = x_1 \cdot x_2 \cdot x_3 \tag{3-5}$$

$$\phi(x) = 1 - (1 - x_1) \cdot (1 - x_2) \cdot (1 - x_3) \tag{3-6}$$

$$\phi(x) = 1 - (1 - x_1) \cdot (1 - x_2 \cdot x_3) \tag{3-7}$$

An initiating event generally leads to a sequence of other events. For example, when a building fire occurs (an initializing event), fire alarms may warn the building residents (one consequential event) or they may fail to operate (the second consequential event). If the fire alarms function, residents may either escape from the building safely or wait for firefighters to assist them in evacuation (third events following the preceding

second event). Such event progressions can be modeled by an event tree analysis. Each event in an event tree has two or more outcomes, and each outcome is conditioned on the occurrence of a previous event. Thus, the initiating event is connected inductively with the final outcomes through the sequences of events depicted in the event tree. Since each outcome has a probability of occurrence, the probability of each final outcome can be calculated by multiplying the conditional probabilities of the sequential events on the path from the initiating event to the final outcome. Event trees also can be used to describe the multiplicity of choices involved in decision analysis, in which case the event tree model is called a decision tree model. Both models are used to compute the probability of occurrence of final outcomes and their consequences (Ang and Tang, 1984; Rausand and Hoyland, 2004).

An example of an event tree and its probabilistic analysis is illustrated in Figure 3-7. Here, the initiating event occurs with probability r_1. Once the initiating event occurs, the second event occurs. The outcomes of the second event are True or False. The probability that the second event is True is $r_{2,T}$, and the probability that the it outputs False is $r_{2,F}$. If the second event results in False, no other events occur and the final outcome 7 is evaluated at the probability of $r_1 \cdot r_{2,T}$. If the second event results in True, the third event occurs and N outcomes (Choice 1, Choice 2, ⋯, Choice N) are possible with the probabilities of $r_{3,1}$, $r_{3,2}$ and $r_{3,N}$, respectively. By continuing the procedure, the probability of each outcome is evaluated. For example, the probability of Outcome 1 is computed as $r_{O1} = r_1 \cdot r_{2,T} \cdot r_{3,1} \cdots r_{N,A}$. By comparing the probabilities of final outcomes,

the most probable outcome can be identified. Furthermore, if the outcomes are expenses or casualties, the consequences can be measured by the weighted average,

$$r_{O1} \cdot Outcome1 + r_{O2} \cdot Outcome2 + \cdots + r_{O7} \cdot Outcome7 \tag{3-8}$$

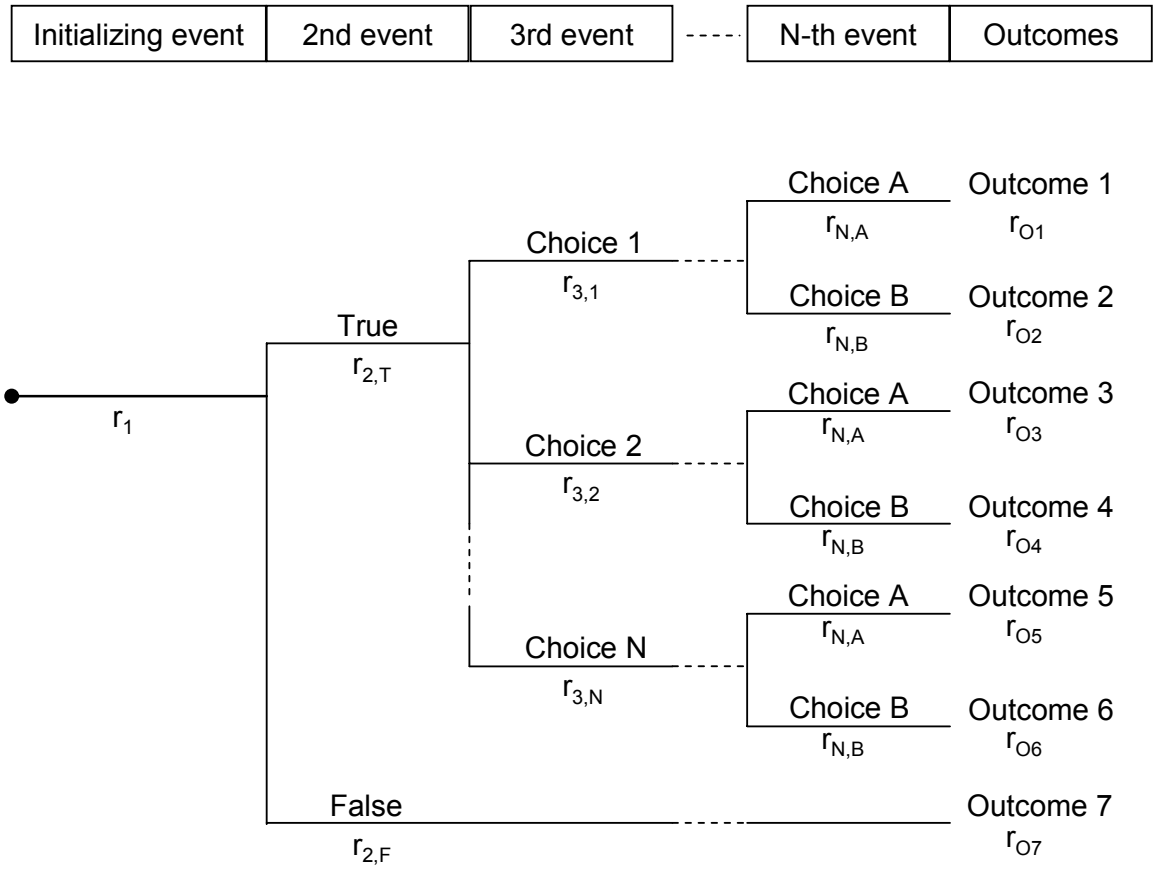

Figure 3-7 An event tree model

3.3 Network Accessibility Assessment

Most civil infrastructure systems are designed to be redundant to maintain their function after a natural or man-made hazard. The number of components, topology of the network, and system redundancy make the infrastructure system complex to analyze. While a simple infrastructure system (or facility within it) can be modeled by a fault tree

model or reliability block diagram and can be analyzed as to whether it has or has not failed after the occurrence of a hazard (e.g. Figures 3.1 - 3.6), a complicated infrastructure system cannot be easily modeled by fault tree models or reliability block diagrams. Furthermore, a highly redundant infrastructure system with high redundancy can have many failure modes.

As noted previously, a facility within an infrastructure system frequently cannot maintain its function without resources or service from other systems (infrastructure interdependency). Furthermore, a facility sometimes cannot function following the occurrence of a hazard even though the facility itself is not physically damaged because other components of the infrastructure system are unable to deliver service to the facility (cascading failure). The interdependencies and the cascading failure can be identified by investigating the accessibility of demand facilities from supply facilities. In other words, supply facilities, such as water storage tanks or electrical power generating plants, provide commodities such as water or electrical power, to demand facilities, such as water distribution nodes or electrical power substations which need the commodities to maintain their function.

One approach to the accessibility assessment is furnished by classical probability theory. For example, Yan and Shaoping (2003) expressed the accessibility of a facility as a union of all path-sets from a supply facility to the facility evaluated. In this approach, all path-sets need to be identified in advance, and the approach must be applied to every facility comprising the infrastructure system one-by-one. In a somewhat different approach, Ang et al. (1996) and Pires et al (1996) used an adjacency matrix. In this approach, the accessibility of all possible pairs of facilities composing an infrastructure

system can be analyzed at once. While this approach is conceptually straightforward, computing time is a significant barrier when the infrastructure system analyzed has many facilities and distributing elements because the size of the adjacency matrix becomes very large.

When modeling an infrastructure system, the directed path through a network between two facilities with a total length that is the minimum is called the shortest path. Algorithms that can identify these shortest paths, which is called the shortest path algorithm, can overcome the difficulties of the two methods above.

Several shortest path algorithms have been proposed in the operations research field. Dijkstra's algorithm (Dijkstra, 1956) and the Floyd-Warshall algorithm (Floyd, 1962; Warshall, 1962) both have been widely used are simple to program. Details of Dijkstra's algorithm can be found in, for instance, Rardin (1997), Kreyszig (1998) or Papadimitriou and Steiglitz (1998). The Floyd-Warshall algorithm has an important advantage over the Dijkstra's algorithm, in that it can find the shortest paths between all pairs of nodes simultaneously. In contrast, Dijkstra's algorithm only can find them one-by-one. Thus, the Floyd-Warshall algorithm is introduced here as the approach to evaluate network accessibility.

In The Floyd-Warshall algorithm (Floyd, 1962; Warshall, 1962), when one facility cannot access another facility, the path length is set equal to infinity (in computation, a very large number), that is, the commodity is prevented from being conveyed between these facilities. The flow direction of the commodity in the distributing element is a key ingredient of accessibility assessment. The Floyd-Warshall algorithm is illustrated as follows:

Input: An n-by-n matrix, where a coefficient $c_{i,j}$ represents the length of distributing element delivering commodities from facility i to facility j.

Output: An n-by-n matrix, where a coefficients $d_{i,j}$ reprensents the length of the shortest path from facility i to facility j.

Begin: for all i except i=j do $d_{i,j}=c_{i,j}$

for i=1,…,n do $d_{i,i}=\infty$

for j=1,…,n do

for i=1,…,n except i=j do

for k=1,…,n except k=j do

$d_{i,k}=\min\{ d_{i,k} , d_{i,j} + d_{j,k} \}$

for all i do $d_{i,i}=0$

End

Figure 3-8 Floyd-Warshall algorithm (modified from Papadimitriou and Steiglitz (1998)

To illustrate the use of the Floyd-Warshall algorithm in finding the shortest paths between pairs of facilities, the simple network model shown in Figure 3-9 is analyzed. Each arrow represents the flow direction of commodities. The number shown with each arrow represents the length of the path between the nodes.

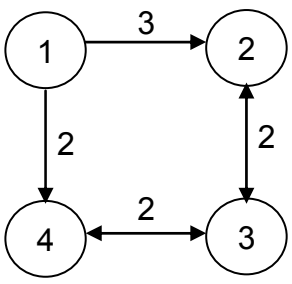

Figure 3-9 A sample network model

The matrix whose coefficients represent the lengths of the paths directly connecting two adjacent nodes are shown as matrix C in Figure 3-10. In this matrix, a coefficient $c_{i,j}$ represents the distance from node i to node j. Since the distance from node i to node i is always 0, the diagonal coefficients are always 0. Infinity (∞) represents two nodes that are not directly connected. (In the computation, a very large number is used instead of ∞.) Since flow directions represented by arrows in Figure 3-9 are considered, the matrix C is not necessarily a diagonal matrix.

$$C = \begin{pmatrix} 0 & 3 & \infty & 2 \\ \infty & 0 & 2 & \infty \\ \infty & 2 & 0 & 2 \\ \infty & \infty & 2 & 0 \end{pmatrix}$$

Figure 3-10 Matrix representing direct path lengths

Before looping with respect to j, distance matrix C is initialized as $D_{j=1}$ by replacing the diagonal coefficients 0 with ∞, as shown in Figure 3-11. The successive stages of the matrix D corresponding to *j* are shown in Figure 3-11.

$$D_{j=1} = \begin{pmatrix} \infty & 3 & \infty & 2 \\ \infty & \infty & 2 & \infty \\ \infty & 2 & \infty & 2 \\ \infty & \infty & 2 & \infty \end{pmatrix} \qquad D_{j=2} = \begin{pmatrix} \infty & 3 & 5 & 2 \\ \infty & \infty & 2 & \infty \\ \infty & 2 & \infty & 2 \\ \infty & \infty & 2 & \infty \end{pmatrix}$$

$$D_{j=3} = \begin{pmatrix} \infty & 3 & 5 & 2 \\ \infty & \infty & 2 & 4 \\ \infty & 2 & \infty & 2 \\ \infty & 4 & 2 & \infty \end{pmatrix} \qquad D_{j=4} = \begin{pmatrix} \infty & 3 & 4 & 2 \\ \infty & \infty & 2 & 4 \\ \infty & 2 & \infty & 2 \\ \infty & 4 & 2 & \infty \end{pmatrix}$$

Figure 3-11 Successive stages of distance matrix D

When j = 2 and i = 1, the coefficients in the first row of $D_{j=2}$ in Figure 3-11 are determined as follows;

for j=2 do

for i=1 do

for k=1

$d_{1,1} = \min\{ d_{1,1} , d_{1,2} + d_{2,1} \}$

$= \min\{ \infty , 3 + \infty\}$

$= \underline{\infty}$

for k=2 skipped since k=j

$d_{1,2} = \underline{3}$

for k=3

$d_{1,3} = \min\{ d_{1,3} , d_{1,2} + d_{2,3} \}$

$= \min\{ \infty , 3 + 2\}$

$= \underline{5}$

for k=4

$d_{1,4} = \min\{ d_{1,4} , d_{1,2} + d_{2,4} \}$

$= \min\{ 2 , 3 + \infty\}$

$= \underline{2}$

Figure 3-12 Floyd-Warshall algorithm solution when j=2 and i=1

$$D = \begin{pmatrix} 0 & 3 & 4 & 2 \\ \infty & 0 & 2 & 4 \\ \infty & 2 & 0 & 2 \\ \infty & 4 & 2 & 0 \end{pmatrix}$$

Figure 3-13 Matrix representing the shortest path lengths

After looping the steps to find the shortest path with respect to j, all diagonal coefficients ∞ are reset equal to 0. Then, the shortest path matrix D in Figure 3-13 is obtained. In this matrix, a coefficient represents the shortest path length from one node to the other node. For example, coefficient $d_{1,3}=4$ means the shortest path from node 1 to node 3 is 4. On the other hand, $d_{3,1}=\infty$ represents that node 1 is not accessible from node 3. As shown in Figure 3-8, the Floyd-Warshall algorithm required $n \cdot (n-1)^2$ iterations to find the shortest path of all pairs of nodes.

3.4 Summary

In this chapter, the mechanisms of infrastructure interdependency are illustrated. Then, the fundamental methods of networked systems, which properly model the effects of infrastructure interaction and cascading failure, are introduced with simple illustrations. Lastly, the Floyd-Warshall algorithm is introduced as a method for identifying the shortest paths through an infrastructure network, and the computational approach to evaluate the accessibility between facilities is represented with a simple example. The techniques and algorithms illustrated in this chapter are used to the proposed methodology of serviceability assessment of a civil infrastructure system in the following chapters.

CHAPTER 4

CHARACTERIZING SEISMIC DEMAND ON INFRASTRUCTURE SYSTEMS

Earthquakes have regional characteristics: epicenters, magnitudes, seismic wave propagation characteristics and ground motions at specific sites. For structural design of new facilities and estimating damage to existing facilities, capturing these regional characteristics is important.

This chapter introduces fundamental characteristics and mathematical models of regional earthquake characteristics in the Central and Eastern United States (CEUS), including earthquake sources, attenuation relationships, ground motion amplifications due to local soil characteristics, and spatial correlation of ground motions. Two methods for specifying seismic hazard are introduced: probabilistic seismic hazard analysis (PSHA) and scenario earthquake (SE) based seismic hazard analysis. The characterization of seismic hazard in this Chapter will be used subsequently to compute seismic intensities such as peak ground acceleration (PGA) and peak ground velocity (PGV) at sites of facilities and distribution elements comprising infrastructure systems after properly selected scenario earthquakes.

4.1 Seismic Hazard

According to Boore (1987 and 2003), the spectrum of ground motion at a site can be evaluated from four ingredients: earthquake source (E), path (P), site (G) and type of motion (I) as follows (see Figure 4-1):

$$Y(M_0, R, f) = E(M_0, f) \cdot P(R, f) \cdot G(f) \cdot I(f) \qquad (4\text{-}1)$$

where M_0 is the seismic moment which is related to the moment magnitude of the earthquake, R is the distance from the source to the site and f is the frequency. The shape and the amplitude of the source spectrum $E(M_0, f)$ are specified from a single corner or double corner frequency spectrum and earthquake size. The path effect spectrum $P(R, f)$ is determined from the geometrical spreading of seismic waves and the epicentral distance to the site. The site effect spectrum $G(f)$ is determined from the local soil condition at the site. Finally, $I(f)$ is used to model the particular local ground motion evaluated from the other three spectra (Boore, 1987 and 2003; Fernandez and Rix, 2006).

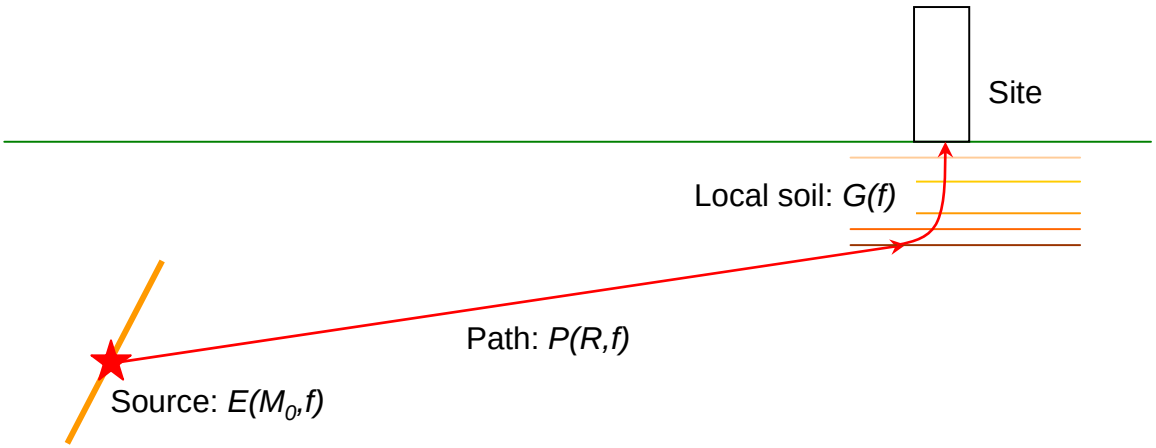

Figure 4-1 Seismic wave path from source to site (modified from Kramer, 1996)

From geological information and historical seismicity, seismic intensities at a site are determined using the following three factors: earthquake sources as a function of earthquake magnitude, attenuation relationships as a function of earthquake magnitude and epicentral distance to the site, and local soil amplification as a function of local soil

condition and seismic intensity at the site. In addition, spatial correlation of seismic intensities is an important factor when analyzing response of an infrastructure system whose facilities and distribution elements are distributed over a wide area.

4.1.1 Earthquake Source

The earthquake source term depends on location of the earthquake epicenter and magnitude. The geographical distribution of epicenters is evaluated from earthquake records and fault locations. The recurrence of an earthquake with a certain magnitude level in a source zone is estimated by the Gutenberg-Richter recurrence law or the bounded Gutenberg-Richter recurrence law (Gutenberg and Richter, 1944; Kramer, 1996).

The Gutenberg-Richter recurrence law models a mean annual frequency of an earthquake whose magnitude is more than m (Kramer, 1996) as follows:

$$\begin{aligned} \lambda_m &= 10^{a-b\cdot m} \\ &= \exp(\alpha - \beta \cdot m) \end{aligned} \tag{4-2}$$

where $\alpha = \ln(10)\cdot a$ and $\beta = \ln(10)\cdot b$. The Gutenberg-Richter recurrence law implies that earthquake magnitudes are exponentially distributed when the range of possible earthquakes in large area are considered. The probability density function of magnitude M for the Gutenberg-Richter recurrence law is expressed as follows:

$$f_M(m) = \beta \cdot \exp(-\beta \cdot m) \tag{4-3}$$

The Gutenberg-Richter recurrence law often is bounded to capture the maximum event believed possible at a site or the minimum event of engineering significance. In this law, the distribution of magnitudes has a maximum (m_{max}), which is determined from

historical or geological evidence. According to Frankel et al. (1996 and 2002), the maximum magnitude is 7.5 for the CEUS. For engineering purposes, a lower threshold magnitude (m_0) is also implemented, which is defined as the magnitude of earthquake (typically a value between 4.0 and 5.0) below which significant damage is unlikely to occur (McGuire and Arabasz, 1990; Kramer, 1996). By considering both the lower threshold magnitude and the maximum magnitude, the mean annual rate of exceedance of an earthquake of magnitude is:

$$\lambda_m = \nu \cdot \frac{\exp[-\beta(m - m_0)] - \exp[-\beta(m_{\max} - m_0)]}{1 - \exp[-\beta(m_{\max} - m_0)]} \tag{4-4}$$

where $\nu = \exp(\alpha - \beta \cdot m_0)$ and $m_0 \le m \le m_{\max}$. The probability density function of magnitude for the bounded Gutenberg-Richter recurrence law is expressed as follows:

$$f_M(m) = \frac{\beta \cdot \exp[-\beta(m - m_0)]}{1 - \exp[-\beta(m_{\max} - m_0)]} \tag{4-5}$$

4.1.2 Ground Motion Attenuation

The decay in seismic waves due to the seismic wave path from source to site is represented by an attenuation relationship, which is determined from many records of measured ground motions from earthquakes occurring in geologically similar zones. Attenuation relationships typically describe a mean or median value of a local ground motion intensity measure (ground motion or spectral ordinate) as a function of the magnitude of an earthquake and the epicentral distance from the epicenter to the site evaluated. The uncertainty associated with these relationships is a major source of uncertainty in seismic risk assessment of civil infrastructure facilities. Several

attenuation relationships for estimating ground motions in the CEUS are available, as described below.

Toro and McGuire (1987) developed attenuation relationships for PGA, PGV and spectral velocities based on historical records and a random vibration model proposed by Hanks and McGuire (1981). These attenuation relationships for PGA and PGV on rock are:

$$\ln\left(PGA_{Toro\&McGuire(1987)}\right) = 2.424 + 0.982 \cdot Mw - 1.004 \cdot \ln(R) - 0.00468 \cdot R \tag{4-6}$$

$$\ln\left(PGV_{Toro\&McGuire(1987)}\right) = -1.717 + 1.069 \cdot Mw - 1.000 \cdot \ln(R) - 0.00391 \cdot R \tag{4-7}$$

where M_w is moment magnitude and R is an epicentral distance. Atkinson and Boore (1990) proposed attenuation relationships for PGA and PGV, and spectral accelerations on hard rock which were derived from an empirically based stochastic ground motion model (Eq.4-1). The relationships for PGA and PGV are:

$$\log_{10}\left(PGA_{Atkinson\&Boore(1995)}\right) = 3.79 + 0.298 \cdot (Mw - 6) - 0.0536 \cdot (Mw - 6)^2 - \log_{10}(R) - 0.00135R \tag{4-8}$$

$$\log_{10}\left(PGV_{Atkinson\&Boore(1995)}\right) = 2.04 + 0.422 \cdot (Mw - 6) - 0.0373 \cdot (Mw - 6)^2 - \log_{10}(R) \tag{4-9}$$

Hwang and Huo (1997) also developed attenuation relationships for PGA and spectral accelerations based on historical records, random vibration theory and a stochastic ground motion model (Eq.4-1), resulting in:

$$\ln\left(PGA_{Hwang(1997)}\right) = -2.904 + 0.926 \cdot Mw - 1.271 \cdot \ln\left(R + 0.06 \cdot e^{0.7 \cdot Mw}\right) - 0.00302 \cdot R \tag{4-10}$$

Toro et al. (1997) proposed the following attenuation relationships for PGA and spectral accelerations on rock based on the predictions of a stochastic ground motion model (Eq.4-1) and ground motion records:

$$\ln\left(PGA_{Toro(1997)}\right) = 2.2 + 0.81(Mw - 6) - 1.27 \cdot \ln\left(\sqrt{R^2 + 9.3^2}\right) - (1.16 - 1.27) \cdot \max\left\{0, \ln\left(\frac{\sqrt{R^2 + 9.3^2}}{100}\right)\right\} - 0.0021 \cdot \sqrt{R^2 + 9.3^2} + \ln(1.52) \tag{4-11}$$

Toro (2003) later modified this relationship by including it as one of a weighted average of three attenuation relationships. The proposed attenuation for PGA on rock is as follows:

$$\ln\left(PGA_{Toro(2002)}\right) = 0.4 \cdot f_1 + 0.4 \cdot f_2 + 0.2 \cdot f_3$$

$$\ln(f_1) = 2.2 + 0.81(Mw - 6) - 1.27 \cdot \ln\left(\sqrt{R^2 + 9.3^2 \cdot e^{(-1.25+0.227Mw)^2}}\right) - (1.16 - 1.27) \cdot \max\left\{0, \ln\left(\frac{\sqrt{R^2 + 9.3^2 \cdot e^{(-1.25+0.227Mw)^2}}}{100}\right)\right\} - 0.0021 \cdot \sqrt{R^2 + 9.3^2 \cdot e^{(-1.25+0.227Mw)^2}} + \ln(1.52)$$

$$\ln(f_2) = 2.2 + 0.81(Mw - 6) - 1.27 \cdot \ln\left(R + 0.0089 \cdot e^{0.6 \cdot Mw}\right) - (1.16 - 1.27) \cdot \max\left\{0, \ln\left(\frac{R + 0.0089 \cdot e^{0.6 \cdot Mw}}{100}\right)\right\} - 0.0021 \cdot R + 0.0089 \cdot e^{0.6 \cdot Mw} + \ln(1.52)$$

$$\ln(f_3) = 2.2 + 0.81(Mw - 6) - 1.27 \cdot \ln\left(\sqrt{R^2 + 9.3^2}\right) - (1.16 - 1.27) \cdot \max\left\{0, \ln\left(\frac{\sqrt{R^2 + 9.3^2}}{100}\right)\right\} - 0.0021 \cdot \sqrt{R^2 + 9.3^2} + \ln(1.52)$$

(4-12)

Finally, the attenuations of PGA and spectral accelerations derived by Campbell (2003) employed a hybrid empirical method which includes the stochastic ground motion model (Eq.4-1). The attenuation relationship is bounded at epicentral distances of 70km and 130km considering the effect of the Mohorovicic discontinuity (Kramer, 1996):

$$\ln\left(PGA_{Campbell(2003)}\right) = 0.0305 + 0.663 \cdot Mw - 0.0427 \cdot (8.5 - Mw)^2 - 1.591 \cdot \ln(R) + (-0.00428 + 0.000483 \cdot Mw) \cdot R + f$$

$$f = \begin{cases} 0 & R \le 70km \\ 0.683 \cdot \ln\left(\frac{R}{70}\right) & 70km < R \le 130km \\ 0.683 \cdot \ln\left(\frac{R}{70}\right) + 0.416 \cdot \ln\left(\frac{R}{130}\right) & 130km < R \end{cases}$$

(4-13)

The six attenuation relationships for PGA and the two attenuation relationships for PGV shown above are plotted in Figures 4.2 and 4.3 for M_w=7.7. Each attenuation relationship leads the median values of PGA or PGV at specific epicentral distances. The aleatory uncertainty, which is due to the shortage of knowledge or data and yields the deviation from the attenuation relationship, must be included, as described subsequently. Furthermore, the difference among the attenuation relationships leads an epistemic uncertainty, which is due to the differences in the modeling approaches on which the attenuation relationships are based. This epistemic uncertainty must also be evaluated properly, which is discussed in the following chapters.

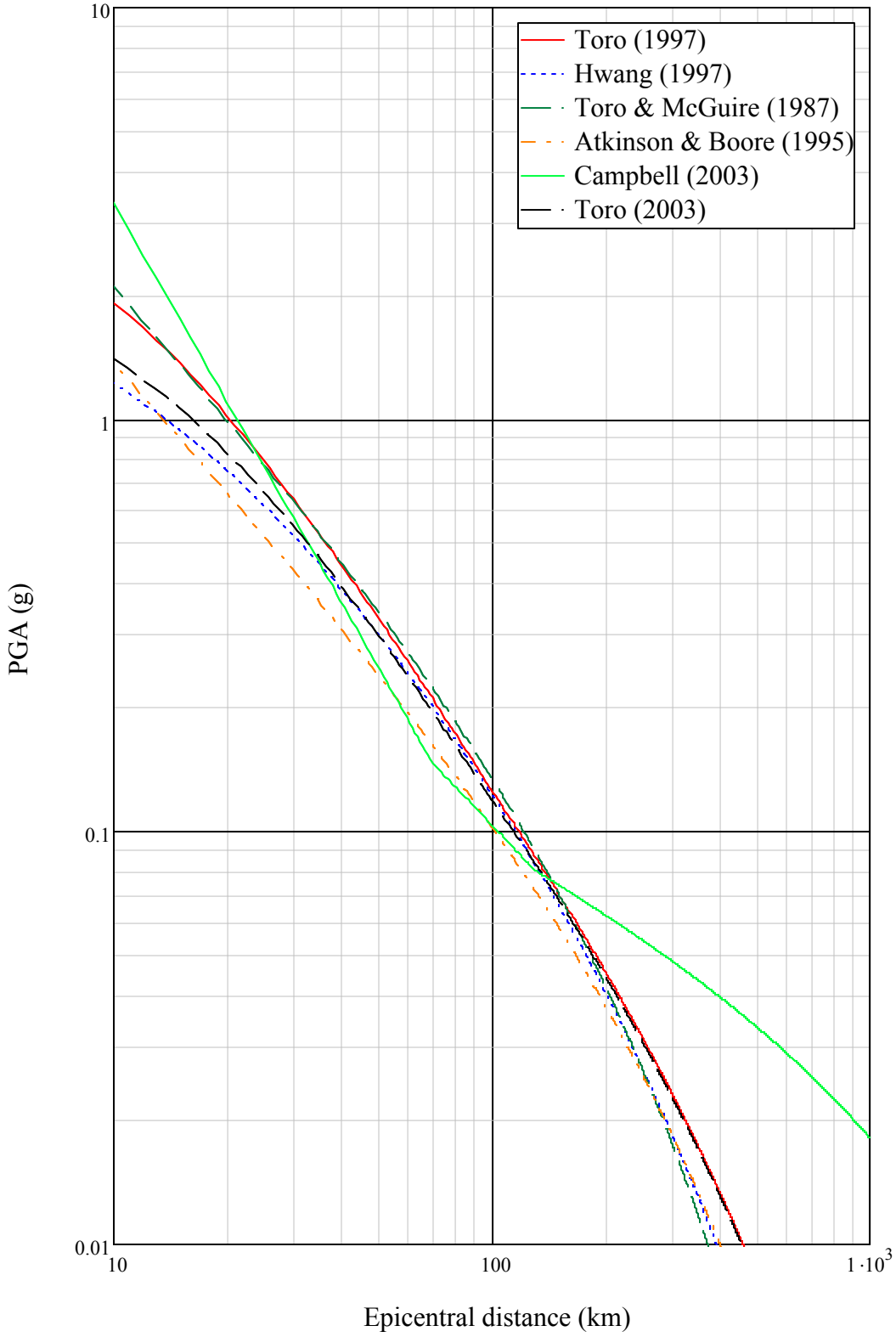

Figure 4-2 Comparison of attenuation relationships for PGA when M_w = 7.7

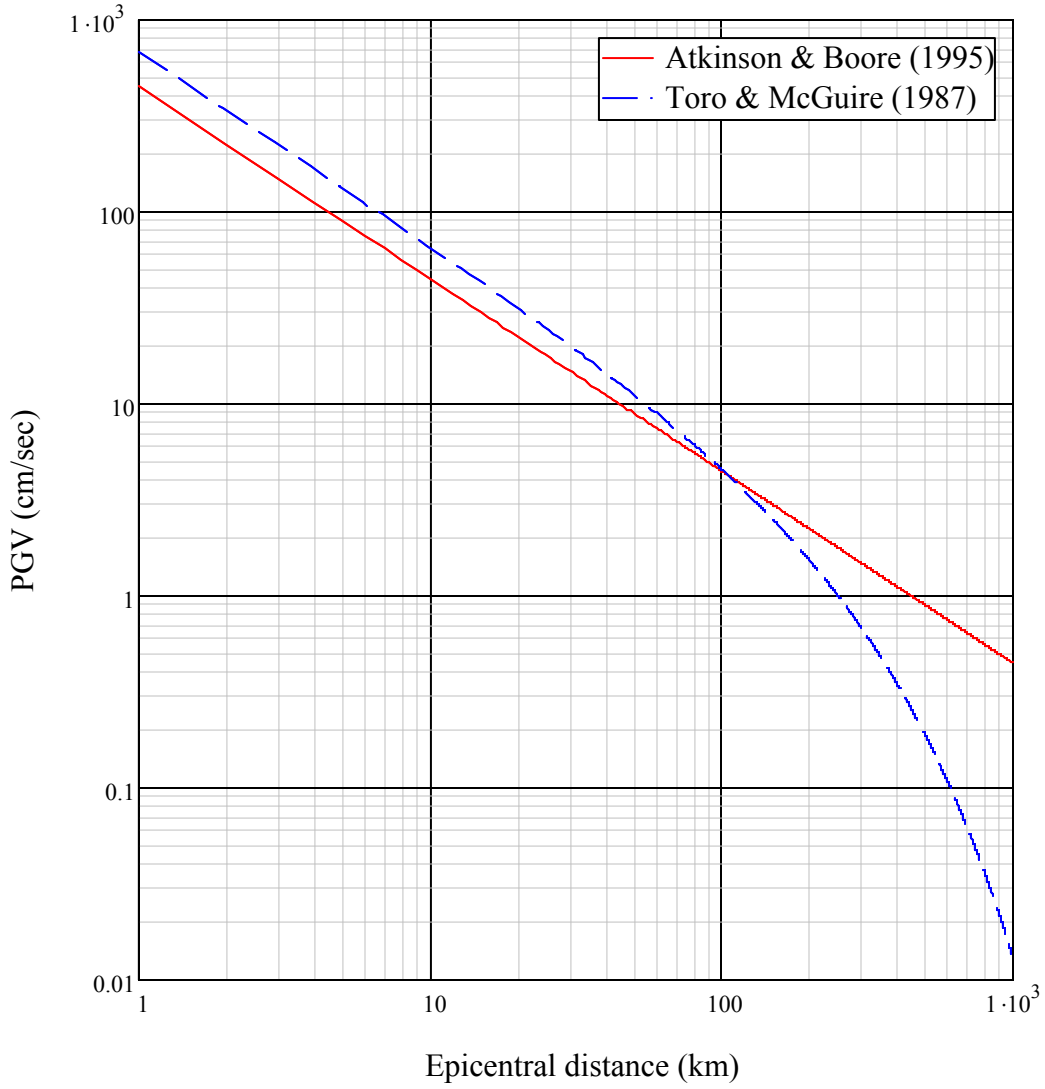

Figure 4-3 Comparison of attenuation relationships for PGV when M_w = 7.7

4.1.3 Local Soil Amplification

Ground motions are amplified or damped as a result of local soil conditions at a site. This effect is captured from knowledge of the profile of local soil layers, the wave velocity in each layer of local soil, the plasticity index (PI) of each soil layer, the over-consolidation ratio (OCR) of each soil layer and ground water level at the local site (Hwang et al, 1997; Dobry et al, 2000). The local amplification effects are represented

numerically by soil amplification factors with respect to the seismic intensity of interest, such as peak ground acceleration, peak ground acceleration, spectral acceleration or spectral velocity.

The local soil amplification factors proposed in the *2003 NEHRP Provisions* (FEMA, 2004) are widely used to estimate the amplification effects of ground motions due to local soil conditions. These factors are classified in six categories (A: hard rock, B: rock, C: dense soil, D: stiff soil, E: soft clay and F: soil requiring site-specific evaluation) mainly by shear wave velocity and standard penetration resistance. The local soil amplification factors proposed in the *2003 NEHRP Provisions* are determined mostly from the ground motion data in California (Hwang et al., 1997), and the characteristics of ground motions in the CEUS may not be similar to those in the Western United States (WUS) (Nuttli, 1981 and 1982). Local soil amplification factors for CEUS regions also have been proposed (e.g., Hwang et al., 1997), but fewer supporting research studies are available.

The local soil amplification factors for PGA and PGV proposed by the *2003 NEHRP Provisions* (FEMA, 2004) are shown in Tables 4-1 and 4-2, respectively. The local soil amplification factors from site category B (rock) to D (stiff soil) for PGA and PGV proposed by the *2003 NEHRP Provisions* (FEMA, 2004) and Hwang et al (1997) are compared in Figures 4-4 and 4-5.

Table 4-1 Short period amplification factor, F_A

Site Class	PGA≤0.25 g	PGA=0.5 g	PGA=0.75 g	PGA=1.00 g	PGA≥1.25 g
A	0.8	0.8	0.8	0.8	0.8
B	1.0	1.0	1.0	1.0	1.0
C	1.2	1.2	1.1	1.0	1.0
D	1.6	1.4	1.2	1.1	1.0
E	2.5	1.7	1.2	0.9	0.9

Table 4-2 1.0-second period amplification factor, F_V

Site Class	S_1≤0.1 g	S_1=0.2 g	S_1=0.3 g	S_1=0.4 g	S_1≥0.5 g
A	0.8	0.8	0.8	0.8	0.8
B	1.0	1.0	1.0	1.0	1.0
C	1.7	1.6	1.5	1.4	1.3
D	2.4	2.0	1.8	1.6	1.5
E	3.5	3.2	2.8	2.4	2.4

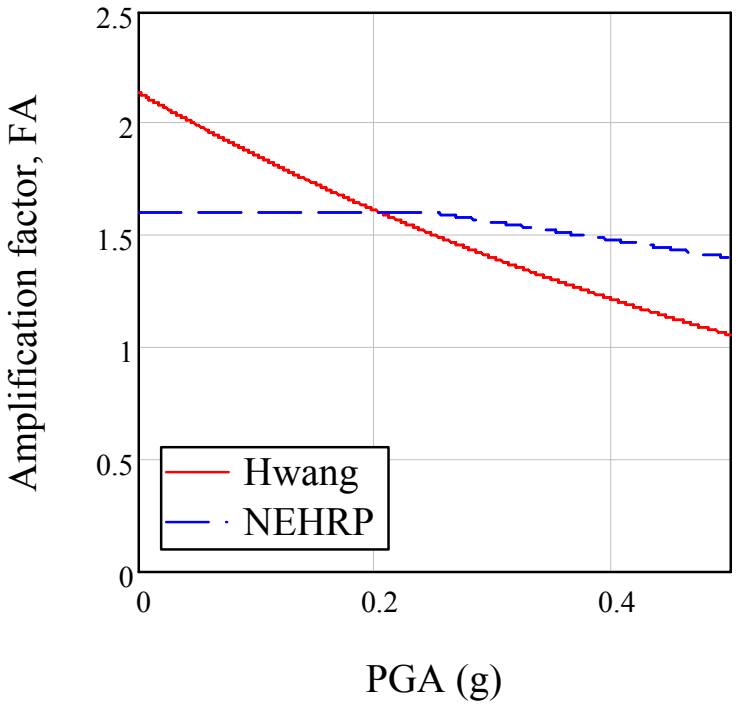

Figure 4-4 Comparison of amplification factors from site category B to D for PGA

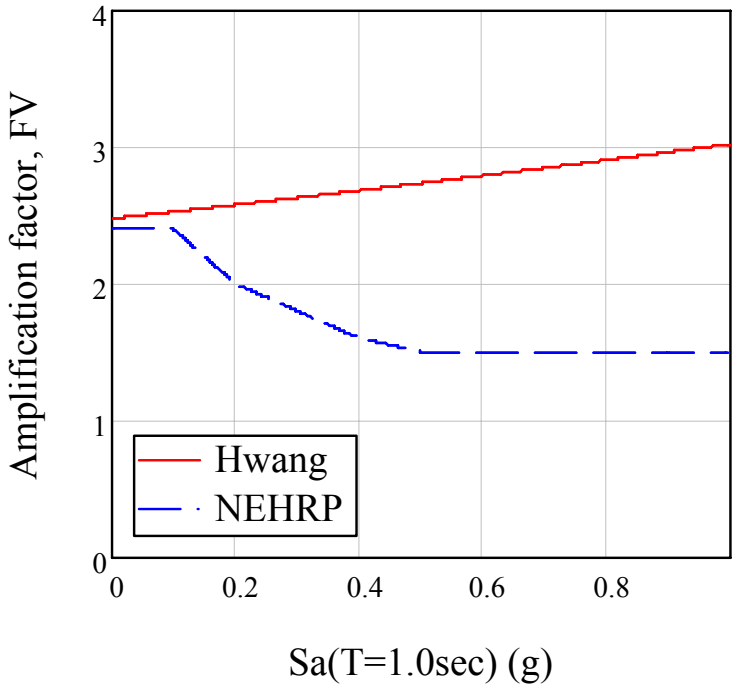

Figure 4-5 Comparison of amplification factors from site category B to D for PGV

According to the *2003 NEHRP Provisions* (FEMA, 2004), the local soil amplification factor for PGA is directly determined from Table 4-1 or from Figure 4-4. On the other hand, to determine the local soil amplification factor for PGV, spectral acceleration at 1.0 second (S_a(T=1.0sec)) is used. The following transformation equation is suggested in HAZUS Technical Manual (FEMA, 1997 and 2003).

$$PGV(in/\sec) = \frac{\left(\frac{386.4}{2\pi} \cdot S_a(T = 1.0\sec)\right)}{1.65} \qquad (4\text{-}14)$$

By multiplying the attenuated seismic intensities by the local soil amplification factors, the, seismic intensities at the surface soil can be computed as follows:

$$PGA_{surface} = PGA_{base} \cdot F_A \tag{4-15}$$

$$PGV_{surface} = PGV_{base} \cdot F_V \tag{4-16}$$

These ground motion intensities will be used subsequently in evaluating the intensities of ground motion impacting the water distribution system and the electrical power transmission system.

4.1.4 Correlation of Seismic Intensities

Since an infrastructure system is composed of many facilities and distributing elements which are distributed over a region, numerous seismic intensities scattered over that same region must be used for its serviceability assessment. When a single scenario earthquake is used for the serviceability assessment, the seismic intensities at sites of components are stochastically dependent to some degree due to the epicentral distances, local soil conditions and the proximity of components. In common engineering applications, such local variations in intensity are captured by the regional variation of first-order statistics of attenuation (e.g. mean or median). The covariance of seismic intensity (a second-order statistical property) is not considered in general.

The variance in seismic intensity is modeled by the standard error associated with the attenuation relationship. The stochastic dependence of the seismic intensities at different sites is modeled by the spatial correlation of seismic intensities (Wesson and Perkins, 2001; Shimomura and Takada, 2004; Takada and Shimomura, 2003 and 2004; Wang and Takada, 2005). Unlike the regional variation captured by the first-order statistics (mean or median) of attenuation, the covariance of seismic intensity models the statistical association (correlation) between intensities at two sites. This covariance

function clearly depends on the geographical distances between sites of components, and may depend on the magnitude and epicentral distances as well.

In the studies by Shimomura and Takada (2004), Takada and Shimomura (2003 and 2004) and Wang and Takada (2005), the spatial correlations of peak ground accelerations and peak ground velocities are described by exponential functions with respect to the geographical distance between two points of interest as follows:

$$R_{LL}\left(\left\|s_i - s_j\right\|\right) = \exp\left(-\frac{\left\|s_i - s_j\right\|}{b}\right) \tag{4-17}$$

$$L_{Xi} = \ln \varepsilon_{Xi} = \ln\left(\frac{X_i}{\overline{X_i}}\right) \tag{4-18}$$

where $R_{LL}(\bullet)$ is the auto-correlation function of L, $\|\bullet\|$ defines the distance between two sites, s_i is the geographical coordinate of a component i, b is a correlation distance which represents the strength of spatial correlation and whose unit is the same as $\|\bullet\|$, ε_{Xi} is the residual of seismic intensity at a site of a component i, X_i is the seismic intensity at the site of a component i, and $\overline{X_i}$ is the median seismic intensity at the site of a component i which is computed from an attenuation relationship. The studies by Shimomura and Takada (2004), Takada and Shimomura (2003 and 2004) and Wang and Takada (2005) using the ground motion records of six earthquakes that have occurred in Japan and Taiwan revealed that correlation distances b typically are about 20 to 30 km for PGA and about 20 to 40 km for PGV.

4.2 Probabilistic Seismic Hazard Analysis

For the seismic hazard analysis, earthquake sources with the potential to affect the sites, seismic wave path from the sources to the sites and local soil conditions of the sites need to be evaluated. In general, the site may be affected by a number of seismic sources and the magnitudes of earthquakes from each seismic source are not deterministic. A probabilistic seismic hazard analysis (PSHA) determines the aggregated effect of the range of possible earthquakes in seismic source zones that are in proximity to a site, weighted by the probability of occurrence of each earthquake (McGuire, 1995; Kramer, 1996). The annual frequency of earthquakes whose seismic intensities at a site exceed a certain value is evaluated as follows:

$$\lambda_{y^*} = \sum_{i=1}^{N_s} \nu_i \int_M \int_R P\left[Y > y^* \mid m, r\right] \cdot f_{M_i}(m) \cdot f_{R_i}(r) dm dr \tag{4-19}$$

where λ_y is the annual frequency rate of earthquakes, N_S is the number of earthquake sources, $\nu_i = \exp(\alpha_i - \beta_i \cdot m_0)$ at earthquake source *i* evaluated from the Gutenberg-Richter's law (Eq.4-2), $P\left[Y > y^* \mid m, r\right]$ is the probability that seismic intensity generated from an earthquake whose magnitude is *m* and epicentral distance is *r* exceeds y^* which is the threshold seismic intensity, $f_{M_i}(m)$ is the probabilistic density function of magnitude of earthquake occurring at source *i*, and $f_{R_i}(r)$ is the probabilistic density function of epicentral distance of earthquake occurring at source *i*. Under the assumption that earthquake occurrence can be modeled as a Poisson process, the PSHA results in the probability that seismic intensities at a site exceed a threshold seismic intensity during a certain interval of time (McGuire, 1995; Kramer, 1996) as follows:

$$P\left[Y_T > y^*\right] = 1 - \exp\left(-\lambda_{y^*} \cdot T\right) \tag{4-20}$$

where T is time.

Probabilistic seismic hazard maps that display contours of seismic intensities corresponding to peak ground acceleration, peak ground velocity or spectral parameters at specific return periods are prepared by the United States Geological Survey (2002b). A PSHA is particularly suited for designing individual facilities since the intensities can be represented at a probabilistically stipulated level of the seismic hazard in codes and other regulatory documents (e.g., 2% probability of exceedance in 50 years) (FEMA, 2004; ASCE, 2005). The seismic hazard maps are created under the assumptions that earthquake occurrence is a Poisson process, implying that earthquake occurrence is time-homogeneous (Frankel et al., 1996). The seismic hazard map for the CEUS, which includes Shelby County, TN, reflects both the New Madrid seismic zone (NMSZ) and a "background" source zone to characterize the uncertainty in source location (Frankel et al, 1996 and 2002).

Since the spatial correlation of seismic intensities shown in the hazard map is lost in the aggregation process of creating the map, the application of the mapped uniform hazard intensities to serviceability assessment of facilities and distribution elements that are spatially distributed over a region and are functionally dependent on each other is questionable. This issue is discussed in further detail in Chapter 5.

A seismic source zone is identified from the historical record of earthquakes. The a-values and the b-values of the Gutenberg-Richter law for a particular source are determined, in general, from the historical records. For the creation of a seismic hazard map of the CEUS, the a-values of the background source zones are estimated by the

earthquake records for a grid with spacing of 0.2 degree in latitude and longitude. However, the b-value of the background source zones is assumed to be 0.95, which is assumed to be constant for most of the CEUS, including Shelby County, TN (Frankel et al, 1996 and 2002). The epicentral distances are determined as the distance between the grid and the site.

The NMSZ is a major earthquake source zone centered in Southeast Missouri and represents a major seismic hazard for several population centers in the Central and Eastern United States (CEUS). Very large earthquakes have occurred historically in this zone, such as the 1811-1812 sequence, and likely will occur in the future. Recent studies of seismicity in the New Madrid region suggest that earthquakes of such magnitudes have a return period of approximately 500 years. The characteristic attenuation of strong ground motion in the Central and Eastern United States is noticeably different from that in the Western United States. According to Nuttli (1982), the 0.25g peak horizontal acceleration contours for the New Madrid earthquake (m_b = 7.2) enclose an area that is about 11 times larger than the comparable area for a southern California earthquake of approximately the same magnitude (M_L = 7.2), and the area enclosed by the 20 cm/sec peak horizontal ground velocity contour was 8.4 times larger. However, the geological and seismological features about the NMSZ are not well researched. Thus, three fictitious faults are used to characterize the uncertainty in epicentral location of earthquakes in the NMSZ whose magnitudes (M_w) are greater than or equal to 3.0 (Fig.4-6) (Frankel et al., 2002).

The earthquakes from these fictitious faults are referred as characteristic earthquakes (Frankel, 1996 and 2002), and their mean recurrence times are assumed to be

500 years. The magnitudes of these characteristic earthquakes and each frequency ratio are M_w=7.3 (the frequency ratio is 15%), M_w=7.5 (20%), M_w=7.7 (15%) and M_w=8.0 (15%) (Cramer, 2001; Frankel et al., 2002).

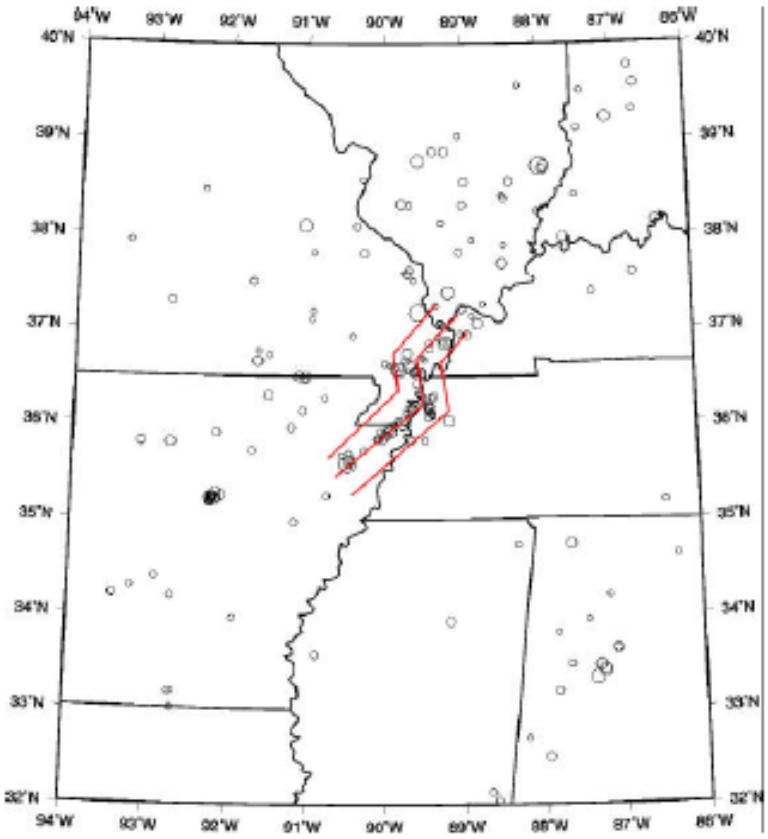

Figure 4-6 Three fictitious faults (red) used to model the New Madrid seismic zone; circles are earthquakes with $M_w \geq 3.0$ since 1976 (Frankel et al, 2002)

4.3 Scenario Earthquake Analysis

Probabilistic seismic hazard analysis (PSHA) provides estimates of the mean annual rate of occurrence (or annual probability) that ground motions exceed a specific intensity (McGuire and Arabasz, 1990). Because a PSHA can be used to determine point or interval estimates of risk based on all possible earthquakes, this method has become a

common seismic risk assessment tool and provides the most informative estimate of earthquake risk at a particular facility site. On the other hand, the results from a PSHA are sometimes difficult for non-specialist decision makers, such as public officials and city planners, to interpret because the significant earthquake threats at the low probabilities of interest in safety analysis of civil infrastructure (on the order of 2% in 50 years, or 0.0004/yr) represent an aggregation of earthquakes events rather than one specific earthquake. This aggregated event fails to model the spatial variability of damaging intensities across a region due to any particular severe earthquake (Eguchi, 1991b; Ishikawa and Kameda, 1994; Chang, et al., 2000; Adachi and Ellingwood, 2007a), and thus may not be appropriate for assessing risk to a distributed infrastructure system.

A risk assessment based on a scenario earthquake avoids these difficulties, but the estimated risk is conditioned on the occurrence of the scenario event. Appropriate scenario events can be determined by a process known as de-aggregation (Bazzurro and Cornell, 1999), which identifies the dominant seismic events contributing to an earthquake hazard of 2% in 50 years, the current basis for building design in the United States (FEMA, 2004; ASCE, 2005), or some other hazard measure for the region being evaluated.

4.3.1 Characteristic Earthquake

Characteristic earthquakes, as well as large historical earthquakes, are often used as scenario earthquakes to assess the damage to facilities. In contrast to a PSHA, SE-based seismic hazard analysis is aimed at investigating the impact of a specific earthquake (usually stipulated in terms of magnitude and epicenter) on a facility or group

of facilities. Such a specification of seismic hazard is useful as a communication tool. Furthermore, McGuire (2001) observed that the SE-based seismic hazard analysis is useful for high seismic regions (e.g. California or Japan) since "a deterministic scenario for this event will allow details to be examined such as ground motion effects caused by rupture propagation." McGuire also noted that, "in moderate and low seismic regions, extreme deterministic scenarios will have probabilities of occurrence that are too low to be useful for most decision purposes."

4.3.2 Deaggregation Analysis

In a SE-based hazard analysis, one specific earthquake is selected from an examination of the seismicity surrounding the site or from a de-aggregation analysis of potential earthquakes. The de-aggregation charts provided by the USGS can be used for selecting this scenario earthquake (USGS, 2002a). Most decision-making regarding public or private investment in seismic risk mitigation focuses on low-probability/high-consequence events. In that case, the earthquake contributing most to the seismic hazard at a stipulated low probability level (e.g., 2% in 50 years) often is selected. Occasionally, an earthquake is simply selected from recordings of severe ground motion (e.g., El Centro, 1940; San Fernando, 1971; Northridge, 1994). Although the scenario earthquake approach is very useful for investigating the damage to an infrastructure system when a specific earthquake occurs, it conveys no quantitative information on the probability of occurrence of the scenario event considered. Thus, the system reliability analysis is conditional in nature.

The results of de-aggregation analyses of six return periods (4975 years, 2475 years, 975 years, 475 years, 224 years and 108 years of return period) at the city of

Memphis, TN obtained by On-line Interactive De-aggregations (USGS, 2002a) are shown in Figures 4-7 to 4-12.

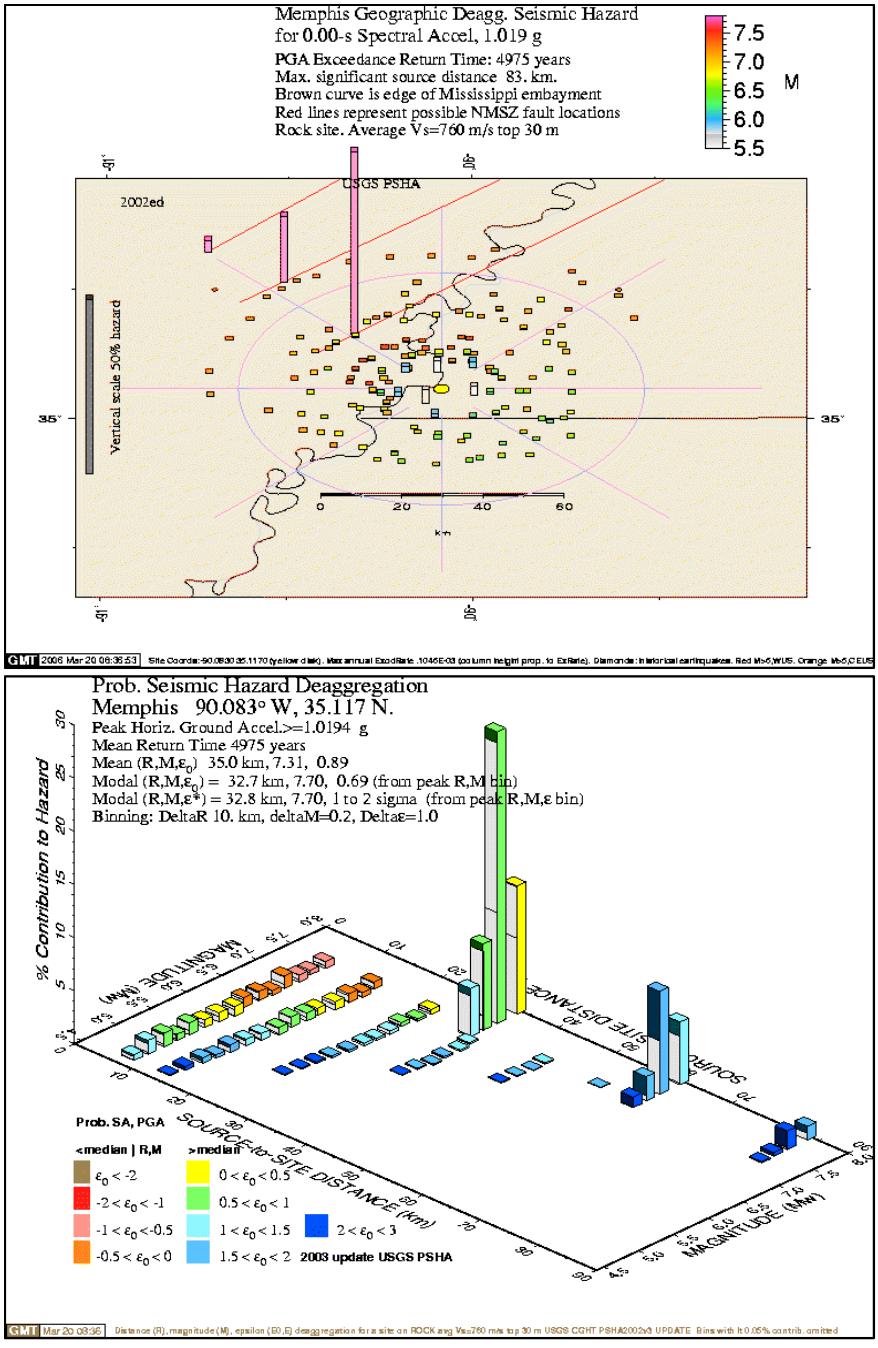

Figure 4-7 Deaggregation results for 4975-year return period (1% probability of exceedance in 50 years) (evaluated from USGS, 2002a)

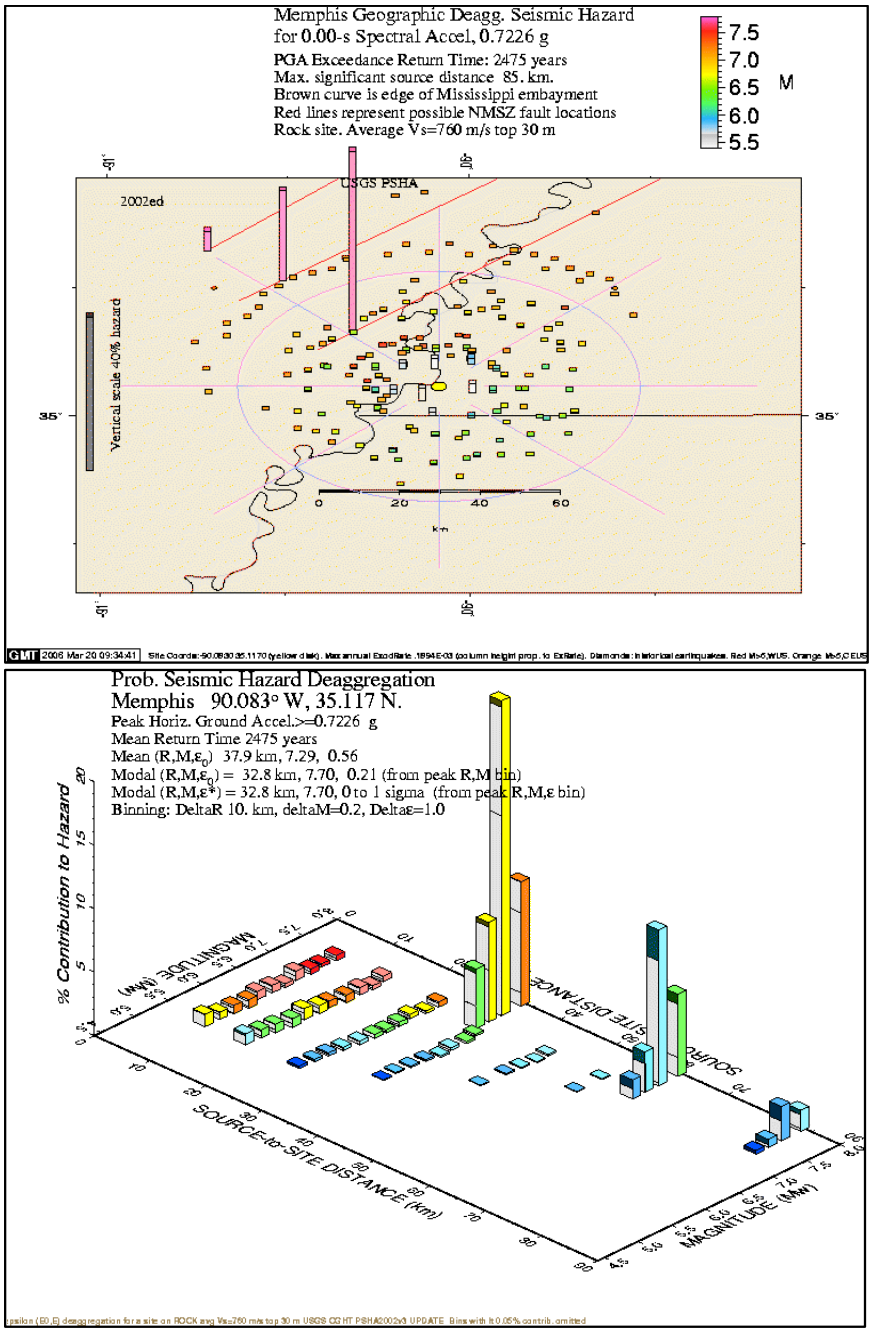

Figure 4-8 Deaggregation results for 2475-year return period (2% probability of exceedance in 50 years) (evaluated from USGS, 2002a)

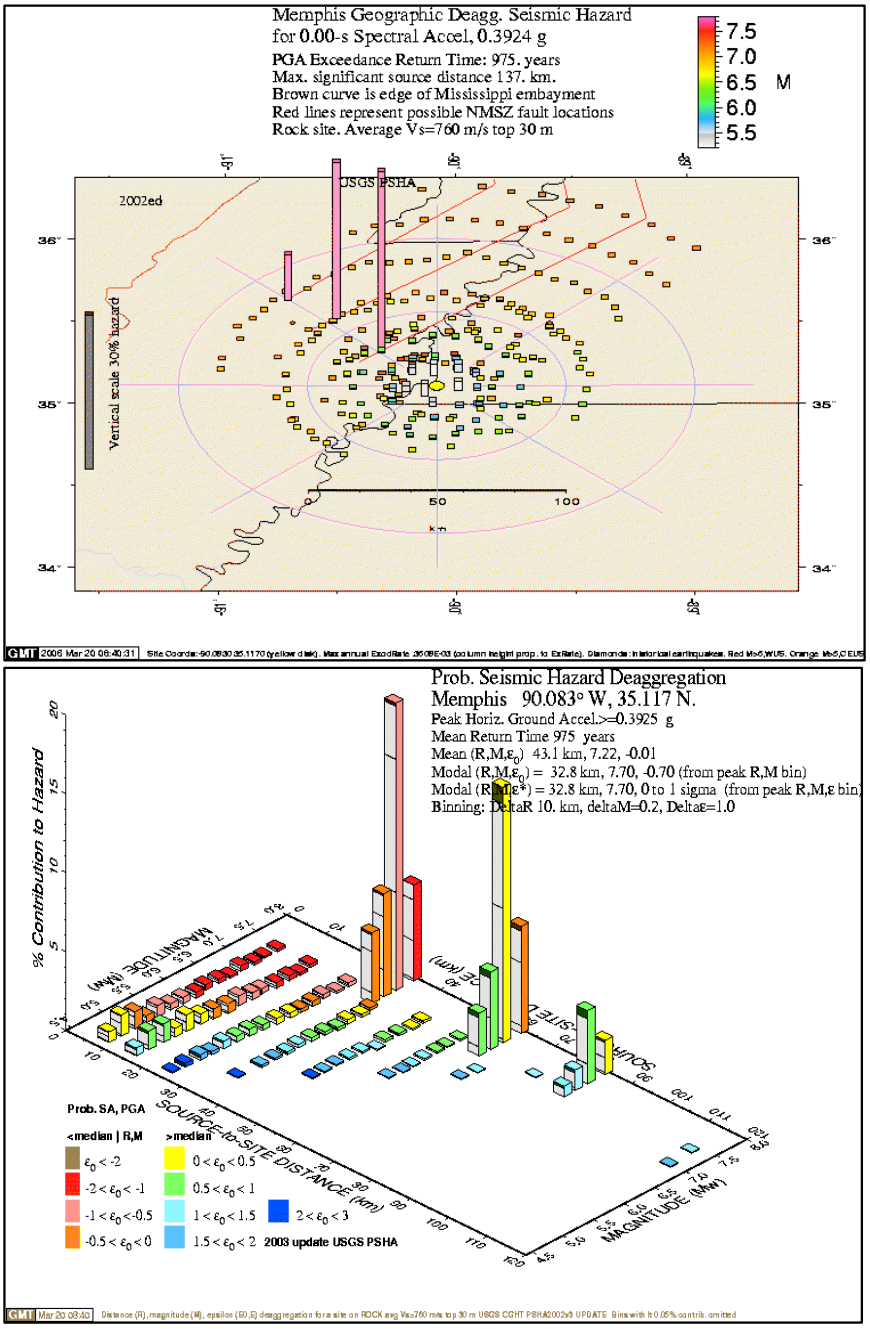

Figure 4-9 Deaggregation results for 975-year return period (5% probability of exceedance in 50 years) (evaluated from USGS, 2002a)

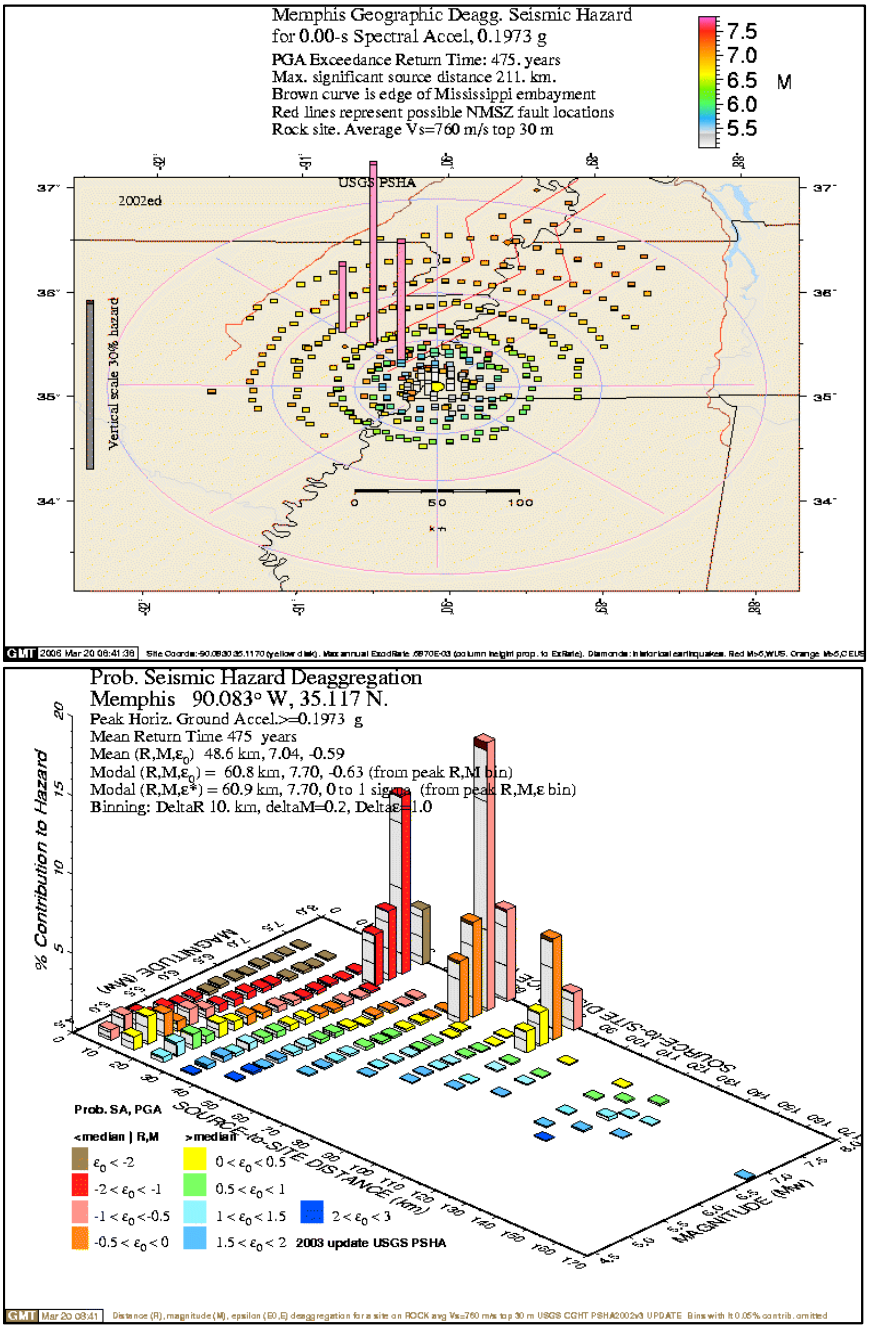

Figure 4-10 Deaggregation results for 475-year return period (10% probability of exceedance in 50 years) (evaluated from USGS, 2002a)

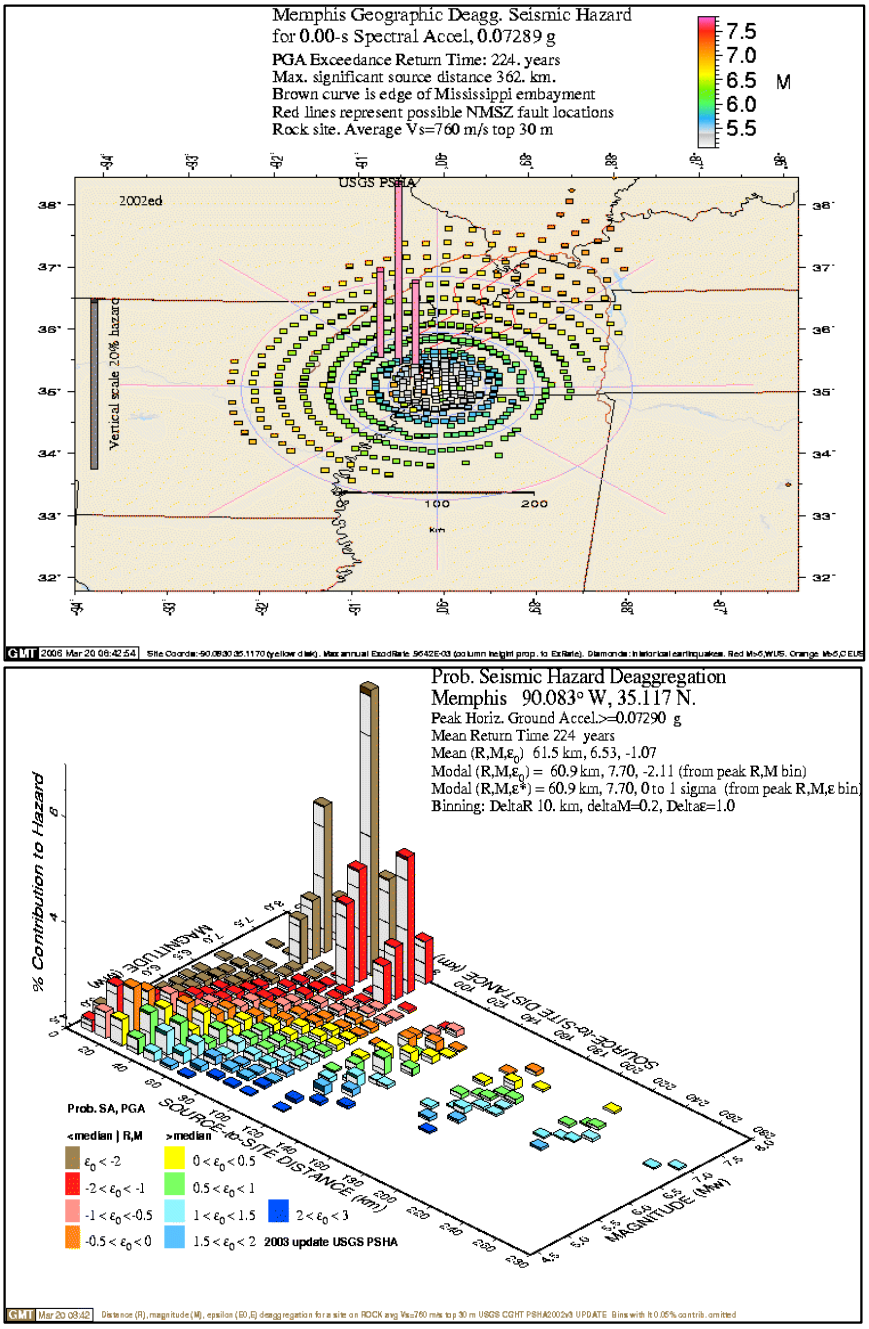

Figure 4-11 Deaggregation results for 224-year return period (20% probability of exceedance in 50 years) (evaluated from USGS, 2002a)

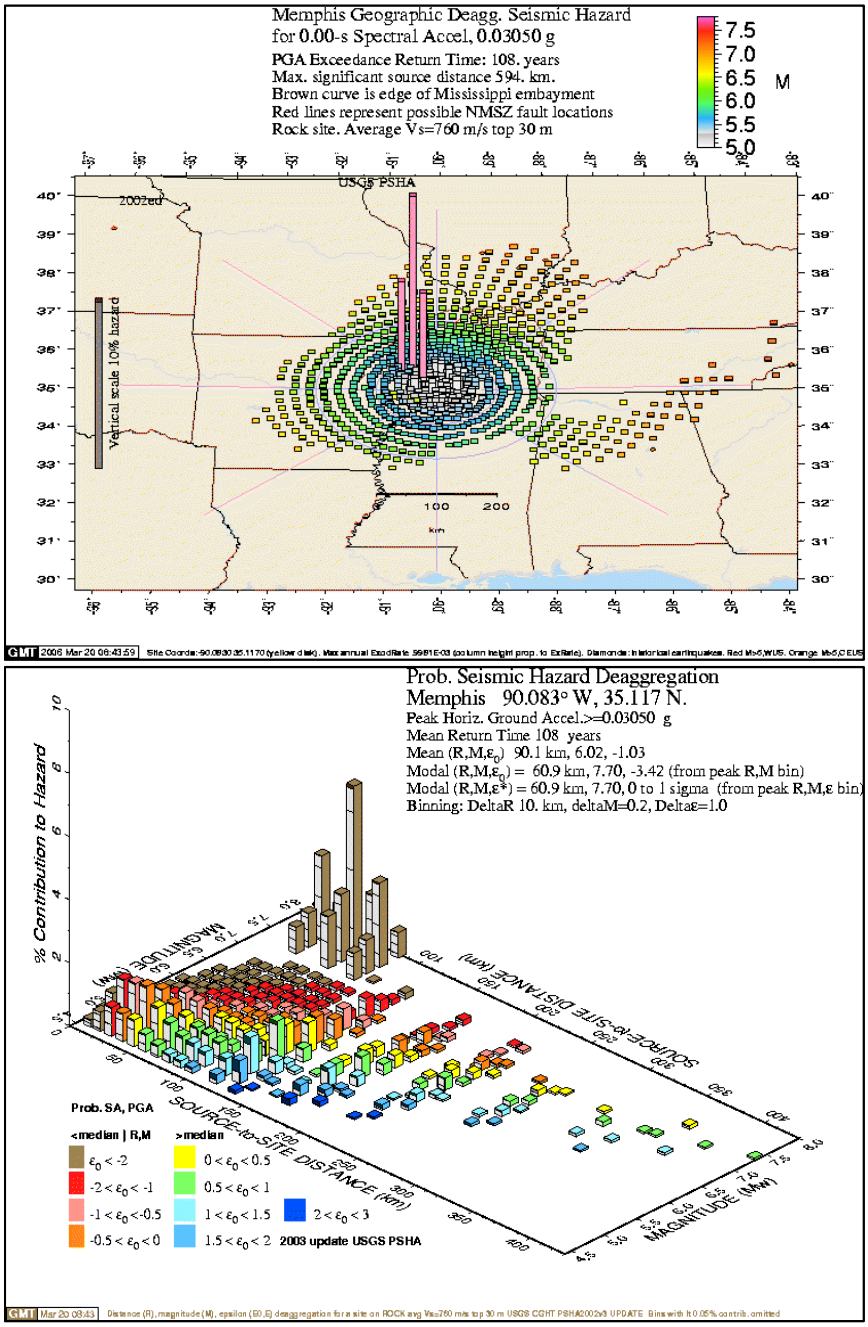

Figure 4-12 Deaggregation results for 108-year return period (50% probability of exceedance in 75 years) (evaluated from USGS, 2002a)

From the de-aggregation at Memphis, TN shown in Figures 4-7 to 4-12, the maximum probable earthquake (MPE) for each return period [one defined as "the largest predicted earthquake that a fault is capable of generating within a specified time period" (Day,

2002)] and the mean earthquake [one with mean magnitude and mean epicentral distance (Bazzurro and Cornell, 1999)] are determined, as summarized in Table 4-3. These de-aggregated earthquakes will be used in Chapters 6 and 7 to assess seismic damage to infrastructure networks.

Table 4-3 MPE and the mean earthquake for each return period

	Maximum probabile earthquake		Mean earthquake	
Return period (years)	Mw	Epicentral Distance to Memphis (km)	Mw	Epicentral Distance to Memphis (km)
4975	7.7	33	7.3	35
2475	7.7	33	7.3	38
975	7.7	33	7.2	43
475	7.7	61	7.0	49
224	7.7	61	6.5	62
108	7.7	61	6.0	90

4.4 Summary

In this chapter, basic approaches to modeling seismic source zones, attenuation relationships of PGA and PGV and amplification of seismic intensities due to local soil conditions were introduced, and differences between probabilistic seismic hazard assessment and scenario-based assessment were summarized. De-aggregation analysis was presented for selecting proper scenario earthquakes. The information summarized in this chapter will be used in Chapters 6 and 7 for the determination of seismic intensities at sites of facilities and distribution elements comprising infrastructure systems.

CHAPTER 5

APPLICABILITY OF PSHA TO A NETWORKED SYSTEM

Probabilistic seismic hazard analysis (PSHA) often provides the basis for designing a facility since it quantifies the seismic intensity in terms of its probability of occurrence during a specific period, taking into account the spectrum of earthquakes likely to contribute to the hazard at that site. A properly conducted PHSA integrates uncertainties of earthquake magnitude, epicentral location, wave propagation expressed by attenuation relationships, and wave amplification due to local soil condition in creating the hazard map, but the effect of interrelations between these factors is lost through the aggregation process. Thus, the applicability of a PSHA to assessing performance of an infrastructure system whose facilities and distribution elements are spatially distributed and are functionally connected (or related) to each other is questionable (Eguchi, 1991b; Chang, 2000).

Figure 5-1 illustrates why aspects of system functionality that depend on the spatial distribution of seismic intensity are not modeled correctly with the PSH-based approach. The upper half of Figure 5-1 shows a simple networked system with two facilities (C_1 and C_2) located between two seismic sources (E_1 and E_2). It is assumed that C_2 requires a commodity (e.g., electrical power, water) from C_1 to maintain its function. The lower half of the figure shows the resistances of the two facilities (R of C_1 and R of C_2) and the attenuation of seismic intensities with increasing distance generated by the two seismic sources (SI of E_1 and SI of E_2). Suppose, for simplicity, that the seismic intensity represented by curve “PSH” is computed under the assumption that the two

seismic zones cause earthquakes with equal frequency. If the average functionality ratio of two facilities in the networked system is evaluated on the basis of the PSH-based approach, the average functionality ratio is 0% since resistances of both facilities fall below the PSH curve. On the other hand, when the functionalities of the two facilities are evaluated for each earthquake separately, the average functionality ratio is 25%; the earthquake from E_1 damages C_1, causing C_2 to lose its function due to cascading failure (implying 0% average functionality ratio), while the earthquake from E_2 damages C_2 but does not damage C_1 (implying 50% average functionality ratio). Figure 5-1 shows clearly that the spatial distribution of seismic intensities in the vicinity of a site cannot be modeled accurately using the PSH-based approach, since no single earthquake can generate a spatial distribution of seismic intensities with peaks at both epicenters 1 and 2.

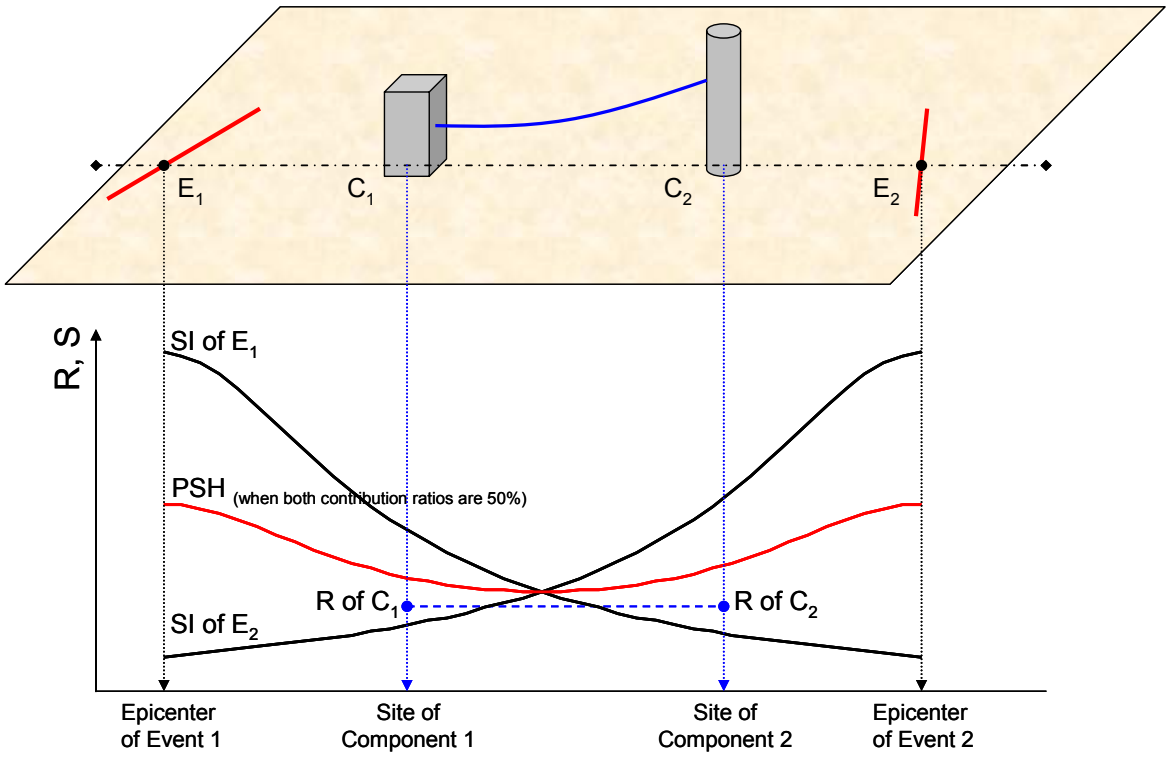

Figure 5-1 Networked system with two seismic zones

There are few studies discussing the applicability of seismic intensities from a seismic hazard map computed by PSHA to serviceability assessment of an infrastructure system. Chang et al. (2000) assessed the expected monetary loss to an infrastructure system in which a small number of earthquakes was selected from all possible earthquakes affecting the system. When these scenario earthquakes are selected "in order to represent different levels of system performance or system damage state" (Chang et al., 2000), they should be selected so that the expected monetary loss due to the selected scenario earthquakes is close to the expected monetary loss due to all possible earthquakes. This methodology works efficiently if the number of selected scenario earthquakes is close to the number of all possible earthquakes in a region. However, there is less advantage of this methodology when civil infrastructure systems in the regions with moderate seismicity are evaluated since the number of possible earthquakes is very large. Furthermore, no clear reason why PSHA is not applicable to assess the serviceability of an infrastructure system was shown in their study.

In Chapter 5, the functionality of a facility within a simple networked system is defined, and its dependence on the functionality of other facilities in the networked system is considered. Then, functionality of facilities in simple networked systems evaluated using probabilistic seismic hazard analysis and scenario earthquake-based analysis is presented. Evaluation of a simple system illustrates some of the difficulties in performing seismic risk analysis of a distributed network based on PSHA and SE-based seismic hazards that would not be as apparent were a realistic network to be evaluated. With these issues identified, the assessment of water and electrical networks in Shelby County, TN will be considered in Chapters 6 and 7.

5.1 Functionality of a Facility in a Networked System

A networked infrastructure system is composed of facilities and connecting elements. Figure 5-2 shows a simple example of a networked system.

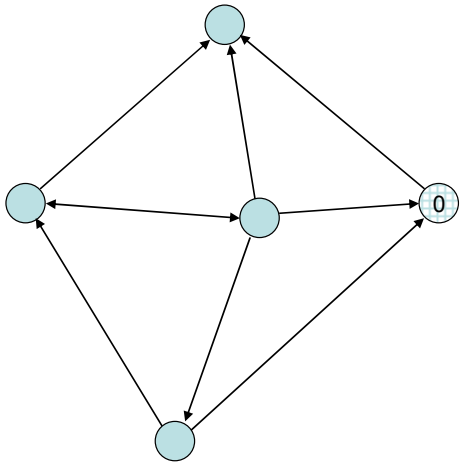

Figure 5-2 Model of a networked system

The circles represent facilities and the arrows represent connecting elements and the directions in which the utility product or commodity (e.g., power, water, or natural gas) flows. Figure 5-2 illustrates a case where the function of facility 0 is affected by the functionalities of the other facilities in the network (cascading failures). When cascading failures are modeled by a reliability block diagram (Rausand and Hoyland, 2004), the function of the facility is expressed as the series system in Figure 5-3. The left square indexed NW represents all facilities of the networked system except facility 0, while the right square indexed 0 represents the target facility. Thus, the survivor function, which represents the functionality ratio of the target facility, is expressed by the following equation when the failures of the facilities are statistically independent events:

$$Rs_0(x_0, x_{NW}) = P[S_0 \cap S_{NW}] = (1 - Pf_0(x_0)) \cdot (1 - Pf_{NW}(x_{NW})) \quad (5\text{-}1)$$

where Rs_0 represents the functionality ratio of the target facility; if $Rs_0 = 0$, the target facility is non-functioning, while if $Rs_0 = 1$ it is fully functioning[1]. Event S_0 represents the event that the facility 0 is functional, while S_{NW} represents the event that the networked system, not including the target facility, is functional. Pf_0 represents the probability of failure of facility 0, Pf_{NW} represents the overall probability of failure of the networked system excluding the facility 0, x_0 is the seismic intensity at the site of the facility 0, and x_{NW} is the vector of seismic intensities for facilities in the networked system excluding the facility 0. These seismic intensities differ for different components in the network, especially for those that are distant from one another. The relation between the survivor function and fragilities is illustrated in Figure 5-4, in which the Pf_{NW} - x surface represents a system fragility curve involving all facilities of the networked system except the facility 0, the Pf_0 - x surface represents the fragility curve of the facility 0, and the Pf_{NW} - Pf_0 - Rs_0 space illustrates the relationship among them (Eq.5-1). Figure 5-4 illustrates the dependence of the functionality ratio of a target facility on the two component fragilities and corresponding seismic intensities. Thus, the system structure and fragility curves both are required to evaluate the functionality ratio of the facilities and the networked system since the system fragility ($Pf_{NW}(x_{NW})$) is dependent on the structure of the system even though the facility fragilities ($Pf_0(x_0)$) are independent of the structure of the network.

[1] We assume here in presenting the basic concepts that each facility can be in one of two states: fully functional or nonfunctional. Later, this assumption will be relaxed.

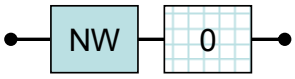

Figure 5-3 Reliability block diagram of the function of a facility within the networked system

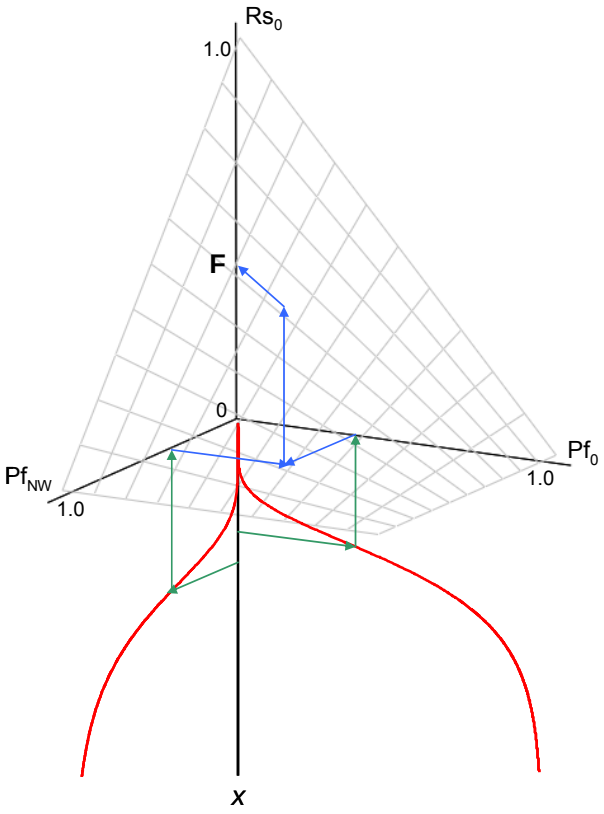

Figure 5-4 Evaluation of facility functionality ratio

The functionality of a facility within a networked system may be highly dependent on the functionality of other facilities in the networked system. In the following sections, the functionality of a facility in a simple networked system evaluated on the basis of a PSHA is compared with the functionality based on a single scenario earthquake. This simple illustration will highlight the drawbacks of relying on a uniform probability hazard map for assessing performance of a distributed networked system.

5.2 Models of Simple Networked Systems

In order to assess the effect of the structure of the networked system represented by block NW on the functionality ratio of facility 0 (see Figure 5-3), systems which have purely series (Figure 5-5) and purely parallel structures (Figure 5-6) are modeled and the functionality ratio of a facility in the network is evaluated. The networked systems in these figures contain facilities that are interconnected by distribution elements. The facility identified by a square represents a supply facility, which generates the commodity distributed in the networked system, such as electrical power or water. The facility identified by a circle is a demand facility, which is a relay point that conveys the commodity from the supply facility to other demand facilities, such as a substation in a power distribution system or a pumping station in a water distribution system, and to customers. Cascading failures of demand facilities occur when they cannot receive the commodity from any supply facility either directly or indirectly as a result of damage to upstream components.

5.2.1 Network Analysis

To illustrate the network analysis in a simple way, Figure 5-5 illustrates a simple series network system, in which the functionality ratios of three facilities 1 to 3 are to be analyzed. Facility 3 is most strongly dependent on the series structure since its functionality ratio is determined by not only the fragility of facility 3 but also the fragilities of facilities 0 to 2. On the other hand, facility 1 is most weakly dependent on the series structure since its functionality ratio is determined only by the fragilities of facilities 0 and 1. The reliability block diagrams describing the functions of facilities 1 to

3 are shown in Figure 5-7 (a) to (c), respectively. The survivor functions for facilities 1 to 3, when the facility failures are statistically independent, are:

$$\begin{aligned} Rs_{S,1}\left(\vec{x}\right) &= P\left[S_0 \bigcap S_1\right] \\ &= \left(1 - Pf_0\left(x_0\right)\right) \cdot \left(1 - Pf_1\left(x_1\right)\right) \end{aligned} \tag{5-2}$$

$$\begin{aligned} Rs_{S,2}\left(\vec{x}\right) &= P\left[S_0 \bigcap S_1 \bigcap S_2\right] \\ &= \left(1 - Pf_0\left(x_0\right)\right) \cdot \left(1 - Pf_1\left(x_1\right)\right) \cdot \left(1 - Pf_2\left(x_2\right)\right) \end{aligned} \tag{5-3}$$

$$\begin{aligned} Rs_{S,3}\left(\vec{x}\right) &= P\left[S_0 \bigcap S_1 \bigcap S_2 \bigcap S_3\right] \\ &= \left(1 - Pf_0\left(x_0\right)\right) \cdot \left(1 - Pf_1\left(x_1\right)\right) \cdot \left(1 - Pf_2\left(x_2\right)\right) \cdot \left(1 - Pf_3\left(x_3\right)\right) \end{aligned} \tag{5-4}$$

Figure 5-6 illustrates a parallel network system, in which the functionality ratio of facility 0 in the networked system (a) and facility 0 in the networked system (b) are to be evaluated. The facility 0 in system (b) sustains the strongest effect of the parallel structure since its functionality ratio depends on the fragilities of all three facilities 1 to 3. On the other hand, facility 0 in system (a) is most weakly dependent on the parallel system structure since its functionality ratio is determined by the fragilities of only facilities 1 and 2. The reliability block diagrams in Figure 5-8 (a) and (b) illustrate the function of facility 0 in systems (a) and (b). Assuming that the facility failures are statistically independent events, the survivor functions of facility 0 in systems (a) and (b) are:

$$\begin{aligned} Rs_{P,(a)}\left(\vec{x}\right) &= P\left[S_1 \bigcup S_2\right] \\ &= 1 - Pf_1\left(x_1\right) \cdot Pf_2\left(x_2\right) \end{aligned} \tag{5-5}$$

$$\begin{aligned} Rs_{P,(b)}\left(\vec{x}\right) &= P\left[S_1 \bigcup S_2 \bigcup S_3\right] \\ &= 1 - Pf_1\left(x_1\right) \cdot Pf_2\left(x_2\right) \cdot Pf_3\left(x_3\right) \end{aligned} \tag{5-6}$$

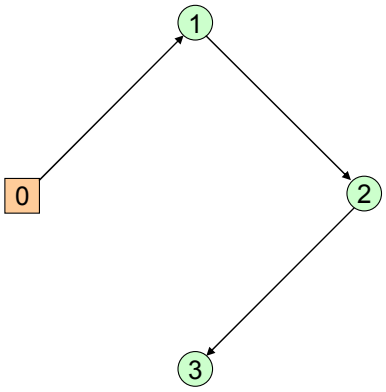

Figure 5-5 A networked system with purely series structure

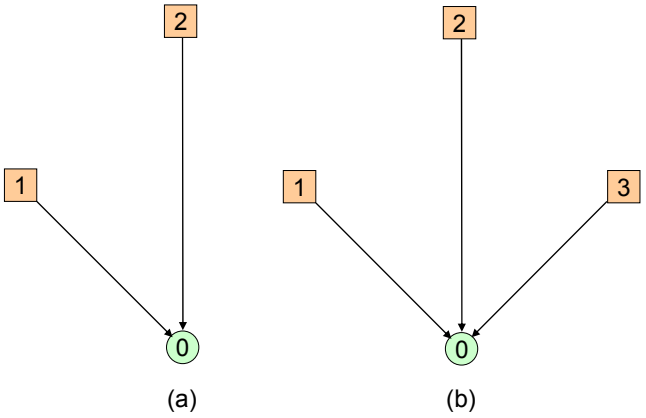

Figure 5-6 The models of networked system with purely parallel structure

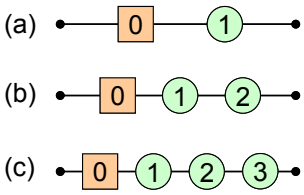

Figure 5-7 The reliability block diagram of the series system

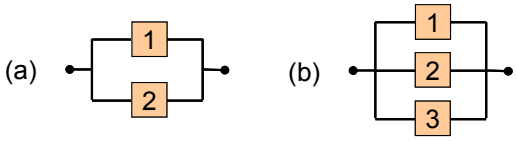

Figure 5-8 The reliability block diagram of the parallel system

5.2.2 Network System Fragilities

The system fragility curves based on these survivor functions are shown in Figure 5-9 under the assumption that all facilities in the network are subjected to the same seismic intensities and the fragility of each facility is described by the log-normal cumulative distribution function:

$$Pf_X(x) = \int_0^x \frac{1}{\sqrt{2\pi}\zeta s} \exp\left[-\frac{1}{2}\left\{\frac{\ln(s)-\lambda}{\zeta}\right\}^2\right] ds \qquad (5\text{-}7)$$

where λ is the mean of ln(X), computed by $\ln(median(X))$, and ζ is the standard deviation of $\ln(X)$. In this simple illustration, all fragilities are defined by $\lambda = \ln(0.4g)$ and $\zeta = 0.4$; these values are typical for fragilities in networked systems (FEMA, 2003).

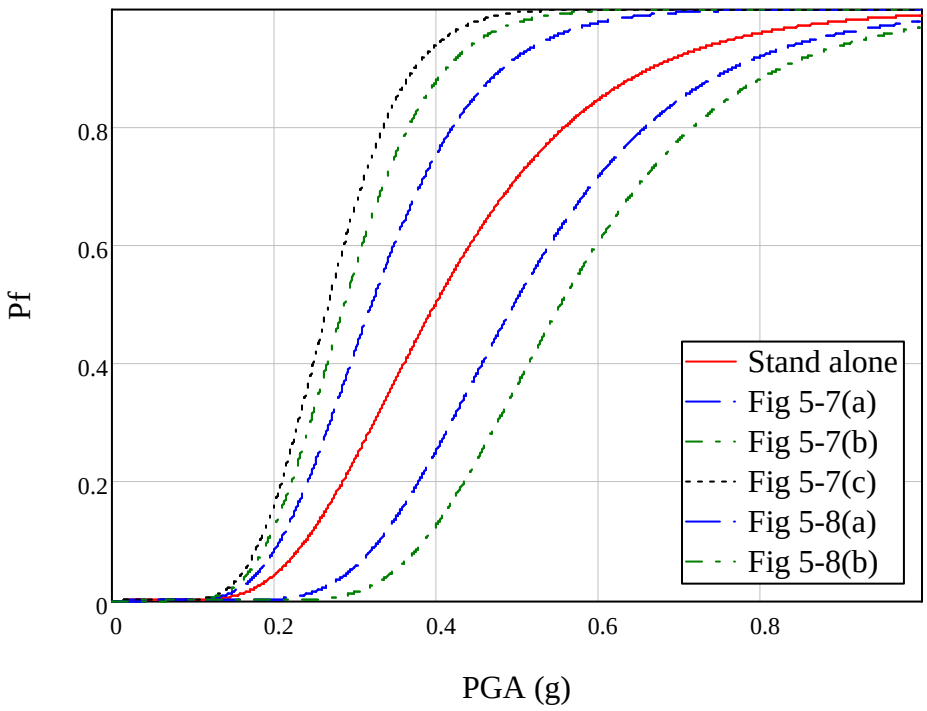

Figure 5-9 System fragility curves (all components subjected to same PGA)

5.2.3 Seismic Intensities

Since the PGA at a site used in the PSHA is determined from seismic intensities generated by all postulated earthquakes proximate to the site, that PGA is dependent on the locations of the seismic source zones. To provide a simple illustration of the effect of earthquake epicentral locations and magnitudes on the estimated risk to the networked system, the following assumptions are made:

1. Earthquakes from two seismic source zones may impact the networked system.
2. Two pairs of seismic source zones are considered. In the first example, the two seismic source zones generate earthquakes with M_w 8.0 and 6.0. In the second example, both seismic source zones generate earthquakes with M_w 8.0. Each zone is assumed to contribute 50% of the earthquake hazard.
3. Epicentral distances of both source zones, measured from the location of the epicenter to the geographic center of the networked system, are arbitrarily set as 30, 40, 50, 60 and 70 km.
4. The azimuth of each epicenter with respect to the target system is defined by an angle θ, which is a uniformly distributed random number in $\left[0^\circ, 360^\circ\right)$.

Figure 5-10 depicts the relation of the location of epicenters and the networked system. The diamond at the center of the figure represents the networked system, with the edges representing the connecting elements and the corners representing the facilities. Each facility is located 10km from the center of the networked system.

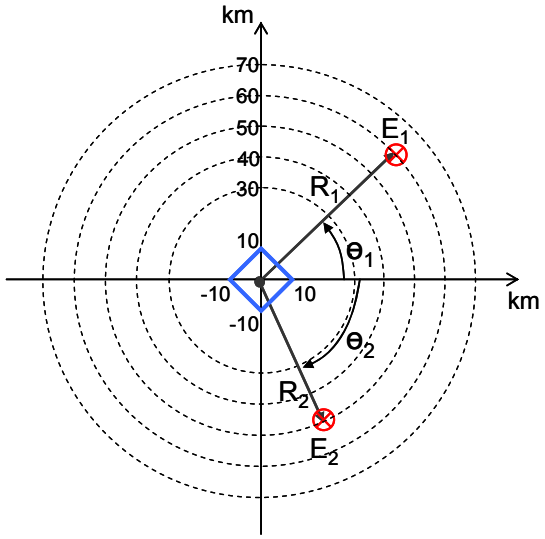

Figure 5-10 Two selected epicenters and the networked system

In order to determine seismic intensities at each facility, the attenuation equation defined in Eq.4-12 (Toro et al., 1997) is used. Figure 5-11 shows the relation between median PGA and the distance from the epicenter to the site evaluated. The logarithmic standard deviation of the PGA associated with Equation 4-12 is 0.6 (e.g., Toro et al., 1997).

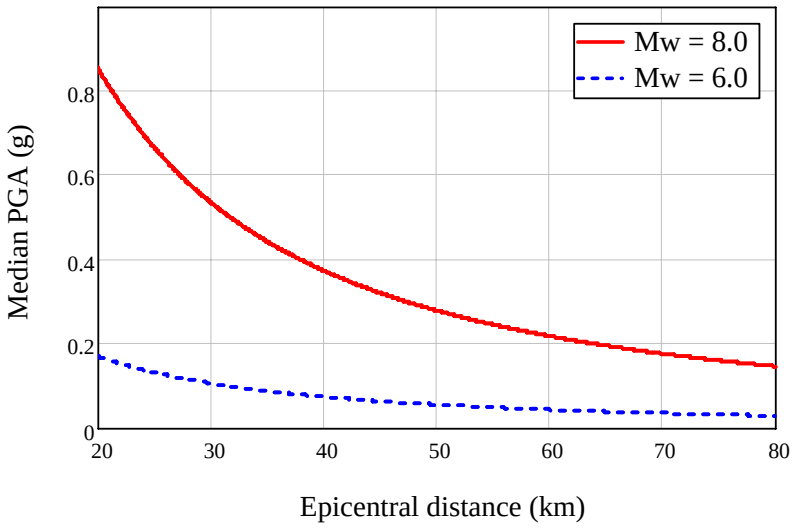

Figure 5-11 Attenuation relations for M_w=8 and M_w =6

Using the simplified scenario earthquake model defined in this section, functionality ratios of facilities are evaluated by both PSHA and the scenario earthquake based approach in the following section. The results of this evaluation illustrate the problems associated with using a PSHA as the basis for functionality assessment of facilities within a networked system.

5.2.4 Functionality of a Facility by PSHA and Scenario Earthquake-based Approaches

Evaluations of the functionality ratio of a facility in a networked system using PSH-based and SE-based approaches utilize the simple models of networked systems and seismic zones summarized previously.

The PSH-based approach (summarized in Figure 5-12 (a)) consists of the following steps:

1. Seismic intensities at the sites of all facilities within the network are computed for two earthquakes which are defined in section 5.3.
2. A weighted average of seismic intensities at each site is computed by weighting the attenuated intensities by the relative frequencies of the contributing earthquakes identified in step 1.
3. The functionality ratio of each facility in the networked system is evaluated using these average seismic intensities and the corresponding survivor function (Eqs. 5-2 to 5-6).

In the SE-based approach (summarized in Figure 5-12 (b)), the functionality ratios of the facilities in a networked system are evaluated for each scenario earthquake, and the resulting facility functionalities are weighted by the probability of occurrence of each

earthquake to arrive at an overall estimate of the facility functionality. If it were possible to take the probability of occurrence of all possible earthquakes into account, then the functionality ratio of a facility evaluated by the SE-based approach would, in fact, be the "exact" functionality ratio of a facility in the networked infrastructure system.

The SE-based approach consists of the following steps:

1. Seismic intensities at the sites of facilities are computed for all possible earthquakes, as in step 1 of the PSH-based approach.
2. The functionality ratio of each facility in the networked system is evaluated using these seismic intensities and a corresponding survivor function.
3. The weighted average functionality ratio of each facility in the networked system is evaluated, taking into account the relative frequency of the corresponding scenario earthquakes.

As noted previously, the PSH-based approach is relatively straightforward, since the USGS seismic hazard map (USGS, 2002b) already reflects the weighted averages of seismic intensities in the vicinity of a site.

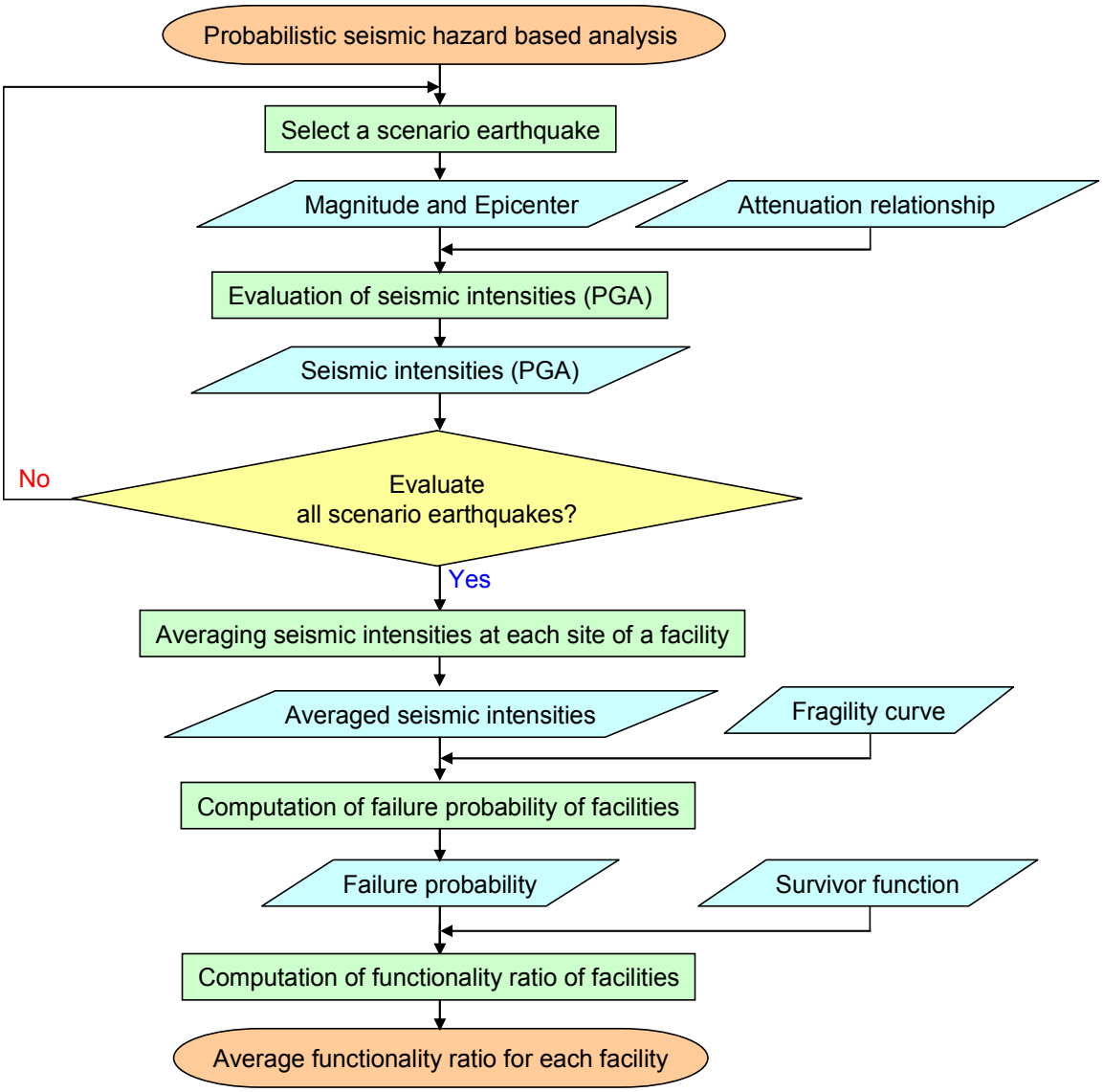
Probabilistic seismic hazard based analysis
Select a scenario earthquake
Magnitude and Epicenter
Attenuation relationship
Evaluation of seismic intensities (PGA)
Seismic intensities (PGA)
No
Evaluate
all scenario earthquakes?
Yes
Averaging seismic intensities at each site of a facility
Averaged seismic intensities
Fragility curve
Computation of failure probability of facilities
Failure probability
Survivor function
Computation of functionality ratio of facilities
Average functionality ratio for each facility

(a)

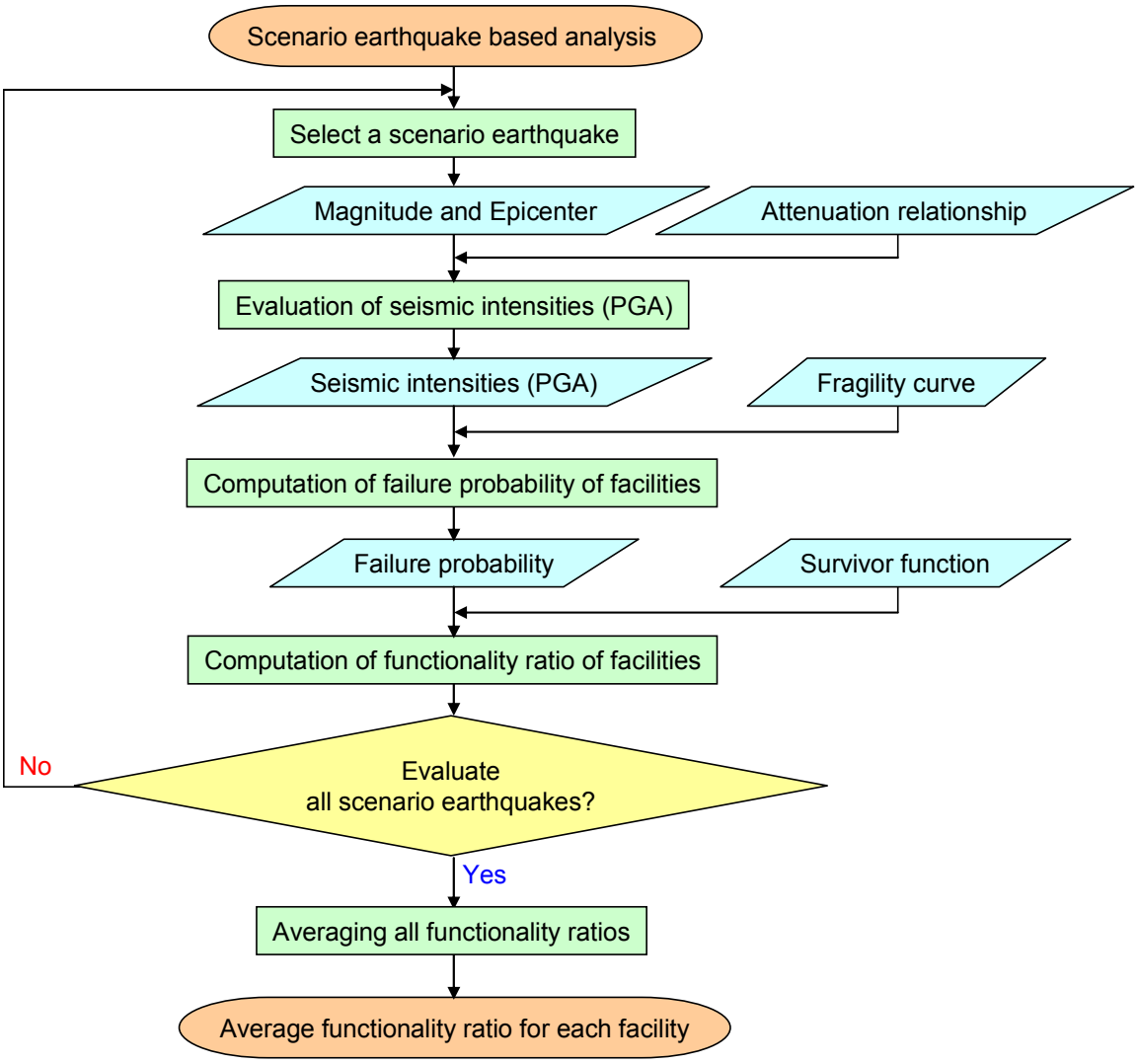

(b)

Figure 5-12 Assessment of functionality ratio of a facility in a networked system based on (a) PSHA and (b) Scenario Earthquake Models

5.3 Estimated functionalities for regional earthquake risks based on PSHA and SE

Following the process illustrated in Figure 5-12 (a) and (b), the functionality ratios of the facilities in the networked systems illustrated in Figure 5-5 and 5-6 are evaluated. From Equations 5-2 to 5-6, the functionality ratios are calculated by applying PGAs from scenario earthquakes or PGAs weighted by contribution ratios. Figure 5-13

to 5-16 display the average functionality ratios corresponding to the facilities within networked systems characterized by series and parallel structures.

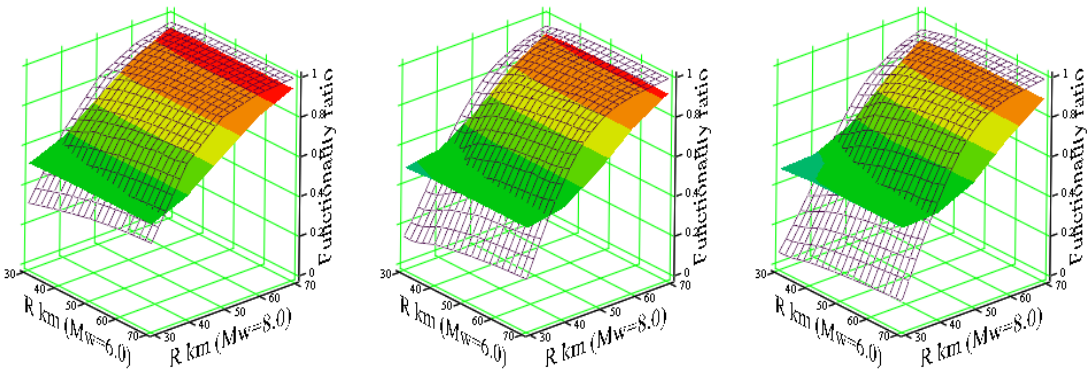

Facility 1 in figure 5 Facility 2 in figure 5 Facility 3 in figure 5

Figure 5-13 Functionality of a facility within a series system: M_w (8.0, 6.0) (Mesh surface: PSH-based approach; Solid surface: SE-based approach)

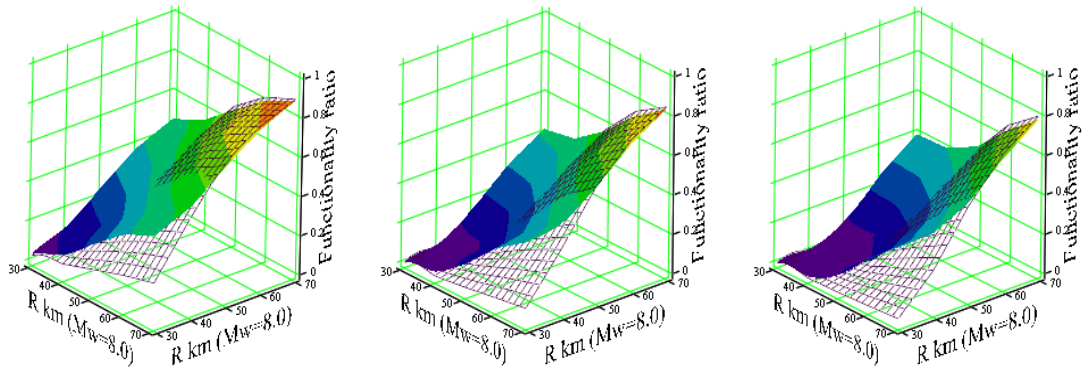

Facility 1 in figure 5 Facility 2 in figure 5 Facility 3 in figure 5

Figure 5-14 Functionality of a facility within a series system: M_w (8.0, 8.0) (Mesh surface: PSH-based approach; Solid surface: SE-based approach)

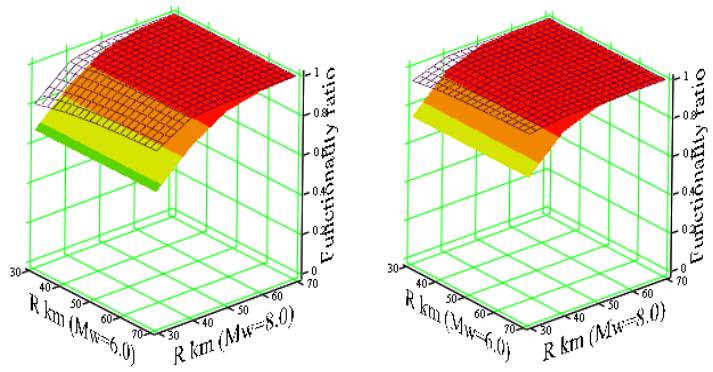

System (a) in figure 6 System (b) in figure 6

Figure 5-15 Functionality of a facility within a parallel system: M_w (8.0, 6.0) (Mesh surface: PSH-based approach; Solid surface: SE-based approach)

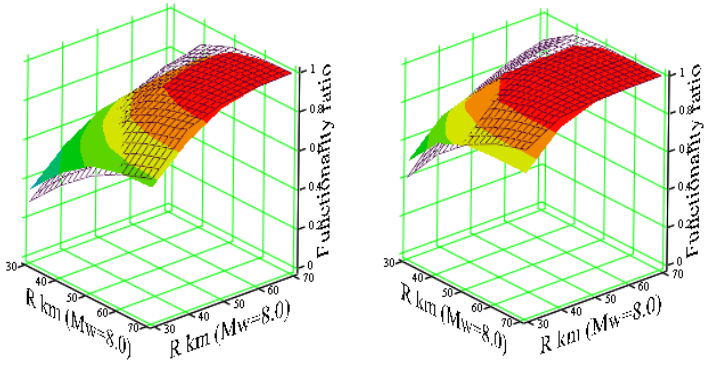

System (a) in figure 6 System (b) in figure 6

Figure 5-16 Functionality of a facility within a parallel system: M_w (8.0, 8.0) (Mesh surface: PSH-based approach; Solid surface: SE-based approach)

Two trends are evident in Figure 5-13 to 5-16. First, when M_w (8.0, 6.0), as shown in Figure 5-13 and 5-15, the functionality ratio of a facility is depends more on the distance of the M_w=8.0 earthquake than on the distance of the smaller M_w=6.0 earthquake; in other words, the larger PGA dominates the functionality ratio of a facility in the networked systems with both series and parallel structures. This can be explained by comparing the attenuations of earthquakes with M_w=6.0 and M_w=8.0 in Figure 5-11. The PGA from the attenuation of the M_w=8.0 earthquake changes drastically at shorter

epicentral distances. This leads to a wider range of functionality ratios for a facility. On the other hand, the PGA from the attenuation of the M_w=6.0 earthquake varies less than for the M_w=8.0 earthquake. Thus, the functionality ratio of a facility due to the M_w=6.0 earthquake has a narrower range.

Second, the functionality ratios of each facility evaluated by the PSH-based approach and the SE-based approach are quite different. For example Figure 5-13, 5-14 and 5-16 show that when the distances of the M_w=8.0 earthquake(s) are larger, the functionality ratios of the three facilities evaluated by the SE-based approach are lower than those by the PSH-based approach. Conversely, for smaller epicentral distances of the M_w=8.0 earthquake(s), the functionality ratios of the three facilities evaluated by the SE-based approach is higher than those by the PSH-based approach. In Figure 5-15, the functionality ratios of facilities evaluated by the SE-based approach are always less than that from the PSH-based approach.

The second trend can be explained by the relation between the fragility curves and the survivor function shown in Figure 5-4. For simplicity, the 3D model in Figure 5-4 is idealized to the 2D models in Figures 5-17 (a) and (b), where the left half surface (Seismic intensity-Failure probability surface) shows a system fragility curve, and the right half surface (Failure probability-Functionality ratio surface) shows a survivor function.

Figure 5-17 (a) illustrates the case when two PGAs generated from two seismic zones are relatively small but are different in value, such as seismic intensities $E_1(M_W = 6.0, R = 50km)$, $E_2(M_W = 8.0, R = 50km)$ in Figure 5-13 and 5-15. Following the SE-based approach illustrated in Figure 5-12 (b), failure probabilities Pf_{E1}

and Pf_{E2} are computed from seismic intensities E_1 and E_2 respectively, and functionality ratios Rs_{E1} and Rs_{E2} are calculated. By weighting the functionality ratios Rs_{E1} and Rs_{E2} with the contribution ratio (50% for each scenario event), the expected functionality ratio $Rs_{SE,1-2}$ is evaluated. In contrast, following the PSH-based approach illustrated in Figure 5-12 (b), seismic intensity $PSHA_{1-2}$ is used to evaluate failure probability $Pf_{PSHA,1-2}$ and functionality ratio $Rs_{PSHA,1-2}$ is computed. By comparing $Rs_{SE,1-2}$ and $Rs_{PSHA,1-2}$, it is concluded that the PSH-based approach results in a larger functionality ratio than the SE-based approach when the two PGAs are relatively small and have difference.

Figure 5-17 (b) illustrates the case when two PGAs generated from two seismic zones respectively are relatively large and are different in value, such as seismic intensities $E_1(M_W = 8.0, R = 40km)$, $E_2(M_W = 8.0, R = 30km)$ in Figure 5-14 and 5-16. In this case, the functionality ratio based on PSH-based approach $Rs_{PSHA,1-2}$ is smaller than the expected functionality ratio based on SE-based approach $Rs_{SE,1-2}$. Other results shown in Figure 5-13 to 5-16 can be explained in a similar way.

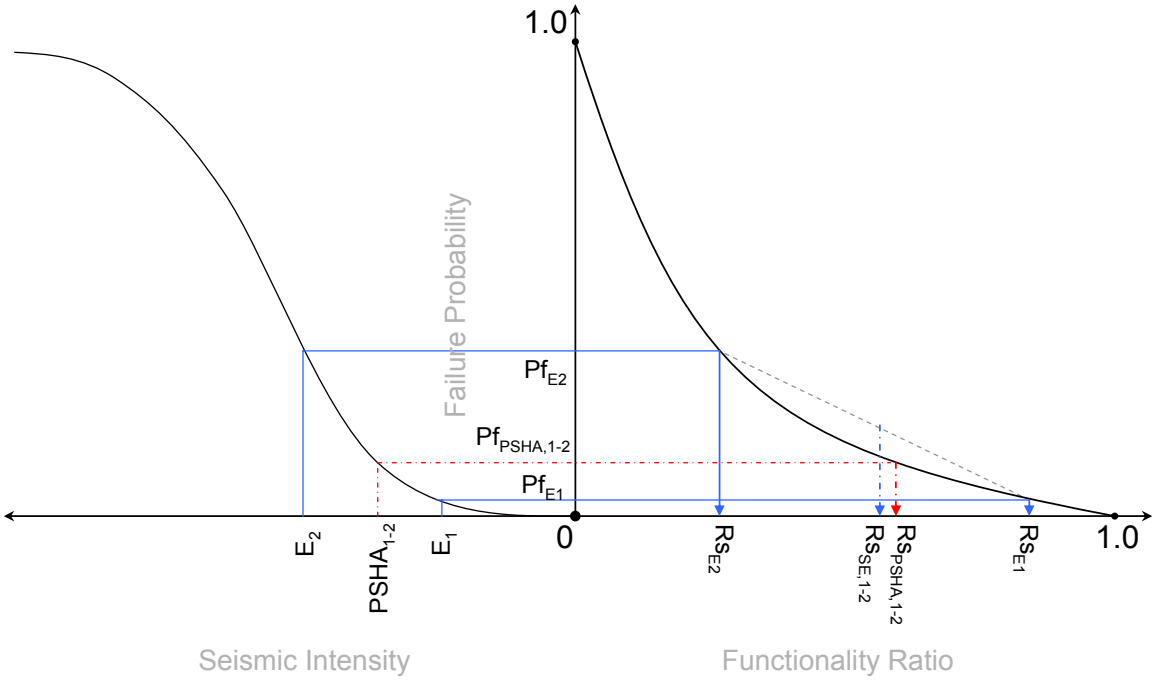

(a) Two seismic intensities are relatively small.

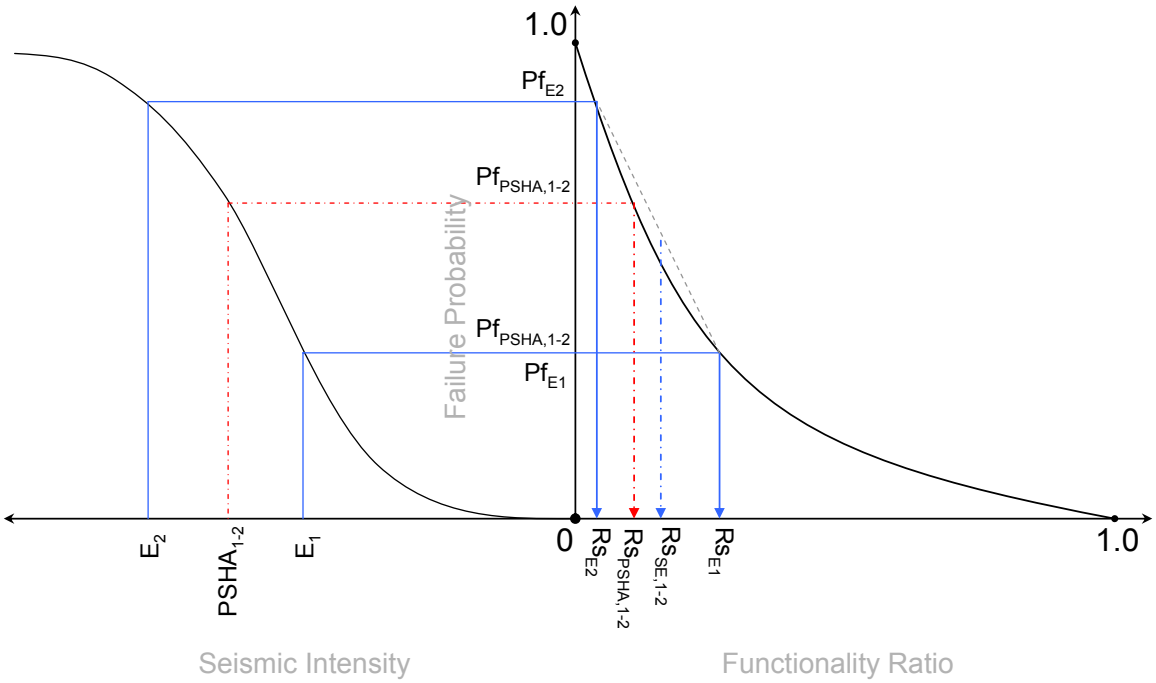

(b)Two seismic intensities are relatively large.

Figure 5-17 The simplified model of Figure 5-4

5.4 Summary

The functionality ratios of facilities within a simple distributed civil infrastructure network were evaluated in this chapter for two alternate specifications of seismic hazard: the PSH-based approach and the SE-based approach. Obstacles to using the PSH-based approach to analyze the functionality ratios of facilities comprising a networked system were assessed.

The function of a facility within a networked system is affected by the functionality of other facilities. Thus, the functionality ratio of a facility is affected by not only its fragility but also the fragility of the entire system. The PSH-based approach generally leads to a facility functionality ratio that is different from what would be evaluated by the scenario based approach. In particular, one may conclude from this study that the use of hazard contours from a PSHA will yield a conservative estimate of performance of a civil infrastructure network only if the network is exposed to high seismic intensities over its entire extent (e.g., $PSHA_{1-2}$ in Figure 5-17(b)). In other cases, the scenario earthquake based seismic hazard analysis will provide a more accurate assessment of damage to a distributed infrastructure system. However, since the functionality ratio of a facility within an infrastructure system is affected by the system topology, fragility curves, magnitudes of earthquakes and the locations of their epicenters, one cannot generalize the conditions under which the PSHA is suitable for the infrastructure system serviceability assessment. Decision-makers should be cautious about accepting such estimates without careful investigation.

CHAPTER 6

SERVICEABILITY ASSESSMENT OF DISTRIBUTED INFRASTRUCTURE SYSTEMS

The electrical power transmission, water and natural gas distribution systems in Shelby County, TN are managed by the Memphis Light, Gas and Water Division (Chang et al., 1996; Shinozuka et al., 1998). Shelby County, TN is located approximately 20 to 100 km from NMSZ and is the largest major population center potentially affected by major earthquakes in the NMSZ. In this chapter, the serviceability assessment of the water distribution and electrical power transmission systems under a single scenario earthquake is considered. Along with the evaluation of effects of spatially correlated seismic intensity on the serviceability assessment of the infrastructure systems, upper and lower bound closed-form solutions for the failure probability of components are derived to reduce the computing time. The effects of infrastructure interdependency on the serviceability of the water distribution system are also evaluated by considering electrical power availability and the effort of the electrical power backup systems.

6.1 Serviceability Assessment Procedure

An infrastructure system is composed of facilities and distributing elements, and several steps are required to assess its serviceability. These steps are summarized in Figure 6-1.

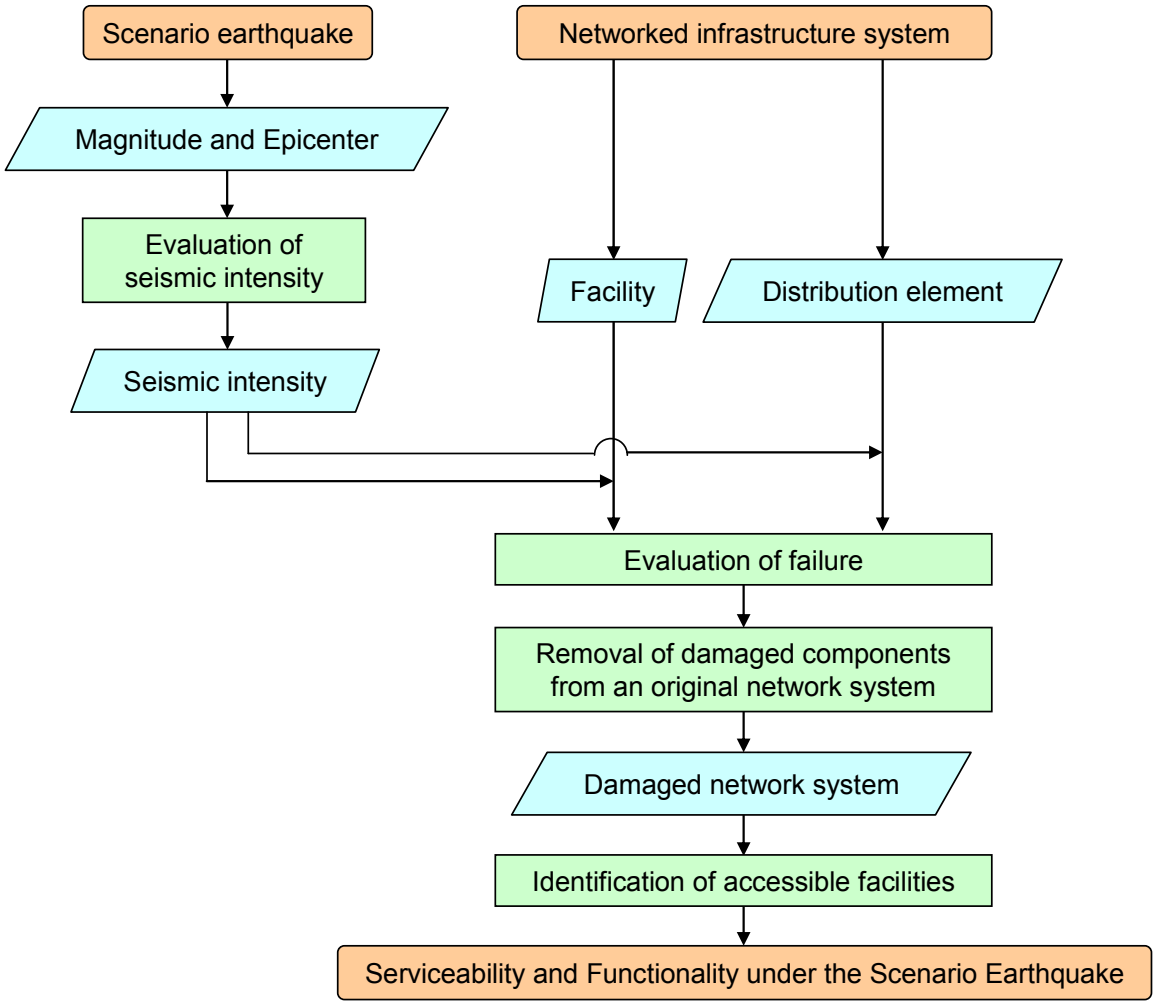

Figure 6-1 Serviceability assessment of an infrastructure system

The "Identification of accessible facilities" step is executed using the Floyd-Warshall shortest path algorithm (Floyd, 1962; Warshall, 1962; Papadimitriou and Steiglitz, 1998) described in Chapter 3. The serviceability of the networked system within a region is defined as the ratio of the satisfied customer demand to total customer demand within the region; the functionality of a facility is defined as the complement failure probability of the facility considering cascading failure due to failure of other facilities and distribution elements.

6.2 Description of Networked Electrical Power Transmission and Water Distribution Systems

The water and electrical power systems in Shelby County consist of numerous facilities and widespread distribution networks. For purposes of illustrating the potential significance of network interdependence and to avoid undue complexity, only major facilities and trunk distributing elements are considered in this study.

Figure 6-2 illustrates the main water distribution system in Shelby County. The water system consists of six elevated storage tanks, nine pumping stations and numerous water distribution nodes connected by buried pipe (Hwang et al, 1998; French and Jia, 1997). Water distribution nodes identified with numbers 16 to 49 are considered as demand facilities, which relay the water to other demand facilities and customers.

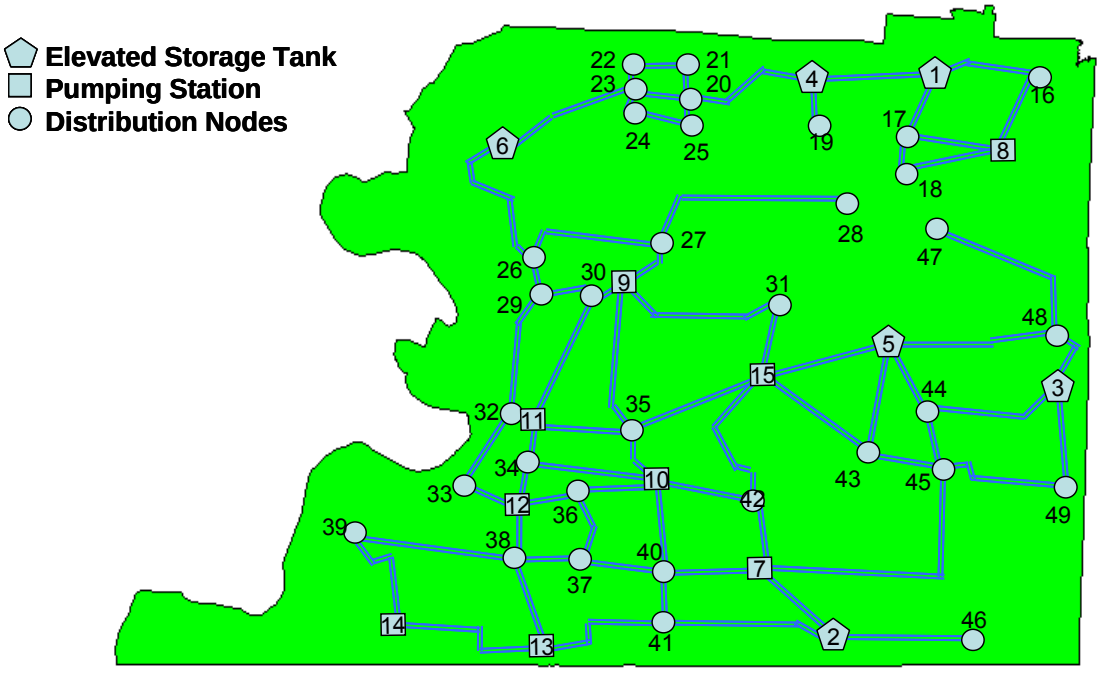

Figure 6-2 Water System in Shelby County, TN. (modified from Chang et al., 1996)

Figure 6-3 illustrates the main electrical power transmission system in Shelby County. The electrical power system consists of eight gate stations, sixteen 23kv substations and twenty-one 12kv substations. Each substation has its own service area within which it provides electrical power to customers (Shinozuka et al, 1998). The service area of each substation is represented by the dashed lines in Figure 6-3. These service areas are required to analyze the dependency of the water system on the electrical power system when infrastructure interaction is considered. Since there is no electrical power generating plant in Shelby County, large substations in the metropolitan area (termed "Gate station") provide the electric power generated by plants outside the county, and are considered as supply facilities for electrical power. The 23kv and 12kv electrical power substations numbered from 9 to 45 are considered as demand facilities. Electrical transmission lines are considered as distributing elements which route the electrical power from gate stations to customers through substations.

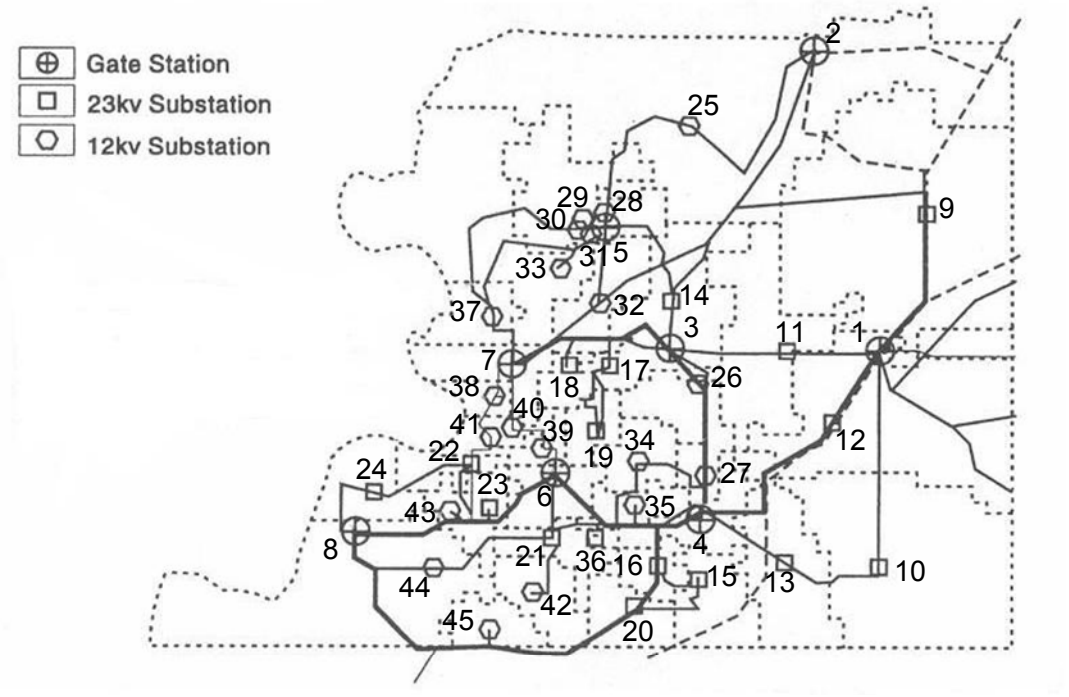

Figure 6-3 Electrical power system in Shelby County, TN. (modified from Shinozuka et al., 1998)

6.3 Damage Assessment of Network Components

6.3.1 Damage Assessment of Distributing Elements

Water and electrical power are delivered from supply facilities to customers through demand facilities and distributing elements. It is assumed that damage to electrical power distribution systems can be assessed from the damage to transmission towers since the transmission lines, which are suspended from the transmission towers, are highly compliant and thus are essentially free from seismic excitation (Jin et al., 2002). Similarly, it is assumed that damage to the distributing elements in the water system can be assessed from the damage to water mains.

Previous research analyzing the seismic vulnerability of water pipes has led to relations between seismic intensity and pipe break density (Katayama et al, 1975; Eguchi, 1991; O'Rourke and Ayala, 1993). The *Guidelines* prepared by the American Lifeline Alliance (ALA) (American Lifelines Alliance, 2001) suggests that damage to water pipe caused by strong ground motion can be expressed as a function of peak ground velocity (PGV):

$$RR = K_1 \cdot (0.00187) \cdot PGV \tag{6-1}$$

where RR is the repair ratio, which is the number of pipe breaks per 1000 feet (305 m) of pipe length, K_1 is a coefficient determined by the pipe material, pipe joint type, pipe diameter and soil condition, and PGV has the units of in/sec. Water pipes installed in the Memphis area before 1960 were unlined cast iron; those installed between 1960 and 1975 were cement-lined cast iron and ductile iron, and those installed after 1975 were ductile iron. Only large-diameter water mains, with diameters from 6 inches to 48 inches (152 mm – 1,220 mm) (Shinozuka et al, 1992; Hwang et al., 1997; Shinozuka, 1998), are

considered in this study. Considering the typical water main and soil conditions in Memphis, it is assumed that K_1=0.5 (ALA, 2001).

In addition to strong ground motion, water pipes can be damaged due to permanent ground displacement (PGD) (Eguchi, 1983; Porter et al., 1992; ALA, 2001). The *ALA Guidelines* suggest that damage to water pipe caused by PGD due to mainly liquefaction can be estimated as follows (ALA, 2001):

$$RR = K_2 \cdot (1.06) \cdot PGD^{0.319} \tag{6-2}$$

where K_2 is a coefficient determined by the pipe material and the pipe joint type. According to Broughton et al. (2001), the flood plains along the Wolf, Loosahatchie and Mississippi Rivers in Shelby County may be susceptible to liquefaction. However, Broughton's liquefaction susceptibility map (Broughton et al., 2001) shows that zones with very high liquefaction susceptibility cover a relatively small area of Shelby County. Furthermore, liquefaction data from the Northridge earthquake (O'Rourke et al, 2000) indicated that permanent ground displacements (PGD) due to liquefaction occurred only in zones where the PGV exceeded 30 inch/sec. (75cm/sec.), a value that is much larger than the attenuated median PGV at any site in Shelby County. Thus, the possibility of pipe break caused by PGD due to liquefaction is neglected.

Under the assumption that the seismic intensity leads to a uniform demand on a water pipe connecting two facilities, the number of pipe breaks can be expressed by the Poisson probability law:

$$P[N = n] = e^{-RR \cdot L} \cdot \frac{(RR \cdot L)^n}{n!} \tag{6-3}$$

where n is the number of pipe breaks, RR is the repair ratio evaluated by Eq.6-1, and L is the length of pipe segment (expressed in terms of 1000-ft (305-m) segments). If, in

addition, it is assumed that a pipe segment cannot deliver water when the segment has at least one pipe break, the failure probability of the pipe segment can be expressed by the exponential distribution.

$$\begin{aligned} P_f &= 1 - P[N = 0] \\ &= 1 - e^{-RR \cdot L} \end{aligned} \tag{6-4}$$

In this study, the events describing failure of each pipe segment are assumed to be statistically independent. The detail of the failure probability of a water pipe is discussed in subsection 6.4.3.

6.3.2 Damage Assessment of Facilities

The functionality of an earthquake-damaged facility is determined by not only the physical damage to the facility itself but also the serviceability of other infrastructure systems to which it is connected. Furthermore, some facilities have backup systems to provide electrical power in the event that the functionality of the primary supporting system is lost or impaired; in this case, the effect of any backup system also should be considered. For example, some water pumping stations have auxiliary electric power generators (Cascos et al., 2004). A fault tree model, such as the simple model shown in Figure 6-4, can be used to integrate the functionalities of the primary and supporting systems in the overall system analysis.

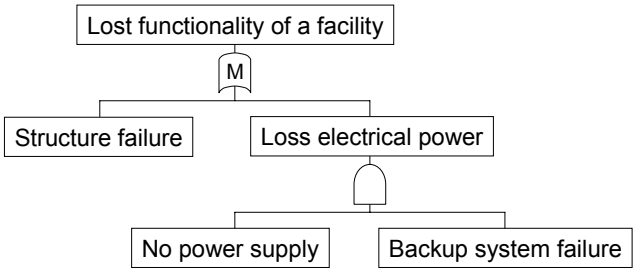

Figure 6-4 Fault tree model of the infrastructure interdependency effect on a facility

Using this fault tree model and assuming, for simplicity, that a facility is either fully-functional or non-functional, the probability of lost functionality of an earthquake-damaged water facility can be presented as;

$$P_f = P\left[F_{Physical} \cup \left(F_{Power} \cap F_{Backup}\right)\right] \quad (6\text{-}5)$$

where P_f is the probability of lost functionality of a water facility, $F_{Physical}$ is the event that the water facility loses its function due to physical damage, F_{Power} is the event that the necessary electrical power is not supplied to the water facility due to the lost function of an electrical power substation whose service area includes this water facility, and F_{Backup} is the event that the electrical power backup system fails to function and cannot supply electrical power to the water facility. The analysis of this fault tree can be performed using the reliability block diagram in Figure 3-6 or the following structure function:

$$\phi(x) = 1 - \left(1 - x_{Physical}\right) \cdot \left(1 - x_{Power} \cdot x_{Backup}\right) \quad (6\text{-}6)$$

where $x_{Physical}$=1 if the water facility is physically non-damaged after an earthquake, and $x_{Physical}$=0 otherwise. Similarly, if electrical power is available to the facility, x_{Power}=1; otherwise x_{Power}=0. If the backup system is non-damaged, x_{Backup}=1; otherwise x_{Backup}=0. Thus, $\phi(x)$=1 if the facility maintains the function after an earthquake; otherwise $\phi(x)$=0. Because of the characteristic of the structure function, x**.** and $\phi(x)$ can take either 1 or 0. These simple models are based on the assumption that the facility is either fully functioning or non-functioning.

The seismic intensities affecting a facility and its backup system at a specific site are assumed to be perfectly correlated due to the proximity of the facility and backup

system, and thus are evaluated at the same seismic intensity. In contrast, intensities affecting facilities and backup systems at different sites are assumed to be stochastically independent. It is assumed that only water pumping stations have backup electrical power facilities.

The probability of physical damage to a facility is modeled by the seismic fragilities that are presented in the *HAZUS MH* (FEMA, 2003) for various lifeline facilities. All fragilities are modeled by log-normal distribution functions that describe the probabilities of entering five damage states (DS), ranging from I (minor) to V (complete), as functions of peak ground acceleration (PGA). As an illustration, Table 6-1 summarizes the parameters of the fragility curves for facilities in the water and electrical power systems having damage state V. The water distribution nodes in the water distribution system (Figure 6-2) are assumed to be undamaged since they are simply the branch points in the piping system needed to distribute the water to customers. The fragilities defined by the parameters in Table 6-1 are plotted in Figure 6-5. As the fragility curve for a backup system, the fragility curve for 12kv substation is used in this study.

Table 6-1 Parameters of fragility curves (DS.V)

	Median (g)	Beta
Gate station	0.47	0.40
23km substation	0.70	0.40
12kv substation	0.90	0.45
Elevated water storage tank	1.50	0.60
Pumping station	1.50	0.80

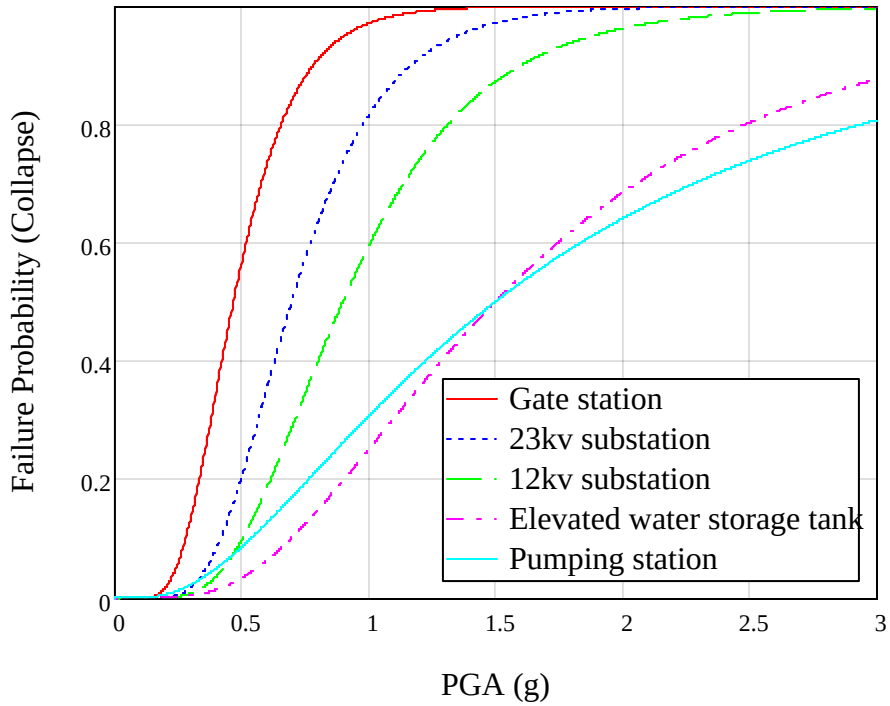

Figure 6-5 Fragility curves of facilities

6.4 Serviceability Assessment of a Networked System subjected to Correlated Seismic Intensities

When a networked system has a series structure, the function is maintained if and only if all components within the networked system are functioning. When a networked system has a parallel structure, the function is maintained if at least one component within the networked system is functioning. A general networked system is modeled as a combination of the two system structures.

6.4.1 Generation of Spatially Correlated Seismic Intensity

The failure probability of a networked system which has a series structure can be calculated as follows:

$$P(F_S) = \sum_{i=1}^{n} P(F_i) - \sum\sum_{i<j}^{n} P(F_i \cap F_j) + \sum\sum\sum_{i<j<k}^{n} P(F_i \cap F_j \cap F_k) - \cdots \quad (6\text{-}7)$$

where $P(\bullet)$ is the probability of an event, F_S is the failure event of a system, n is the number of components in the system and F_i is the failure event of a component i. Since the failure mode of a series system involves component failure events that are neither perfectly correlated nor mutually statistically independent, the failure probability of a system has (first-order) lower and upper bounds (Cornell, 1967):

$$\max_{i=1}^{n}[P(F_i)] \le P(F_S) \le 1 - \prod_{i=1}^{n}[1 - P(F_i)] \quad (6\text{-}8)$$

The failure probability of a networked system is equal to the lower bound when all component failure events are stochastically dependent, and is equal to the upper bound when all component failure events are statistically independent.

When a networked system has a parallel structure, its failure probability can be calculated as:

$$P(F_S) = P\left(\bigcap_{i=1}^{n} F_i\right) \quad (6\text{-}9)$$

The failure probability of a system with a parallel structure has upper and lower bounds:

$$1 - \sum_{i=1}^{n}[1 - P(F_i)] \le P(F_S) \le \min_{i=1}^{n}[P(F_i)] \quad (6\text{-}10)$$

The failure probability of the system is equal to the lower bound when all component failure events are statistically independent, and is equal to the upper bound when all component failure events are stochastically dependent. As a practical matter, this lower bound is approximately zero in realistic systems.

Since components within a networked system are distributed over a geographical area in which the intensity of ground motion can be modeled as a stochastic field, seismic intensities at the locations of components from the scenario earthquake are correlated. Seismic intensity is often modeled by a log-normal random variable since an attenuated seismic intensity at the site is modeled as a product of a function of earthquake magnitude, epicentral distance to the site, fault characteristics and local site characteristics (see Sec.3.4.2 of Kramer (1996) for details). Thus, to evaluate network reliability, a method for generating vectors of correlated lognormal random variables is required. A mathematical approach to generate a correlated log-normal random vector is illustrated in Kiureghian and Liu (1986) and Ditlevsen and Madsen (1996).

6.4.2 Bounds on Failure Probabilities of Facilities

As noted previously, Takada and Shimomura (2003, 2004), Shimomura and Takada (2005) and Wang and Takada (2005) found that the correlation of logarithmic residuals of seismic intensities at two sites can be evaluated using Equations 4-17 and 4-18. Seldom is there sufficient information on seismic wave propagation or local site conditions to define correlation distance b. Accordingly, we consider two extreme cases: perfectly correlated seismic intensities and perfectly independent seismic intensities. Statistically independent seismic intensities are generated as follows:

$$X_i = \overline{X_i} \cdot \varepsilon_{Xi} \tag{6-11}$$

where ε_{Xi} is the residual of seismic intensity, defined by a lognormal distribution. On the other hand, perfectly correlated seismic intensities are generated as,

$$X_i = \overline{X_i} \cdot \varepsilon_X \tag{6-12}$$

where ε_X is a lognormal random variable, which is the same for all components within a networked system.

6.4.3 Bounds on Failure Probabilities of Distribution Elements

The water main is modeled as a line superposed on the stochastic field describing seismic intensity and the PGV varies over its length. Thus, the failure probability of a water pipe can be computed by considering the number of pipe breaks to be a spatially non-homogeneous Poisson process (Rausand and Hoyland, 2004):

$$P_f = 1 - \exp\left(-\int_L RR\left(PGV(s)\right) ds \right) \tag{6-13}$$

where RR(•) is the repair ratio expressed as a function of PGV(s) (Eq.6-1) which is a function of site s, and L is the length of a water pipe. Since PGV(s) is a continuous function along the length of pipe, PGV values at discrete points need to be used. When a single PGV value is used to compute P_f of a water pipe of length L (Figure 6-6(a)), the spatial distribution of PGV for a water pipe may not be modeled correctly if the length L is too long for the segment to be considered as one discrete component. In this case, L should be divided into a sufficient number of short length water pipe segments, with PGV assigned to each segment, to compute P_f of the pipe (Figure 6-6(b)) as follows:

$$P_f = 1 - \exp\left(-\sum_{i=1}^{m} RR\left(PGV_i\right) \cdot \Delta L_i \right) \tag{6-14}$$

where PGV_i is a PGV value for a water pipe segment i, ΔL_i is the length of a water pipe segment i, and m is the number of water pipe segments.

The number of pipe segments required to achieve an accurate estimate of P_f depends on the correlation distance, b, of the seismic intensity. If b=0 km, the seismic intensities at the two sites are statistically independent. Figure 6-7 illustrates the relation between the number of segments of water pipe and P_f of the water pipe calculated by Eq.6-21 with three correlation distances: b=0 km, 10 km, and 30 km. The length of the water pipe L is 20 km. The distribution of PGV over the length of water pipe increases linearly from PGV=12 in/s at one end to PGV=15 in/s at the other end. The coefficient of variation of PGV is 60%. Figure 6-7 shows that P_f increases as the number of pipe segments increases, and that this trend holds for all three correlation distance cases. In other words, if the number of segments is small, there is a potential risk that P_f will be underestimated. Thus, a larger number of segments should be chosen to avoid underestimating P_f.

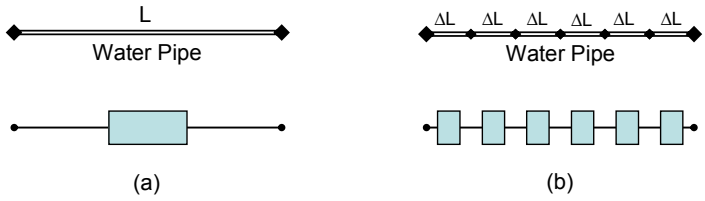

Figure 6-6 PGV distribution along a water pipe:
(a) An original water pipe and its reliability block diagram
(b) A segmented water pipe and its reliability block diagram

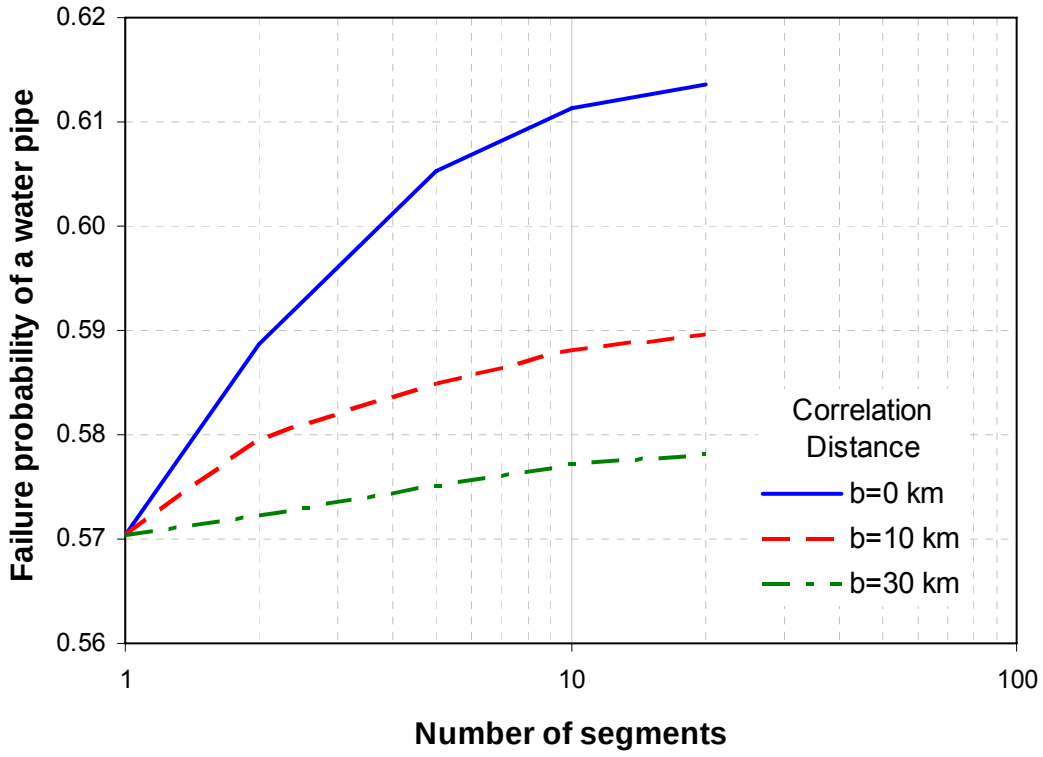

Figure 6-7 Relation between number of segmentation of a water pipe and failure probability of a water pipe

As with the facilities, determination of correlation distance b in Eq.4-17 is problematic. Thus, two extreme cases (perfectly correlated seismic intensities and perfectly independent seismic intensities) are considered. When a segmented water pipe is modeled as a series system with short segment lengths (Figure 6-6(b)), an upper-bound estimate of failure probability is obtained if the PGVs are modeled as statistically independent random variables, and has a lower bound if the PGVs are modeled as perfectly correlated variables (Eq.6-8).

The repair ratio RR is actually a function of PGV, and thus is a random variable. Removing the conditioning on RR and assuming that the seismic intensities are statistically independent, the failure probability is as follows:

$$\begin{aligned} E[P_f] &= E[P[\exists N_i \neq 0, i = 1 \cdots m]] \\ &= 1 - E[P[\forall N_i = 0, i = 1 \cdots m]] \\ &= 1 - \prod_{i=1}^{m} \int_{PGV_i} P[N = 0 \mid PGV_i = pgv_i] \cdot P[PGV_i = pgv_i] \\ &= 1 - \prod_{i=1}^{m} \int_0^{\infty} \exp(-RR(PGV_i) \cdot \Delta L_i) \cdot f_{PGV_i}(pgv_i) \cdot dpgv_i \\ &= 1 - E\left[\exp\left(-\frac{CL}{m}\sum_{i=1}^{m} PGV_i\right)\right] \\ &= 1 - E\left[\exp\left(-\frac{CL}{m}\sum_{i=1}^{m} \overline{PGV_i} \cdot \varepsilon_{PGVi}\right)\right] \end{aligned} \tag{6-15}$$

where N_i is the number of pipe breaks within a pipe segment i, pgv_i is the PGV for pipe segment i, described by a lognormal random variable whose median is computed by the attenuation relationship and coefficient of variation is 60%, f.(•) is a lognormal probability density function, ΔL_i is assumed to be same in all elements, C=K•0.00187, $\overline{PGV_i}$ is the median value of PGV for a water pipe segment i, and ε_{PGVi} is the residual of the PGV for a water pipe segment i. To avoid underestimating the failure probability, the limit of the expected failure probability is evaluated when m goes to infinity:

$$\begin{aligned} \lim_{m\to\infty} E[P_f] &= \lim_{m\to\infty}\left\{1 - E\left[\exp\left(-\frac{CL}{m}\sum_{i=1}^{m} PGV_i\right)\right]\right\} \\ &= 1 - E[\exp(-CL\mu_{PGV})] \end{aligned} \tag{6-16}$$

where μ_{PGV} is the average PGV for the entire length of pipe.

Conversely, when the seismic intensities along the pipe length are perfectly correlated, the unconditional failure probability is,

$$
\begin{aligned}
E\left[P_f\right] &= 1 - E\left[\exp\left(-\frac{CL}{m}\sum_{i=1}^{m} PGV_i\right)\right] \\
&= 1 - E\left[\exp\left(-\frac{CL}{m}\sum_{i=1}^{m} \overline{PGV_i}\cdot\varepsilon_{PGV}\right)\right]
\end{aligned}
\tag{6-17}
$$

The last right-hand member in Eq.6-24 has a similar expression as that under statistically independent seismic intensities. The critical difference is that ε_{PGV}, which is the residual of the PGV, is assumed to be constant with respect to a pipe segment i. To avoid the underestimation of failure probability, the limit of the expected failure probability is evaluated when m goes to infinity:

$$
\begin{aligned}
\lim_{m\to\infty} E\left[P_f\right] &= \lim_{m\to\infty}\left\{1 - E\left[\exp\left(-\frac{CL}{m}\sum_{i=1}^{m} \overline{PGV_i}\cdot\varepsilon_{PGV}\right)\right]\right\} \\
&= 1 - E\left[\exp\left(-CL\mu_{PGV}\varepsilon_{PGV}\right)\right] \\
&= 1 - G_{\varepsilon_{PGV}}\left(-CL\mu_{PGV}\right)
\end{aligned}
\tag{6-18}
$$

where $G_{\varepsilon_{PGV}}(\bullet)$ is the moment generating function of ε_{PGV}. Thus, the failure probability of a water main is,

$$
1 - G_{\varepsilon_{PGV}}\left(-CL\mu_{PGV}\right) \le E\left[P_f\right] \le 1 - E\left[\exp\left(-CL\mu_{PGV}\right)\right] \tag{6-19}
$$

The upper and lower bounds in Eq.6-26 are (1) independent of correlation distance, and (2) independent of the number of segments used to idealize the pipe. The first characteristic avoids the difficulty of determination of the autocorrelation in intensity when there is insufficient data. The second characteristic removes the dependence of failure probability on pipe segmentation (which is a modeling choice rather than a physical attribute of the water distribution system) and enhances the efficiency of the computation of network serviceability. Though the use of Eqs.6-18, 6-19, 6-23 and 6-25 will cause errors in the results of serviceability assessment of infrastructure systems, this

enables seismic intensities to be generated without information on correlation distance b (Eq.4-17). A comparison of exact and approximate failure probabilities is made later in this chapter.

6.5 Serviceability Assessment of Infrastructure Systems

Using the de-aggregation analysis provided by the USGS (2002a) at the City of Memphis, a scenario earthquake, with magnitude M_w 7.7 and epicenter located at 35.3N and 90.3W, is selected to apply the serviceability assessment of the water distribution system and the electrical power transmission system. This scenario earthquake is the Maximum Probable Earthquake (MPE) at a 2475-year return period, which corresponds to 2% probability of exceedance in 50 years (Table 4-3). The average epicentral distance of this scenario event to the city of Memphis is about 33 km.

The seismic intensity at a site from an earthquake with magnitude M_w and epicentral distance R from that site is determined by an attenuation relationship, modified by the local soil conditions. The attenuation relationships illustrated in Section 4.1 describe the median ground motion intensity (defined as either peak ground or spectral parameters) as a function of moment magnitude M_w and epicentral distance R. There is considerable scatter around the estimated median, and the coefficients of variation (COV) in the ground motions predicted by these attenuation curves typically are on the order of 0.50-0.70. According to Hwang et al. (1998), Shelby County is located within the Mississippi embayment, and the local site conditions in the region correspond mainly to site categories D and E as specified in the *2003 NEHRP Provisions* (FEMA, 2004).

In this study, the attenuation relationships for PGA and PGV proposed by Atkinson and Boore (1995) is selected since they both are based on the same ground

motion records and computational approach; the coefficient of variation associated with this relationship, which measures the aleatory uncertainty in ground motion intensity at the site (Toro et al., 1997) is set equal to 0.60. The soil condition is assumed to be categorized by site category D over the entire area in the absence of detailed information on local site conditions, and the local soil amplification factors defined in the *2003 NEHRP Provisions* (FEMA, 2004) are used.

The procedure followed for serviceability assessment of the infrastructure systems following an earthquake, considering the effects of the infrastructure interdependency and the effort of the electrical power backup system under the correlated seismic intensities (PGA and PGV), is summarized in Figure 6-8.

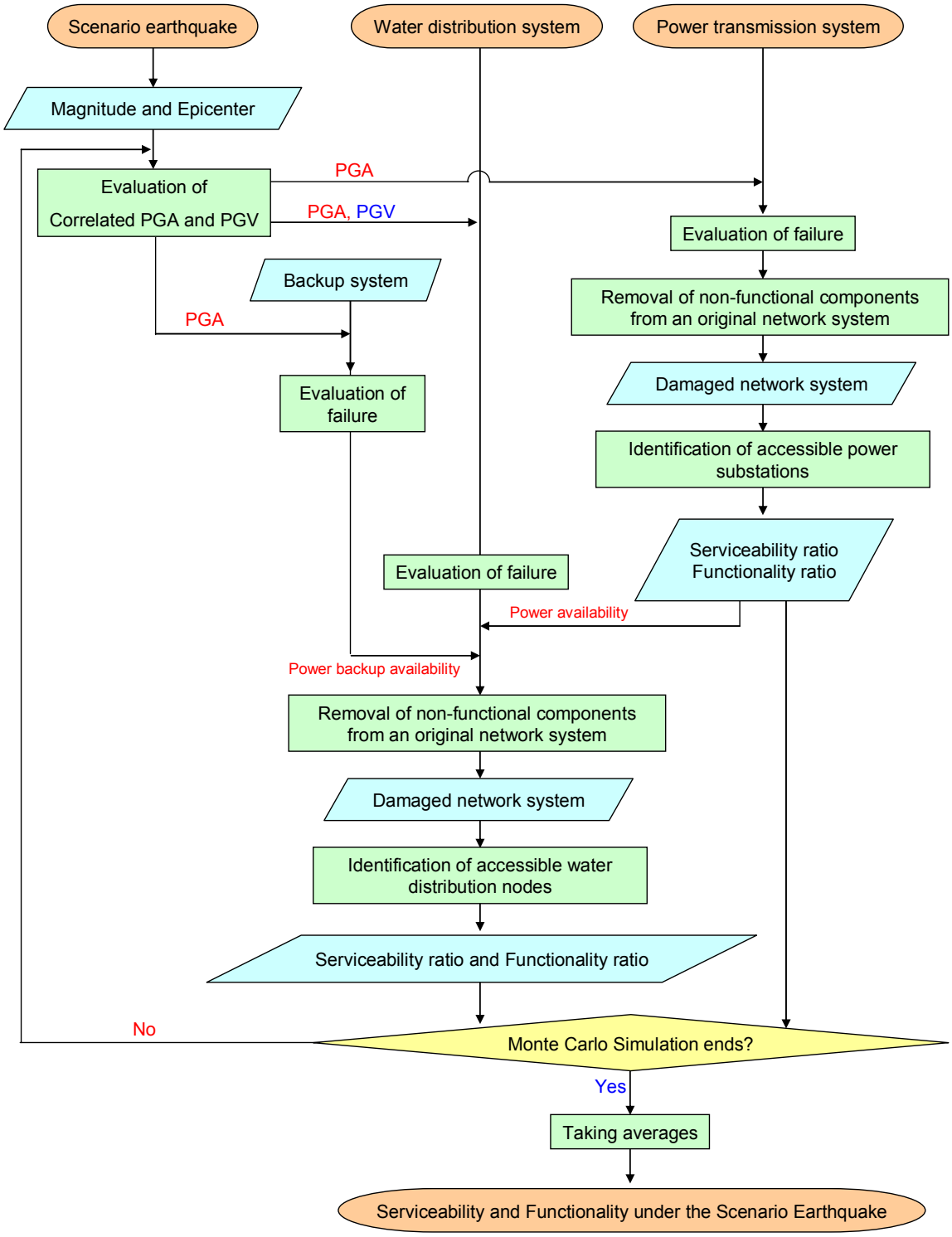

Figure 6-8 Flow chart of the serviceability assessment of infrastructure systems considering infrastructure interdependency

In most cases, customers in a particular service area receive water or power from a facility serving that area. Thus, the serviceability of the water distribution system following the earthquake is directly related to the number of water distribution nodes in the network which remain accessible from at least one supply facility following the earthquake. In a similar way, the serviceability of the power system following the earthquake is determined from the number of substations which are accessible from at least one gate station. In this case, a measure of the serviceability ratio can be computed as:

$$P[S \le s] = P\left[S \le \frac{\sum_{i=1}^{N} (\omega_i \cdot X_i)}{\sum_{i=1}^{N} \omega_i} \right] \tag{6-20}$$

where S is the serviceability ratio of an infrastructure system defined on the domain [0,1], where s = 0 implies complete loss of serviceability, while s = 1 implies unimpaired function, ω_i is a weighting factor assigned to facility i, and X_i represents the functionality ratio of facility i. Since only two states - non-functioning and fully-functioning - are considered, X_i is modeled as the outcome of a Bernoulli trial: $X_i = 1$ if facility i is non-damaged and can receives its commodity from at least one supply facility (full-function), otherwise $X_i = 0$ (non-function). N is the number of water distribution nodes or number of substations. The weighting factor ω_i is dependent on the goal of the serviceability assessment. For example, if the number of customers who can receive the resources after an earthquake is of interest, ω_i might be determined by the number of customers in the service area of the facility i. Similarly, the amount of sales in the service area of facility i can determine the weighting factor when industrial productivity

is of concern. If the importance level of all demand nodes is same, Eq.6-27 can be rewritten as:

$$P[S \le s] = P\left[S \le \frac{\sum_{i=1}^{N} X_i}{N} \right] \tag{6-21}$$

In this study, the serviceability of the water distribution system and those of the electrical power transmission system are determined from the functionality X_i of the water distribution nodes and the 23kv and 12kv substations, respectively. Furthermore, it is assumed that all nodes in the water distribution system and all substations in the electrical power system have the same importance level for customers. The serviceability ratio of the water distribution system and those of the electrical power transmission system both are determined from Eq.6-28. The mean functionality ratio of water facility i is defined as the average of X_i.

The evaluation of the average serviceability ratio and the average functionality ratio of the water distribution system and those of the electrical power transmission system considering the effect of aleatory uncertainty in seismic intensities is performed using Monte Carlo simulation, with the number of trials set equal to 10,000. Since general infrastructure systems are comprised of a very large number of facilities and distributing elements, the short periodicity of certain pseudo-random number generating algorithms may be of concern. Accordingly, pseudorandom numbers in this analysis are generated using the Mersenne Twister algorithm (Matsumoto and Nishimura, 1998) which has long periodicity (2^{19937}-1) and 623-dimensional equi-distribution, while the pseudo-random numbers generated by the classical and widely used linear congruential generating algorithm has at most 5-dimensional equi-distribution. The programming

source codes written in C-language provided by Matsumoto (1997) and Wada (2002) are used in this study.

6.5.1 Water Distribution System

Figure 6-9 illustrates the effects of spatially correlated seismic intensity on the serviceability of the water distribution system. The serviceability is evaluated with three correlation distances: b=0 km (the seismic intensities are statistically independent each other), 30 km and Infinity in Eq.4-17 for both PGA and PGV. The case b=Infinity represents the case when seismic intensities are perfectly correlated. In Figure 6-9, items identified as 16 to 49 represent water distribution nodes, as shown in Figure 6-2.

Figure 6-9 shows that the functionality ratio at water distribution nodes ranges widely, from 0.01 at node 28 to 0.67 at node 44 when b=0 km, from 0.05 at node 28 to 0.70 at node 44 when b=30km, and from 0.07 at node 28 to 0.71 at node 44 when b=Infinity. This range of values can be attributed to the relative distances of the nodes from water storage tanks which supply water to the node, the damage of such water storage tanks, and the redundancy of the earthquake-damaged water system. Conversely, if the demand facilities are located far from supply facilities (e.g. node 39) or if their redundancy of accessibility is poor (e.g. node 28), their residual serviceability ratio becomes small.

Figure 6-9 reveals three trends: (1) the functionality ratio of any water distribution node increases when the spatial correlation of seismic intensity is stronger, (2) the functionality ratio changes in some nodes (e.g., nodes 20 to 27 and 29 to 42) more than others when the functionality ratio in b=0km and in b=30km are compared, and (3) the

functionality ratio changes slightly in all nodes when the functionality ratio in b=30km and in b=Infinity are compared.

The first trend implies that the Shelby County water distribution system behaves more like a series system than a parallel system since the components connected in series return the larger serviceability ratio (the complement of system failure probability) in the networked system with stronger correlation effect (Eq.6-8). This implies that the water distribution system has small redundancy as a networked system. The serviceability ratio of the entire water distribution system shows that the water distribution system behaves more like a series system.

The second trend appears at water distribution nodes that either are located a long distance from any elevated water storage tank or are located in northwestern Shelby County, which is close to the epicenter of the scenario earthquake used in this study. In either situation, the trend reflects the fact that the range of system failure probabilities shown in Eq.6-8 is large when the failure probabilities of components are large. This means either that the components are located closer to the epicenter of the scenario earthquake or that the number of components locating between elevated water storage tanks and the water distribution node focused on is large.

The third trend is explained by Figure 6-7, which shows that the system failure probability changes more rapidly when correlation distances are short under a specific number of segments (e.g. P_f with b=0km and b=30km under N=10).

From the results shown in Figure 6-9, one might conclude that the effect of spatially correlated seismic intensity on the serviceability assessment of the water distribution system is not negligible, especially in case that either the function of

components located close to the epicenter of the scenario earthquake or the function of components located far from water storage tanks is evaluated, and in case that the correlation distance is assumed to be relatively small (e.g. b=0~30km in this study). Furthermore, the importance of spatial correlation effects is clear when the serviceability ratio of the entire water distribution system is evaluated.

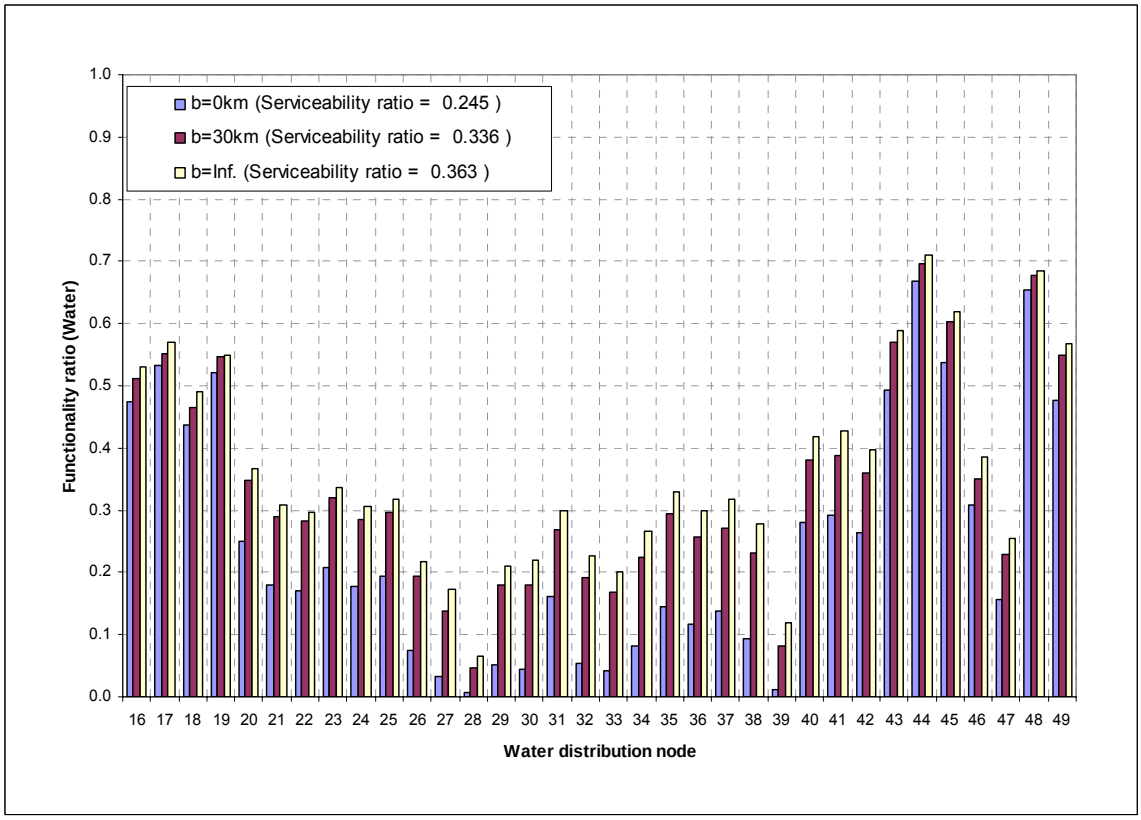

Figure 6-9 Functionality ratio of water distribution nodes (effect of spatially correlated seismic intensity)

Figure 6-10 illustrates the results of three additional serviceability analyses: (1) Functionality of the water distribution system is not dependent on electrical power availability ($F_{Power} = \phi$ in Eq.6-5 or $x_{Power}=0$ in Eq.6-6); (2) Functionality of the water distribution system is dependent on electrical power availability but backup electrical

power sources are not installed or are unavailable ($F_{Backup} = \Omega$ in Eq.6-5 or $x_{Backup}=1$); and (3) Functionality of the water distribution system is dependent on electrical power availability and backup power systems are installed.

The dependence of serviceability of the water distribution system on availability of electrical power is significant. Furthermore, the impact of power backup systems on serviceability of the water system is noticeable; Figure 6-10 shows that the functionality of the water distribution nodes are improved if a source of electrical power can be assured. Thus, availability of backup electrical power systems following a large earthquake is important to maintain the functionality of the water system in this case study.

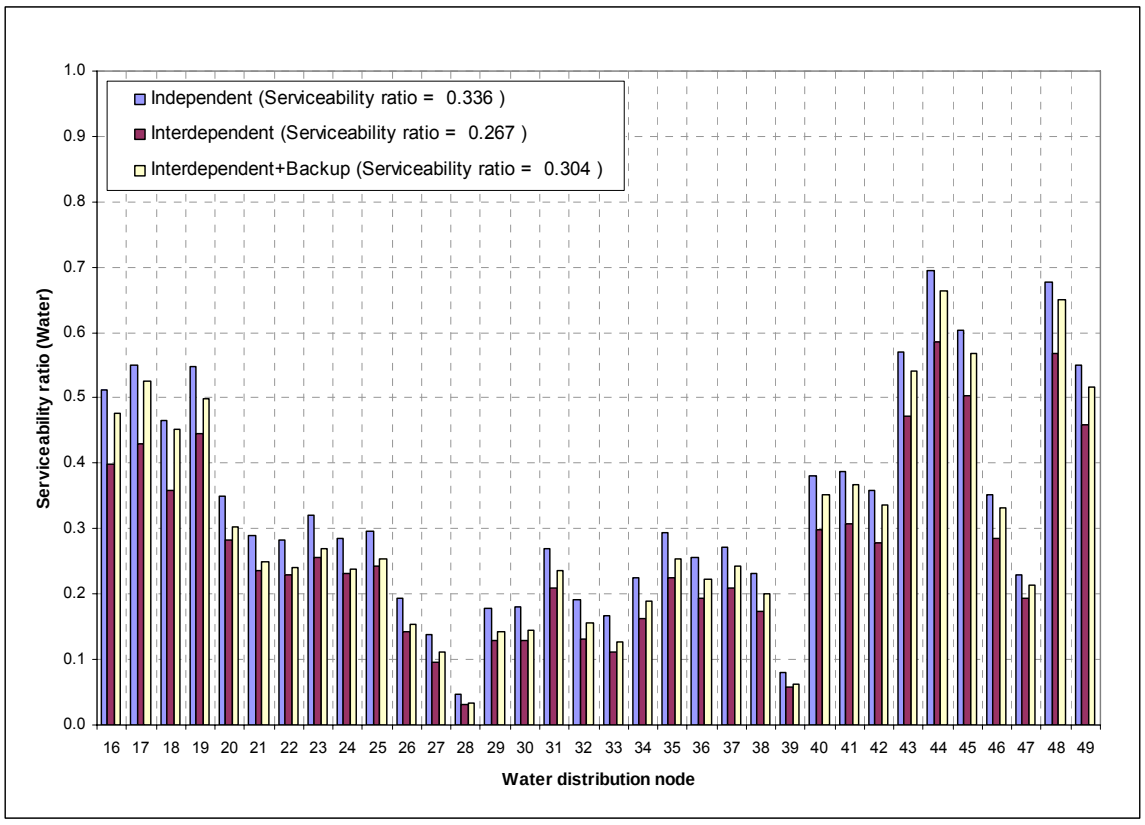

Figure 6-10 Functionality ratio of water distribution system (effect of infrastructure interdependency and electrical power backup systems)

6.5.2 Electrical Power Transmission System

Figure 6-11 illustrates the effects of spatially correlated seismic intensity on the serviceability of the electrical power transmission system. The serviceability is evaluated with three correlation distances: b=0 km, 30 km and Infinity in Eq.4-17. In Figure 6-11, items identified as 9 to 45 represent electrical power substations, as shown in Figure 6-3.

Figure 6-11 shows that the functionality ratio of substations ranges widely from 0.24 at node 24 to 0.79 at node 9 when b=0 km, from 0.35 at node 24 to 0.74 at node 44 when b=30km, and from 0.37 at node 24 to 0.71 at node 9 when b=Infinity. This range of values can be attributed to their relative distances from the gate stations which supply power to the substation, the damage of such substations, and the redundancy of the earthquake-damaged electrical power transmission system.

In contrast to the results for the water distribution system shown in Figure 6-9, the increase in correlation distance does not always cause the functionality ratio of the substations to increase. This implies that electrical power transmission system behaves as a mix of parallel and series systems. Since the components connected in series return the larger serviceability ratio (the complement of system failure probability) in the networked system with stronger correlation effect (Eq.6-8) and the components connected in parallel return the smaller serviceability ratio with stronger correlation effect (Eq.6-10), some substations (e.g. 9, 10, 27 and 32) behave more like component in a parallel system and other substations (e.g. 19, 22, 23 and 24) behave more like components in a series system. The mixed effects of connection in series and in parallel are apparent in some substations (e.g. 16, 20 and 44). The serviceability ratio of the entire electrical power transmission system likewise represents the mixed effects.

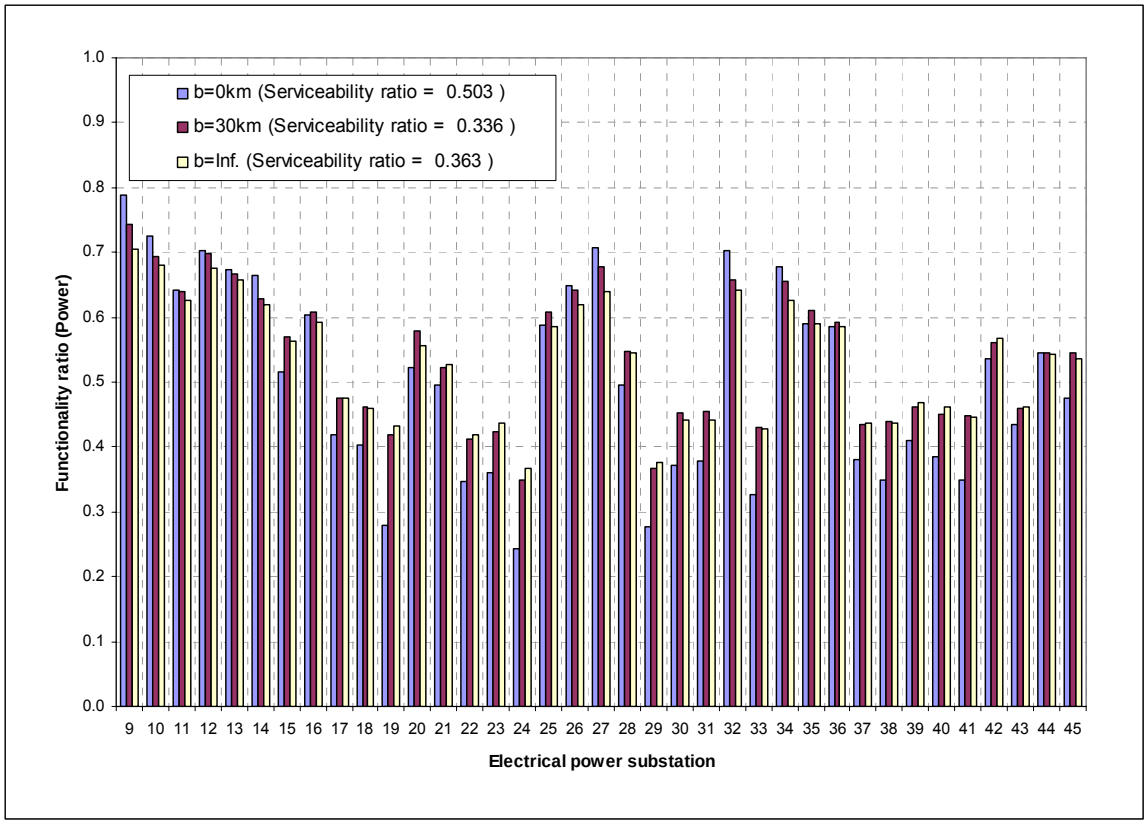

Figure 6-11 Functionality ratio of electrical power substations (effect of spatially correlated seismic intensity)

6.5.3 Serviceability Bounds on Water Distribution System

The serviceability bounds of the water distribution system are evaluated by the approximate procedure developed above, leading to an estimate of bounds of the mean functionality ratio at each water distribution node and bounds of the mean serviceability ratio of the entire water distribution system.

Figure 6-12 illustrates the result of the serviceability assessment of the water system under the assumption that the correlation distance b=30 km for PGA and PGV, which is reasonable according to Takada and Shimomura (2003 and 2004), Shimomura and Takada (2004) and Wang and Takada (2005). Infrastructure interdependency is not considered in this analysis.

The exact solutions are obtained by dividing each water main into 20 equal-length segments; at this level of discretization, about $275 \cdot 10^7$ iterations are needed to obtain all exact solutions of the water distribution system by the Floyd-Warshall algorithm. The upper bound on failure probability of a water pipe is computed under the assumption that the PGVs along the length of pipe are statistically independent using Eq.6-23, to avoid difficulties in determining the number of pipe segments and to reduce computing time; this yields a lower bound (LB) solution to the functionality ratio of each distribution node and the serviceability ratio of the water distribution system. In contrast to the exact solution, only about $118 \cdot 10^3$ iterations are required to obtain all LB solutions from the Floyd-Warshall algorithm. The lower bound on failure probability of a water pipe is computed under the assumption that the PGVs along the length of pipe are perfectly correlated using Eq.6-28; this yields a upper bound (UB) solution on a functionality ratio of each distribution node and a serviceability ratio of the water distribution system. But, since no closed-form solution for the moment generating function of the log-normal distribution used for ε_{PGV} in Eq.6-25 exists, there is no advantage to obtaining UB solutions in this case study. However, since UB solutions are unconservative, this is not a practical problem. In this case study, UB solutions are evaluated by segmenting each water main into 20 equal-length segments using Eq.6-24 with m=20, in place of using the closed-form (Eq.6-25).

As would be expected, the exact functionality ratio in Figure 6-12 is between the upper bound (UB) and the lower bound (LB). The maximum difference between the upper and the lower bounds of functionality ratio is 0.082 at distribution node 40; the maximum difference between the exact functionality ratio and the lower bound is 0.063

at distribution node 20, which is small enough for the LB solution to be used in practical applications. The difference in serviceability ratio between UB and LB is 0.051, while the difference between the exact solution and the LB is 0.041. The required number of iterations to obtain a LB solution from the Floyd-Warshall algorithm is only 0.0043% of the number required to obtain an exact solution. Thus, the LB solution for network serviceability ratio is useful in a practical sense for decision-making.

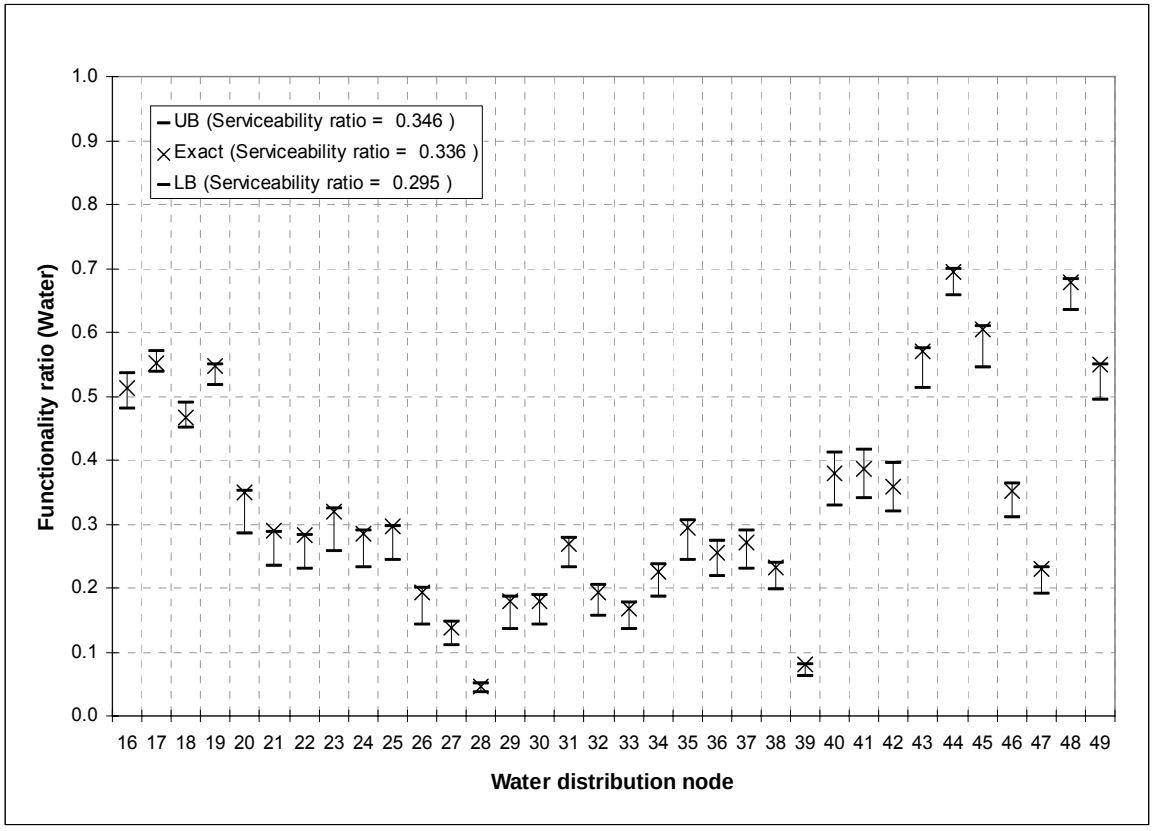

Figure 6-12 Bounds on functionality ratio of water distribution system (correlation distance b=30km)

6.6 Summary

The serviceability of the water distribution system and the electrical power transmission system following a scenario earthquake was presented in this chapter, taking

into account spatial correlations in seismic demand on facilities within the system. Seismic intensities (PGA and PGV) representing demands on the network system were modeled as a stochastic field along connecting elements in the distribution network. Lower and upper bounds on the failure probability were obtained by assuming that the seismic intensity field is fully correlated over the network or is effectively uncorrelated from point to point. The bounds are independent of how the piping system is discretized in the network analysis, which otherwise would increase the dimensions of the random vectors required to model spatial variation in seismic demands on the system.

The feasibility of this method was demonstrated by an application to the water distribution system in Shelby County, TN. The case study revealed that the functionality of the water distribution nodes and the serviceability of the water distribution system evaluated by using the upper and lower bounds are sufficiently close to the exact results that the bounds would be useful for practical risk mitigation decision purposes. A lower bound solution can be obtained at only 0.0043% of the computational effort required for an exact solution. Since the number of iterations required to obtain a Floyd-Warshall solution to network serviceability is proportional to the cube of the number of nodes in the system, as described in Section 3.3, the lower bound solution should be even more efficient when more complicated networked systems are analyzed.

CHAPTER 7

SERVICEABILITY ASSESSMENT BASED ON UNIFORM SEISMIC HAZARD CONTOURS

In Chapter 6, the serviceability of infrastructure systems under a scenario earthquake was assessed. However, such an assessment for a single scenario earthquake, which occurs with a low but non-quantified probability, does not provide enough information to estimate the cost of insurance to cover the expected losses due to a spectrum of possible earthquakes impacting the community, to design new infrastructure systems, and to retrofit existing infrastructure systems. The expected serviceability of infrastructure systems due to a spectrum of possible earthquakes, ranging from the frequent to infrequent, is required for these decisions. While the probabilistic seismic hazard map for a stipulated return period provided in the *ASCE Standard 7* (ASCE, 2005) and the USGS (2002b) can be applied for a site-specific seismic hazard analysis, such maps may not be suitable to evaluate the serviceability of a spatially distributed infrastructure system (Eguchi, 1991b; Ishikawa and Kameda, 1994; Chang et al., 2000; McGuire, 2001; Adachi and Ellingwood, 2007a), for the reasons introduced in Chapter 5.

In this chapter, the drawbacks of using a probabilistic seismic hazard analysis to assess risk to a spatially distributed infrastructure system, which were identified using the simple networked systems in Chapter 5, are explored more fully using the electrical power transmission system in Shelby County, TN. (Adachi and Ellignwood, 2007c). The expected serviceability of the water distribution system and the electrical power transmission system is evaluated by considering the spectrum of possible earthquakes for

six return periods (4975, 2475, 975, 475, 224 and 108 years) (Adachi and Ellignwood, 2007d).

7.1 Applicability Assessment of PSHA to a Real Networked System

In Chapter 5, the functionality ratios of facilities evaluated by the probabilistic seismic hazard (PSH) based and the scenario earthquake (SE) based approaches were compared using simple networked systems impacted by only two seismic zones. In this section, the PSH-based and the SE-based characterizations of hazard are applied to the evaluation of the electrical power distribution system in Shelby County, TN shown in Figure 6-3.

7.1.1 Determination of Scenario Earthquakes

As illustrated in Ch.4, a PSHA considers all possible earthquakes affecting a region of interest. De-aggregation analysis determines the contributing earthquakes with their relative contributions at a certain return period. In this study, such earthquakes and corresponding spatially distributed peak ground accelerations (PGAs) are obtained from a deaggregation analysis at Memphis provided by the U.S. Geological Survey (2002a) for a 2475-year return period earthquake event, which corresponds to a 2% probability of exceedance in 50 years (Figure 4-8). This de-aggregation analysis reveals a large number of contributing earthquakes at this probability level; for the purposes herein, the ten most likely earthquakes, which contribute about 75% of the total hazard, are selected (Table 7-1). In order to determine a PGA that is comparable to the PGA obtained directly from the PSHA and to have a consistent basis for comparison, the original contribution ratios are normalized in the last column of Table 7-1 to sum to 100%. The epicentral distances

R shown in Table 7-1 are the approximate distances between each epicenter and Memphis. The attenuation relationship proposed by Toro, Abrahamson et al. (1997) with coefficient of variation of 0.6 is used to evaluate the PGA at the sites of facilities comprising the electrical power transmission system. The maximum and minimum PGA at all facility sites due to each scenario earthquake and the weighted PGA by the modified contribution ratio are shown in Table 7-2.

Table 7-1 Ten scenario earthquakes

Longitude (W)	Latitude (N)	Epicentral Distance to Memphis	Mw	Contribution ratio (%)	Modified contribution ratio (%)
90.3	35.3	33km	8.0	9.78	13.07
			7.7	24.78	33.10
			7.5	7.85	10.49
			7.3	4.70	6.28
90.5	35.5	61km	8.0	6.44	8.61
			7.7	12.26	16.38
			7.5	3.18	4.24
			7.3	1.52	2.03
90.7	35.6	83km	8.0	1.64	2.19
			7.7	2.70	3.61
Total				**74.86**	**100.00**

Table 7-2 Maximum and minimum PGA

Event	1	2	3	4	5	6	7	8	9	10	Weighted PGA
maxPGA (g)	0.62	0.55	0.50	0.73	0.30	0.33	0.35	0.40	0.27	0.31	0.45
minPGA (g)	0.28	0.25	0.23	0.32	0.15	0.17	0.20	0.23	0.16	0.19	0.27

7.1.2 Serviceability Assessment of the Electrical Power Transmission System under Uniform Seismic Hazard

The study of simple networked systems in Chapter 5 revealed that the fragilities of both individual facilities and the structure of the system network affect the functionalities of facilities within the network. Thus, two fragility curves corresponding

to “complete” and “extensive” damage states, which are defined in HAZUS MH (FEMA, 2003), are used to model the performance of each facility in this section. The fragilities are modeled by lognormal distributions, with parameters listed in Table 7-3. The serviceability assessment procedure is the same as that illustrated in Section 6.6. The number of networks analyzed by Monte Carlo simulation for purposes of estimating functionality and serviceability is 10,000, with the pseudorandom numbers being generated by the Mersenne Twister algorithm (Matsumoto and Nishimura, 1998) as before.

Table 7-3 Parameters of fragility curves (from FEMA, 2003)

Damage state	Gate station		23kv substation		12kv substation	
	median (g)	beta	median (g)	beta	median (g)	beta
Complete	0.47	0.40	0.70	0.40	0.90	0.45
Extensive	0.20	0.35	0.35	0.40	0.45	0.45

7.1.3 Results and Discussion

The functionality ratios of substations and the average functionality ratios are shown in Figures 7-1 and 7-2 for the “complete” and “extensive” damage states identified above. The numbers on the horizontal axis correspond to the substation numbers in Figure 6-3. Figure 7-1 shows that the functionality ratios of most substations evaluated by the PSH-based analysis are slightly larger than those evaluated by the SE-based analysis when the “complete” damage state fragilities are used. Conversely, Figure 7-2 shows that the functionality ratios of facilities evaluated by the PSH-based analysis are smaller than those evaluated by the SE-based analysis when the “extreme” damage state fragility is used. In this situation, then, using the PSH-based analysis will lead to a pessimistic appraisal of the readiness of the network following a great earthquake.

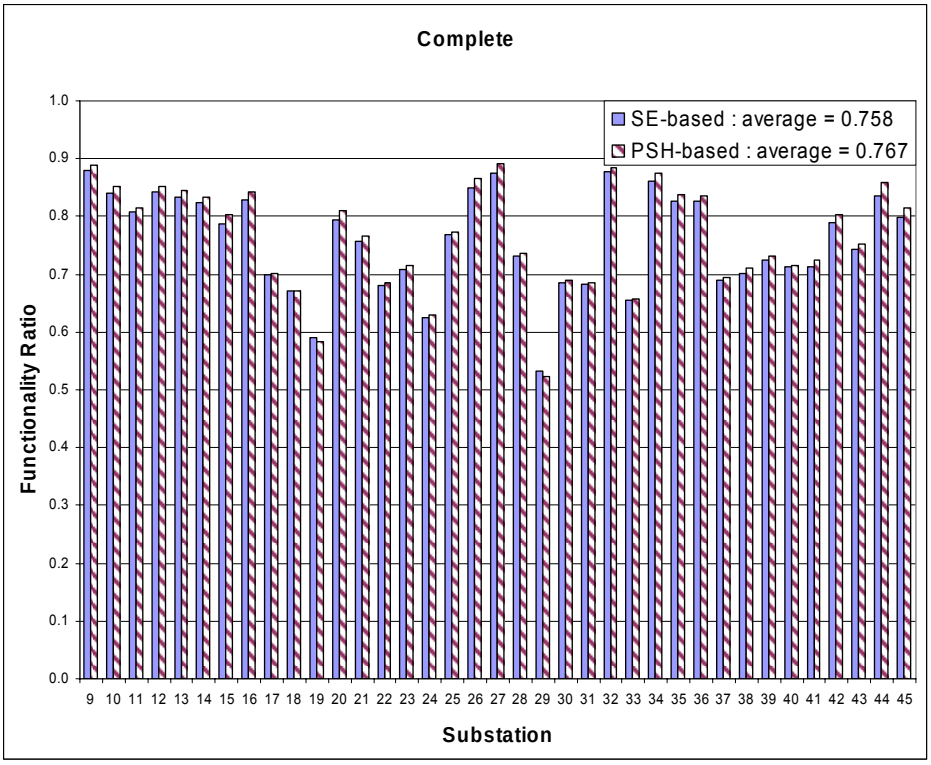

Figure 7-1 Functionality ratios of facilities: complete damage state

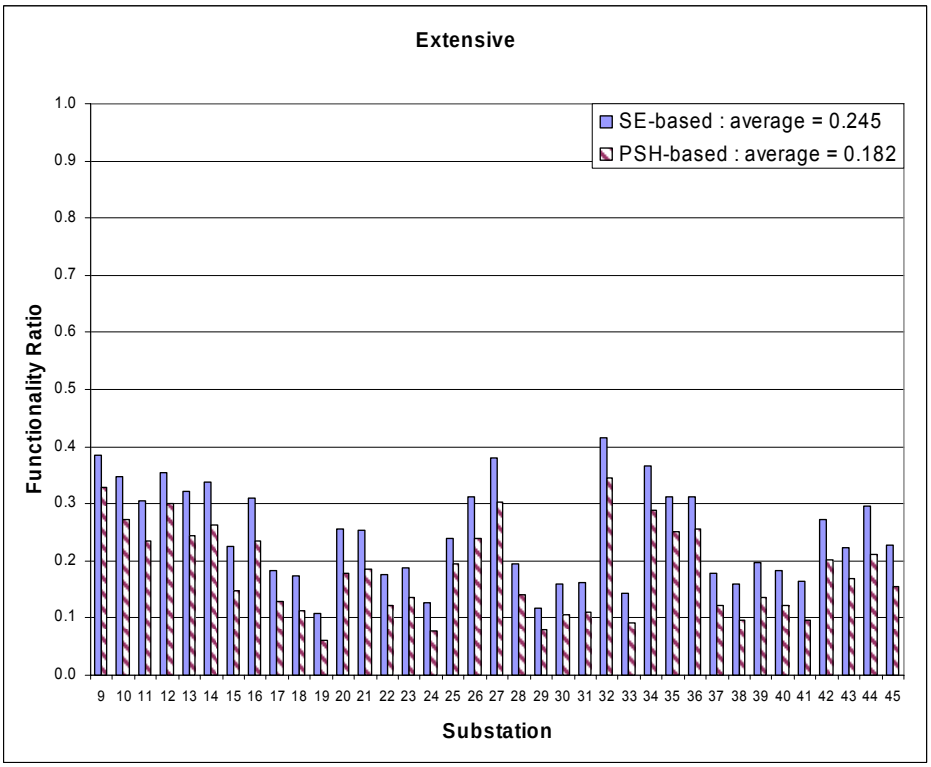

Figure 7-2 Functionality ratios of facilities: extensive damage state

The trends shown in Figures 7-1 and 7-2 can be explained by the relation between the system fragility curve and the survivor function in Figures 7-3 and 7-4. In Figures 7-3 and 7-4, E_a and E_b represent seismic intensities due to scenario earthquakes identified in Table 7-1: $E_a = \min(E_1, E_2, \cdots, E_{10})$ and $E_b = \max(E_1, E_2, \cdots, E_{10})$. (The eight remaining intensities are not shown for simplicity). In contrast, the seismic intensity from the *PSHA* represents the weighted average of the ten seismic intensities (E_1, E_2,…, E_{10}). The seismic intensity from the PSHA is within the domain $[E_a, E_b]$.

When the fragility curves for the "complete" damage state are used, Figure 7-3 shows that the functionality ratio determined from the SE-based analysis $Rs_{SE,Complete}$ is smaller than the functionality ratio from the PSH-based analysis $Rs_{PSHA,Complete}$. On the other hand, when the fragility curves for the "extensive" damage state are used, Figure 7-4 shows that the estimated failure probabilities are higher, even though the ten seismic intensities (E_1, E_2,…, E_{10}) and the *PSHA* are the same as those in Figure 7-3. The functionality ratio due to the SE-based analysis $Rs_{SE,Extensive}$ is larger than the functionality ratio due to the PSH-based analysis $Rs_{PSHA,Extensive}$.

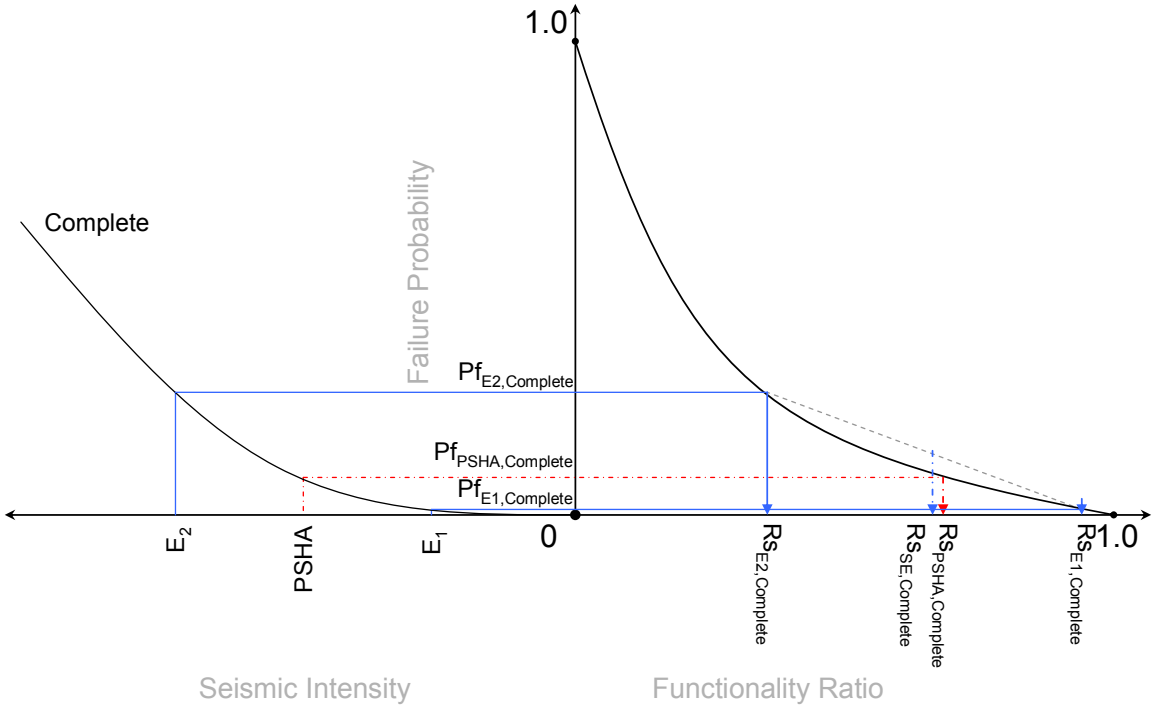

Figure 7-3 Functionality ratios evaluated under different system fragility curves: Fragility curve of complete damage state

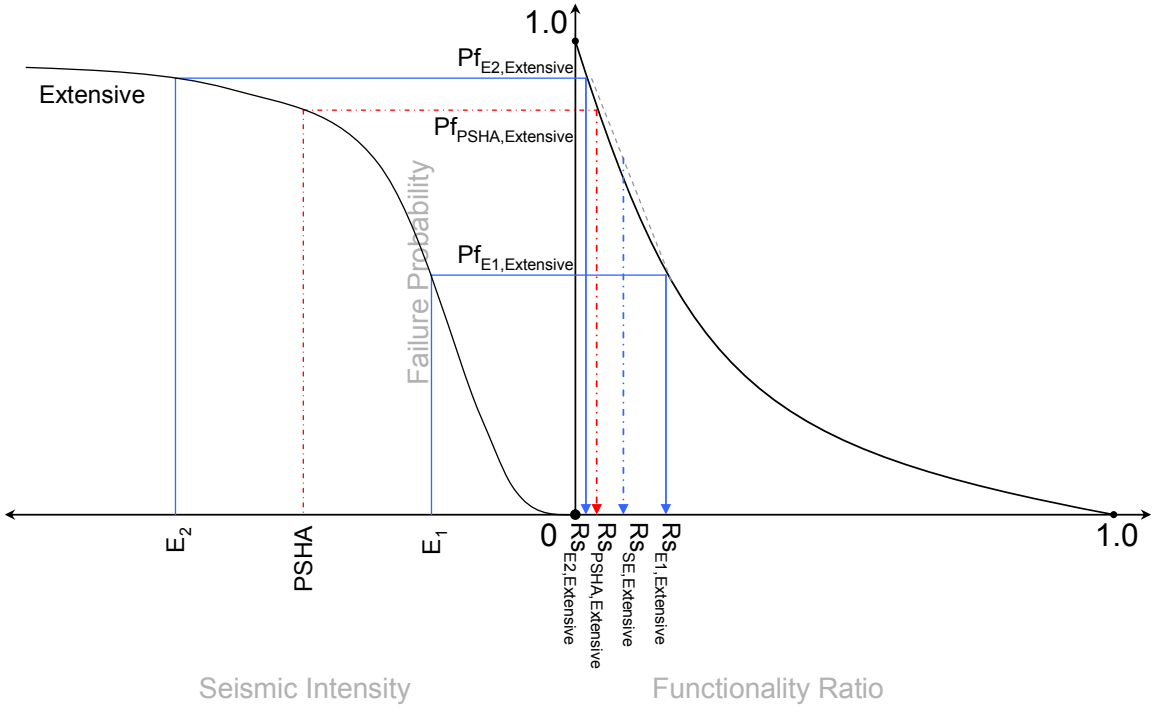

Figure 7-4 Functionality ratios evaluated under different system fragility curves: Fragility curve of extensive damage state

7.2 Serviceability Assessment under Uniform Seismic Hazard

The probabilistic seismic hazard (or uniform hazard) map is not suitable for assessing performance of spatially distributed infrastructure systems, and yet all possible earthquakes should be considered to evaluate the serviceability of infrastructure systems at a stipulated seismic hazard. According to Frankel et al. (1996 and 2002), earthquakes have occurred not only in the New Madrid seismic zone (NMSZ) but in the entire region surrounding Shelby County, TN, referred to as the background source zone. To evaluate the serviceability of infrastructure systems under a specified seismic hazard, the following steps should be followed:

1. For serviceability assessment for earthquakes identified as coming from the NMSZ;
    1.1. One earthquake from the NMSZ is generated, whose magnitude and epicenter are randomly determined; the frequency of magnitudes and epicenters are determined from the results of deaggregation assessment at Shelby County at a specific return period.
    1.2. The serviceability of the infrastructure system is assessed using the earthquake generated in Step 1.1 as a scenario earthquake, as illustrated in Chapter.6.
    1.3. Steps 1.1-1.2 are repeated to generate enough number of scenario earthquakes which include earthquakes with small frequency in the NMSZ. As an independent check, a plot of epicenters on the geographical map and a graph of magnitudes vs. epicentral distances should be compared with the results of the USGS deaggregation assessment used in Step 1.1.

2. For serviceability assessment due to earthquakes from the background source zones;
    2.1. One earthquake from the background source zones whose magnitude and epicenter are randomly determined is generated. The frequency of magnitudes and epicenters are determined from the results of deaggregation assessment at Shelby County at the specified return period.
    2.2. The serviceability of the infrastructure system is assessed using the earthquake generated in Step 2.1 as a scenario earthquake, as illustrated in Chapter 6.
    2.3. Steps 2.1-2.2 are repeated to generate a sufficient number of scenario earthquakes, which include earthquakes with small frequency in the NMSZ. A plot of epicenters on the USGS de-aggregation map and a graph of magnitudes vs. epicentral distances is compared with the results of de-aggregation assessment used in Step 1.
3. The average serviceability of the infrastructure system is computed by averaging the serviceability due to the earthquakes from NMSZ and the serviceability due to the earthquakes from the background source zones. The frequency ratios for the earthquakes from the NMSZ and from the background seismic zones are used as the weighting factors for averaging.
4. Steps 1-3 are repeated at different return periods, and a plot of the serviceability ratio vs. the annual frequency, which is the inverse the return period, is developed.

The generation of earthquakes from the NMSZ and from the background source zone is explained next.

7.2.1 Modeling Earthquakes from the New Madrid Seismic Zone

According to Frankel et al. (1996 and 2002), the New Madrid seismic zone is the only major seismic zone near to Shelby County, TN. (Figure 4-6). As a result of the deaggregation analysis for Memphis, the epicenters of earthquakes generated at the NMSZ at any return period are aggregated to three specific epicenters. Table 7-4 represents the locations of the earthquake epicenters, their magnitudes and their relative frequencies at each return period. The earthquakes whose frequency ratios are in boldface are the maximum probable earthquakes (MPE).

Table 7-4 Twelve characteristic earthquakes from NMSZ and their relative frequency

Longitude (W)	Latitude (N)	Epicentral Distance to Memphis	Mw	Frequency(%) Return period (years)					
				4975	2475	975	475	228	108
90.3	35.3	33km	8.0	16.18	12.91	8.16	5.14	3.88	3.74
			7.7	**36.88**	**32.71**	**24.38**	16.72	12.92	12.45
			7.5	10.88	10.36	8.76	6.51	5.16	4.98
			7.3	6.10	6.20	5.97	4.90	4.03	3.90
90.5	35.5	61km	8.0	7.90	8.50	9.08	8.61	7.65	7.47
			7.7	13.00	16.19	21.67	**25.22**	**25.13**	**24.87**
			7.5	3.05	4.19	6.56	8.93	9.89	9.94
			7.3	1.32	2.00	3.65	5.86	7.45	7.66
90.7	35.6	83km	8.0	1.72	2.17	2.90	3.52	3.72	3.73
			7.7	2.33	3.57	6.22	9.48	11.99	12.39
			7.5	0.46	0.83	1.74	3.13	4.63	4.93
			7.3	0.17	0.36	0.92	1.99	3.55	3.96
Total				100.00	100.00	100.00	100.00	100.00	100.00

7.2.2 Modeling Earthquakes from the Background Seismic Source Zones

In contrast to the NMSZ, the background seismic source zones are modeled as a number of seismic zones which are meshed by 0.2° in latitude and longitude in the CEUS

(Frankel et al., 1996 and 2002). Using the record of historical earthquakes, the a-values of the Gutenberg-Richter recurrence law are evaluated (Gutenberg and Richter, 1944; Kramer, 1996). The b-value of the Gutenberg-Richter recurrence low is 0.95, which is constant for the entire CEUS (Frankel et al., 2002). The maximum magnitude 7.5 is used for the bounded Gutenberg-Rechter recurrence law (Kramer, 1996). As results of de-aggregation analysis, the epicenters of the earthquakes occurring in the background seismic source zone are scattered throughout the area surrounding Shelby County at each return period (Figures 4-7 to 4-12). Since it is not feasible to identify each de-aggregated earthquake from the result of the de-aggregation analysis, a computer simulation is performed to determine the epicenter and the magnitude of earthquakes under the following assumptions;

- The frequency of a de-aggregated earthquake with magnitude (M_w) and epicentral distance (R) follows the list which is obtained as a result of the deaggregation analysis (e.g. de-aggregated earthquakes for 2475-year return period listed in Table 7-5). Since the deaggregation analysis shows the frequency of each binned M_w and R, it is assumed that M_w and R are uniformly distributed within the bin. Thus, M_w and R are computed as follows:

$$M_W = \overline{M}_W + \Delta m \tag{7-1}$$

$$R = \overline{R} + \Delta r \tag{7-2}$$

where $\overline{M}$ is the de-aggregated magnitude (e.g. M_w listed in Table 7-5), Δm is a random number which is uniformly distributed within [-0.1, 0.1), $\overline{R}$ is the de-aggregated epicentral distance (e.g. the epicentral distance listed in Table 7-5) and Δr is uniformly distributed random number within [-5.0, 5.0).

- The epicenter of the earthquake determined in the previous step is determined by an epicentral distance (R) and a randomly generated rotational angle (ɵ) whose frequency is distributed between [0°, 360°) based on the number of earthquakes identified in the results of deaggregation analyses in each octant (Figure 7-5).

Table 7-5 De-aggregated earthquakes from the background seismic zone at Memphis, TN (2475-year return period)

Epicentral distance, R (km)	Magnitude (Mw)	Frequency (%)
6.7	7.19	1.071
6.9	7.39	1.715
7.0	6.79	3.104
7.1	6.42	2.482
7.1	6.20	2.765
7.2	6.99	1.766
7.3	6.59	1.283
7.4	5.61	2.469
7.5	5.40	4.188
7.5	5.21	2.380
7.5	5.03	5.260
7.5	4.80	5.785
7.5	4.61	2.600
7.6	5.81	2.804
7.9	6.01	2.854
14.1	4.61	0.889
14.3	4.80	2.617
14.5	5.04	3.159
14.6	5.21	1.732
14.7	5.40	3.659
14.8	5.62	2.702
15.2	5.81	2.884
15.3	7.39	1.830
15.3	6.59	2.160
15.3	6.22	3.650
15.5	6.43	2.706
15.7	7.01	2.473
15.7	6.01	2.964
15.9	7.19	1.364
15.9	6.79	2.549
23.6	5.05	0.313
24.0	5.21	0.267
24.3	5.40	0.788
24.4	5.62	0.779
24.6	5.81	1.084
24.8	6.01	0.966
24.9	6.99	1.440
25.2	6.22	1.245
25.3	7.39	1.673
25.4	7.19	0.872
25.4	6.79	1.474
25.4	6.60	0.974
25.4	6.43	1.283
34.2	6.01	0.381
34.3	7.18	0.618
34.4	6.22	0.521
34.4	5.81	0.237
34.6	6.42	0.601
34.8	6.78	0.889
34.9	7.00	0.716
35.2	6.60	0.559
44.4	6.43	0.220
44.6	6.78	0.402
44.8	6.99	0.428
44.9	7.38	0.572
45.2	7.20	0.288
54.4	7.39	0.301
54.5	7.01	0.241
Total		100.000

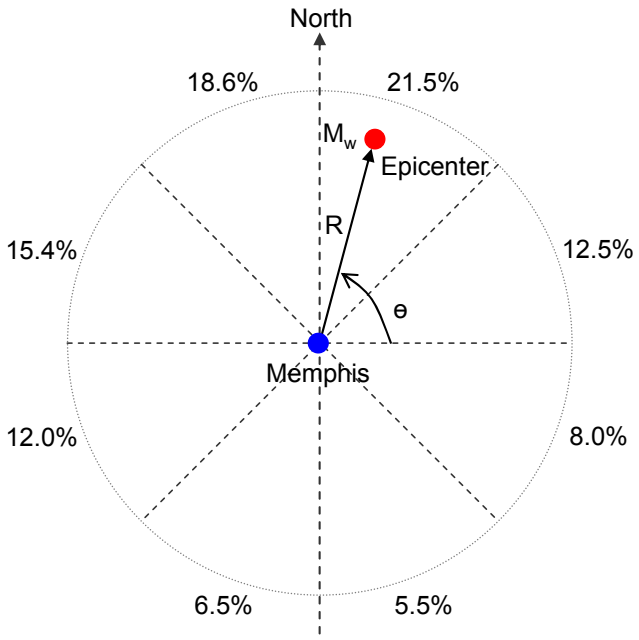

Figure 7-5 Determination of the epicenter of the earthquake from the background seismic source zone

To confirm the simulated earthquakes generated from the background seismic source zones, the map on which the simulated epicenters are plotted and the graph of the magnitudes vs. the epicentral distance are compared with a map and the graph obtained from the de-aggregation analysis (e.g., Figure 7-6 vs. Figure 4-6 for 2475-year return period).

In Figure 7-6, 2500 simulated earthquakes are plotted. The relations between the epicentral distance and the magnitude agree reasonably well with the results of deaggregation analysis shown in Figure 4-6.

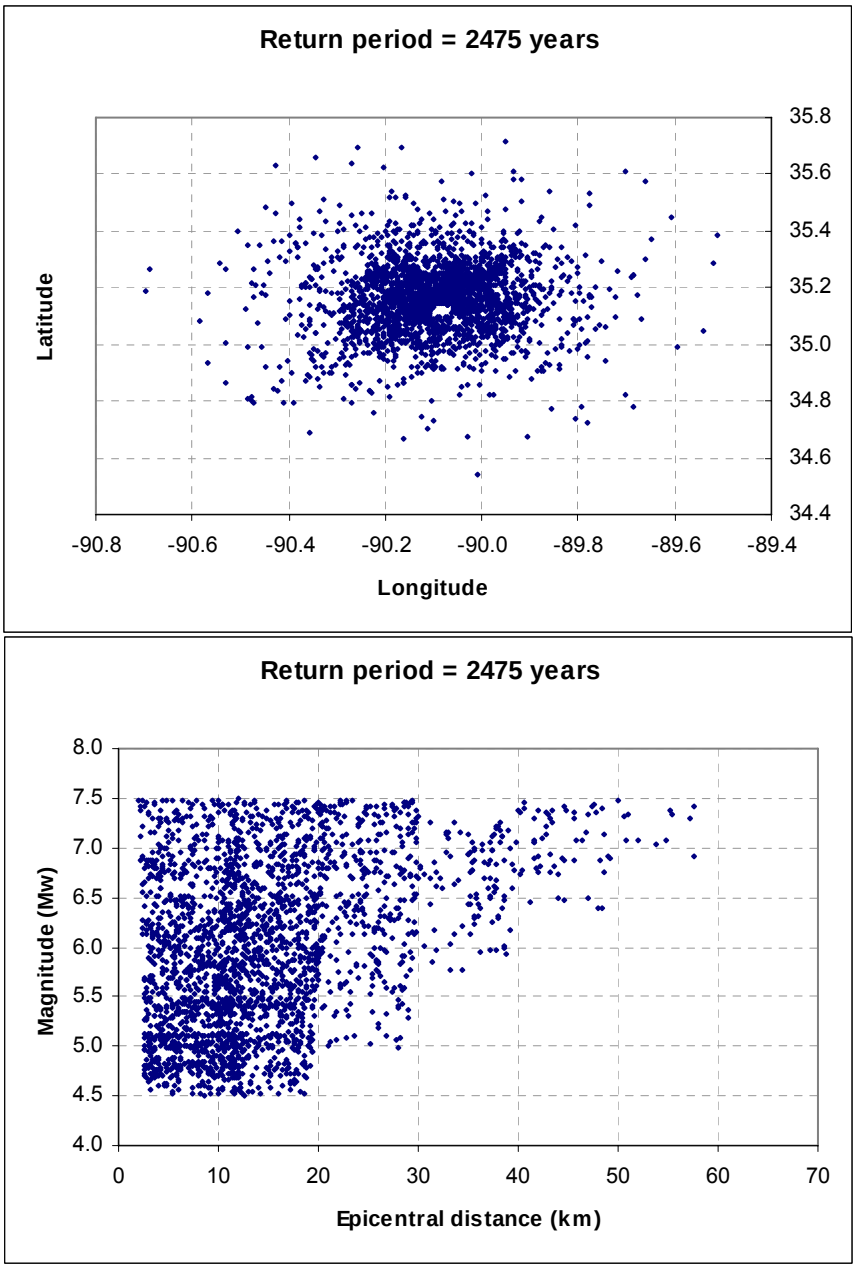

Figure 7-6 Distributions of epicenters, magnitudes and epicentral distances of simulated earthquakes for 2475-year return period

7.2.3 Probabilistic Seismic Hazard Assessment for Infrastructure Systems

To evaluate the serviceability of the water distribution system and the electrical power transmission system for each return period, the serviceability assessment

illustrated in Chapter 6 must be conducted for all possible earthquakes from the sites surrounding the infrastructure system at each return period, treating each earthquake as a scenario earthquake. The process is summarized in Figure 7-7. The process "Serviceability assessment" is illustrated in Figure 6-8. The serviceability assessment for the NMSZ is performed twelve times since twelve scenario earthquakes are used as characteristic earthquakes within the NMSZ (Table 7-4). N must be large enough for the earthquakes with small frequency to be generated while looping. In this study, N=5000 for each return period. When the loop is finished, 12 results are weighted by their frequency ratios in Table 7-4, and N results of the background earthquake source zone are arithmetically averaged. To assess the serviceability of an infrastructure system due to the probabilistic seismic hazard, these two results must be averaged using weighting factors representing the frequencies of earthquake occurrence at NMSZ and at the entire background source zones. These frequencies, which are obtained from the results of de-aggregation analysis, are listed as a function of return period in Table 7-6.

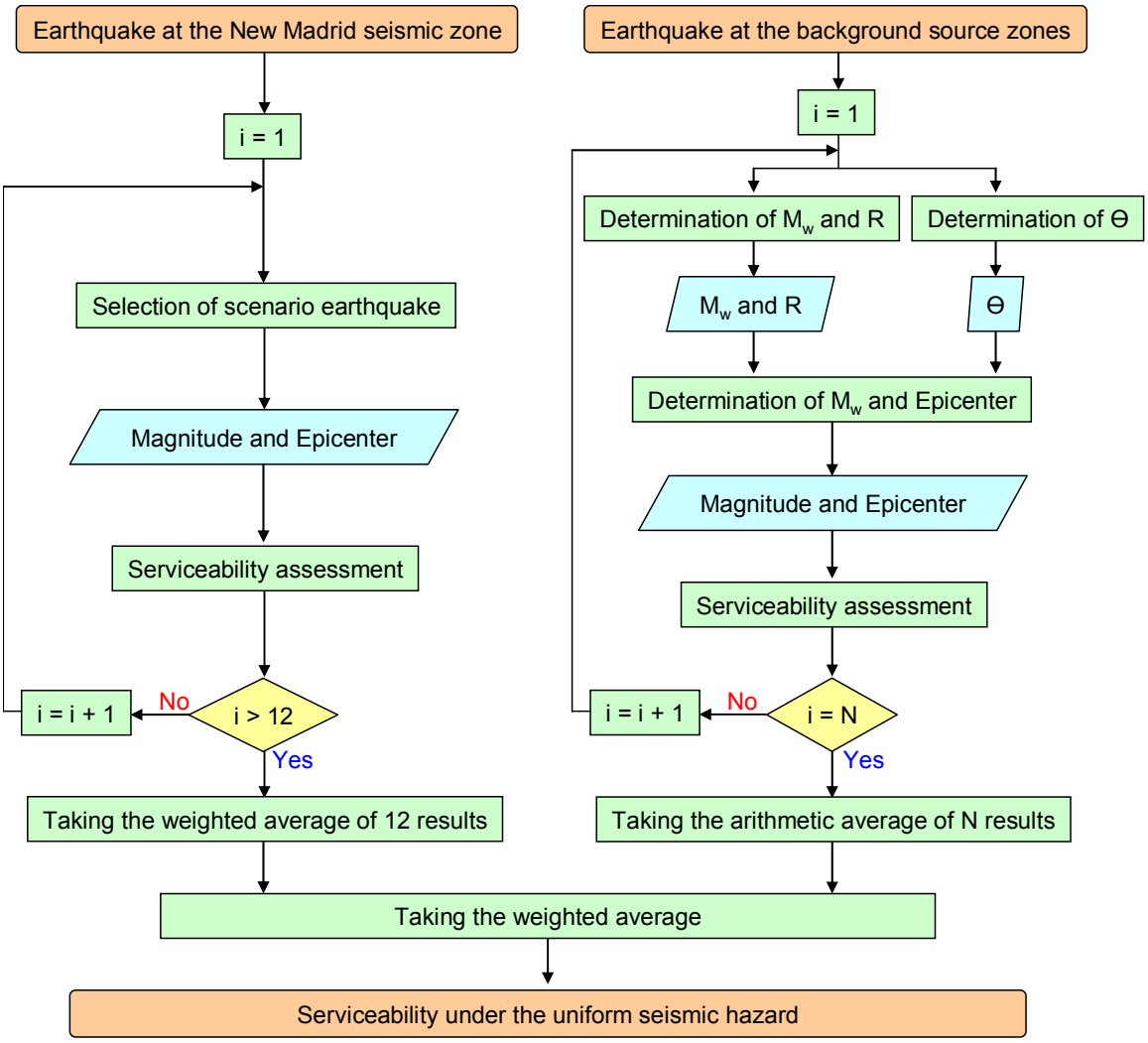

Figure 7-7 Flow chart of the serviceability assessment of the infrastructure systems under PSHA

Table 7-6 Contribution ratio of earthquake source zones to the uniform seismic hazard at Shelby County, TN at each return period

Earthquake source zone	Frequency (%)					
	Return period (years)					
	4975	2475	975	475	224	108
NMSZ	74.46	75.76	74.69	67.27	43.15	21.60
Background zones	25.54	24.24	25.31	32.74	56.85	78.40
Total	100.00	100.00	100.00	100.00	100.00	100.00

7.2.4 Serviceability Risk for Networked Systems

Following the procedure summarized in the previous section, the serviceability ratios of the electrical power transmission system and the water distribution system are calculated at 6 return periods. The parameters used to compute the serviceability ratios utilize the following models:

- The attenuation relationships for PGA and PGV proposed by Atkinson and Boore (1995),
- The local soil amplification factors proposed by the *2003 NEHRP Provisions* (FEMA, 2004),
- The correlation distance b in Eq.4-17 for PGA and PGV is 0 km; in other words, spatial correlation effects are neglected,
- The set of the fragility curves for the components of the water distribution system proposed in HAZUS MH (FEMA, 2003), and
- The infrastructure interdependency effect is not considered for the water distribution system.

The serviceability ratios of the entire water distribution system and the entire electrical power transmission system, which are evaluated using five categories of seismic zones or earthquakes, are plotted in Figures 7-14 and 7-15 with respect to the annual frequency, which is the reciprocal of the return period: 0.0002 for 4975-year return period, 0.0004 for 2475-year return period, 0.0010 for 975-year return period, 0.0021 for 475-year return period, 0.0045 for 224-year return period and 0.0093 for 108-year return period. In Figures 7-14 and 7-15, the curves labeled NMSZ represent serviceability ratios computed using only the earthquakes from the NMSZ; curves labeled

BGSZ represent the serviceability ratios computed using the earthquakes only from the background seismic zone; PSH represents serviceability ratios computed using the earthquakes from both the NMSZ and BGSZ, which is the exact solution evaluated by the process shown in Figure 7-7; MeanCE represents serviceability ratios computed using the mean characteristic earthquake identified in Table 4-3; and MPE represents serviceability ratios computed using the MPE listed in Table 4-3.

Figure 7-8 shows that the serviceability ratio of the water distribution system in Shelby County, which is a moderate seismic region, would be evaluated too conservatively if the MPE were chosen as the scenario event; the MeanCE is a better scenario earthquake to evaluate the seismic resistance of the water distribution system, although the estimated serviceability ratios are on the non-conservative side at larger annual frequencies such as 0.0021 and 0.0045.

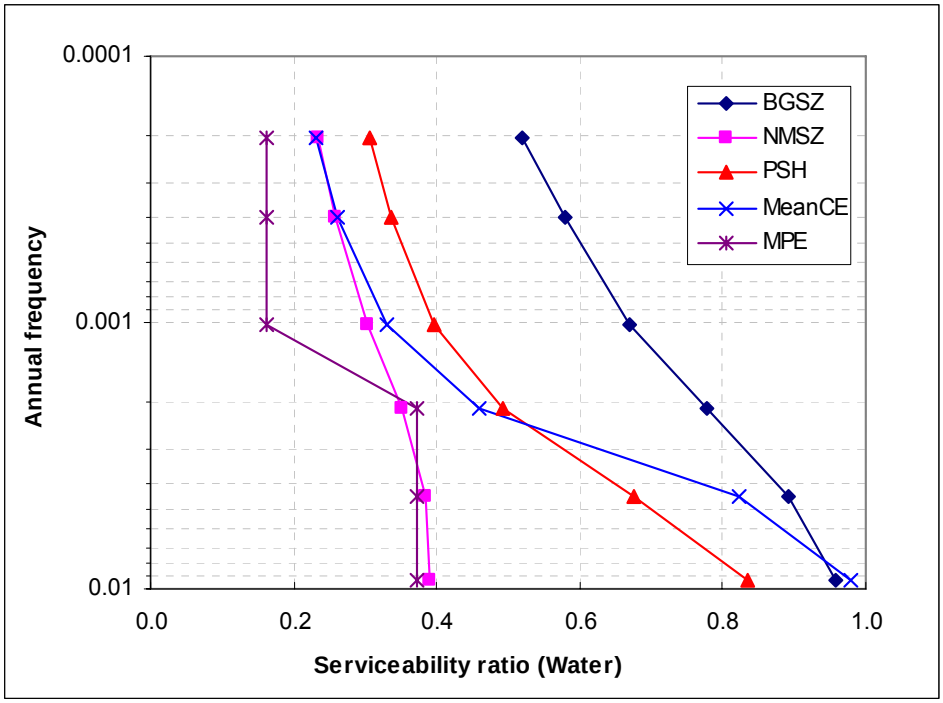

Figure 7-8 Serviceability ratio of the water distribution system at six annual frequencies

Similar to the water distribution system, Figure 7-9 clearly indicates that the use of the MPE results in an overly conservative serviceability ratio for the electrical power transmission system at any annual frequency except 0.0010; the MeanCE is a better scenario earthquake for evaluating the seismic resistance of the system though it results in the non-conservative ratios at larger annual frequencies such as 0.0010, 0.0021, 0.0045 and 0.0093.

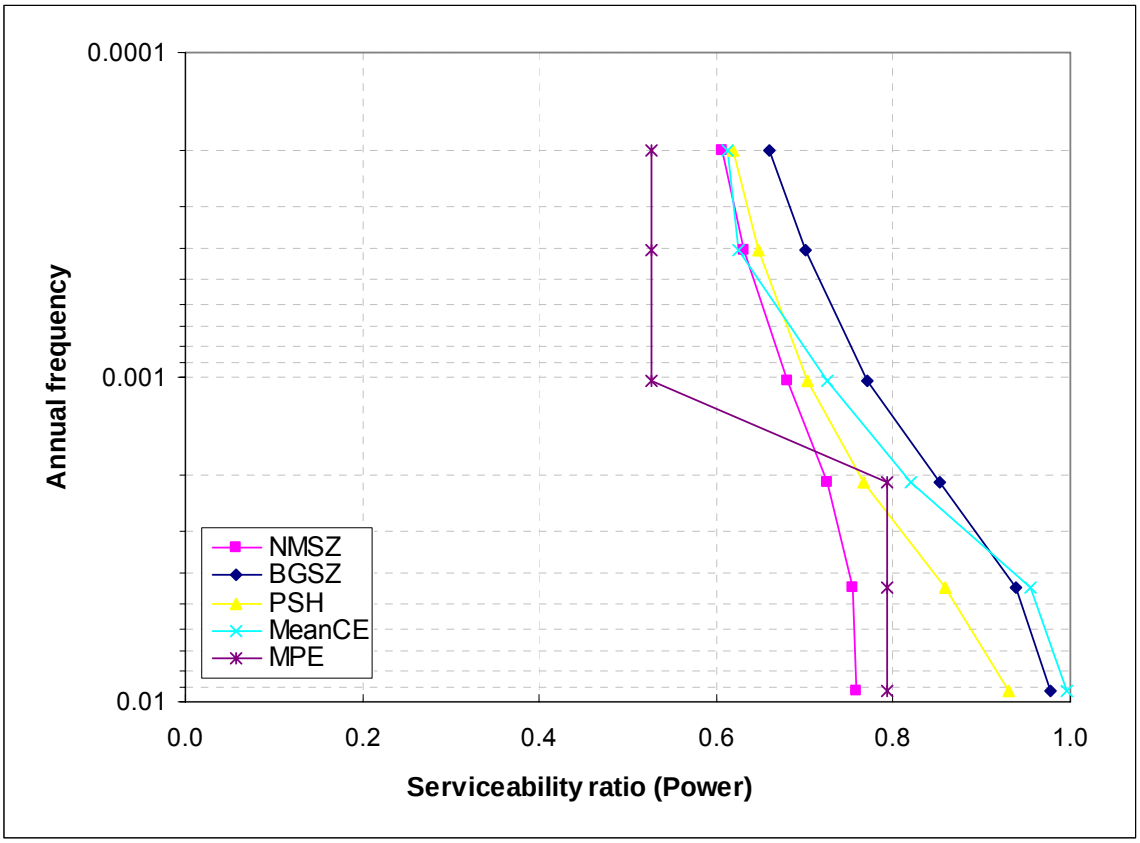

Figure 7-9 Serviceability ratio of the electrical power transmission system at six annual frequencies

7.3 Summary

The serviceability of the water distribution system and the electrical power transmission system in Shelby County, TN under a uniform seismic hazard was evaluated

in this chapter. The earthquakes which occurred at NMSZ and BGSZ were identified through a deaggregation analysis. The earthquakes occurring within the NMSZ were modeled as twelve characteristic scenario earthquakes which had deterministic magnitudes and epicenters, respectively. On the other hand, the earthquakes occurring within the BGSZ were modeled by 5000 earthquakes whose epicenters and magnitudes were randomly determined using the results of deaggregation analysis.

The serviceability assessments of the water distribution system and the electrical power transmission system showed that the maximum probable earthquake, which often has been used as a scenario earthquake, may lead to estimates of serviceability ratios of both the water distribution system and the electrical power transmission system that are considerably in error. Estimates obtained using the mean characteristic earthquake as a scenario event (MeanCE) are closer to exact serviceability ratios in most instances, although the MeanCE may occasionally result in unconservative estimates of serviceability ratios at larger annual frequencies.

CHAPTER 8

UNCERTAINTY AND SENSITIVITY ASSESSMENT

The serviceability assessment of the water distribution and electrical power transmission systems is based on numerous assumptions and modeling parameters: the attenuation relationships for PGA and PGV, the local soil amplification factors for PGA and PGV, the spatial correlation of PGA and PGV, the water pipe break ratios and the fragility curves for the water storage tanks, the water pumping stations, the electrical power substations and backup systems. These modeling parameters affect the serviceability and the functionality ratios, and their selection contributes uncertainty to the results of the network analysis. Such uncertainties are classified into two types: aleatory uncertainty (inherent randomness) and epistemic uncertainty (knowledge-based uncertainty) (Ang and Tang, 2006).

8.1 Aleatory and Epistemic Uncertainties

The aleatory uncertainty arises from naturally occurring random factors. The aleatory uncertainty generally cannot be reduced through more information or data, but it can be estimated more accurately (with higher confidence) with additional information. On the other hand, the source of epistemic uncertainty is incomplete knowledge; such uncertainties can be reduced when more information is collected. The epistemic uncertainty contains modeling uncertainty, which represents difference between the actual physical process and the simplified model used to predict the physical process, and parametric uncertainty, which represents uncertainty in the values of the parameters that are used in the model, respectively (Toro et al., 1997; Ang and Tang, 2006).

In seismic hazard analysis, a major source of aleatory uncertainty is the variability in the ground motion attenuation with respect to the estimated mean or median; this uncertainty is modeled by a log-normal distribution, as described previously. The uncertainty is represented numerically by the standard deviation or coefficient of variation (or log-standard deviation) of the probability distribution. On the other hand, the epistemic (modeling) uncertainty can be depicted by an event tree model, which represents the different modeling assumptions and decisions made by the analyst. The branches extending from each node are assigned weights in such a way that they sum to unity. The weights are assigned by the analyst to reflect the relative confidence in each option.

8.1.1 Source of Uncertainty

The case studies in the previous chapters included the aleatory uncertainties arising from the attenuation of seismic intensity from source to site and the fragility curves. Both uncertainties are modeled by log-normal distributions whose median values are determined by the attenuation relationships or the fragility curves. The log-standard deviation is defined to be 60% for the attenuation relationships and is set equal to the values listed in Table 6-1 for the fragility curves. The epistemic uncertainties due to the modeling assumptions made in the previous analyses can be analyzed by the event tree models shown in Figures 8-1 to 8-3.

Figure 8-1 represents the event tree model for evaluating the PGA at a site. In the process to evaluate the PGA, four steps are required. First, the scenario earthquake is determined. For the scenario earthquake-based seismic hazard analysis, the magnitude and the epicenter (from the USGS website) are assumed to be unique, and no other choice

is considered. Second, the attenuation relationship must be selected. For the CEUS, at least six attenuation relationships have been proposed (Toro and McGuire, 1987; Atkinson and Boore, 1990; Hwang and Huo, 1997; Toro et al., 1997; Toro, 2003; Campbell, 2003). Those equations are given in Eqs.4-6, 4-8, 4-10 to 4-13 and are plotted in Figure 4-2 for the case when magnitude M_w is 7.7. The weighting factor for each attenuation relationship is assumed to be 1/6 for purposes of illustration (implying that each attenuation law is viewed as equally plausible). This decision may be controversial. For example, the attenuation relationship proposed by Hwang and Huo (1997) may be assigned a smaller weighting factor than the other attenuation relationships, reflecting the fact that it is less commonly used than the others. However, Hwang and Huo's attenuation relationship was developed specifically for the Mid-America region, while the other attenuation relationships apply to the entire CEUS. In any event, this assignment of weights can reflect the judgment of the analyst and allows variations in the serviceability estimates to be traceable directly to this assumption and subsequently revised, if necessary. The local amplification factors for the CEUS are taken from the *2003 NEHRP Provisions* (FEMA, 2004) and Hwang et al. (1997). Though the amplification factor proposed by the *2003 NEHRP Provisions* is more widely used for the seismic hazard analysis than the amplification factor proposed by Hwang et al. (1997), the weighting factor for each site amplification factor is set equal to 0.5, since the Hwang et al. (1997) study focused specifically on the CEUS. The spatial correlation of PGA is characterized by the correlation distance shown in Eq.6-17. Since the correlation distance (km) is determined from the domain $[0,\infty)$, two extreme values are selected: 0 km and infinity, implying , respectively, perfect independence and dependence in ground

motion intensity at two sites. The weighting factors for these assumptions of correlation distance are 0.5 for each.

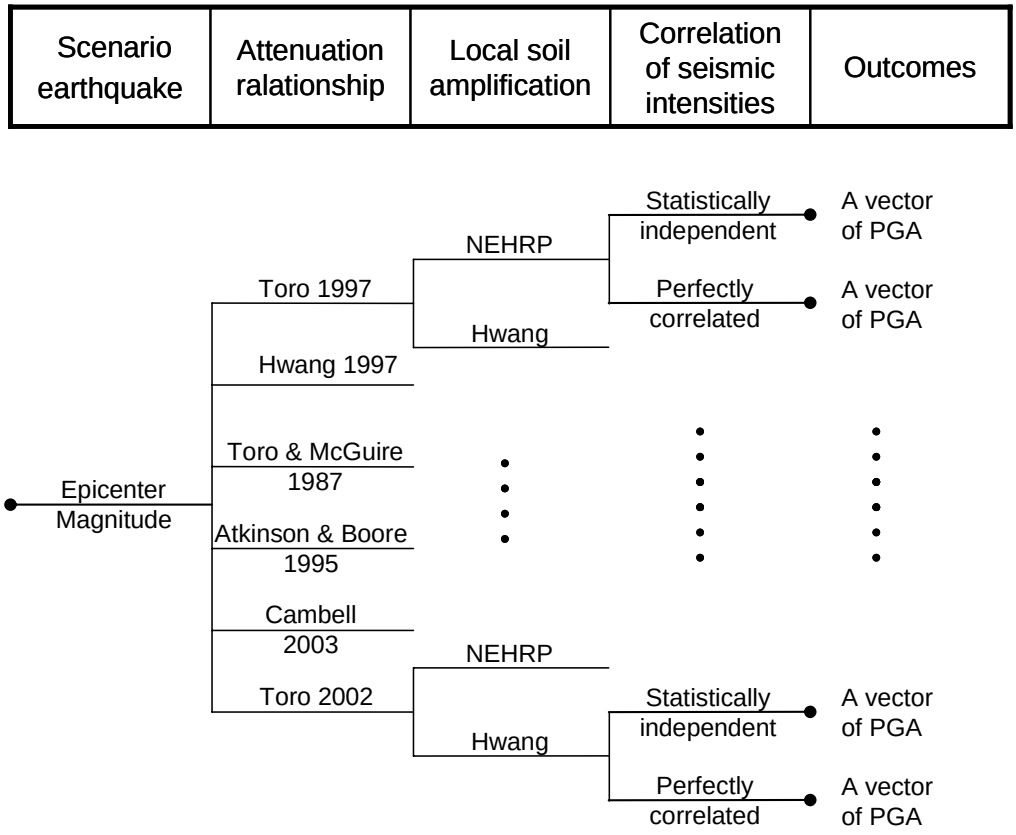

Figure 8-1 Event tree model for the determination of PGA

Similarly, Figure 8-2 represents the event tree model describing the modeling assumptions for evaluating the PGV at a site. Here, two attenuation relationships have been proposed for the CEUS, which are shown in Eqs.4-7 and 4-9 (Toro and McGuire, 1987; Atkinson and Boore, 1990), and their weighting factors are assumed 0.5 for each, each relation being equally plausible in the seismological community. The other modeling parameters are defined as same as those for PGA illustrated in Figure 8-1.

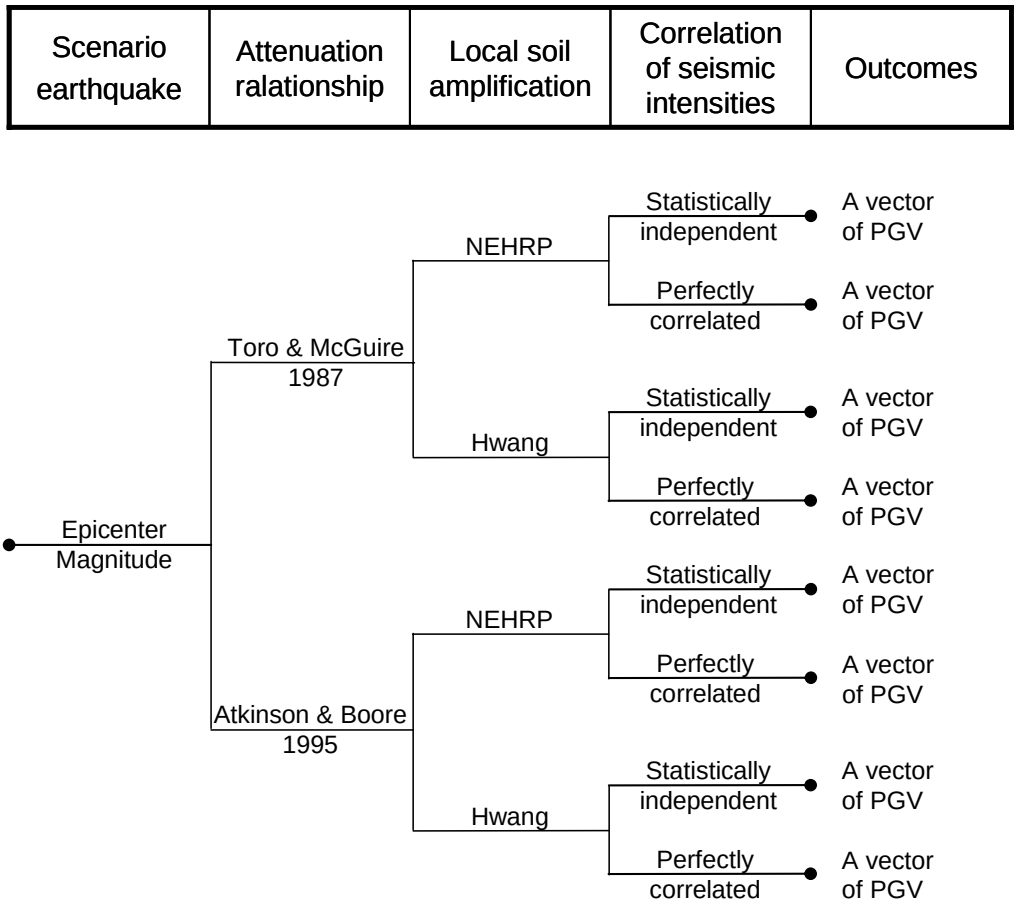

Figure 8-2 Event tree model for the determination of PGV

Figure 8-3 shows the event tree model for evaluating the serviceability ratio and the functionality ratio for the water distribution system and the electrical power transmission system.

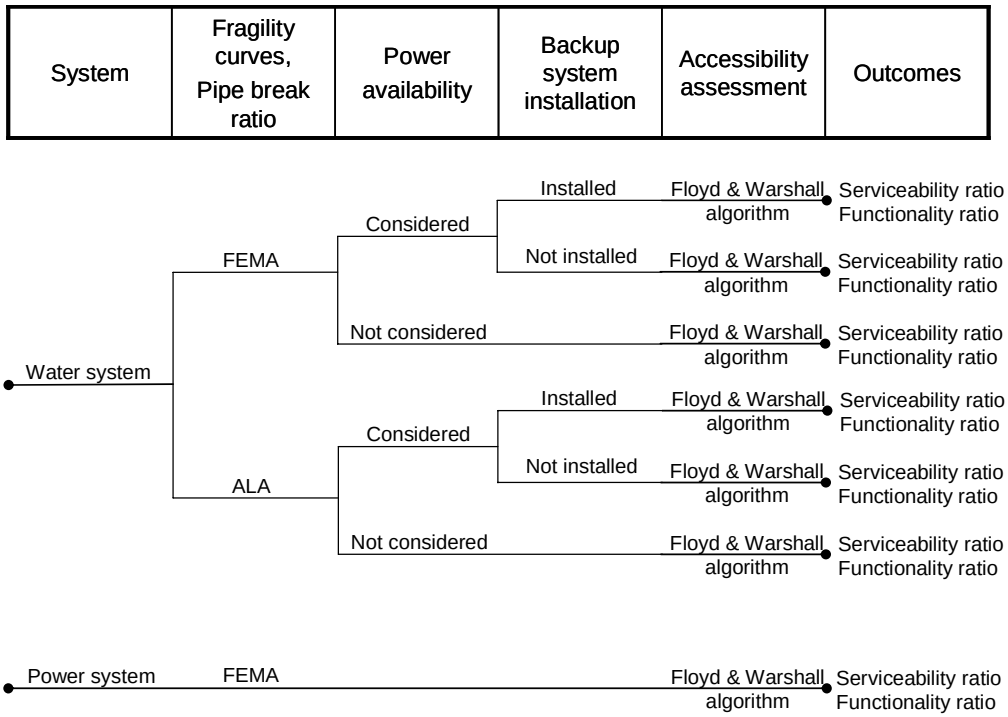

Figure 8-3 Event tree models for the determination of serviceability ratio and functionality ratio of water distribution system and electrical power transmission system

In the modeling process summarized in Figure 8-3, five steps are required. First, an infrastructure system is selected. Second, a set of fragility curves to support the system analysis are determined. For example, HAZUS MH (FEMA, 2003), the *ALA guideline* (ALA, 2001), Eidinger (2001) proposed fragility curves for water storage tanks, defined by log-normal distributions with parameters summarized in Table 8-1. The fragility curves are plotted in Figure 8-4. HAZUS MH (FEMA, 2003) provides the fragility curve for a water pumping station; the parameters are shown in Table 8-1 and the fragility is plotted in Figure 6-5. Ballantyne and Taylor (1991), O'Rourke and Ayala (1993), Toprak (1998), O'Rourke and Jeon (1999), the *ALA guideline* (ALA, 2001) and Eidinger (2001), HAZUS MH (Federal Emergency Management Agency, 2003) developed alternate water pipe break ratio functions, which are listed in Table 8-1 and

plotted in Figure 8-5. Fragilities and water pipe break ratios provided by the *ALA Guideline* (ALA, 2001) and HAZUS MH (FEMA, 2003) are selected because they apply to any water pipe; the weighting factor assigned to each source is 0.5. Fragilities for specific electrical power substations have been developed by Pires et al. (1996), Ang et al. (1996) and Jin et al. (2002), Hwang and Chou (1998) and Dong and Shinozuka (2003); however, since these studies all focus on a specific power substation, only the substation fragilities provided by HAZUS MH (FEMA, 2003) are used. The fragility parameters were summarized in Table 6-1 and the fragility curves were plotted in Figure 6-5.

Table 8-1 Parameters of lognormal distribution for fragility curves of components of the water distribution system

	Elevated steel tank	Water pumping station	Pipe break ratio (breaks/1000km)
	Median PGA, Beta	Median PGA, Beta	Vulnerability function
FEMA (2003)	1.50, 0.60	1.50, 0.80	$0.3*0.0001*PGV^{2.25}$
ALA (2001)	1.00, 0.55	NA	0.5*0.00187*PGV
Eidinger, J. (2001)	1.00, 0.55	NA	0.5*0.00187*PGV
Toprak, S. (1998)	NA	NA	$0.00023*PGV^{1.62}$
O'Rourke,M. and Jeon, S.S. (1999)	NA	NA	$(PGV/266)^{1.22}$
O'Rourke and Ayala (1993)	NA	NA	$(PGV/50)^{2.63}$

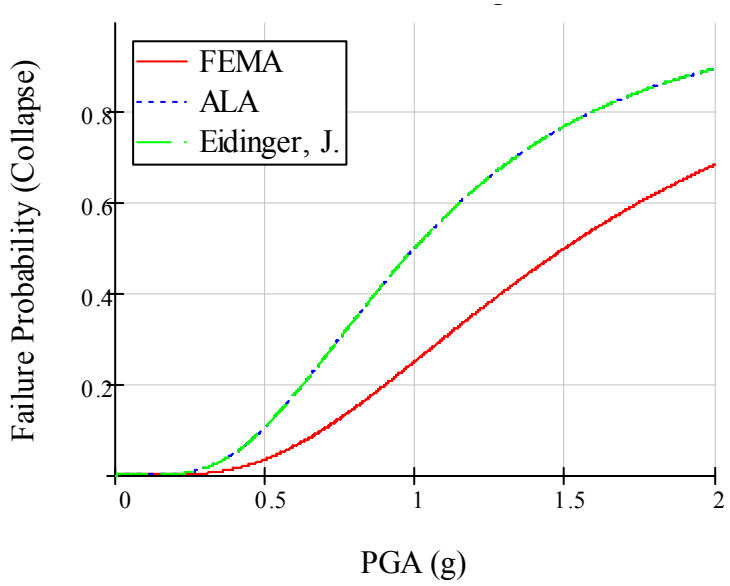

Figure 8-4 Fragility curves for an elevated water storage tank

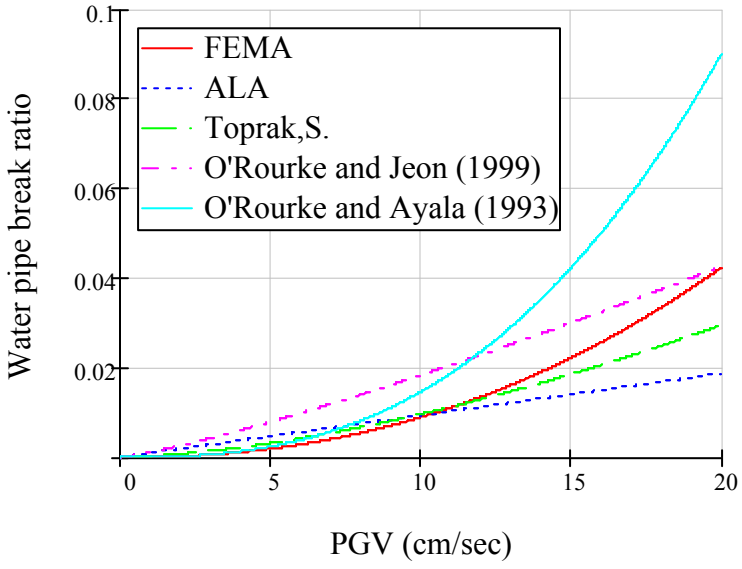

Figure 8-5 Water pipe break density

Third, for the seismic assessment of the water distribution system, whether the infrastructure interdependency effect due to electrical power availability is, or is not, considered is selected. Fourth, when infrastructure interdependency effect is considered,

whether or not the power backup system is installed must be selected. Fifth, only the shortest path algorithm is used for the accessibility assessment method. The last three steps ("Power availability", "Backup system installation" and "Accessibility assessment") are not the sources of epistemic uncertainty. However, they are included in the event trees since they are necessary to complete the accessibility assessment of a water distribution system and an electrical power transmission system.

8.1.2 Reduction of Number of Sets of Modeling Parameters

To perform a "full-factorial" analysis of sensitivity, 2304 sets of modeling parameters would have to be considered (see Table 8-2: column "Full factorial design"). Since this is not practical, the number of sets of modeling parameters must be reduced. The theory of experimental design (Cox and Reid, 2000; Wu and Hamad, 2000; Antony, 2003; Recab and Shaikh, 2005) can be used to reduce the number of experiments by neglecting certain higher-order interactions among modeling parameters. For example, when an experiment has four modeling parameters which have two choices each, $2^4=16$ runs are performed as the full factorial design. On the other hand, by applying a fractional factorial experimental design of resolution IV[1], the number of required runs can be reduced to $2^{4-1}=8$ runs (Recab and Shaikh, 2005). By performing the fractional factional experimental design of resolution IV, only the interactions between one modeling parameter and one other modeling parameter or two other modeling parameters are observed. Generally speaking, the higher-order interactions are less important (Cox and Reid, 2000; Wu and Hamad, 2000; Antony, 2003; Recab and Shaikh, 2005).

[1] "Resolution R implies that no effect involving i factors is aliased with effects involving less than R-i factors." (Wu and Hamad, 2000)

Thus, for the serviceability assessment of the water distribution and the electrical power transmission systems, some modeling parameters are grouped: local soil amplification factors, correlation distances and fragility curves. The local soil amplification factors for PGV in the *2003 NEHRP Provisions* (FEMA, 2004) are always used if the local soil amplification factors for PGV in the *2003 NEHRP Provisions* (FEMA, 2004) are used, and vice versa. If b_{PGA} =0 km is used for the correlation distance of PGA, b_{PGV}=0 km is also used. Furthermore, if the fragility proposed in HAZUS MH (FEMA, 2003) is used for an elevated water storage tank, the water pipe break density proposed in HAZUS also is used. As a result of this grouping, the sensitivity assessment can be performed under 288 sets of modeling parameters [2]. The choices of modeling parameters are shown in Table 8-2 (column "Grouping").

After the fractional factional experimental design of resolution IV is applied to four modeling parameters (attenuation relationships for PGV, local soil amplification factors for PGA and PGV, correlation distances for PGA and PGV, and fragility curves of components of the water distribution system), 144 combinations[3] of modeling parameters are required for the sensitivity assessment. The final choices of modeling parameters are shown in Table 8-2 (column "Fractional factorial design of resolution IV") and Table 8-3. Table 8-4 shows the twenty-four sets of modeling parameters for the attenuation relationship for PGA proposed by Toro and McGuire (1987). A similar approach is taken for the other five attenuation relationships for PGA.

[2] 6 (attenuation relationships for PGA) x 3 (infrastructure interdependency effects) x 2^4 (the full factional experimental design) = 288

[3] 6 (attenuation relationships for PGA) x 3 (infrastructure interdependency effects) x 2^{4-1} (the fractional factional experimental design of resolution IV) = 144

Table 8-2 Number of sets of modeling parameters in each step

Factor	Choice of factors		
	Full factorial design	Grouping	Fractional factorial design of resolution IV
Attenuation relationship for PGA	Toro and McGuire (1987) Atkinson and Boore (1990) Hwang and Huo (1997) Toro, Abrahamson et al. (1997) Toro (2003) Campbell (2003)	Toro and McGuire (1987) Atkinson and Boore (1990) Hwang and Huo (1997) Toro, Abrahamson et al. (1997) Toro (2003) Campbell (2003)	Toro and McGuire (1987) Atkinson and Boore (1990) Hwang and Huo (1997) Toro, Abrahamson et al. (1997) Toro (2003) Campbell (2003)
Attenuation relationship for PGV	Toro and McGuire (1987) Atkinson and Boore (1990)	Toro and McGuire (1987) Atkinson and Boore (1990)	(Table 8-3)
Local soil amplification factor for PGA	NEHRP (FEMA, 2004) Hwang, Lin et al. (1997)	NEHRP (FEMA, 2004) Hwang, Lin et al. (1997)	
Local soil amplification factor for PGV	NEHRP(FEMA, 2004) Hwang, Lin et al. (1997)		
Spatial correlation for PGA	0km Infinity	0km Infinity	
Spatial correlation for PGV	0km Infinity		
Fragility curve for an elevated storage tank	FEMA ALA	FEMA ALA	
Fragility curve for pipe break density	FEMA ALA		
Infrastructure interdependency and power backup installation	Independent Interdependent Interdependent + Backup	Independent Interdependent Interdependent + Backup	Independent Interdependent Interdependent + Backup
Total number of sets of factors	**2304**	**288**	**144**

Table 8-3 The sets of modeling parameters in the design of experiments

Attenuation equation PGV	Local soil		Correlation distance		Fragility curves
	PGA	PGV	PGA	PGV	
Atkinson&Boore	NEHRP	NEHRP	0km	0km	FEMA
Toro&McGuire	Hwang	Hwang	Infinity	Infinity	ALA
Atkinson&Boore	Hwang	Hwang	0km	0km	ALA
Toro&McGuire	NEHRP	NEHRP	Infinity	Infinity	FEMA
Atkinson&Boore	NEHRP	NEHRP	Infinity	Infinity	ALA
Toro&McGuire	Hwang	Hwang	0km	0km	FEMA
Toro&McGuire	NEHRP	NEHRP	0km	0km	ALA
Atkinson&Boore	Hwang	Hwang	Infinity	Infinity	FEMA

Table 8-4 Design of experiment for one attenuation relationship for PGA

Run	Factor							
	Attenuation equation		Local soil		Correlation distance		Fragility curves	Power availability/ Backup system
	PGA	PGV	PGA	PGV	PGA	PGV		
1	Toro&McGuire	Atkinson&Boore	NEHRP	NEHRP	0km	0km	FEMA	Not considered
2	Toro&McGuire	Toro&McGuire	Hwang	Hwang	Infinity	Infinity	ALA	Not considered
3	Toro&McGuire	Atkinson&Boore	Hwang	Hwang	0km	0km	ALA	Not considered
4	Toro&McGuire	Toro&McGuire	NEHRP	NEHRP	Infinity	Infinity	FEMA	Not considered
5	Toro&McGuire	Atkinson&Boore	NEHRP	NEHRP	Infinity	Infinity	ALA	Not considered
6	Toro&McGuire	Toro&McGuire	Hwang	Hwang	0km	0km	FEMA	Not considered
7	Toro&McGuire	Toro&McGuire	NEHRP	NEHRP	0km	0km	ALA	Not considered
8	Toro&McGuire	Atkinson&Boore	Hwang	Hwang	Infinity	Infinity	FEMA	Not considered
9	Toro&McGuire	Atkinson&Boore	NEHRP	NEHRP	0km	0km	FEMA	Considered
10	Toro&McGuire	Toro&McGuire	Hwang	Hwang	Infinity	Infinity	ALA	Considered
11	Toro&McGuire	Atkinson&Boore	Hwang	Hwang	0km	0km	ALA	Considered
12	Toro&McGuire	Toro&McGuire	NEHRP	NEHRP	Infinity	Infinity	FEMA	Considered
13	Toro&McGuire	Atkinson&Boore	NEHRP	NEHRP	Infinity	Infinity	ALA	Considered
14	Toro&McGuire	Toro&McGuire	Hwang	Hwang	0km	0km	FEMA	Considered
15	Toro&McGuire	Toro&McGuire	NEHRP	NEHRP	0km	0km	ALA	Considered
16	Toro&McGuire	Atkinson&Boore	Hwang	Hwang	Infinity	Infinity	FEMA	Considered
17	Toro&McGuire	Atkinson&Boore	NEHRP	NEHRP	0km	0km	FEMA	Considered+Backup
18	Toro&McGuire	Toro&McGuire	Hwang	Hwang	Infinity	Infinity	ALA	Considered+Backup
19	Toro&McGuire	Atkinson&Boore	Hwang	Hwang	0km	0km	ALA	Considered+Backup
20	Toro&McGuire	Toro&McGuire	NEHRP	NEHRP	Infinity	Infinity	FEMA	Considered+Backup
21	Toro&McGuire	Atkinson&Boore	NEHRP	NEHRP	Infinity	Infinity	ALA	Considered+Backup
22	Toro&McGuire	Toro&McGuire	Hwang	Hwang	0km	0km	FEMA	Considered+Backup
23	Toro&McGuire	Toro&McGuire	NEHRP	NEHRP	0km	0km	ALA	Considered+Backup
24	Toro&McGuire	Atkinson&Boore	Hwang	Hwang	Infinity	Infinity	FEMA	Considered+Backup

Following the serviceability assessment using all 144 sets of modeling parameters, a numerical average is taken of all resulting serviceability and functionality ratios. The resulting mean values of the serviceability and the functionality ratios (in a Bayesian sense) include both aleatory and epistemic uncertainty.

8.2 Effects of Uncertainties on Serviceability Assessment

Using the fault tree models, statistical data and experimental design summarized above, the serviceability assessment of the water distribution system and the electrical power transmission system considering the effects of uncertainties are performed.

8.2.1 Serviceability Assessment considering Aleatory and Epistemic Uncertainty under a Scenario Earthquake

Figures 8-6 and 8-7 illustrate the serviceability and functionality ratios of the water distribution and electrical power transmission systems, respectively, considering the effects of aleatory uncertainty and epistemic uncertainty. In Figure 8-6, the water distribution nodes located in northwest Shelby County, which is close to the epicenter of the scenario earthquake used in this study, have small functionality ratios compared with other water distribution nodes located far from the epicenter since they suffers the larger seismic intensities (e.g. nodes 23 and 26). Furthermore, some water distribution nodes located far from any water storage tank also have a smaller functionality ratio than the nodes located close to any storage tank (e.g. nodes 28 and 39). The effects of infrastructure interdependency (electrical power availability) on the serviceability assessment of the water distribution system are noticeable. When the infrastructure interdependency effects are considered, the functionality ratios of all water distribution nodes are decreased because the possibility that electrical power will be unavailable decreases the functionality of the water distribution nodes. This implies that to neglect infrastructure interdependency effects leads to un-conservative serviceability estimates. Installation of electrical power backup increases the functionality ratios of the all water distribution nodes; the recovered functionality ratios approach the functionality ratios of the water distribution nodes estimated under the assumption that electrical power is independent.

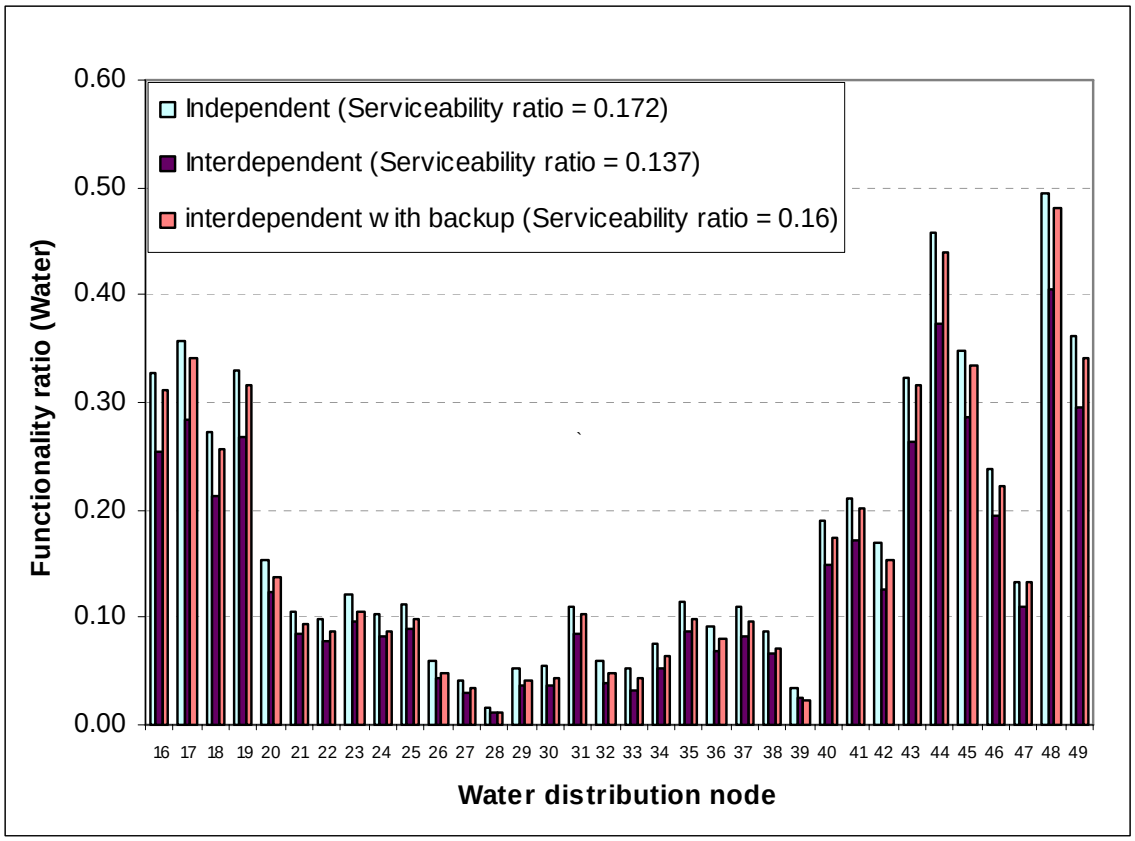

Figure 8-6 Serviceability assessment of water distribution system considering aleatory and epistemic uncertainties

In contrast to the performance of water distribution nodes, electrical substations located close to the epicenter do not always exhibit smaller functionality ratios (e.g. figure 6-19, substation 25) than those located far from the epicenter. On the other hand, the functionality ratios of substations located far from any gate station are relatively small compared with those located closed to any gate station. This implies that the serviceability of the electrical power distribution system is more sensitive to the redundancy of the networked system than to the failure probability of individual substations within the network (epicentral distance to the location of substations).

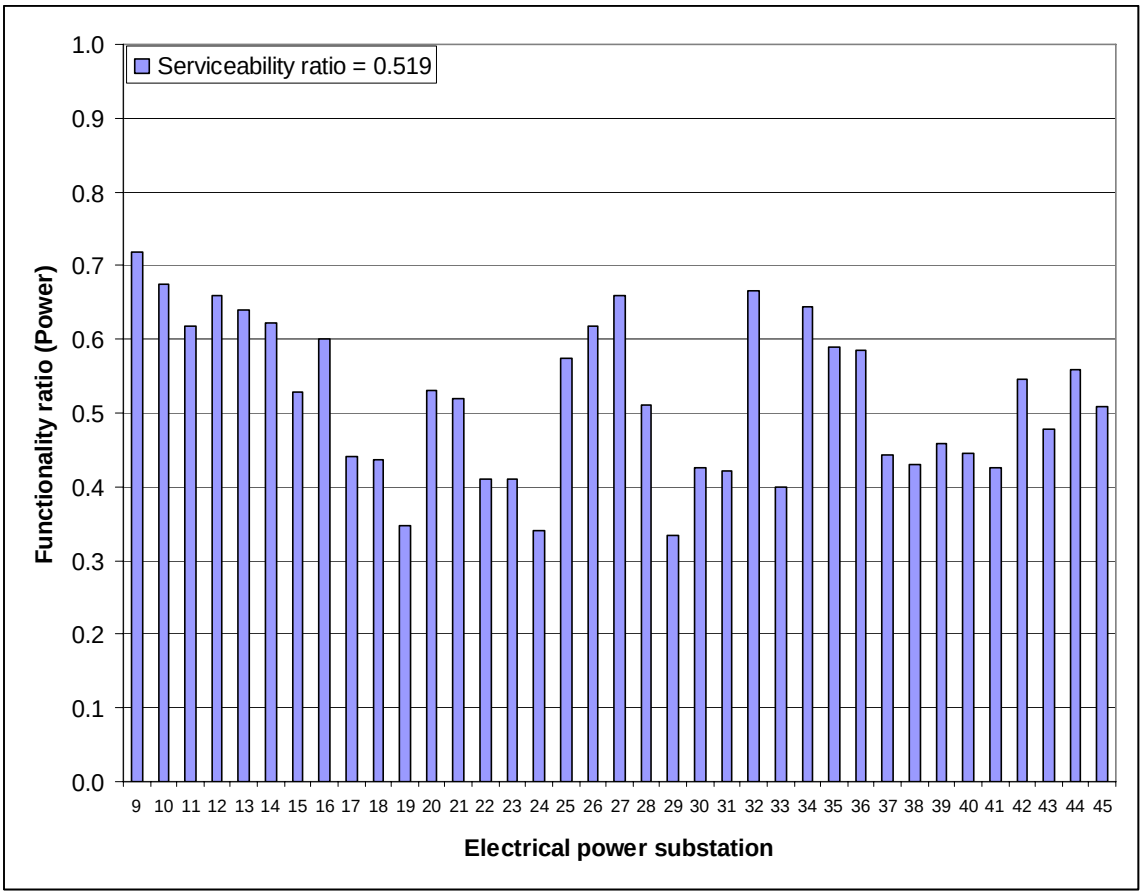

Figure 8-7 Serviceability assessment of electrical power transmission system considering aleatory and epistemic uncertainties

8.2.2 Serviceability Assessment considering Aleatory and Epistemic Uncertainty under a Uniform Seismic Hazard

In this section, the serviceability ratios of the water distribution and electrical transmission systems in Shelby County are evaluated for uniform seismic hazard at six return periods considering aleatory and epistemic uncertainties. To integrate such aleatory and epistemic uncertainties, the serviceability assessment must be performed with respect to all possible combinations of modeling parameters, as illustrated in the event tree models described previously in Figures 8-1 to 8-3. Since the serviceability

assessment is performed using all earthquakes which are obtained by deaggregation analysis of the uniform seismic hazard, the event tree models are also applied to these earthquakes. The sources of uncertainties are discussed in Section 8.1. The modeling parameters were summarized in Tables 8-2 to 8-4.

The aleatory uncertainty represented by the attenuation relationships and the fragility curves and the epistemic uncertainty represented by the choice of modeling parameters, such as attenuation relationships, local soil amplification factors, fragility curves of facilities and water pipe break densities, are integrated using the theory of experimental design as described in the previous section. Figures 8-8 and 8-9 show the serviceability ratio of the water distribution system and the electrical power transmission system considering aleatory and epistemic uncertainties.

Figure 8-8 illustrates the serviceability ratios of the water distribution system under several assumptions regarding earthquake modeling. The curve labeled BGSZ represents the serviceability ratio computed using only the earthquakes from the background seismic zone; NMSZ represents the serviceability ratio computed using only the earthquakes from the NMSZ; PSH represents the serviceability ratio computed using the earthquakes from both NMSZ and BGSZ, the so-called exact serviceability ratio. Since the contribution ratio of the BGSZ increases gradually as the annual frequency increases (Table 7-6), the serviceability ratio identified by PSH, which is close to that of NMSZ at small annual frequencies, approaches that of the BGSZ as the annual frequency increases. This trend shows the serviceability ratio obtained from considering only scenario earthquakes in the NMSZ may underestimate the resistance of the water

distribution system to earthquakes with relatively short return periods (e.g. 975-year, 224-year and 108-year return periods).

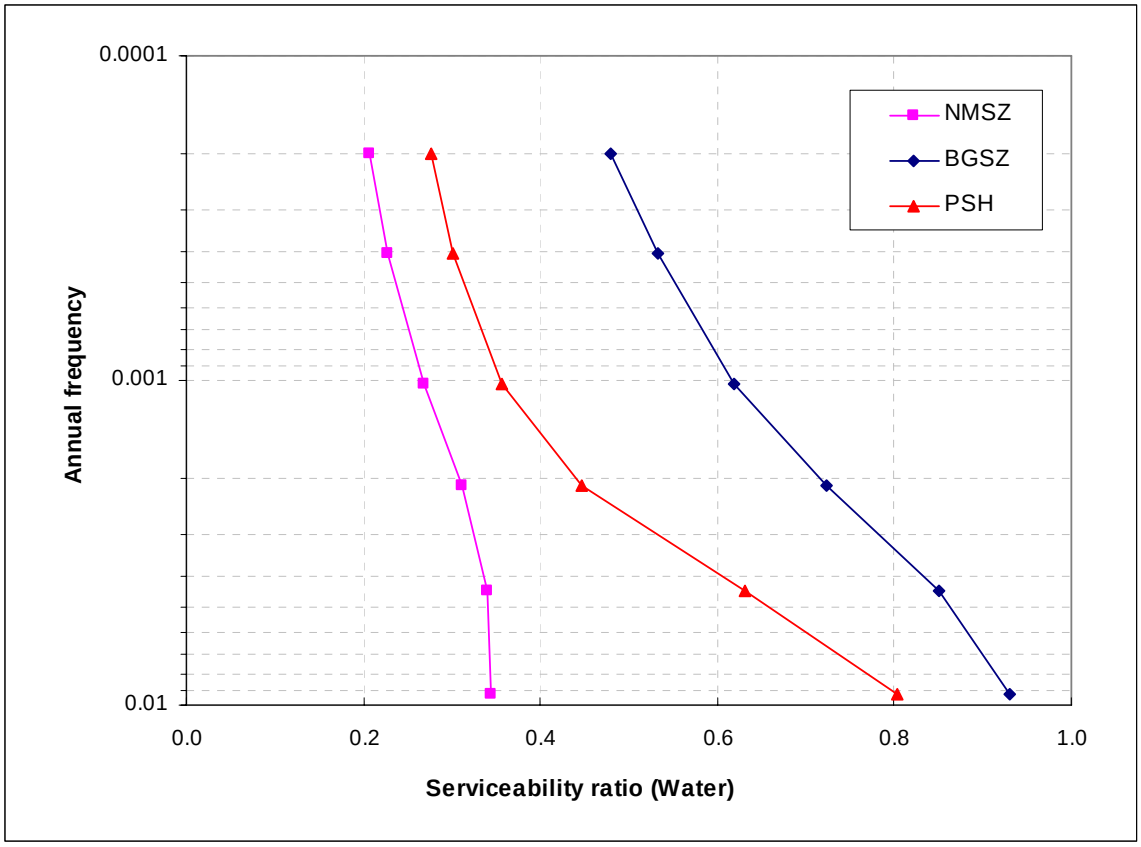

Figure 8-8 Serviceability assessment of water distribution system considering aleatory and epistemic uncertainties under uniform seismic hazard

Figure 8-9 illustrates the serviceability ratios of the electrical power transmission system at the six return periods considered. As shown in Figure 8-8, the serviceability ratio defined by PSH, which is close to that of the NMSZ when the annual frequency is small, approaches that of the BGSZ as the annual frequency increases since the contribution ratio of the BGSZ increases gradually as the annual frequency increases (Table 7-6). However, this trend is less noticeable than it was in the serviceability assessment of the water distribution system (Figure 8-8) since the serviceability ratios

following earthquakes from both the NMSZ and BGSZ remain relatively large. This is because the failures of the distribution elements (e.g., electrical power transmission towers and cables) in the electrical power network are not considered for the serviceability assessment, and the electrical power transmission system has high redundancy, which keeps the serviceability ratio relatively higher than in the water distribution system.

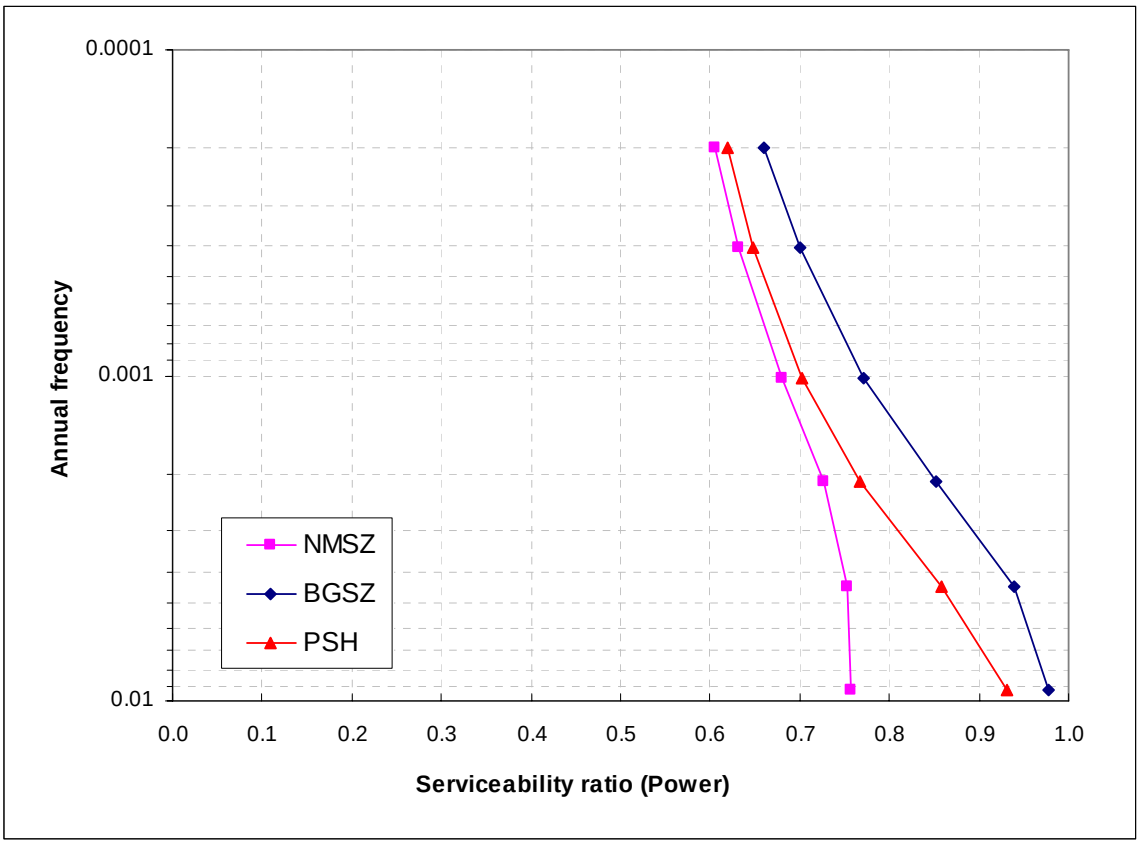

Figure 8-9 Serviceability assessment of electrical power transmission system considering aleatory and epistemic uncertainties under uniform seismic hazard

8.3 Sensitivity Analysis of Serviceability Estimation

The proposed serviceability assessment involves numerous modeling parameters such as attenuation equations for PGA and PGV, local soil amplification factors for PGA

and PGV, correlation distance of PGA and PGV, component fragilities, and water pipe break ratios. Engineers and decision makers may wish to know which factors are the most influential on the serviceability or functionality ratios in order to select proper modeling parameters or to target investments in additional data acquisition or risk management. Such assessment is called sensitivity assessment.

8.3.1 Sensitivity Assessment under a Scenario Earthquake

In order to assess the effect of a specific modeling parameter on the results, the effect of all other modeling parameters need to be integrated. For example, to identify the sensitivity of the results to the local soil amplification factors provided in the *2003 NEHRP Provisions* (FEMA, 2004) vs those proposed by Hwang et al. (1997), the following two network analyses would be required:

- Serviceability assessment using the local soil amplification factors proposed by the *2003 NEHRP Provisions* and all possible sets of other modeling parameters, and
- Serviceability assessment using the local soil amplification factors proposed by Hwang et al. and all possible sets of other factors.

In the following sections, sensitivity assessments of the serviceability and the functionality ratios are performed to the water distribution system and the electrical power distribution system without considering infrastructure interaction effect.

8.3.1.1 Water Distribution System

Figure 8-10 shows the sensitivity of the serviceability of the water distribution system due to the attenuation relationships for PGA. In all attenuation relationships for

PGA, the water distribution nodes located either in the northwest region of Shelby County, which is close to the epicenter of the scenario earthquake used in this study (e.g. nodes 23 and 26), or far from any water storage tank, result in relatively small functionality ratios compared with ratios at nodes located close to storage tanks (e.g. nodes 38 and 47). When water distribution nodes are located close to the epicenter and far from any water storage tank, their functionality ratios are very small (e.g. nodes 28 and 39).

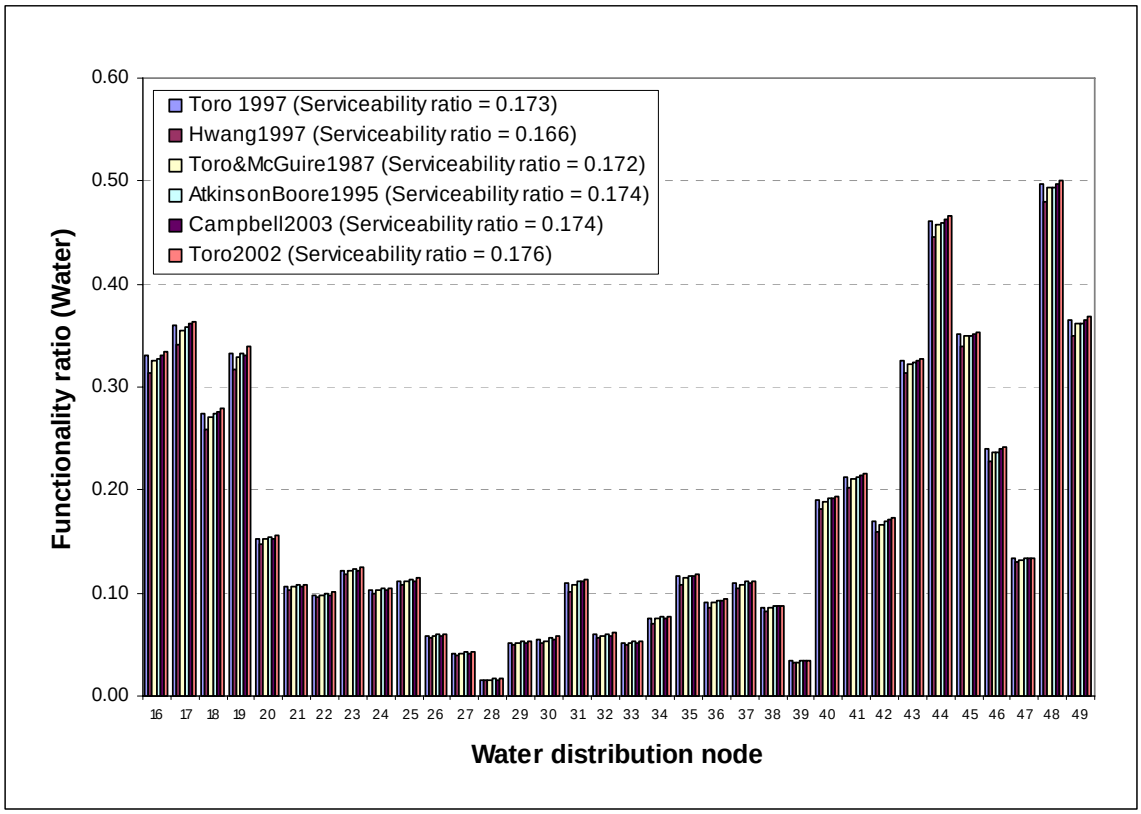

Figure 8-10 Sensitivity of water distribution system serviceability to attenuation relationships for PGA

Figure 8-11 shows the sensitivity of the serviceability of the water distribution system to the attenuation relationships for PGV. At all water distribution nodes, the functionality ratio computed using the attenuation relationship proposed by Toro and

McGuire (1987) is smaller than the ratio computed using the Atkinson and Boore (1995) attenuation. Note that the Toro/McGuire attenuation relationship estimates a larger PGV for epicentral distances less than about 100km (Figure 4-3), a distance within which all water distribution nodes are located.

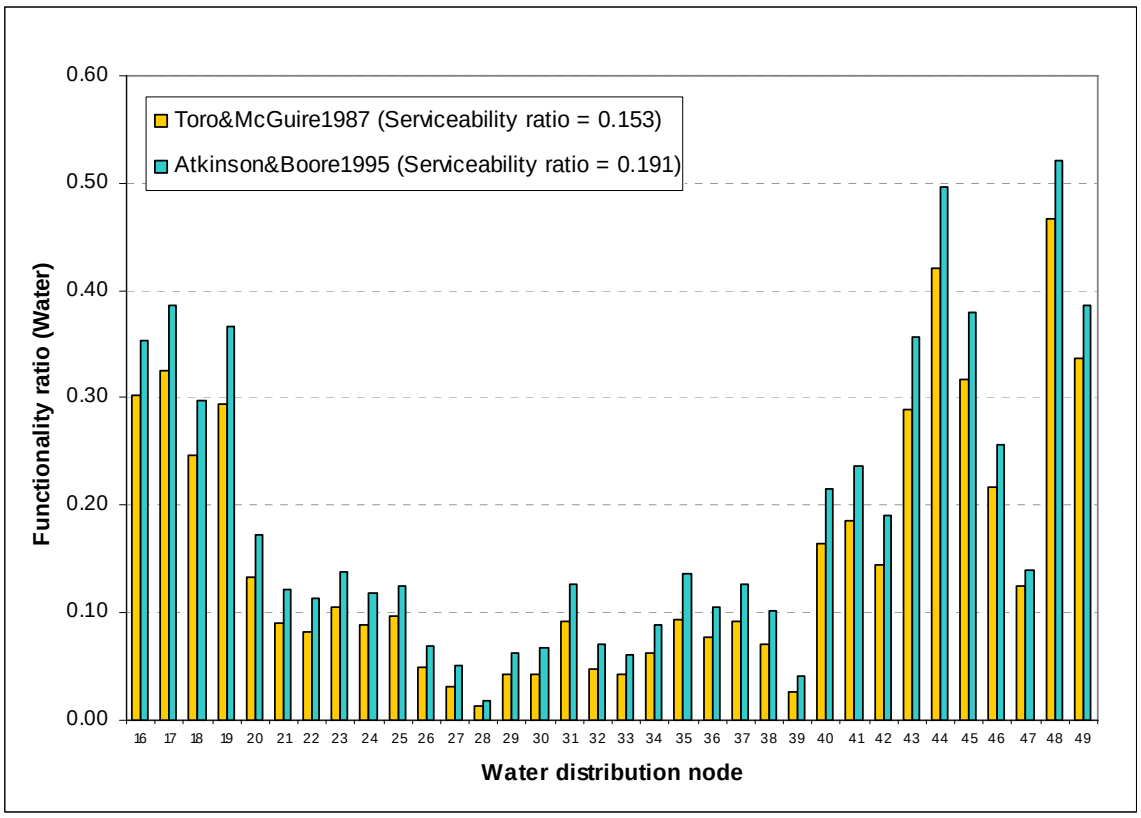

Figure 8-11 Sensitivity of water distribution system serviceability to attenuation relationships for PGV

Figure 8-12 illustrates the sensitivity of the serviceability of the water distribution system to the local soil amplification factors for PGA and PGV. At all water distribution nodes, the functionality ratio computed using the local soil amplification factor proposed by Hwang et al (1997) is smaller than the ratio computed using the factors in the *2003 NEHRP Provisions* (FEMA, 2004). It might be recalled that the local soil amplification factor for PGV proposed by Hwang et al. is larger for all seismic intensities (Figure 4-5),

while the amplification factor for PGA crosses the *NEHRP* amplification at around PGA=0.2g. The results in Figures 8-12 and 8-13 show that the PGV is the most important factor for evaluating serviceability of the water distribution system. This observation implies that the water mains, whose failure is determined by PGV, are more important to the serviceability of the water distribution system than water storage tanks and water pumping stations.

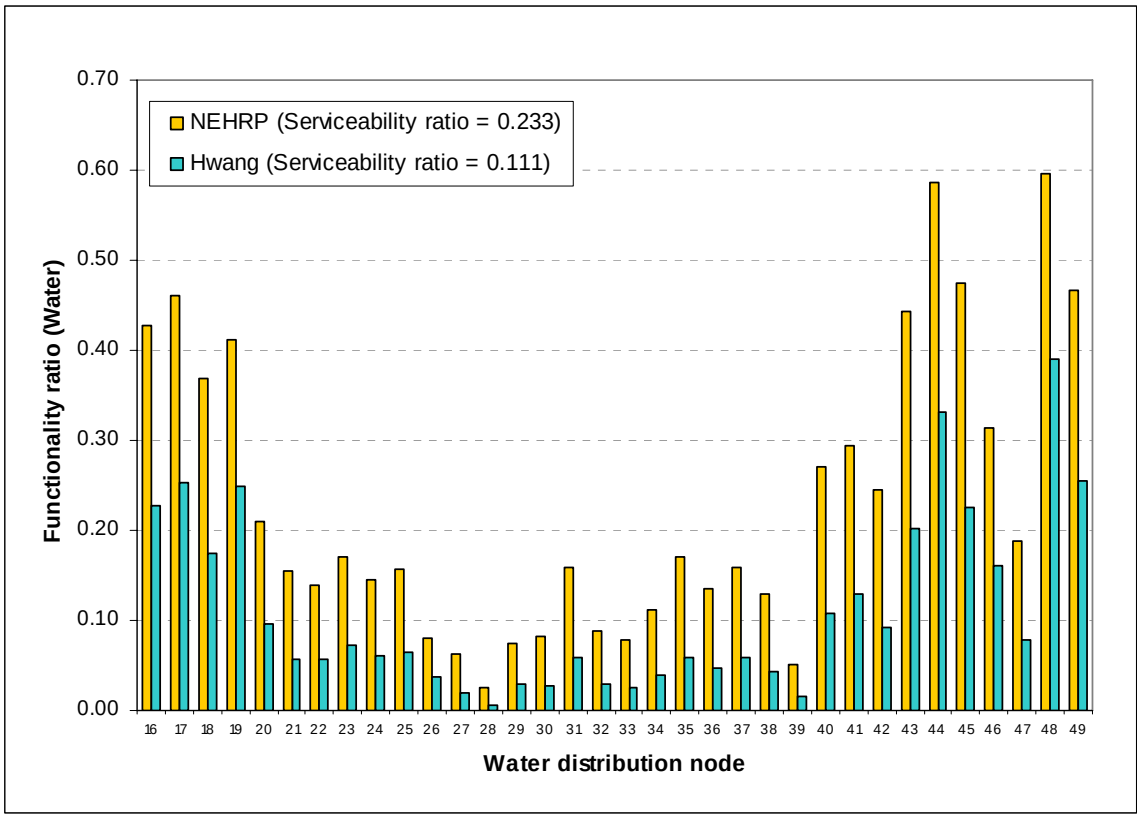

Figure 8-12 Sensitivity of water distribution system serviceability to local soil amplification factors

The sensitivity of the serviceability of the water distribution system due to the correlation distance for PGA and PGV is illustrated in Figure 8-13. At all water distribution nodes, the functionality ratios computed assuming that the correlation distance b=0 km result in a smaller value than that computed under the assumption that

the correlation distance b=Infinity. Considering the fact that system failure probability is larger when failure events of components are statistically independent (Eq.6-5), one can conclude that the water distribution system in Shelby County behaves more like a series than a parallel system and lacks redundancy.

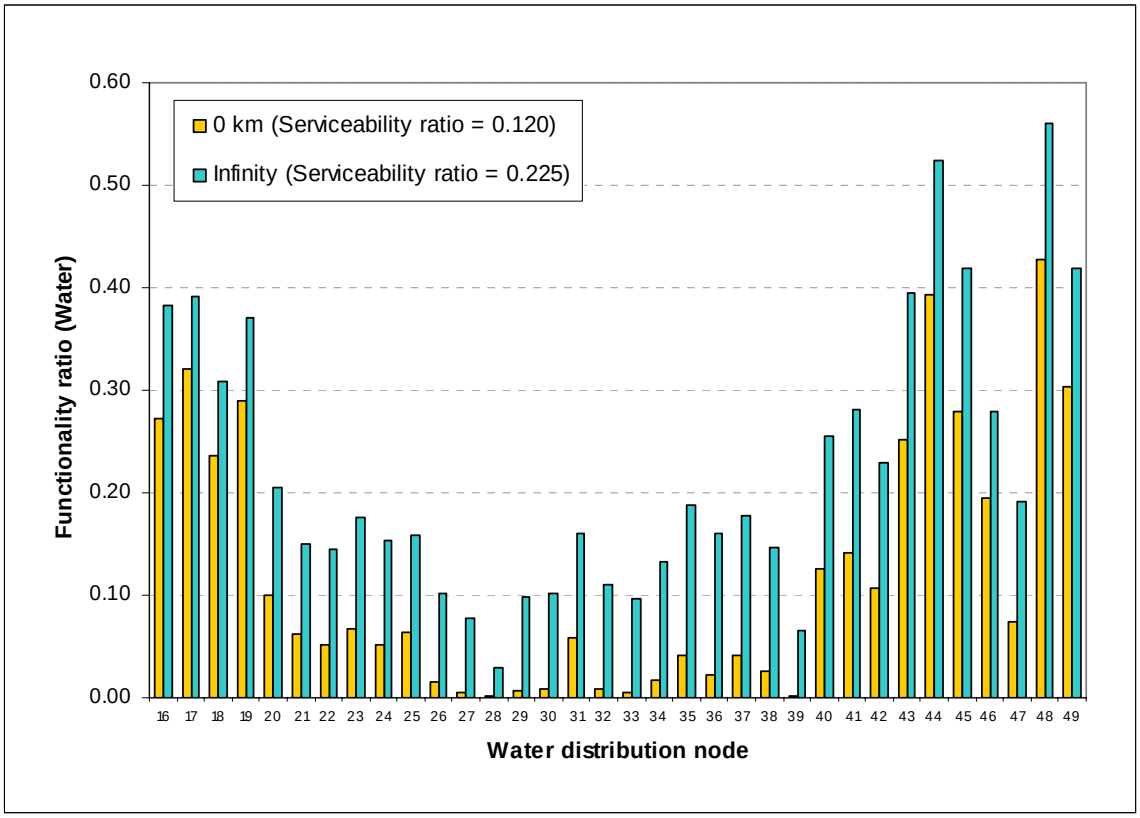

Figure 8-13 Sensitivity of water distribution system serviceability to correlation distance

Figure 8-14 shows the sensitivity of the serviceability of the water distribution system to the assumed fragility of an elevated water storage tank and the water pipe break density. At all nodes, the functionality ratios computed using the fragilities proposed by HAZUS MH (FEMA, 2003) are smaller than those using the *ALA Guideline* (ALA, 2001). The water pipe break density embedded in HAZUS MH is higher, at PGV>10 cm/sec, than that proposed by the *ALA Guideline* (ALA, 2001) (Figure 8-5), while the failure

probability of an elevated storage tank is smaller at all values of PGA (Figure 8-4). This fact reinforces the previous observation that water pipes, whose failure is determined by PGV, are more important to the serviceability of the water distribution system than water storage tanks and water pumping stations.

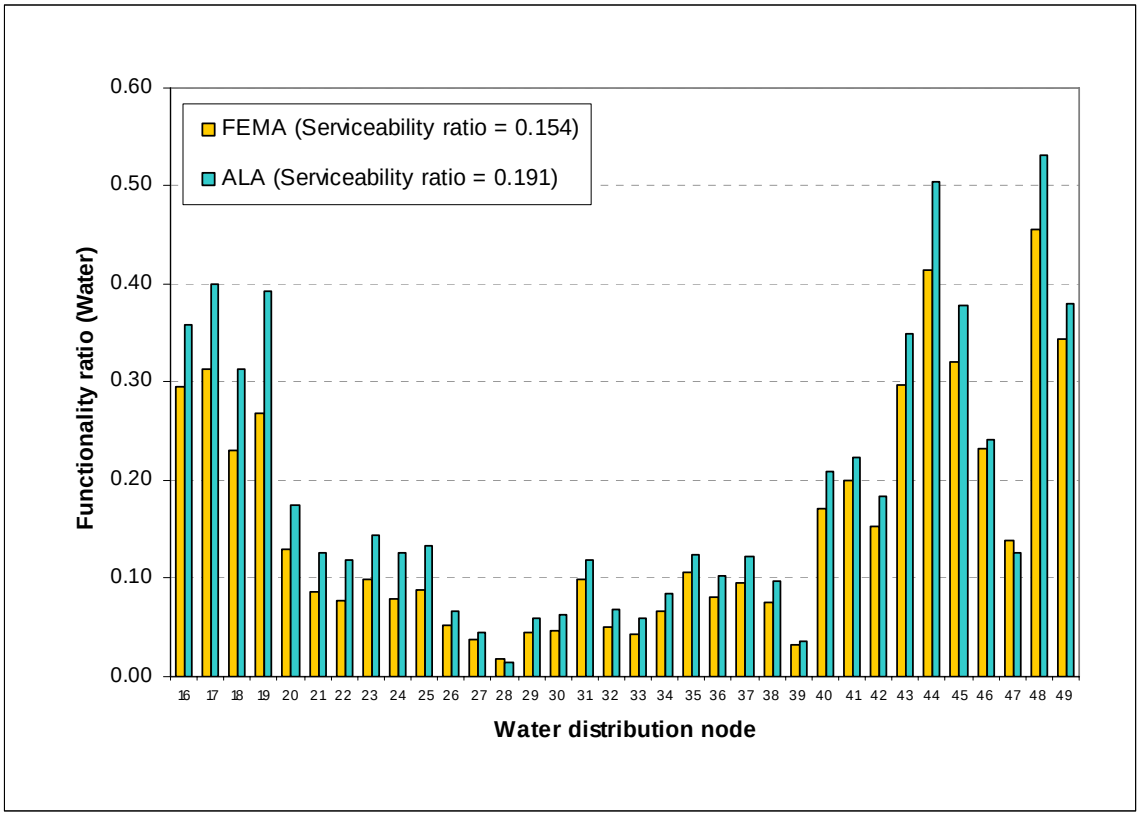

Figure 8-14 Sensitivity of water distribution system serviceability to fragility curves

To determine the modeling parameter to which the serviceability assessment of the water distribution system is the most sensitive, a statistical approach is applied, as summarized in Figure 8-15 (Recab and Shaikh, 2005). The contribution ratios of five modeling parameters to the functionality ratio of each water distribution node and to the serviceability ratio of the entire system are listed in Table 8-5.

Step 1: Evaluate $T=\Delta_A^2+\Delta_B^2+\Delta_C^2+\Delta_D^2+\Delta_E^2$.

where $\Delta_\bullet$: the maximum difference with respect to factor •

A : the attenuation relationship for PGA

B : the attenuation relationship for PGV

C : the local soil amplification factors for PGA and PGV,

D : the correlation distances for PGA and PGV, and

E : the fragility curve and the water pipe break density.

Step 2: Calculate the contribution of factor A as Δ_A^2/T

Step 3: Repeat Step 2 for factors B, C, D and E.

Figure 8-15 Identification of important modeling parameters

The contribution ratios in red and in blue in Table 8-5 represent the most and the second most significant modeling parameter for the functionality ratio and the serviceability ratio, respectively. The functionality ratios at all nodes and the serviceability ratio for the system are uniformly sensitive to the local soil amplification factors and the correlation distance. In contrast, the effects of component fragilities vary widely from node to node (e.g. the second most contributed modeling parameter for nodes 17 to 19, while the least contributed modeling parameter for node 46). Thus, it can be concluded that the local soil amplification factors, the correlation distance and the component fragilities all are important for determining the functionality ratio of individual nodes, while the local soil amplification factors and the correlation distance are important for assessing the serviceability ratio of the entire water distribution system. The attenuation relationships for PGA and PGV appear to be less important for the serviceability assessment of the system as a whole.

Table 8-5 Contribution ratio of modeling parameters to the serviceability assessment of the water distribution system

Functionality ratio	Attenuation relationship		Amplification factor	Correlation distance	Fragility curves
	PGA	PGV			
Node 16	0.8%	4.3%	67.7%	20.3%	6.9%
Node 17	0.8%	6.2%	71.8%	8.5%	12.7%
Node 18	0.7%	5.1%	71.8%	9.6%	12.7%
Node 19	1.0%	9.4%	48.5%	12.3%	28.8%
Node 20	0.2%	5.5%	46.8%	40.1%	7.4%
Node 21	0.1%	4.7%	47.7%	39.4%	8.1%
Node 22	0.1%	5.5%	37.4%	47.4%	9.6%
Node 23	0.1%	4.6%	39.8%	47.2%	8.3%
Node 24	0.1%	4.2%	34.7%	50.2%	10.8%
Node 25	0.2%	3.8%	41.4%	44.2%	10.4%
Node 26	0.1%	3.8%	19.7%	74.3%	2.1%
Node 27	0.2%	5.3%	24.8%	69.1%	0.6%
Node 28	0.1%	2.1%	32.7%	64.6%	0.5%
Node 29	0.1%	3.5%	19.0%	75.4%	2.0%
Node 30	0.2%	4.9%	24.5%	68.6%	1.7%
Node 31	0.6%	5.5%	44.8%	47.1%	2.0%
Node 32	0.2%	3.7%	22.6%	71.1%	2.4%
Node 33	0.2%	3.1%	23.3%	70.8%	2.6%
Node 34	0.3%	3.5%	26.8%	67.8%	1.6%
Node 35	0.3%	4.8%	34.7%	59.3%	1.0%
Node 36	0.2%	2.8%	26.8%	68.5%	1.7%
Node 37	0.2%	4.2%	33.2%	60.1%	2.2%
Node 38	0.1%	4.2%	31.2%	62.4%	2.2%
Node 39	0.1%	4.5%	23.7%	71.5%	0.2%
Node 40	0.3%	5.5%	56.1%	35.2%	3.0%
Node 41	0.4%	5.3%	54.9%	38.4%	1.1%
Node 42	0.5%	5.0%	56.6%	35.5%	2.4%
Node 43	0.3%	5.1%	67.8%	23.5%	3.3%
Node 44	0.5%	5.9%	67.2%	17.9%	8.6%
Node 45	0.2%	4.3%	69.6%	22.1%	3.7%
Node 46	0.5%	5.0%	71.9%	22.3%	0.2%
Node 47	0.0%	0.8%	45.5%	53.0%	0.7%
Node 48	0.7%	4.4%	61.4%	25.3%	8.2%
Node 49	0.5%	3.7%	71.9%	21.7%	2.1%
Serviceability Ratio	**0.4%**	**4.9%**	**51.7%**	**38.2%**	**4.8%**

8.3.1.2 Electrical Power Transmission System

Figure 8-16 shows the sensitivity of the serviceability of the electrical power transmission system to the attenuation relationship for PGA. In any attenuation relationship for PGA, the substations located either in northwest Shelby County, which is

close to the epicenter of the scenario earthquake, or far from any gate station exhibit the smallest functionality ratios (e.g. substations 19, 24 and 29).

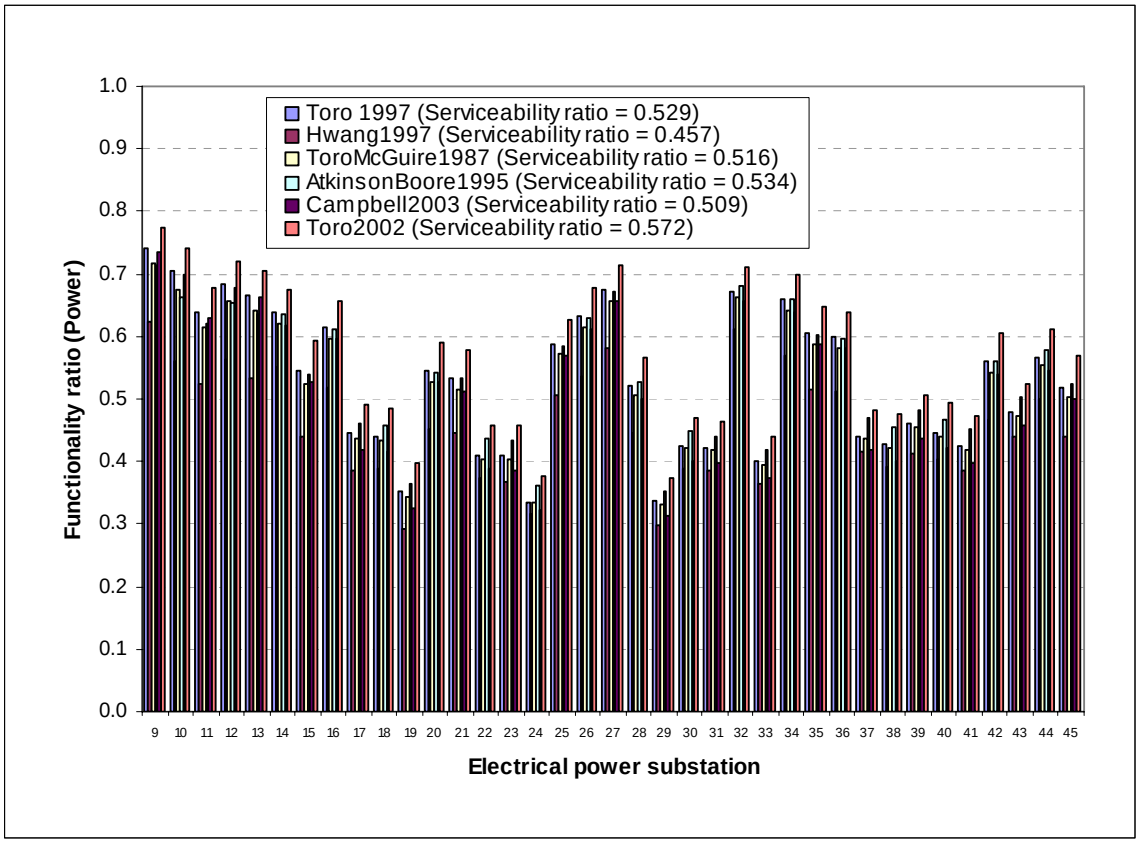

Figure 8-16 Sensitivity of electrical power transmission system serviceability to attenuation relationships for PGA

The sensitivity of the serviceability of the electrical power transmission system to the local soil amplification factor for PGA is illustrated in Figure 8-17. Some substations (e.g. substations 9, 10, 12 and 13) located far from the epicenter indicate smaller functionality ratios under the local soil amplification factor proposed by Hwang et al. (1997) since that amplification factor returns larger value at small PGA, and vice versa.

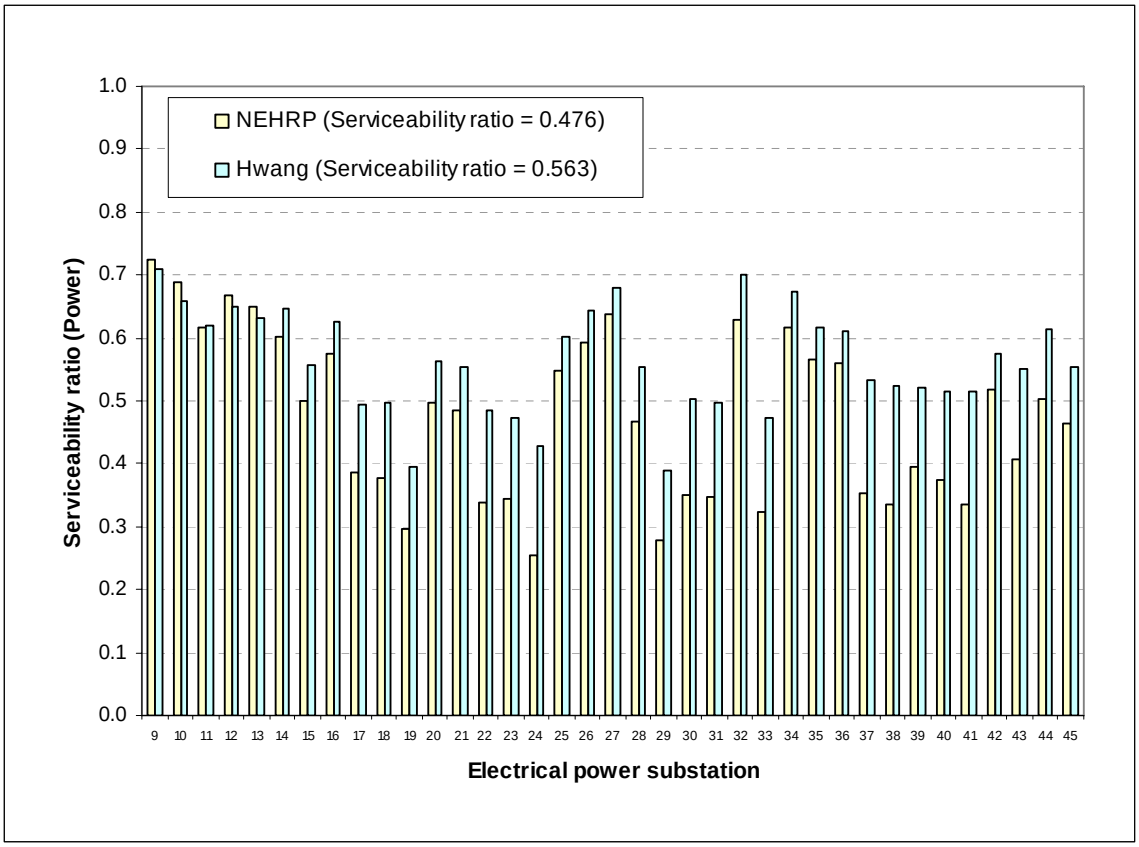

Figure 8-17 Sensitivity of electrical power transmission system serviceability to local soil amplification factors

Figure 8-18 shows the sensitivity of the serviceability of the electrical power transmission system to the correlation distance for PGA. Some substations (e.g., substations 9, 16, 27, 32 and 34) are networked in such a way that they behave as if they are part of a parallel system. Since a parallel system furnishes a lower bound on system failure probability when failure events are statistically independent (Eq.6-10), this explains why these substations indicate large functionality ratios when correlation distance b=0 km. Other substations (e.g. substations 19 and 42), whose functionality ratios are larger when correlation distance b = Infinity, are connected in series from any gate station. Such substations have less redundancy than other substations in the network.

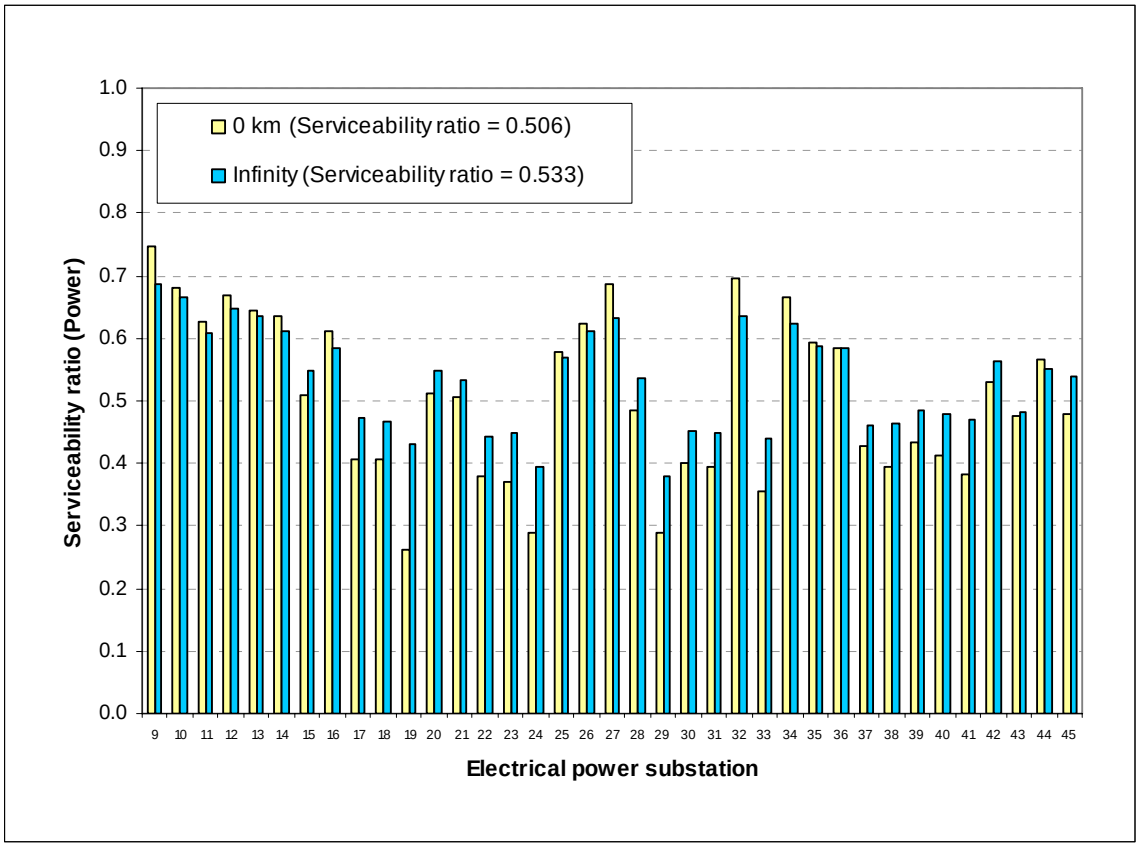

Figure 8-18 Sensitivity of electrical power transmission system serviceability to correlation distance

As was done for the water distribution system, a statistical approach was applied to determine the modeling parameter to which the serviceability assessment is most sensitive (Figure 8-15). The contribution ratios of three modeling parameters to the functionality ratio of each substation and to the serviceability ratio of the entire electrical power transmission system are summarized in Table 8-6. The contribution ratios in red and in blue represent the most and the second most important modeling parameter for the functionality ratio and the serviceability ratio, respectively. The functionality ratio and the serviceability ratio both are sensitive to the attenuation relationship for PGA and the local soil amplification factors in all cases. The effect of correlation distance for PGA varies widely from node to node (e.g., the most significant for substation 19; least

significant for node 46). Thus, it can be concluded that while all three modeling parameters may be important to determine the functionality ratios of the individual substations, the attenuation relationship for PGA and the local soil amplification factor are the most important factors in assessing the serviceability ratio of the entire electrical power transmission system.

Table 8-6 Contribution ratio of modeling parameters to the serviceability assessment of the electrical power transmission system

Functionality ratio	Attenuation relationship for PGA	Amplification factor	Correlation distance
Substation 9	84.8%	0.6%	14.5%
Substation 10	96.7%	2.8%	0.5%
Substation 11	98.5%	0.0%	1.5%
Substation 12	97.0%	1.1%	1.8%
Substation 13	98.6%	1.2%	0.3%
Substation 14	85.4%	10.8%	3.8%
Substation 15	83.3%	11.0%	5.8%
Substation 16	85.5%	11.2%	3.3%
Substation 17	41.4%	42.6%	16.0%
Substation 18	35.3%	51.1%	13.6%
Substation 19	22.6%	19.9%	57.5%
Substation 20	77.9%	16.5%	5.6%
Substation 21	77.7%	19.5%	2.8%
Substation 22	21.7%	65.9%	12.4%
Substation 23	27.0%	52.7%	20.3%
Substation 24	7.7%	67.7%	24.6%
Substation 25	83.9%	15.5%	0.6%
Substation 26	88.3%	10.8%	0.9%
Substation 27	78.8%	7.6%	13.6%
Substation 28	57.3%	32.1%	10.6%
Substation 29	21.6%	47.7%	30.7%
Substation 30	20.0%	72.1%	7.9%
Substation 31	19.5%	71.1%	9.4%
Substation 32	53.3%	27.4%	19.2%
Substation 33	16.7%	62.7%	20.5%
Substation 34	77.3%	13.7%	9.0%
Substation 35	87.3%	12.6%	0.1%
Substation 36	85.2%	14.8%	0.0%
Substation 37	11.9%	85.2%	2.9%
Substation 38	15.0%	74.9%	10.1%
Substation 39	32.3%	58.7%	9.0%
Substation 40	25.2%	61.6%	13.2%
Substation 41	16.4%	67.4%	16.2%
Substation 42	82.2%	13.2%	4.6%
Substation 43	26.3%	73.5%	0.2%
Substation 44	50.4%	48.4%	1.2%
Substation 45	82.2%	13.2%	4.6%
Serviceability Ratio	**55.5%**	**35.0%**	**9.6%**

8.3.2 Sensitivity Assessment under a Uniform Seismic Hazard

Sensitivity assessment of the serviceability ratio and the functionality ratio is performed to the water distribution system and the electrical power distribution system

under the uniform seismic hazard at six return periods. Infrastructure interaction effects are not considered.

8.3.2.1 Water Distribution System

Figure 8-19 shows the sensitivity of the serviceability of the water distribution system to the six attenuation relationships for PGA. The difference in the serviceability ratio is very small at all annual frequencies. Thus it is concluded that the serviceability ratio of the water distribution system is not sensitive to the attenuation relationship chosen for PGA.

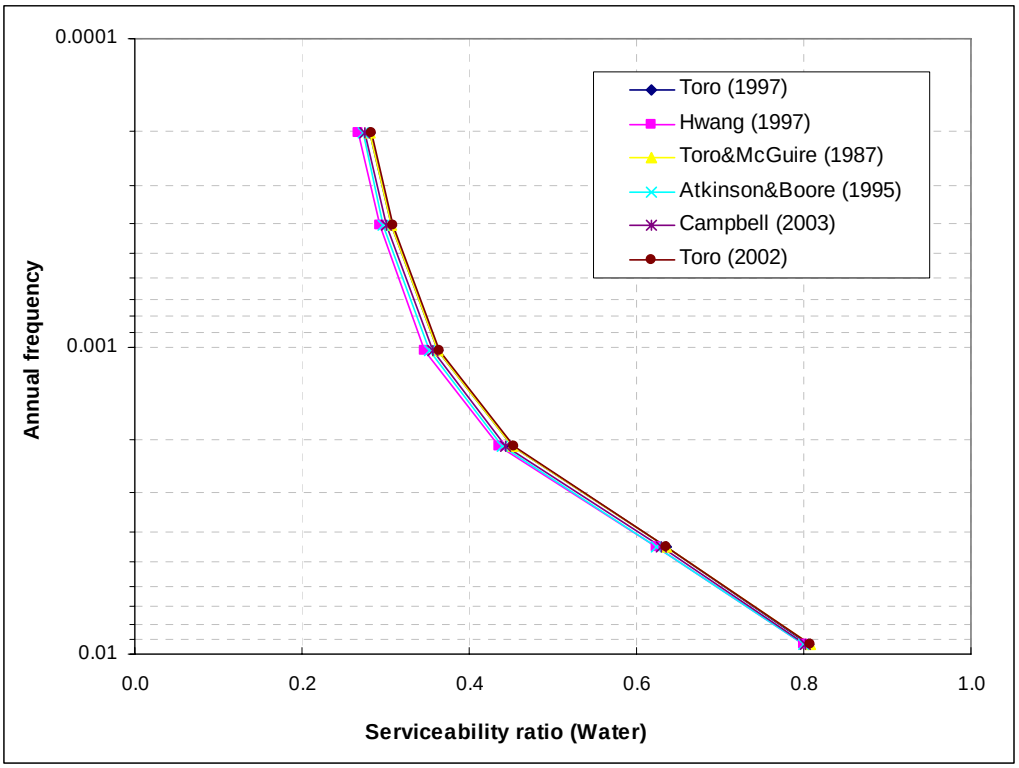

Figure 8-19 Sensitivity of water distribution system serviceability to attenuation relationships for PGA under uniform seismic hazard

The sensitivity of the serviceability of the water distribution system to the two attenuation relationships for PGV is summarized in Figure 8-20. The same trend is seen as PGA attenuation; the difference in serviceability ratio is very small. The serviceability

ratio of the water distribution system appears insensitive to the attenuation relationships for PGV.

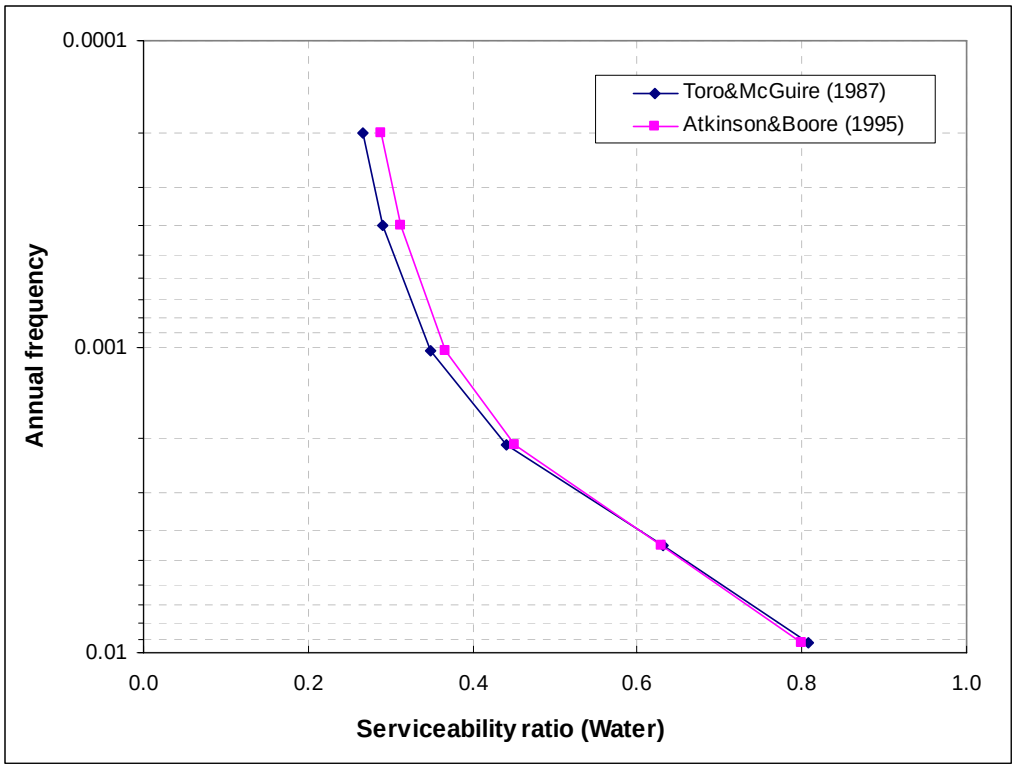

Figure 8-20 Sensitivity of the water distribution system serviceability to attenuation relationships for PGV under uniform seismic hazard

The dependence of the serviceability of the water distribution system on the local soil amplification factors for PGA and PGV is illustrated in Figure 8-21. The differences of the serviceability ratio are affected by the local soil amplification factor for PGV more than the amplification factor for PGA since the amplification factor for PGV proposed by Hwang et al. (1997) is larger than the amplification factor proposed by the *2003 NEHRP Provisions* at all values of PGV. Thus, the water pipe break, which is determined by PGV, dominates the determination of the serviceability of the entire water distribution network at all annual frequencies.

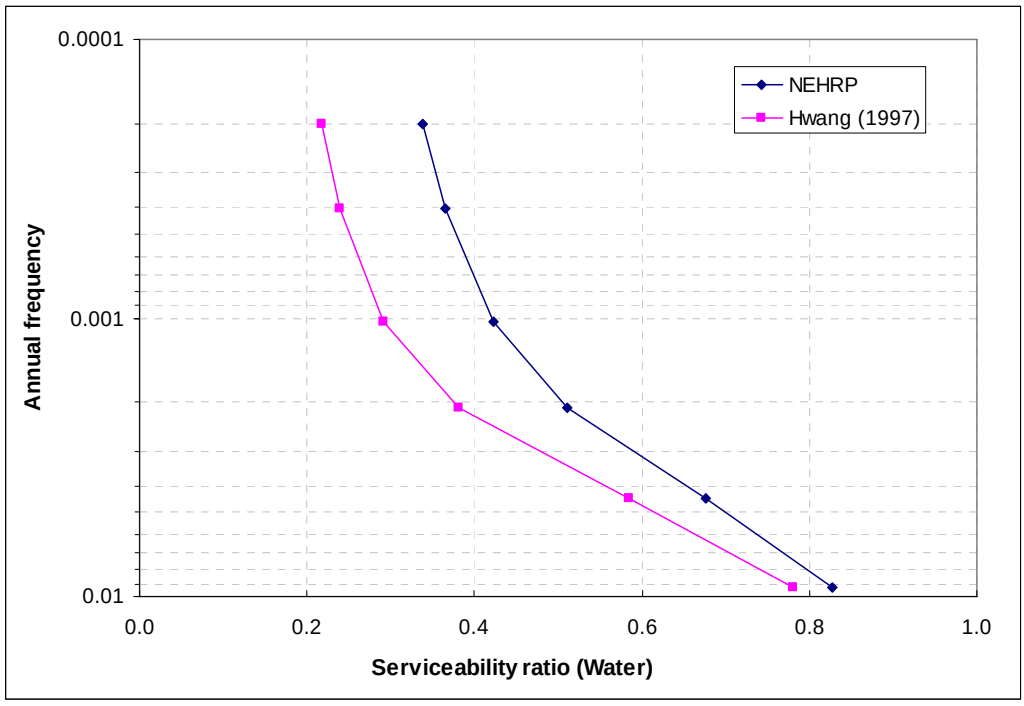

Figure 8-21 Sensitivity of water distribution system serviceability to local soil amplification factors under uniform seismic hazard

Figure 8-22 illustrates the sensitivity of the serviceability of the water distribution system to the correlation distances for PGA and PGV. The effect of the spatial correlation of PGA and PGV is relatively large at small annual frequencies (e.g. 0.0002, 0.0004 and 0.001-annual frequencies), but the effect becomes less important as the annual frequency increases (e.g. 0.0045 and 0.0093-annual frequencies).

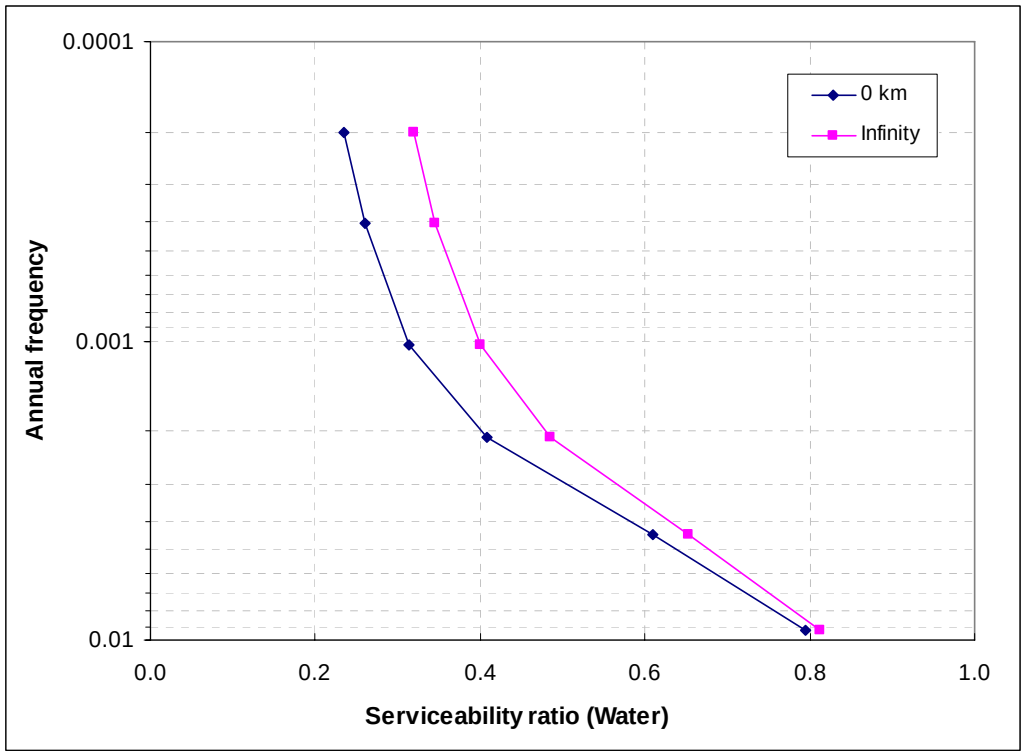

Figure 8-22 Sensitivity of water distribution system serviceability to correlation distance under uniform seismic hazard

The impact of choice of seismic fragility of an elevated water storage tank and the water pipe break density on the resulting serviceability of the water distribution system is illustrated in Figure 8-23. The two lines intersect at 0.0021-annual frequency because the functions of the water pipe break densities proposed by HAZUS MH (FEMA, 2003) and the *ALA Guideline* (ALA, 2001) cross at a PGV of 10 cm/sec. Earthquakes at large annual frequencies (e.g., 0.009-annual frequency) generate mostly small seismic intensities, and at these small seismic intensities (<10cm/sec.), the water pipe break ratio in HAZUS MH (FEMA, 2003) returns a smaller break ratio than the break ratio proposed by the *ALA Guideline* (ALA, 2001). Thus, the serviceability ratio using the water pipe break ratio by HAZUS MH (FEMA, 2003) is higher than the serviceability ratio using the break ratio by the *ALA Guideline* (ALA, 2001). The explanation is similar at small

annual frequencies (e.g., 0.0002-annual frequency). There, however, the difference is so small that the fragility curves and the water pipe break ratios have negligible impact on the serviceability ratio of the water distribution system.

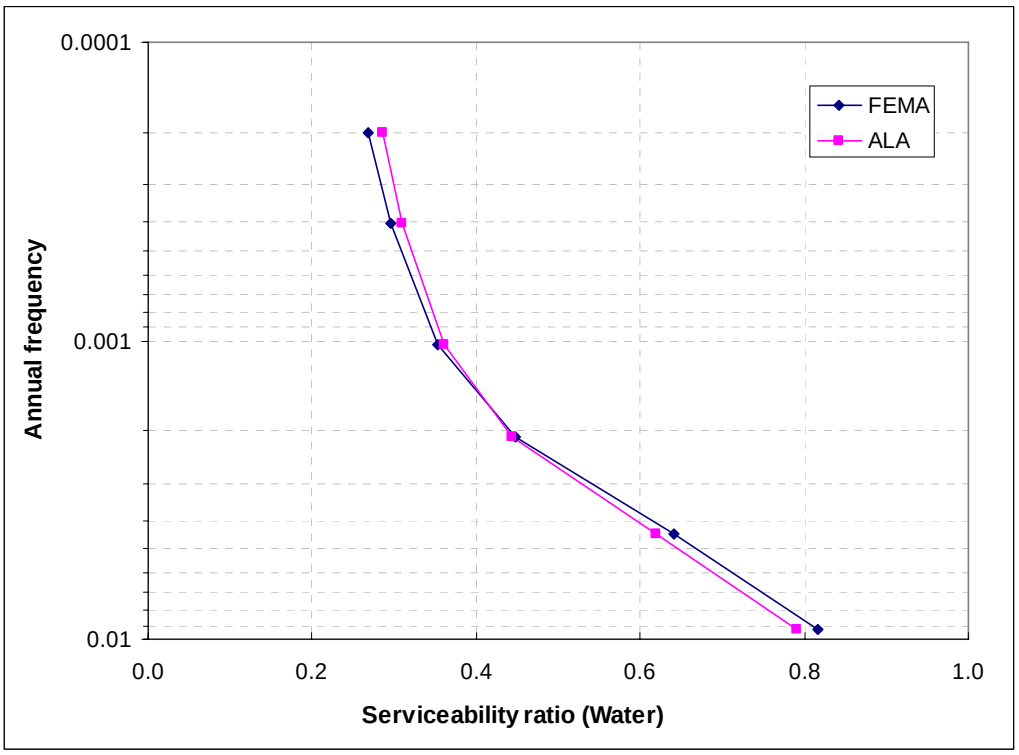

Figure 8-23 Sensitivity of water distribution system to fragility curves and water pipe break ratios under uniform seismic hazard

The statistical approach illustrated in Figure 8-15 is applied to determine the modeling parameters to which the serviceability assessment is most sensitive. The contribution ratios of five key modeling parameters to the serviceability ratio of the entire water distribution system are presented in Table 8-7. The contribution ratios in red and in blue represent the most important and the second most important modeling parameters to the serviceability ratio, respectively. As was seen previously, the serviceability ratio is especially sensitive to the local soil amplification factors and the correlation distance. In

contrast, the attenuation relationships for PGA and PGV are relatively unimportant for the serviceability assessment of the water distribution system.

Table 8-7 Contribution ratio of modeling parameters to the serviceability assessment of the water distribution system under the uniform seismic hazard

Return period (years)	Annual frequency	Attenuation relationship		Amplification factor	Correlation distance	Fragility curves
		PGA	PGV			
4975	0.0002	1.1%	2.3%	64.3%	30.9%	1.3%
2475	0.0004	1.2%	2.0%	66.2%	29.9%	0.8%
975	0.0010	1.2%	1.3%	68.1%	29.2%	0.2%
475	0.0021	1.2%	0.5%	72.5%	25.7%	0.1%
224	0.0045	1.4%	0.1%	76.6%	17.7%	4.2%
108	0.0093	1.6%	2.6%	68.6%	8.8%	18.3%

8.3.2.2 Electrical Power Transmission System

The sensitivity of the serviceability of the electrical power transmission system to the six attenuation relationships for PGA is summarized in Figure 8-24. The serviceability ratio is more sensitive to the attenuation relationships for PGA at smaller annual frequencies than at larger annual frequencies. In contrast to the results for the water distribution system shown in Figure 8-19, Figure 8-24 suggests that the difference in the serviceability ratio of the electrical power transmission system resulting from the choice of attenuation relationships for PGA is noticeable. Thus, PGA attenuation may be an important modeling parameter for serviceability assessment of electrical transmission systems.

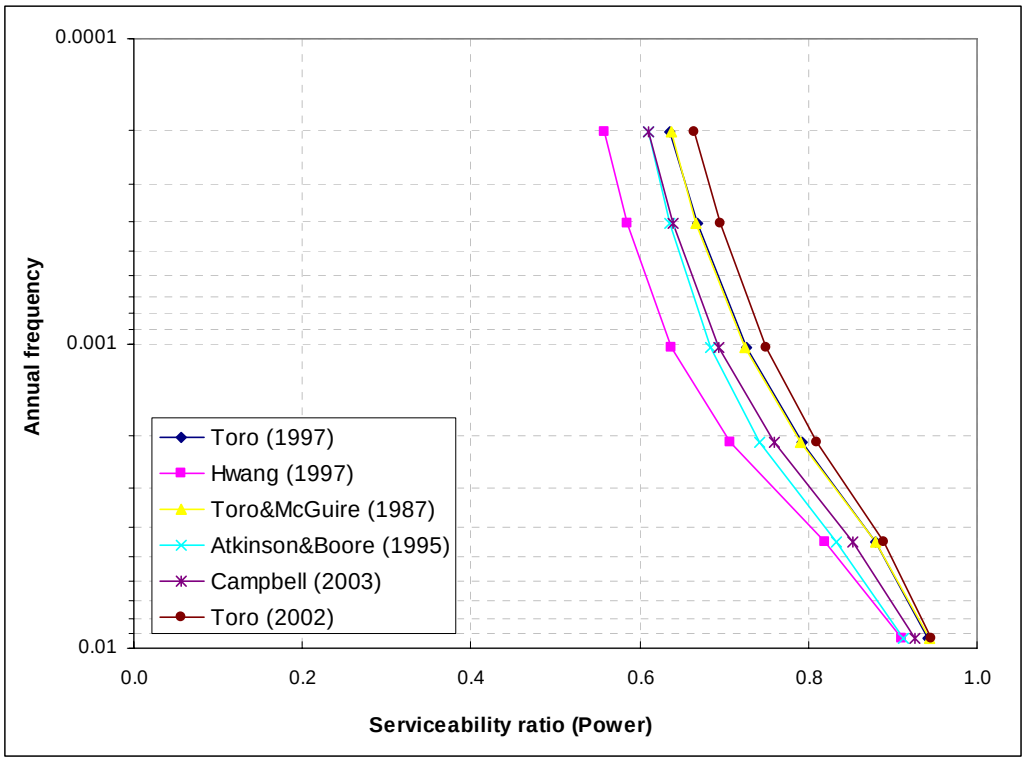

Figure 8-24 Sensitivity of electrical power transmission system serviceability to attenuation relationships for PGA under uniform seismic hazard

Figure 8-25 shows the sensitivity of the serviceability of the electrical power transmission system to the local soil amplification factors for PGA. The large difference at 0.0002-annual frequency follows from the fact that the amplification factor for PGA proposed by Hwang et al. (1997) is smaller than the amplification factors proposed by the *2003NEHRP Provisions* (FEMA, 2004) at larger values of PGA. The smaller amplification factor leads smaller estimated failure probabilities, yielding the larger serviceability ratio. Overall, it is concluded that the serviceability ratio of the electrical power transmission system is sensitive to the local soil amplification factors for PGA only at small annual frequencies.

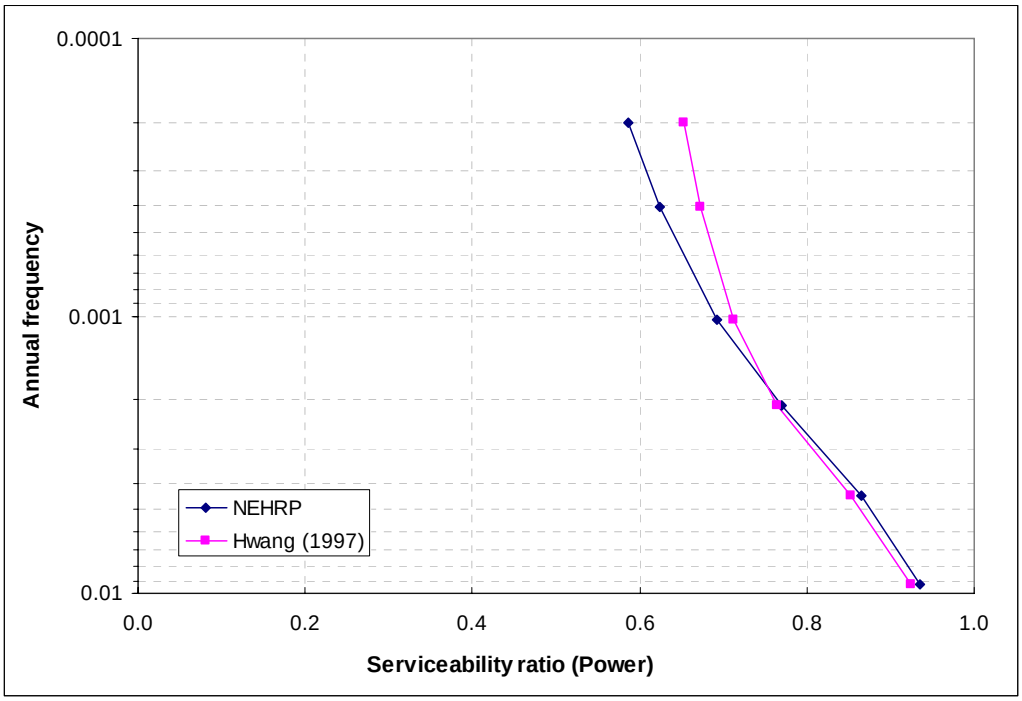

Figure 8-25 Sensitivity of electrical power transmission system serviceability to local soil amplification factors under uniform seismic hazard

Figure 8-26 shows the impact of correlation distance for PGA on the electrical system serviceability. The effect of the spatial correlation of PGA is small at all annual frequencies, indicating that this modeling parameter has a negligible impact on the serviceability ratio of the electrical power transmission system.

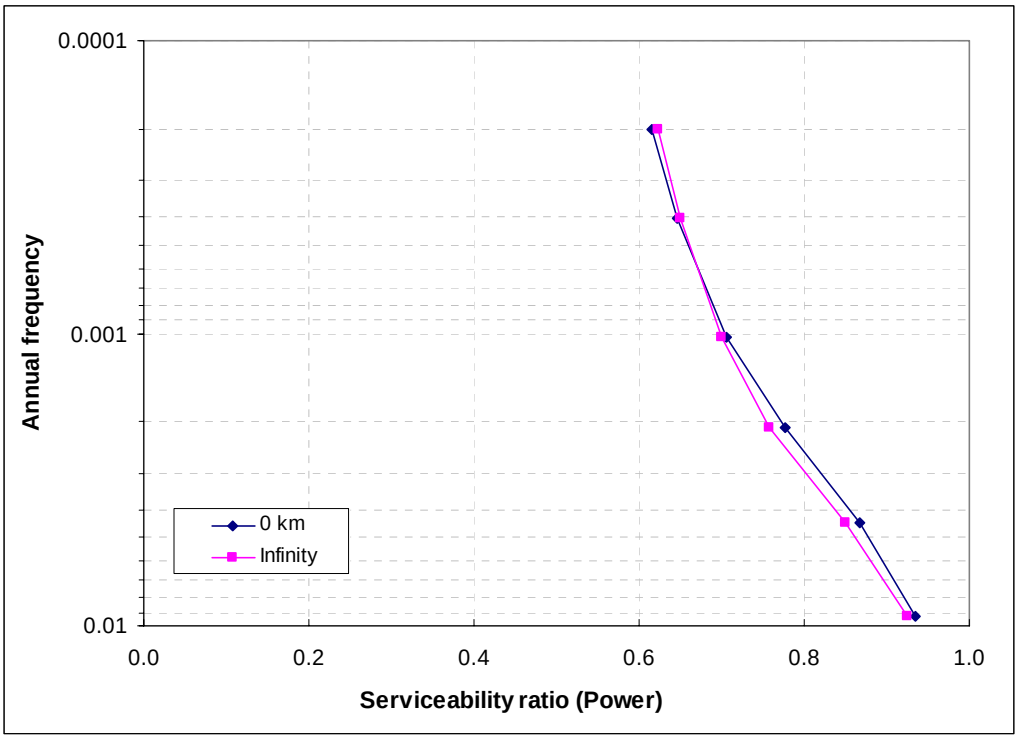

Figure 8-26 Sensitivity of electrical power transmission system to correlation distance under uniform seismic hazard

As in the case of the water distribution system, the contribution ratio, which is determined in Figure 8-15, determines the modeling parameter to which the serviceability assessment is most sensitive. The contribution ratios of three key modeling parameters to the functionality ratio of each substation and to the serviceability ratio of the electrical power transmission system are summarized in Table 8-8. Those in red and blue represent the most important and the second most important modeling parameters for the serviceability ratio, respectively. The serviceability ratio of the electrical power transmission system clearly is most sensitive to the attenuation relationship for PGA, and at smaller annual frequencies, the local soil amplification factor for PGA is also an important modeling parameter. It should be noted that the latest codes and regulatory

documents use the 0.0004-annual frequency (2,475-year return period or 2% probability of exceedance in 50 years) for earthquake-resistant design.

Table 8-8 Contribution ratio of modeling parameters to the serviceability assessment of the electrical power transmission system under the uniform seismic hazard

Return period (years)	Annual frequency	Attenuation relationship	Amplification factor	Correlation distance
4975	0.0002	72.1%	27.4%	0.5%
2475	0.0004	84.0%	16.0%	0.1%
975	0.0010	96.9%	2.8%	0.3%
475	0.0021	97.0%	0.2%	2.8%
224	0.0045	91.5%	3.2%	5.3%
108	0.0093	87.6%	6.8%	5.5%

8.4 Summary

The effects of uncertainties and the impact of modeling parameters were assessed in this chapter. The aleatory uncertainties of PGA and PGV were considered by modeling them as log-normal random variables; the median values were evaluated from the attenuation relationships for PGA and PGV, while the logarithmic standard deviation representing scatter in the ground motion data was set at the typical value of 60%. The epistemic uncertainties, which come from the choice of modeling parameters such as attenuation relationships, local soil amplification factors, correlation distances, fragility curves and water pipe break ratios, were modeled using the event tree models.

Considering the serviceability assessment under the scenario earthquake, the functionality ratios of facilities which either were located close to the epicenter or some distance from any supply facilities return were invariably smaller than the ratios of the other facilities. Under the uniform seismic hazard, a serviceability assessment using only the characteristic earthquakes within the NMSZ, might underestimate serviceability ratios.

The impact of the choice of modeling factors on the serviceability assessment was also analyzed in this chapter. The serviceability assessment of the water distribution system was found to be particularly sensitive to the local soil amplification factors and the correlation distances for PGA and PGV. In contrast, the impact of the attenuation relationships, fragility curves and water pipe break ratios were relatively small at all facilities and return periods. The correlation distance in seismic intensities was relatively unimportant for the serviceability assessment of the electrical power transmission system.

CHAPTER 9

SUMMARY, CONCLUSIONS AND FUTURE WORK

Civil infrastructure systems are essential to the smooth functioning of society. The operability and efficiency of such systems is made possible through interconnections with other infrastructure systems and by the availability of the commodities supplied by those systems. The complexity of interdependent infrastructure systems can lead unpredictable performance following natural or man-made events and accidents. Understanding the nature of these interdependencies is an important starting point to avoid or minimize damage or disruption arising from localized failures in such systems.

This study has explored the serviceability assessment of interdependent water distribution and electrical transmission systems from the standpoint of seismic risk. The case studies have illustrated the significant contribution to risk of system non-serviceability arising from its dependency on interfacing systems and the errors that may result if the seismic performance of each system is assessed without considering such interdependencies.

9.1 Summary and Conclusions

The serviceability assessment of an infrastructure system in this study has a number of following attributes, which represent advances in network evaluation over the approaches taken in previous research: (1) It addresses system interdependency effects explicitly; (2) It incorporates the effect of spatially correlated seismic intensities on the system serviceability assessment; (3) It examines limitations on the applicability of the uniform seismic hazard as a measure of seismic demand on the serviceability of a

distributed network; (4) It compares the serviceability of an infrastructure system estimated from a scenario earthquake to that estimated from a uniform seismic hazard, pointing out the shortcomings of basing the serviceability on the latter hazard model; (5) It examines the effect of aleatory and epistemic uncertainties for the serviceability assessment; and (6) It displays the sensitivity of the network serviceability to modeling parameters, thereby pointing the way to further data acquisition and development.

The first attribute utilizes the following techniques of system reliability assessment: fault tree modeling, reliability block diagram, structure functions and the Floyd-Warshall shortest path algorithm. The fault tree model captures the infrastructure interdependency effects simply and accurately. The reliability block diagram and the structure function facilitate modeling the infrastructure system whose components are interconnected. These techniques lead to an expression of system safety in binary form (e.g., 0: non-function, 1: normal-operation) The Floyd-Warshall shortest path algorithm facilitates rapid and efficient evaluation of network serviceability following system damage by an earthquake. Application of the system reliability analysis to the water distribution and the electrical power transmission systems in Shelby County, TN revealed that the functionality of key components may be strongly affected by the function of other connected facilities; in particular, the serviceability of the water distribution system is highly dependent on availability of electrical power, and power backup systems play a key role for ensuring continued function of the water distribution system. Due to the installation of power backup systems, the serviceability of the water distribution system considering interaction effects from the electrical power transmission system increases to the point where the water distribution system behaves as if it is independent of the

electrical power transmission system. The studies by Dueñas-Osorio (2005) and Dueñas-Osorio et al. (2006a and 2006b) also evaluated the impact of infrastructure interdependency. However, the graph theory has not been commonly applied in infrastructure system serviceability assessment, and the integration and interpretation of the graph theory estimates in the context of other system assessments may present a challenge. Furthermore, those studies did not assess the importance of power backup systems.

With regard to the second attribute, the assessment of the effect of spatially correlated seismic intensities on the serviceability of both water distribution and electrical transmission systems revealed that the performance of both systems was strongly dependent on the degree of spatial correlation. Furthermore, the effect of spatially correlated seismic intensities on functionality of a facility is dependent on the facility targeted. The accuracy in the estimate of failure probability of the water pipe depends on the segmentation of the pipelines as it relates to the spatial variability in the seismic demand. Although the Floyd-Warshall shortest path algorithm decreases computing effort involved in serviceability assessment, refined segmentation of water pipes increases the computing effort. A closed-form approximate solution to this system reliability analysis was developed, which is independent of the number of segments, reduces the execution time required for the Floyd-Warshall shortest path algorithm significantly, and yields a conservative solution that is sufficiently close to the exact solution to be used in practical system analysis.

The third attribute was achieved through a comparison of the component functionality ratios evaluated by the use of contours of the averaged seismic intensities to

averaged component functionality ratios evaluated by seismic intensities generated from each earthquake. This comparison suggested that the use of the probabilistic seismic hazard analysis as a basis for network serviceability assessment yields conservative estimates of performance only if the network is exposed to high seismic intensities over its entire extent. Otherwise, the use of the probabilistic seismic hazard contours leads to estimates of network serviceability that are sufficiently non-conservative that they should not be used for decision-making. A similar result, which was obtained when the serviceability of the electrical power transmission system was considered, confirmed the hidden risk of the use of a PSHA as the basis for assessing the serviceability of a networked system. Since the infrastructure system serviceability assessment performed by Dueñas-Osorio (2005) and Dueñas-Osorio et al. (2006a and 2006b) was performed using seismic intensities taken directly from the USGS probabilistic seismic hazard map, the results from the earlier study may differ from those presented in this study, where the spatial correlation in intensity was taken into account.

The forth attribute was accomplished by assessing the serviceability of the water .and electrical systems in Shelby County under a uniform seismic hazard established using both the New Madrid seismic zone and the background source zones, which are simulated from the results of the deaggregation analysis. Assessing the serviceability of either the water distribution system or the electrical power transmission system on the basis of the maximum probable earthquake, which is often used as a scenario earthquake for purposes of system assessment, appears to result in a quite conservative estimate of the serviceability ratio of either infrastructure system compared with the exact serviceability ratio in a certain return period. A serviceability assessment

using a mean scenario earthquake appears to be preferable for determining a retrofit plan for an existing infrastructure system or a design for a new system.

The fifth attribute was achieved by integrating aleatory and epistemic uncertainties into the serviceability assessment of the water distribution system and the electrical power transmission system. The median values of PGA and PGV at sites of components are computed from attenuation relationships for PGA and PGV; the associated coefficient of variation due to attenuation is assumed 60%, which is a major source of aleatory uncertainty. On the other hand, the epistemic uncertainty, which comes from the choice of modeling parameters, is displayed through decision tree models. Accordingly, this study clearly illustrates the role of uncertainty modeling on network performance.

The sixth and final attribute was to assess the sensitivity of the serviceability estimates for the water and electrical systems to the choice of modeling parameters. The result of this sensitivity assessment revealed that the functionality of components within each system is affected by different factors at different return periods. Overall, the local soil amplification factor and the strength of spatial correlation of seismic intensities are the factors that are most significant for estimating the serviceability of both the water distribution system and the electrical power transmission system. Conversely, the attenuation model chosen for PGA and PGV appears to be unimportant for the water distribution systems. However, the choice of attenuation model is important for assessing serviceability of the electrical power transmission system.

The sensitivity analysis reduces the difficulty in selecting parameters or relationships for network risk assessment, as it allows the network analyst to focus on the

subset of parameters that are essential to achieve accurate estimates of performance and risk.

9.2 Applications and Recommendations for Future Study

The methods and the outcomes described herein appear applicable to the following infrastructure system problems:

- The methods described herein for serviceability assessment of infrastructure systems are constructed from fundamental techniques such as fault tree models, the reliability block diagrams and the structure functions. This fact allows the methods to be easily integrated into existing engineering decision models.
- The serviceability assessment of infrastructure systems is often applied to estimate indirect economic losses to industries. Thus, the proper evaluation of serviceability after an earthquake, allowing for inter-dependencies in systems, may enhance the accuracy of such loss estimates.
- The proposed serviceability assessment methodology will facilitate decision making to increase the performance of existing infrastructure systems within a limited budget (such as by connecting facilities with new distributing elements, by building new facilities, or by retrofitting existing facilities or distributing elements). Importance indices (e.g., Birnbaum's measure or Criticality importance measure (Rausand and Hoyland, 2004)) can help establish priorities in identifying those facilities and distributing elements the early repair of which would most improve the serviceability of an existing system. The importance indices can be computed using the results of the probabilistic analysis presented in this study.

The present research also has identified some issues for future research:

- Interdependencies at higher levels - those in telecommunication systems, gas distribution pipelines, transportation systems and computer networks – should be integrated into the serviceability assessment. Not only the information such as locations, fragilities of components, but a careful investigation as to how such infrastructure systems interact is necessary;
- The network serviceability assessment should take into account progressive damage states in facilities that reduce, but do not eliminate, the flow of commodities. To achieve this, the Floyd-Warshall shortest path algorithm must be replaced by another shortest path algorithm (e.g., the Ford-Fulkerson algorithm (Papadimitriou and Steiglitz, 1998)) that allows partial function of key components to be modeled. Experience has indicated that the Ford-Fulkerson algorithm requires vastly more data than the Floyd-Warshall algorithm that is the basis for the accessibility analysis in this dissertation. Additional data, such as the capacity of facilities and distributing elements and customer demands, are needed. The capacity of facilities may be assumed, e.g., from the dimensions of water tanks, the number of seismically vulnerable electric components such as buses, circuit breakers and disconnect switches in an electrical power substation (Shinozuka et al, 1998) or the diameter and construction of water mains. Also, customer demands may be assumed by the average consumption per person per day (e.g., 80-100 gallons of water per day per person at home (USGS, 2005)). Furthermore, the relationship between damage state of facilities and distribution elements and their residual capacities must be established. Residual capacities of

components, in percent, may be assumed by the use of the relationship such as PGA vs. damage states (DS) and DS vs. residual capacities illustrated in ATC 13 (ATC, 1985), ATC 25 (ATC, 1991), ATC 25-1 (ATC, 1992) and HAZUS MH (FEMA, 2003).

REFERENCES

Adachi, Takao and Ellingwood, Bruce R. (2007a). "Assessment of probabilistic seismic hazard analysis applied to the networked civil infrastructure systems." Manuscript under review by Journal of Infrastructure Systems, American Society of Civil Engineers (ASCE).

Adachi, Takao and Ellingwood, Bruce R. (2007b). "Serviceability of earthquake-damaged water systems: effects of electrical power availability and power backup systems on system vulnerability", Reliability Engineering and System Safety. (In press).

Adachi, Takao and Ellingwood, Bruce R. (2007c). "Serviceability assessment of a municipal water system under spatially correlated seismic intensities." Manuscript under review by Computer-Aided Civil and Infrastructure Engineering, Blackwell Publishing.

Adachi, Takao and Ellingwood, Bruce R. (2007d). "Serviceability Assessment of an Electrical Power Transmission System under the Uniform Seismic Hazard." Manuscript under review by Structure and Infrastructure Engineering, Taylor and Francis.

Antony, Jiju (2003). Design of Experiments for Engineers and Scientists. Burlington, MA.: Butterworth-Heinemann.

American Lifelines Alliance (2001). Seismic Fragility Formulations for Water Systems Part 1 Guideline. Washington D.C.: American Lifeline Alliance (ALA).

American Society of Civil Engineers (2005). Minimum Design Loads for Buildings and Other Structures (ASCE Standard 7-05). Washington D.C.: American Society of Civil Engineers (ASCE).

Ang, A. H.-S.; Pires, J.A. and Villaverde, R. (1996). "A model for the seismic reliability assessment of electric power transmission systems." Reliability Engineering and System Safety **51**: 7-22.

Ang, Alfredo H-S. and Tang, H. Wilson (1984). Probability Concepts in Engineering Planning and Design Volume II Design, Risk, and Reliability. New York, NY: John Wiley & Sons.

Ang, Alfredo H-S. and Tang, H. Wilson (2006). Probability Concepts in Engineering – Emphasis on Applications to Civil and Environmental Enginering. 2nd ed. New York, NY: John Wiley & Sons.

Applied Technology Council (1985). Earthquake Damage Evaluation Data for California (ATC 13), Redwood City, CA: Apllied Technology Council (ATC).

Applied Technology Council (1991). Seismic Vulnerability and Impact of Disruption of Lifelines in The Conterminous United States (ATC 25). Redwood City, CA: Apllied Technology Council (ATC).

Applied Technology Council (1992). A Model Methodology for Assessment of Seismic Vulnerability and Impact of Disruption of Water Supply Systems (ATC 25-1). Redwood City, CA: Apllied Technology Council (ATC).

Atkinson, G.M. and Boore, D.M. (1990). "Recent trends in ground motion and spectral response relations for North America." Earthquake Spectra. **6**(1): 15-35.

Atkinson, G.M. and Boore, D.M. (1995). "Ground-motion Relations for Eastern North America." Bulletin of the Seismological Society of America **85**: 17-30.

Balducelli, C., Bologna, S., Di Pietro, A., Vicolo, G. (2005). "Analysing interdependencies of critical infrastructures using agent discrete event simulation." International Journal of Emergency Management **2**(4): 306-318.

Ballantyne, Donald B. and Taylor, Craig (1991). "Earthquake loss estimation modeling of the Seattle water system using a deterministic approach." Lifeline Network Reliability, Technical Council on Lifeline Earthquake Engineering monograph No.4. 747-760.

Bazzurro, P. and Cornell, C.A. (1999). "Disaggregation of Seismic Hazard." Bulletin of the Seismological Society of America. **89**(2): 501-520.

Boore, D. M. and Atkinson, G. (1987). "Stochastic prediction of ground motion and spectral response parameters at hard-rock site in eastern North America." Bulletin of Seismological Society of America. **77**: 440-467.

Boore, D. M. (2003). "Simulation of Ground Motion Using the Stochastic Method." Pure and Applied Geophysics. **160**(3-4): 635-676.

Broughton, A.T. Van; Arsdale, R.B. and Broughton, J.H. (2001). "Liquefaction susceptibility mapping in the city of Memphis and Shelby County, Tennessee." Engineering Geology. **62**: 207-222.

Campbell, K.W. (2003). "Prediction of strong ground motion using the hybrid empirical method and its use in the development of ground-motion (attenuation) relations in eastern North America." Bulletin of the Seismological Society of America. **93**(3): 1012-1033.

Cascos, George; Ciaccia, Julius; Tripp, Jennifer; Bella, Joe; Qussar, Saleh and Lacey, Marcia (2004). "Emergency Backup Power Supply." American Water Works Association Journal. **96**(1): 41-43.

Chang, S.E.; Seligson, H.A. and Eguchi, R.T. (1996). Estimation of the Economic Impact of Multiple Lifeline Disruption: Memphis Light, Gas and Water Division Case Study (NCEER-96-0011). Buffalo, N.Y.: The Multidisciplinary Center for Earthquake Engineering Center (MCEER).

Chang, S.E.; Shinozuka, Masanobu and Moore, James E. II (2000). "Probabilistic earthquake scenarios: extending risk analysis methodologies to spatially distributed systems." Earthquake Spectra.**16**(3): 557-572.

Chen, Walter W.; Shih, Ban-Jwu; Chen, Yi-Chih; Hung, Jui-Huang and Hwang, Howard H. (2002). "Seismic response of natural gas and water pipelines in the Ji-Ji earthquake." Soil Dynamics and Earthquake Engineering. **22**(9): 1209-1214.

CNN.COM (2006). "Tokyo suffers rush-hour power cut" Retrieved 15 August 2006 from <http://www.cnn.com/2006/WORLD/asiapcf/08/13/japan.powerout.reut/>.

Cox, D.R. and Reid, N. (2000). The theory of the design of experiments. Boca Raton, FL: Chapman & Hall/CRC press.

Cramer, Chris H. (2001). "A seismic hazard uncertainty analysis for the New Madrid seismic zone." Engineering Geology. **62**(1-3): 251-266.

Cornell, C.A. (1967). "Bounds on the reliability of structural systems." Journal of Structural Division, American Society of Civil Engineering. **93**(ST1): 171-200.

Day, Robert W. (2002). Geotechnical Earthquake Engineering Handbook. New York, NY: McGraw-Hill.

Delhe, A.: Bungum, H. and Kvamme, L.B. (1990). "Attenuation Models Inferred from Intraplate Earthquake recordings" Earthquake Engineering and Structural Dynamics. **19**: 1125-1141.

Dijkstra, E.W. (1959). "A note on two problems in connecting with graphs." Numerische Mathematik. **1**: 269-271.

Ditlevsen, O. and Madsen, O. (1996). Structural Reliability Methods. Chichester, NY: Wiley.

Dobry, R.; Borcherdt, R.D.; Crouse, C.B.; Idriss, I.M.; Joyner, W.B.; Martin, G.R.; Power, M.S.; Rinne, E.E.; Seed, R.B. (2000). "New site coefficients and site classification system used in recent building seismic code provisions." Earthquake Spectra. **16**(1): 41-67.

Dong, X.J.; Shinozuka, M. (2003). "Performance analysis and visualization of electric power systems" Proceedings of SPIE - The International Society for Optical Engineering. **5057**: 645-654.

Dueñas-Osario, Leonardo (2005). Interdependent Response of Networked Systems to Natural Hazard and Intentional Disruptions. Diss. Georgia Institute of Technology.

Dueñas-Osorio, Leonardo, James I. Craig and Barry G. Goodno (2006a). "Seismic

response of critical interdependent networks." Earthquake Engineering and Structural Dynamics, (In press).

Dueñas-Osario, Leonardo; Craig, James I. and Goodno, Barry J. (2006b). "Interdependent response of networked systems" Journal of Infrastructure Systems, (In press).

Eguchi, R. (1983). "Seismic Vulnerability Models for Underground Pipes, Earthquake behavior and safety of oil and gas storage facilities, buried pipelines and equipment." American Society of Mechanical Engineers (ASME) PVP-77: 368-373.

Eguchi, R.T. (1991a). "Early Post-Earthquake Damage Detection for Underground lifelines." Final report to the National Science Foundation, Dames and Moore P.C., Los Angeles, CA.

Eguchi, R.T. (1991b). "Seismic hazard input for lifeline systems." Structural Safety. **10**: 193-198.

Eguchi, Ronald T. and Honegger, Douglas G. (2003). "Standard Guidelines to Assess the Seismic Fragility of Water Transmission Systems." Proceedings of the Sixth U.S. Conference and Workshop on Lifeline Earthquake Engineering, American Society of Civil Engineers (ASCE): 504-511.

Eidinger, John (2001). Seismic fragility formulations for water systems (web site report). Oakland, CA: G&E engineering systems Inc.

Federal Emergency Management Agency (1997). HAZUS 97 Technical Manual. Washington D.C.: Federal Emergency Management Agency (FEMA).

Federal Emergency Management Agency (2003). HAZUS MH MR1 Technical Manual. Washington D.C.: Federal Emergency Management Agency (FEMA).

Federal Emergency Management Agency (2004). FEMA 450: the 2003 NEHRP Recommended Provisions for New Buildings and Other Structures. Washington D.C.:Federal Emergency Management Agency (FEMA).

Fedora, Philip A. (2004). "Reliability Review of North American Gas/Electric System Interdependency" Proceedings of the 37th Hawaii International Conference on System Sciences, IEEE.

Fernandez, J.A. and Rix, G.J. (2006). "Soil Attenuation Relationships and Seismic Hazard Analyses in the Upper Mississippi Embayment." Eighth U.S. National Conference on Earthquake Engineering 8NCEE, San Francisco, California.

Floyd, R.W. (1962). "Algorithm 97: Shortest Path." Comm. ACM 5. **6**: 345.

Frankel, A.; Mueller, C.; Barnhard, T.; Perkins, D.; Leyendecker, E.; Dickman, N.; Hanson, S. and M. Hopper (1996). National seismic-hazard maps: documentation June 1996. U.S. Geological Survey, Open-file Report 96-532.

Frankel, Arthur D.; Petersen, Mark D.; Mueller, Charles S.; Haller, Kathleen M.; Wheeler, Russell L.; Leyendecker, E.V.; Wesson, Robert L.; Harmsen, Stephen C.; Cramer, Chris H.; Perkins, David M. and Rukstales, Kenneth S. (2002). Documentation for the 2002 Update of the National Seismic Hazard Maps. U.S. Geological Survey Open-file Report, 02-420.

French, S. P. and Jia, X. (1997). "Estimating Societal Impacts of Infrastructure Damage with GIS" URISA Journal. **9**(1): 31-43.

Gillette, J. L., Fisher, R. E., Peerenboom, J. P., Whitfield, R. G. (2002). "Analyzing water/wastewater infrastructure interdependencies." 6th International Conference on Probabilistic Safety Assessment and Management. San Juan.

Gutenberg, B. and Richter, C.F. (1944). "Frequency of Earthqueks in California." Bulletin of the Seismological Society of America. **34**(4): 1985-1988.

Haimes, Y.Y. and Jiang, P. (2001) "Leontief-based model of risk in complex interconnected infrastructures." Journal of Infrastructure Systems. **7**(1): 1-12.

Yacov Y. Haimes; Barry M. Horowitz; James H. Lambert; Joost R. Santos;

Chenyang Lian; and Kenneth G. Crowther. (2005a) “Inoperability Input-Output Model for Interdependent Infrastructure Sectors. I: Theory and Methodology.” Journal of Infrastructure Systems. **11**(2): 67-79.

Yacov Y. Haimes; Barry M. Horowitz; James H. Lambert; Joost R. Santos; Chenyang Lian; and Kenneth G. Crowther. (2005b) “Inoperability Input-Output Model for Interdependent Infrastructure Sectors. I: Case Studies.” Journal of Infrastructure Systems. **11**(2): 80-92.

Hanks, T.C. and McGuire, R.K. (1981) “The character of high-frequency strong ground motion.” Bulletin of Seismological Society of America. **71**: 2071-2095.

Hwang, H.H.M., Lin, Huijie and Huo, Jun-Rong (1997). “Site coefficients for design of builings in eastern United States.” Soil Dynamics and Earthquake Engineering. **16**: 29-40.

Hwang, H. and Huo, J. (1997). “Attenuation relations of ground motion for rock and soil sites in eastern United States.” Soil Dynamics and Earthquake Engineering. **16**: 363-372.

Hwang, Howard H.M.; Lin, Huijie and Shinozuka, Masanobu (1998). “Seismic performance assessment of water delivery systems.” Journal of Infrastructure systems. **4**(3): 118-125.

Hwang, Howard H.M.; Chou, Tien (1998). “Evaluation of seismic performance of an electric substation using event tree/fault tree technique” Probabilistic Engineering Mechanics. **13**(2): 117-124.

International Electrotechnical Commission (1997). Functional safety of electrical/electronic/programmable electronic safety-related systems. Piscataway, N.J.: International Electrotechnical Commission (IEC) 61508.

Ishikawa, Y. and Kameda, H. (1994). “Scenario earthquake vs. probabilistic seismic hazard.” Proceedings of the International Conference on Structural Safety and Reliability (ICOSSAR'93). **3**: 2139-2146.

Jin, X.; Cheng, T.C.; Shinozuka, M and Dong, X. (2002). “Seismic Performance Analysis for LADWP Power System” Beijing, People's Republic of China: Power Systems and Communications Infrastructure for the future.

Katayama, T.; Kubo, K. and Sato, N. (1975). “Earthquake damage to water and gas distribution lines.” Proceedings of the U.S. National Conference on Earthquake Engineering: 396-405.

Kiureghian, A.D. and Liu, P. (1986). “Structural reliability under incomplete probability information.” Journal of Engineering Mechanics Engineering. **113**(1): 85-104.

Kramer, L.S. (1996). Geotechnical earthquake engineering. Upper Saddle River, N.J.: Prentice Hall.

Kreyszig, Erwin (1998). Advanced Engineering Mathematics. 8th ed. New York, NY: Wiley.

Kuwata, Yasuko and Takada, Shiro (2003). “Seismic Risk Assessment and Upgrade Strategy of Hospital-lifeline Performance.” Advancing Mitigation Technologies and Disaster Response for Lifeline Systems, Technical Council on Lifeline Earthquake Engineering Monograph No.25: 82-91.

Leontief, Wassily W. (1951). “Input-Output economics.” Scientific American. **185**(4): 15.

Leontief, Wassily W. (1986). Input-Output Economics. 2nd ed. New York, N.Y.: Oxford University Press.

Matsumoto, M. and Nishimura, T. (1998). “Mersenne twister: 623-dimensionally equidistributed uniform pseudorandom number generator.” ACM Transactions on Modeling and Generation methods and applications of Monte Carlo method. **8**(1): 3-30.

Matsumoto, M. (1997). “Mersenne Twister: A random number generator" Retrieved 25 September 2006 from <http://www.math.sci.hiroshima-u.ac.jp/~m-mat/MT/emt.html>.

McGuire, R.K. and Arabasz, W.J. (1990). “An introduction to probabilistic seismic hazard analysis.” Geotechnical and Environmental Geophysics. **1**: 333-353.

McGuire, R.K. (1995). “Probabilistic seismic hazard analysis and design earthquakes: closing the loop.” Bulletin of the Seismological Society of America. **85(**5): 1275-1284.

McGuire, R.K. (2001). “Deterministic vs. probabilistic earthquake hazards and risks.” Soil Dynamics and Earthquake Engineering. **21**: 377-384.

McGuire, Robin K. (2004). Seismic Hazard and Risk Analysis (MNO-10). Oakland, CA: Earthquake Engineering Research Institute.

Melchers, R.E. (1999). Structural Reliability Analysis and Prediction. 2nd ed. Chichester; NY. John Wiley & Sons.

McGuire, W., Gallagher, Richard H. and Ziemian, Ronald D. (2000). Matrix Structural Analysis. 2nd ed. New York, NY: John Wiley & Sons, Inc.

Newman, D.E., Nkei, Bertrand, Carreras, B.A., Dobson, I., Lynch, V.E. and Gradney, Paul (2005). “Risk assessment in complex interacting infrastructure systems.” Proceedings of the Annual Hawaii International Conference on System Sciences, IEEE.

Niigata Prefecture (2004). Information on damages due to 2004 Mid Niigata earthquakes. Retrieved April 2005 from <http://www.pref.niigata.jp/content/jishin/higai.html>. (in Japanese).

Nojima, Nobuoto and Sugito, Masata (2003). “Development of a Probabilistic Assessment Model for Post-Earthquake Residual Capacity of Utility Lifeline Systems.” Proceedings of the Sixth U.S. Conference and Workshop on Lifeline Earthquake Engineering: 707-716.

North American Electric Reliability Council (NERC) (2004). Gas/Electricity Interdependencies and Recommendations. Prinston, NJ: North American Electric Reliability Council.

Nuttli, Otto W. (1981). “Similarities and Differences between Western and Eastern United States Earthquakes, and Their Consequences for Earthquake Engineering.” Conference article of Earthquakes and Earthquake Engineering: The Eastern United States; Assessing the Hazard - Evaluating the Risk: 25-51.

Nuttli, Otto W. (1982). “The Earthquake Problem in The Eastern United States.” ASCE Journal of Structure Division. **108**(ST6): 1302-1312.

O'Rourke, M. and Ayala, G. (1993). “Pipeline damage due to wave propagation.” Journal of Geotechnical Engineering. **119**(9): 1490-1498.

O'Rourke, Michael J. and So, Pak (2000). “Seismic Fragility Curves for On-Grade Steel Tanks.” Earthquake Spectra. **16**(4): 801-815.

O'Rourke, T.D. and Jeon, S.S. (2000). “Seismic Zonation for Lifelines and Utilities.” Proceedings of the Sixth International Conference on Seismic Zonation, Earthquake Engineering Research Institute.

O'Rourke, T.D. and Jeon, S.S. (1999). “Factors affecting the earthquake damage of water distribution systems.” Proceedings of the 1999 5th U.S. Conference on Lifeline Earthquake Engineering: Optimazing Post-Earthquake Lifeline System Reliability. **16**: 379-388.

O'Rourke, Michael and Deyoe, Erik (2004). “Seismic damage to segmented buried pipe” Earthquake Spectra; **20**(4): 1167-1183.

Papadimitriou, H. Christos and Steiglitz, Kenneth (1998). Combinational Optimization – Algorithms and Complexity-. Mineola, NY: Dover Publications.

Peerenboom, James P., Fisher, Ronald E., Rinaldi, Steven M. and Kelly, Terrance K. (2002). “Studying the Chain Reaction” Retrieved 2 November 2006 from < http://www.eei.org/magazine/editorial_content/nonav_stories/2002-01-01-chain.htm>.

Pires, J.A.; Ang, A.H-S. and Villaverde, R. (1996). “Seismic reliability of electrical power transmission systems.” Nuclear engineering and design. **160**: 427-439.

Porter, K.A.; Scawthorn, C.; Honegger, D.G.; O'Rourke, T.D. and Blackburn, F. (1992). "Performance of Water Supply Pipelines in Liquefied Soil." Proceedings of 4th US-Japan Workshop on Earthquake Disaster Prevention for Lifeline Systems: 3-17.

Quimpo, Rafael G. and Wu, Sue-Jen (1997). "Condition assessment of water supply infrastructure." Journal of Infrastructure Systems. **3**(1): 15-22.

Rardin, L.Ronald (1997). Optimization in Operations Research. Upper Saddle River, N.J.: Prentice Hall.

Rausand, M. and Hoyland, A. (2004). System Reliability Theory –Models, Statistical Methods, and Applications-. 2nd ed. Hoboken, NJ: Wiley Interscience.

Recab, Kamel and Shaikh, Muzaffar (2005). Statistical Design of Experiments with Engineering Applications. Boca Raton, FL: CRC Press.

Rinaldi, S.M. (2004). "Modeling and simulating critical infrastructures and their interdependencies." Proceedings of the 37th Annual Hawaii International Conference on System Sciences: 873-880.

Rinaldi, Steven M.; Peerenboom, James P. and Kelly, Terrence K. (2001). "Identifying, understanding, and analyzing critical infrasrtfure interdependencies." IEEE Control Systems Magazine. **December**: 11-25.

Robert, Benoit (2004). "A method for the study of cascading effects within lifeline networks." International Journal of Critical Infrastructures. **1**(1): 86-99.

Rose, Adam; Benavides, J; Chang S.E.; Szczesniak, P and Lim,D. (1997). "The Regional Economic Impact of an Earthquake: Direct and Indirect Effects of Electricity Lifeline Disruptions." Journal of Regional Science. **37**(3): 437-458.

Ross, M. Sheldon (1992). Applied Probability Models with Optimization Application. Mineola, NY: Dover Publications.

Ross, M. Sheldon (2003). Introduction to Probability Models. 8th ed. Burlington, MA: Academic Press.

Satyanarayana, A. and Wood, R. Kevin (1985). "A linear-time algorithm for computing K-terminal reliability in series-parallel networks." SIAM Journal of Computing. **14**(4): 818-832.

Scawthorn, Charles; Chen, Wai-Fah and Chen Chen (2003). Earthquake Engineering Handbook. Boca Raton, FL: CRC Press.

Shimomura, T. and Takada, T. (2004). "Estimation for seismic ground motion using macro-spatial correlation model." Proceedings of 3rd Asian-Pacific Symposium on Structural Reliability and Its Applications: 139-148.

Shinozuka, M.: Hwang, H. and Murata, M. (1992). "Impact on Water Supply of a Seismically Damaged Water Delivery System." Lifeline Earthquake Engineering in the Central and Eastern U.S.: 43-57.

Shinozuka, M.; Rose, A. and Eguchi, R.T. (1998). Engineering and Socioeconomic Impact of Earthquake –an analysis of electricity lifeline disruptions in the New Madrid area- (MCEER Monograph Series 2). Buffalo, NY: Multidiciplinary Center for Earthquake Engineering Research.

Shinozuka, M; Cheng, Tsen-Chung; Feng, Maria Q. and Mau, Sheng-Taur (1999). "Seismic Performance Analysis of Electric Power Systems." MCEER Research Progress and Accomplishments 1997-1999: 61-69.

Shinozuka, Masanobu; Chang, Stephanie E.; Eguchi, Ronald T.; Abrams, Daniel P.; Hwang, Howard H.M. and Rose, Adam (1997). "Advances in Earthquake Loss Estimation and Application to Memphis, Tennessee." Earthquake Spectra. **13**(4): 739-758.

Takada, Shiro and Imanishi, Tatsuhiko (2003). "Time and Space Restoration Process and Prediction of Recovery Period for Damaged Water Supply Systems Based on GIS Data of The 1995 Kobe Earthquake." Technical Council on Lifeline Earthquake Engineering Monograph 25: 39-48.

Takada, T. and Shimomura, T. (2003). “Macro-spatial correlation of seismic ground motion of the 1999 Chi-Chi earthquake.” Architectural Institute of Japan (AIJ) Journal of Structural and Construction Engineering. **565**: 41-48. (in Japanese).

Takada, T. and Shimomura, T. (2004). “Macro-spatial correlation structural of seismic ground motion of the 1999 Chi-Chi earthquake.” Proceedings of 9th ASCE Specialty Conference on Probabilistic Mechanics and Structural Reliability.

Thoft-Christensen, P. and Baker, M.J. (1982). Structural Reliability Theory and Its Applications. Berlin, NY: Springer-Verlag.

Thoft-Christensen, P. and Muratsu, Y. (1986). Application of Structural Systems Reliabilty Theory. Berlin, NY: Springer-Verlag.

Tierney, K.J. (2000). “Improving earthquake loss estimation: review, assessment and extension of loss estimation methodologies.” MCEER Research Progress and Accomplishments 1997-1999: 12-27.

Toprak, S. (1998). Earthquake effects on buried lifeline systems. Diss. Cornell University.

Toro, G.R. (2002). Modification of the Toro et Al. (1997) Attenuation Equations for Large Magnitudes and Short Distances. Boulder, CO: Risk Engineering Inc.

Toro, G.R. and McGuire, R.K. (1987). “An investigation into earthquake ground motion characteristics in eastern north America.” Bulletin of the Seismological Society of America. **77**(2): 468-489.

Toro, G.R.; Abrahamson, N.A. and Schneider, J.F. (1997). “Model of Strong Ground Motions from Earthquakes in Central and Eastern North America: Best Estimates and Uncertainties.” Seismological Research Letters. **68**(1): 41-57.

U.S. Geological Survey (1996). “National Maps 1996.” Retrieved 27 August 2006 from <http://earthquake.usgs.gov/research/hazmaps/products_data/1996/natlmap.php>.

U.S. Geological Survey (2002a). “Interactive Deaggregations, 2002.” Retrieved 27 August 2006 from <http://eqint.cr.usgs.gov/eq-men/html/deaggint2002-06.html>.

U.S. Geological Survey (2002b). “2002 USGS National Seismic Hazard Maps, Conterminous United States.” Retrieved 27 August 2006 from <http://earthquake.usgs.gov/research/hazmaps/products_data/2002/us2002.php>.

U.S. Geological Survey (2005). “Water Science for Schools, Water Q&A: Water use at home.” Retrieved 10 February 2007 from <http://ga.water.usgs.gov/edu/qahome.html>.

U.S. Nuclear Regulatory Commission (1981). Fault Tree Handbook. NUREG-0492. Washington, DC: Nuclear Regulatory Research.

US-Canada Power System Outage Task Force (2004). Final Report on the August 14th Blackout in the United States and Canada. Washington D.C.: US-Canada Power System Outage Task Force (PSOTF).

Wada, I. (2002). Good Random Numbers and Bad Random Numbers. Retrieved 25 September 2006 from < http://www001.upp.so-net.ne.jp/isaku/rand.html> (in Japanese).

Wang, M. and Takada, T. (2005). “Macrospatial correlation model of seismic ground motions.” Earthquake spectra. **21**(4): 1137-1156.

Wagner, Janet M.; Shamir, Uri; Marks, David H. (1988a). “Water Distribution Reliability: Analytical Methods.” Journal of Water Resources Planning and Management: **114**(3): 253-275.

Wagner, Janet M.; Shamir, Uri; Marks, David H. (1988b). “Water Distribution Reliability: Simulation Methods.” Journal of Water Resources Planning and Management: **114**(3): 276-294.

Warshall, S. A. (1962). “Theorem on Boolean Matrices.” The Journal of the ACM **9**:11-12.

Wesson, Robert L. and Perkins, David M. (2001). “Spatial Correlation of Probabilistic Earthquake Ground Motion and Loss.” Bulletin of the Seismological Society of America **91**(6): 1498-1515.

Wong, F.S.; Dong, W.; Weimin, L. (1995). “Lifeline performance and business recovery.” Proceedings of the 4th U.S. Conference on Lifeline Earthquake Engineering **6**: 96-103

Wu, C.F. Jeff and Hamad, Micheal. (2000). Experiments -Planning, Analysis, and Parameter Design Optimization-. Hoboken, NJ: Wiley Interscience.

Yang, Han and Shaoping, Sun (2003). “Seismic Reliability of Urban Pipeline Network Systems.” Proceedings of the Sixth U.S. Conference and Workshop on Lifeline Earthquake Engineering: 445-454.

Yates, Roy D. and Goodman, David J. (2005). Probability and Stochastic Processes -A Friendly Introduction for Electrical and Computational Engineers-. 2nd ed. Hoboken, NJ: John Wiley & Sons, Inc.

VITA

Takao Adachi was born in Osaka, Japan in 1976, but spent his childhood in Wakayama, Japan. He earned a Bachelor's degree in Architectural Engineering from Nagoya University in 1999, completing research on the fragility assessment of earthquake-damaged buildings after the 1995 Kobe earthquake using the theory of structural reliability. He pursued his graduate studies in Architectural Engineering at the University of Tokyo, receiving the Master's degree in 2001. His Master's thesis was on the topic of optimal reliability assessment of building structures considering their lifetime impact on the natural environment and their lifetime cost. He enrolled as a doctoral student in the School of Civil and Environmental Engineering at the Georgia Institute of Technology in the fall of 2003, receiving a Master's degree in 2005. His current research interests include serviceability assessment of civil infrastructure systems damaged by earthquakes, system reliability analysis, operations research, and probability and statistics applied to engineering decision-making. He was awarded the Grand Prize by SAIC for his paper, "Serviceability Assessment of a Municipal Water System under Spatially Correlated Seismic Intensities: Approximate Closed-Form Bounds," which was developed from his thesis research.